Newer Synthetic Strategies for Novel Polyheteroaromatic (PHA) Compounds and Some of Their Photophysical Studies

A Dissertation Submitted to the

Indian Institute of Technology Guwahati

As Partial Fulfilment for the Degree of

Doctor of Philosophy (Ph.D.)

Submitted by

Sabina Yashmin

Roll No – 186122031

Under Supervision of

Prof. Abu Taleb Khan

Department of Chemistry
Indian Institute of Technology Guwahati
Guwahati-781039, Assam

Indian Institute of Technology Guwahati
Department of Chemistry
Guwahati – 781039, India
Tel. No.: +91-361-2582343
Fax No.: +91-361-2582349
e-mail: sabina@iitg.ac.in

Mrs. Sabina Yashmin
Research Scholar

DECLARATION

I, Sabina Yashmin, enrolled in the Ph.D. program in July 2018 in the Department of Chemistry at IIT Guwahati. I started my research endeavors under the guidance of Prof. Abu Taleb Khan in September 2018. I would also like to mention that the Institute was closed for 10 months due to the Covid-19 pandemic. Unfortunately, conducting research work was not feasible during that period, and I lost a valuable period in my research career.

I do hereby declare that the matter embodied in this thesis entitled "**Newer Synthetic Strategies for Novel Polyheteroaromatic (PHA) Compounds and Some of Their Photophysical Studies**" is the result of investigations carried out by me under the supervision of Prof. Abu Taleb Khan in the Department of Chemistry, Indian Institute of Technology Guwahati, India.

In keeping with the general practice of reporting scientific observations, due acknowledgements have been made wherever the work described is based on the findings of other investigators.

.

Sabina Yashmin

IIT Guwahati
2nd February, 2024

Sabina Yashmin
Roll No.- 186122031

Indian Institute of Technology Guwahati
Guwahati – 781039, India
Tel. No.: +91-361-2582305
Fax No.: +91-361-2582349
e-mail: atk@iitg.ac.in

Dr. Abu T. Khan
Professor of Chemistry

CERTIFICATE

This certifies that Mrs. Sabina Yashmin has been working in my research group since September 2018 as a registered PhD student. I want to mention that the Institute was closed for ten months due to the Covid-19 pandemic. Therefore, she lost ten months. Otherwise, she would have achieved more in research publications.

I am forwarding her thesis entitled "**Newer Synthetic Strategies for Novel Polyheteroaromatic (PHA) Compounds and Some of Their Photophysical Studies**", which is being submitted for the Ph.D. (Science) Degree from this institute.

I certify that she has fulfilled all the requirements according to the rules of this Institute regarding the investigations embodied in her thesis, and this work has not been submitted elsewhere for a degree.

IIT Guwahati
2nd February, 2024

Prof. A. T. Khan
(Thesis Supervisor)

DEDICATED TO

My Parents, Sisters, Brother

&

My Husband

ACKNOWLEDGEMENTS

I am delighted to use this moment to convey my heartfelt appreciation and thanks to everyone who has supported and encouraged me throughout my PhD studies. Your contributions have been invaluable, and this thesis would not have been possible without each one of you.

Above all, I would like to convey my sincere thanks and gratitude to Professor Abu T. Khan, my supervisor, for granting me the invaluable opportunity to work under his guidance. His mentorship, scientific insights, enthusiasm, and inspiration played a pivotal role in navigating the scope of work summarized in this thesis. I am thankful for his intense faith in me and for always showing me the right direction throughout this journey. His support, advice, and guidance have greatly contributed to my professional and personal growth. I have learned a lot from this precious time spent with him, and I will treasure these lessons for a lifetime. I am also grateful for his love and affection; he always holds a special place in my heart.

I am grateful to Prof. P. K. Iyer, Chairman of the Doctoral Committee, and other Doctoral Committee members, Prof. S. S. Ghosh and Prof. Bhubaneswar Mandal, for their intellectual support, encouragement, insightful suggestions, and sincere evaluation throughout my doctoral study.

My honest regards to all the faculty members of the Department of Chemistry. I especially thank Dr. Kalishankar Bhattacharyya, Assistant Professor in the Department of Chemistry at IIT Guwahati, for his contributions to the computational study of establishing the reaction mechanism.

I sincerely appreciate the collaboration with Prof. Priyabrata Banerjee, Principal Scientist of the Surface Engineering & Tribology Group at CSIR-Central Mechanical Engineering Research Institute, and his student, Dr. Riyanka Das, in our Photophysical Studies. Their dedicated efforts are highly valued, and I sincerely thank them.

I am highly indebted to Dr. Lokman Hakim Choudhury, Professor & Head, Department of Chemistry, IIT Patna, and Dr. Radhakrishnanand P, Professor at NIPER Guwahati, for their generous support in providing HRMS data. Additionally, I thank their students for recording the HRMS data of the organic compounds.

I express my sincere gratitude for the research fellowship, access to instrumental facilities offered by IIT Guwahati, and all the additional support, including the delightful campus, which has made this five-year journey truly memorable.

I extend special appreciation to the Central Instrument Facility at IIT Guwahati for granting access to the 600 MHz NMR, X-ray, and HRMS facilities. Additionally, my gratitude goes to the North East Centre for Biological Sciences and Healthcare Engineering, IIT Guwahati, for providing the 500 MHz NMR facility.

I want to express my gratitude to all the Department of Chemistry staff members for their helpful and cooperative nature. I want to offer a special acknowledgement to Mr. Imdadul Islam for instructing me on the operation of the 500 MHz NMR equipment and Dr. Babulal Das for assisting with the single crystal XRD studies during my Ph.D. work.

Furthermore, I have had the privilege of sharing this journey with the wonderful individuals in my laboratory. I am pleased to acknowledge the remarkable lab seniors, namely Dr. Suchandra Bhattacharjee, Dr. Radhakrishna Gattu, Dr. Santa Mondal, Dr. Saghir Ali, Dr. Rashid Ali, and my current labmates Anjela Xalxo, Ujjwal Jyoti Goswami, Dr. Arnab Mandal, Ahmad Ali, Simra Faraz, Mukesh Kumar, Anil R Pawar, Satyajit Singh, Nisha Rani, Halida Khatun, Eman Ali, and Gyani Yumnum. I consider myself fortunate to have shared countless joyful moments with them. They have all been fantastic, supportive, and cooperative in every circumstance. Each has contributed to my learning experience in the lab and my life.

I also had the opportunity to work with some dedicated M. Sc. and summer trainees Kharou M, Karthik M, Anukampa Chakravarty, Sampriti Mukherjee, Tejas Thorat, Lubna Naaz, Musfika Khatun.

I express my deepest love and gratitude to all my friends Bittu Lama, Rinki Brahma, Sandeep Kumar, Sagnik Dey, Debjyoti Pal, Pran Gobinda Nandi, Bikoshita Porashar, Vinay Arora, Tanumay Sarkar, Priyanka Adhikari, Tirupati Roy, Indraneel Debnath, Aritra Mitra, Monuranjan Konwar. Without their support, this journey would be incomplete. I will cherish the beautiful and joyful time I have spent with them for my lifetime. I am especially thankful to my friends Santa Mondal, Bittu Lama, Rinki Brahma, Sandeep Kumar and Ujjwal Jyothi Goswami for contributing to my personal and professional growth.

I extend my profound gratitude to my late grandmother Mrs. Mahuda Begam, uncles, aunts, cousins, father-in-law, mother-in-law, sister-in-law, and all other relatives for their endless love, support, and blessings throughout my life. A special gratitude is expressed to my uncles, Mr. Mamud Hossain and Dr. Ahmad Hossain, for being my role model. I am also grateful to all my friends and teachers, including those from my childhood, who have made direct and indirect contributions to my life.

Finally, I extend my deepest gratitude, love, and respect to my parents, Mr. Shaikh Iqbal Hossain and Mrs. Farida Begum. Their immense sacrifices and unconditional love at every stage of my life motivated me to overcome all challenges. They courageously confronted challenges to impart their moral values, moulding me into a good human. To my wonderful and loving sisters and my brother, Sabrina Parveen, Sayma Sadaf, and Shaikh Yasir Hossain, I express my love, affection, and gratefulness for their unwavering support, kindness, and significant presence in my life. I owe my entire life to them.

I am greatly indebted to my dear husband, Sk Rafiqul Rahaman, for his endless moral support and encouragement throughout the journey. I express my sincere gratitude, utmost love and respect for him. I pray to the almighty to spend a blissful and peaceful life with him.

At last, I express my gratitude to the Almighty. May he bless us all with his kindness and mercy.

Sabina Yashmin

GENERAL REMARKS

The present investigations were carried out at the Department of Chemistry, Indian Institute of Technology Guwahati, Guwahati -781 039, Assam, during the period from September 2018 to January 2024 as a doctoral student under the supervision of Prof. Abu T. Khan. The analytical samples were routinely dried *in a vacuum* at 50 ^{o}C. In TLC experiments, silica gel G (SRL) or silica gel GF 254 (SRL) employed as an adsorbent was used. Column chromatography was carried out with silica gel (60-120 mesh, Merck or SRL), for purifications of the reaction mixture. Biotage flash chromatography was also used for purification. After purification, the solvent was usually removed in a rotatory evaporator using Büchi R-114V and Büchi R-300 instrument. Melting points were determined using a Büchi melting point apparatus. IR spectra were recorded on the Perkin-Elmer 281 IR spectrophotometer. $CDCl_3$ and DMSO-d_6 were used to record the NMR spectrum. The standard chemical shift value for $CDCl_3$ and DMSO-d_6 are considered 7.26 and 2.50 ppm in ^{1}H NMR spectra, and 77.16 and 39.52 in case of ^{13}C NMR spectra respectively. Using TMS as an internal standard, ^{1}H NMR spectra were recorded on Bruker 400 MHz, Bruker 500 MHz and Bruker 600 MHz spectrometers. Similarly, ^{13}C NMR spectra were recorded on Bruker 100 MHz, Bruker 125 MHz, and Bruker 150 MHz spectrometer TMS as the internal reference; chemical shifts (δ scale) are reported in parts per million (ppm). ^{1}H NMR spectra are reported in the order of multiplicity, number of protons, and coupling constant (*J* value) in hertz (Hz); signals were characterized as s (singlet), d (doublet), t (triplet), m (multiplet), brs (broad singlet), dd (doublet of doublet), dq (doublet of the quartet), dt (doublet of triplet) and ddt (doublet of a doublet of triplet). HRMS spectra were recorded using ESI (TOF) mode. Crystal data were collected with Bruker Smart Apex-II CCD diffractometer using graphite monochromated MoKα radiation (λ = 0.71073 Å) at 296 K.

CONTENTS OF THE THESIS

ABBREVIATION

Ac	Acetyl
AcOH	Acetic Acid
Ac_2O	Acetic Anhydride
AIBN	Azobisisobutyronitrile
AIE	Aggregation-Induced Emission
aq.	Aqueous
Bn	Benzyl
Bu	Butyl
***t*-Bu**	*tert*-Butyl
***t*-BuOK**	Potassium *tert*-Butoxide
Bz	Benzoyl
CCDC	Cambridge Crystallographic Data Centre
CDC	Cross Dehydrogenative Coupling
CSA	(±)-Camphor-10-sulfonic Acid
DABCO	1,4-diazabicyclo[2.2.2]octane
DCE	1,2-Dichloroethene
DCM	Dichloromethane
DFT	Discrete Fourier Transform
DMF	*N*, *N*-Dimethylformamide
DMSO	Dimethyl Sulfoxide
DNA	Deoxyribonucleic Acid
EDG	Electron-Donating Group
EWG	Electron-Withdrawing Group
ESI (TOF)	Electrospray Ionization (Time-of-Flight)

Et	Ethyl
EtBr	Ethidium Bromide
Et_3N	Triethylamine
EtOH	Ethanol
g	gram
h	hour
HIV	Human Immunodeficiency Virus
HRMS	High-Resolution Mass Spectrometry
HCl	Hydrochloric Acid
$In(OTf)_3$	Indium Triflate
IR	Infrared
***m*-CPBA**	*m*-Chloroperoxybenzoic Acid
MCR	Multicomponent Reaction
Me	Methyl
mg	Milligram
mp	Melting Point
ms	Molecular Sieves
MW	Microwave
NBS	*N*-Bromosuccinimide
NMR	Nuclear Magnetic Resonance
OFETs	Organic Field Effect Transistors
OLEDs	Organic Light-emitting Diodes
OPVs	Organic Photovoltaics
OSCs	Organic Semiconductors
ORTEP	Oak Ridge Thermal Ellipsoid Program

PAHs	Polycyclic Aromatic Hydrocarbons
PHAs	Polyheteroaromatic Compounds/Polycyclic Heteroaromatic Compounds
$Pd(OAc)_2$	Palladium (II) Acetate
Ph	Phenyl
Pr	Propyl
ppm	Parts per Million
Py	Pyridine
***p*-TSA**	*p*-Toluenesulfonic Acid
ROS	Reactive Oxygen Species
rt	Room Temperature
S_N2	Bimolecular Nucleophilic Substitution
TBAB	Tetrabutylammonium Bromide
TBHP	*tert*-Butyl Hydroperoxide
TEMPO	(2,2,6,6-Tetramethylpiperidin-1-yl)oxyl
TFA	Trifluoroacetic Acid
THF	Tetrahydrofuran
TLC	Thin-Layer Chromatography
TMS	Tetramethylsilane
TfOH	Triflic Acid
w	Weight
XRD	X-ray Diffraction
$Yb(OTf)_3$	Ytterbium(III) Triflate

CHAPTER I

A Review on Polyheteroaromatic Compounds (PHAs)

1.1. Introduction to Polyheteroaromatic Compounds (PHAs)

1.1a. Polycyclic Aromatic Hydrocarbons (PAHs) and Polyheteroaromatic Compounds (PHAs)

Polycyclic aromatic hydrocarbons (PAHs) are aromatic compounds characterized by two or more fused benzene rings arranged in various structural configurations devoid of heteroatoms within their rings.[1a-e] Naphthalene, with its two aromatic rings, serves as the simplest representative, while examples of three-ring compounds are anthracene, phenanthrene, and phenalene. The tetracyclic PAHs encompass chrysene, tetracene, triphenylene, and pyrene, while examples of pentacyclic PAHs include perylene, pentacene, and benzopyrene. Representatives of the PHAs containing different numbers of rings are illustrated[1b-c] in **Figure 1.1**. PAHs containing up to four rings are classified as light PAHs, whereas those with more than four rings are categorized as heavy PAHs. Heavy PAHs exhibit greater stability and toxicity than their light counterparts. PAHs comprising solely carbon and hydrogen arranged in intricate ring systems, based on their benzene ring arrangements, showcase a diverse range of physical, chemical, and toxicological characteristics.[1d-e]

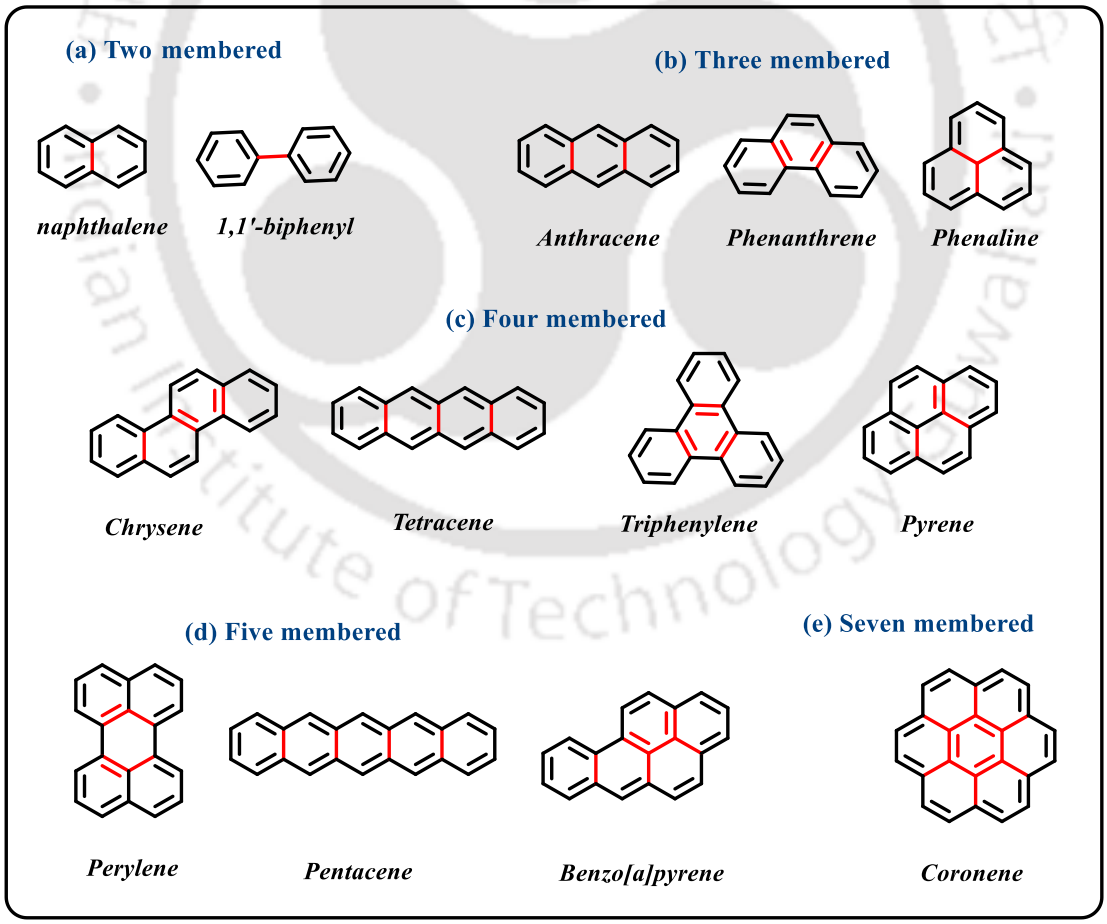

Figure 1.1. A few examples of polycyclic aromatic hydrocarbon (PAH).

When an electron-rich heteroatom (N, O, or S) or an electron-deficient heteroatom (B) is introduced into a PHA skeleton, they are called **Polyheteroaromatic Compounds (PHAs)**.[3] It is also described as Polycyclic heteroaromatic compounds. They can have one or many heteroatoms. Many of them can be fused by multiple polycyclic systems, such as naphtho[1,2-*b*]benzofuran, composed of benzofuran and naphthalene ring. A few simple examples are shown in **Figure 1.2**.

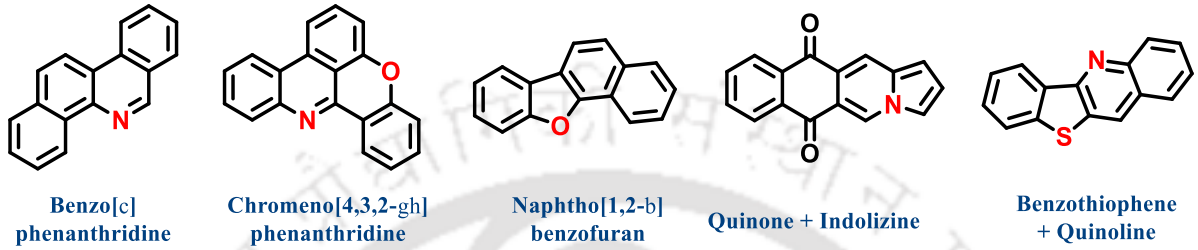

Figure 1.2. A few examples of Polyheteroaromatic compounds (PHAs).

1.1b. Fusion Patterns and Edge Topologies

Polycyclic heteroaromatic molecules display considerable structural diversity in terms of the number and connectivity of constituent rings, heteroatom pattern, and peripheral substitution. PHAs have specific fusion patterns. They can be *ortho*-fused, *peri*-fused, and *macro*-fused, as shown in **Figure 1.3**. In *ortho* fusion, two rings are connected through an edge; in a *peri*-fused system, three rings are attached through a peri-fusion point. Macro fusion is observed for macrocyclic compounds.

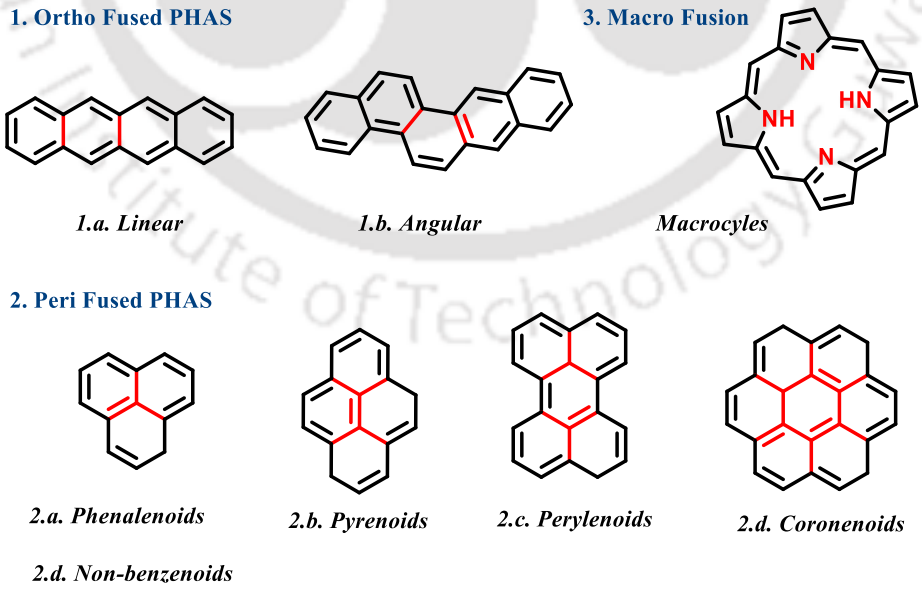

Figure 1.3. Classifications of polycyclic aromatic frameworks based on their fusion patterns.

Conversely, polycyclic aromatic compounds with different edge topologies exhibit considerably different physical and chemical properties. Typical edge structures of the polycyclic aromatic framework are presented[3a-b] in **Figure 1.4**. It includes **bay regions**, armchair edges, and L-regions (zigzag edges) with isolated CH bonds. **K-regions** show isolated carbon-carbon double bonds that do not belong to the Clar sextet. Cove and fjord regions cause non-planarity due to the prevailing steric hindrance. Similarly, the **N region** can be in a ring with continuous HC-CH-CH connectivity. In contrast, the **M region** is defined as a ring with HC-CH-CH-CH connectivity (**Figure 1.4b)**.

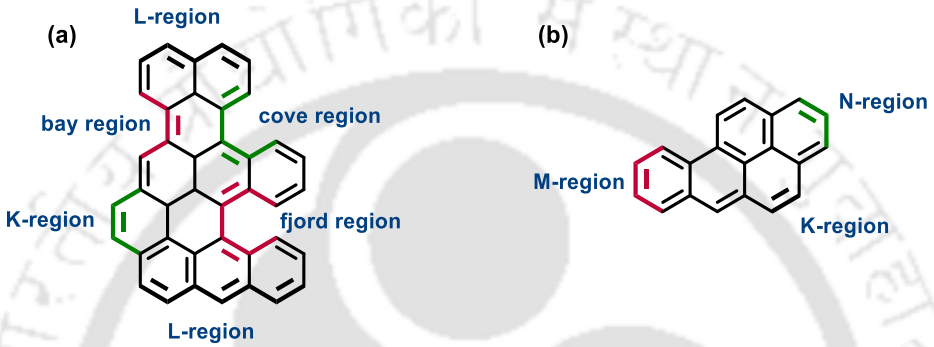

Figure 1.4. Edge topologies of polycyclic aromatic frameworks.

1.1c. Why PHAs are so Important?

The chemistry of heteroaromatic compounds is a vast discipline, spanning nearly two centuries of research. The focus of heterocyclic chemistry has evolved, encompassing many topics in synthetic and physical organic chemistry, natural product research, molecular biology, and materials science. The interest in polycyclic heteroaromatic molecules (PHAs) can be traced back to the initial investigations of natural and synthetic dyes such as xylindein, coerulein, flavonthrone, etc, as illustrated[4a,b] in **Figure 1.5**.

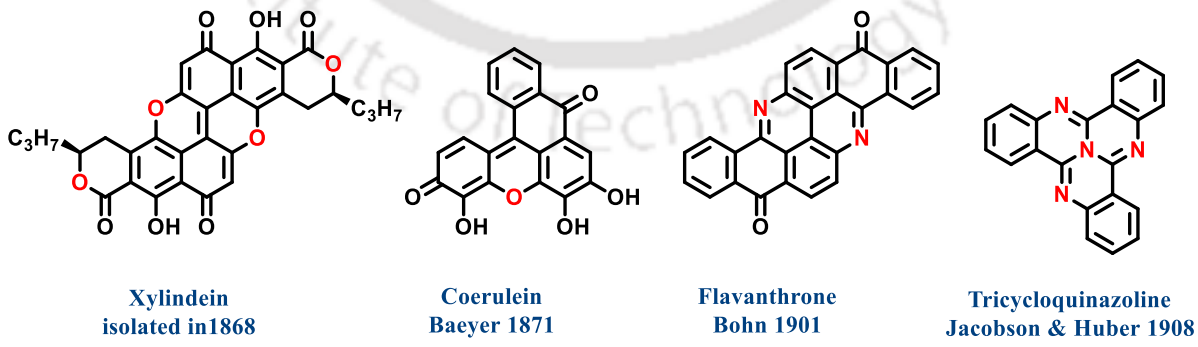

Figure 1.5. Very early examples of PHAs, used as dye.

Overcoming the barrier of appropriate analytical methods, it expanded from dyestuff research to supramolecular chemistry to the growing interest in porphyrin analogues. Depending on the number and placement of heteroatom donors, PHAs can offer monodentate, chelating, or macrocyclic coordination.[5] This helps them to be used as a ligand in coordination chemistry, studying biological and photophysical properties, and catalysts in many reactions. PHAs find applications in various forms, such as self-assembling materials,[6a] liquid crystals,[6b] porous structures,[6c] nanofibers,[6d] and gels[6e] (**Figure 1.6**). They have immense importance in drug discovery for their widespread biological activities such as anti-cancer, anti-tumor, etc.[7]

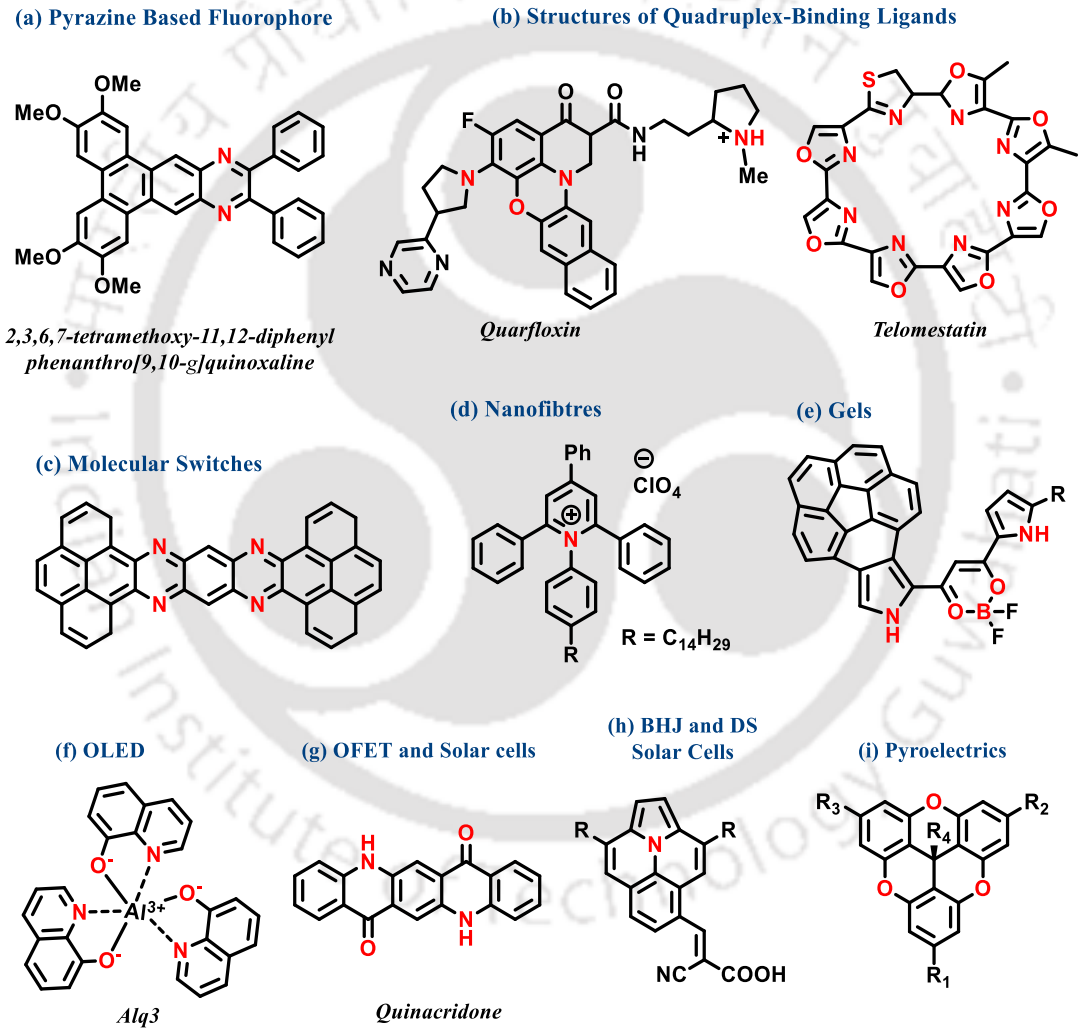

Figure 1.6. Few examples of PHAs having numerous applications.

At the turn of the 21st century, the research on large polycyclic heteroaromatics gained new impetus with the discovery of graphene and the prospect of its application in molecular electronics. The incorporation of a heteroatom increases the three-dimensional inter/intramolecular interactions. Modifying the topology and heteroatom content of the π-conjugated system can tune the key features of the electronic structure, including the band gap, optical absorption spectra, photoluminescence, redox behaviour, and solubility very flexibly. As a result, many families of PHAs are attractive objects of photophysical investigations and have been explored as NIR-active dyes,[8a] two-photon absorbers,[8b] and fluorescence sensors. The presence of heteroatoms facilitates the design of stable π-aromatic cations,[8c] high-spin organic molecules.[8d] By judicious choice of ring fusion, heteroatom doping, and substitution, PHAs can be tailored into **organic semiconductors (OSCs)** such as organic field-effect transistors (OLEDs)[9a] and organic light-emitting diodes (OFETs).[9b] Photovoltaic applications of PHAs encompass both bulk-heterojunction (BHJ) and dye-sensitized (DS) solar cells.[9c] A few examples are displayed in Figure 1.6.9. Macrocyclic heteroaromatic systems are also very useful for OLED making.[24b-d]

1.2. Synthetic Methodologies of Polyheteroaromatic Compounds (PHAs)

PHAs have penetrated nearly every field of chemistry for their immense significance. Chemists have, over time, devised numerous synthetic methods tailored to different types of PHAs based on specific needs. However, there is no standardized approach that precisely regulates synthetic achievements. The successful synthesis of new PHA compounds, with practical applications in mind, is a testament to chemists' relentless hard work and efforts.

In the subsequent section of this review (**Section 1.2**), we will delve into the commonly employed methods of organic synthesis that have facilitated the realization of diverse PHAs.

1.2a. A General Synthetic Approach towards PHAs

The primary challenge in the synthetic chemistry of PHAs revolves around the necessity to devise effective annulation strategies. Given the structural diversity of PHA systems and the intricate nature of existing ring fusion patterns, various synthetic approaches have arisen. These approaches are often applicable, albeit in a somewhat restricted manner, to specific classes of compounds. The fundamental operations for forming rings can be broadly categorized as *ortho*- and *peri*-annulations. *Ortho*-annulations typically result in lateral or peripheral extensions of the pre-existing fused framework. However, mainstream annulation strategies for creating heteroatom-containing fused π-systems generally adhere to four fundamental protocols, as depicted in **Figure 1.7**.

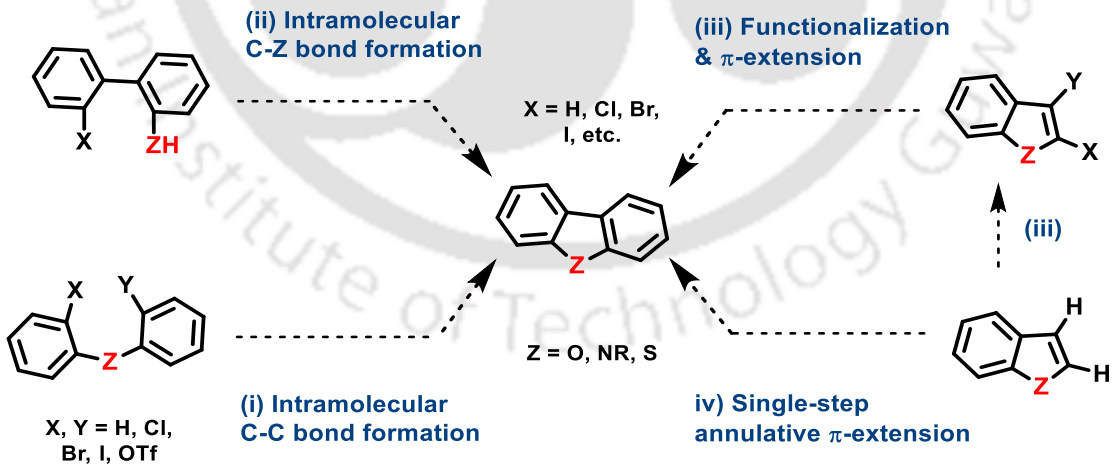

Figure 1.7. Traditional synthetic protocols of PHAs.

These protocols include: (**i**) intramolecular carbon−carbon bond formation of diaryl hetero ethers, (**ii**) intramolecular carbon−heteroatom bond formation of biaryl alcohols, amines, and sulfides, (**iii**) stepwise functionalization and π-extension of heteroarenes, and (**iv**) single-step annulation π-extension (APEX) of unfunctionalized heteroarenes.[10a,b]

Multi-Step Synthesis of PHAs

Although annulative π-extension (APEX) of unfunctionalized heteroarenes is a single-step process, the above-mentioned synthetic methods (**i**), (**ii**), and (**iii**) mostly rely on stepwise reaction for the synthesis of π-extended fused heteroaromatics. A stepwise preparation is widely adopted as a general and conventional synthetic strategy to obtain PHAs[11c,d] (**Scheme 1.1**). These multistep protocols are composed of three elementary steps:

- **(a)** prefunctionalization such as halogenation, metalation, and/or the introduction of the heteroatom for the unfunctionalized aromatics;
- **(b)** component assembly between functionalized aromatics by intermolecular CAr–heteroatom (CAr–Z) or CAr–CAr bond formation to afford polyarylated precursors;
- **(c)** a final "stitching-up" cyclization via intramolecular CAr–CAr or CAr–Z bond formation to craft PHAs.

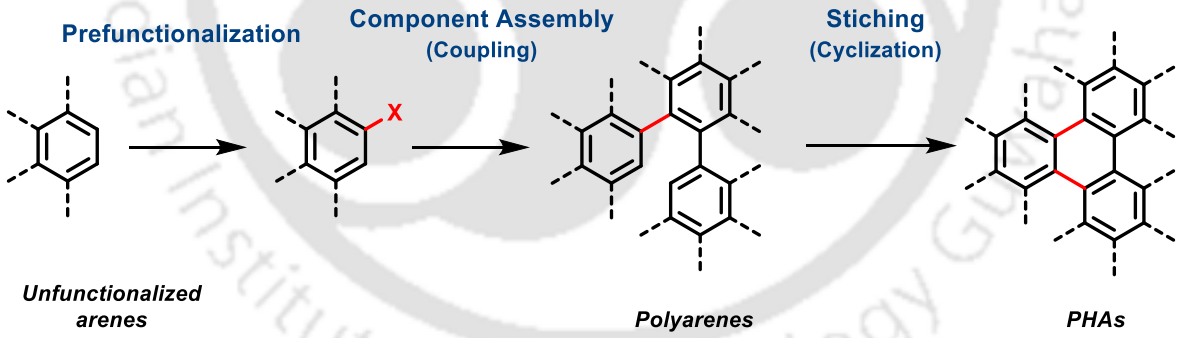

Scheme 1.1. Classical strategy towards multi-step synthesis of PHAs.

These strategies are employed judiciously for the advancement of the PHAs using a variety of synthetic tools, which are metal-promoted homocoupling, inter- and intramolecular cross-coupling reactions, Diels−Alder reactions, ring-closing metathesis, alkyne cyclizations, photocyclizations and so on. These methodologies are explained very briefly, and suitable examples of the synthesis of polyheteroaromatics are provided throughout this section.

1.2b. Annulative π-Extension (APEX)

The concept of annulative π-extension (APEX) involves the direct C−H arylation of unfunctionalized arenes or heteroarenes, simultaneously forming one or more fused aromatic rings. APEX applied to straightforward aromatic substrates through C−H activation is an efficient synthetic shortcut for synthesising polycyclic aromatic hydrocarbons (PAHs) and PHAs, employing a π-extending agent (**Figure 1.2a**). This approach offers advantages over traditional synthetic methods regarding step-economy and the ability to fine-tune the structure and properties at later stages.[10,11]

In the year 2017, Ozaki *et al.* documented APEX reactions involving heteroarene templates like thiophenes, benzofuran, and *N*-tosylindole using a palladium catalyst, silver salts, and *o*-chloranil (**Scheme 1.2b**).[11a] The inclusion of π-extending agents such as dimethyldibenzosilole and dimethyldibenzogermole, in combination with silver hexafluorophosphate or silver triflate, facilitated the one-step synthesis of a diverse range of π-extended fused heteroarenes. This methodology presents clear advantages over existing stepwise π-extension methods, emphasizing improvements in step- and atom economy.

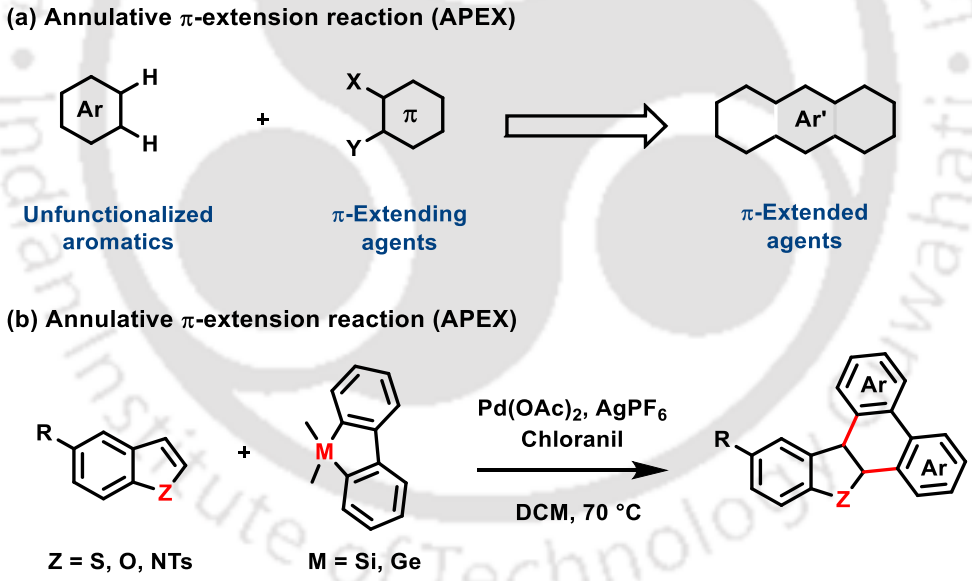

Scheme 1.2. Annulative π-extension (APEX) reactions.

On the other hand, hetero-APEX reactions can directly construct one or more fused heteroaromatic structures, including hexagonal and non-hexagonal rings, using heteroatom-embedded-π-extending agents (**Scheme 1.3a**). For instance, by performing hetero-APEX reactions with π-extending agents embedded with nitrogen, oxygen, sulfur, boron, or phosphorus atoms, the construction of new pyridine, pyrrole, pyrylium, furan, thiopyrylium, thiophene, borole, phosphabenzene, and phosphole rings will be realized.

These reactions can be defined as aza-APEX, oxa-APEX, thia-APEX, bora-APEX, and phospha-APEX, respectively.[11c]

In 2005, Musgrave and colleagues published findings on an oxa-APEX reaction that produced polycyclic furan from either veratrole or anisole and 9,10-phenanthrenequinone at 180 °C without solvent and in the presence of a catalytic amount of $SnCl_4 \cdot 5H_2O$ (**Scheme 1.3b**).[11b] The reaction involved electron-rich arenes attacking one of the carbonyls in the electron-deficient 1,2-diketone. This process led to the formation of a Friedel–Crafts-type reaction intermediate. Subsequently, a quinomethane structure was generated through the elimination of H_2O. The ensuing steps in the reaction sequence included the elimination of H_2O, oxy-cyclization, and aromatization, ultimately forming

the targeted polycyclic furan compound.

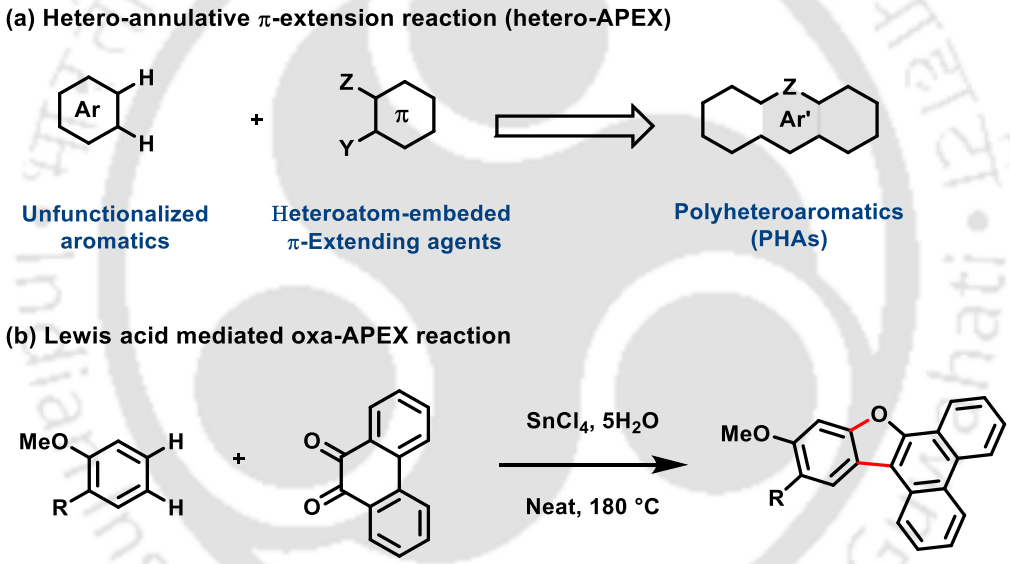

Scheme 1.3. Hetero-annulative π-extension (hetero-APEX) reactions.

1.2c. π-Extended Decarboxylative Annulation (PEDA)

The π-extended decarboxylative annulation (PEDA) represents an enhanced evolution of the one-step annulation approach for π-extension (APEX). In 2019, Zhang *et al*. pioneered the Pd (II)-catalyzed synthesis of phenanthridines or benzocarbazoles from indole-2-carboxylic acids, utilizing cyclic diaryliodonium salts as a π-extension agent.[12a] The carboxylic acid functionality serves dual purposes, acting as both a traceless directing group for *ortho* C−N or C−C coupling and a reactive group for the cascade annulation in a highly step-economic manner (**Scheme 1.4**).

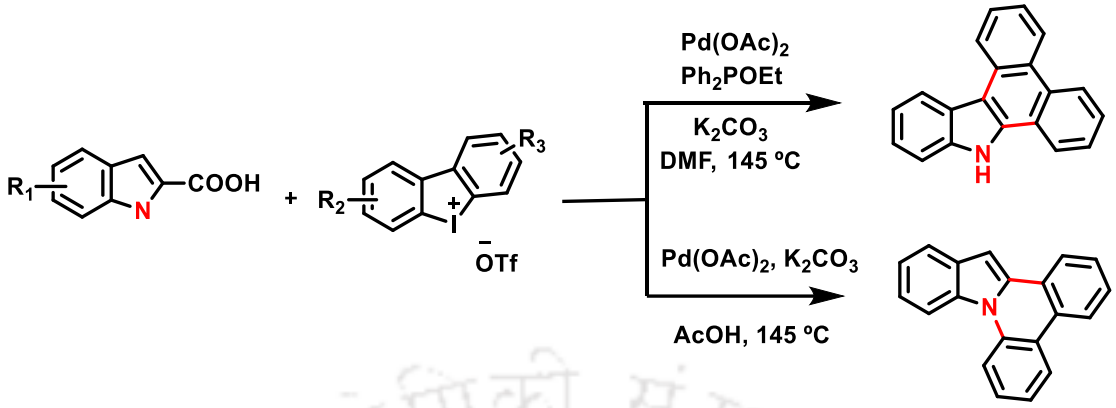

Scheme 1.4. Example of a π-extended decarboxylative annulation (PEDA) reaction.

In 2020, Hu *et al.* presented a new approach for the synthesis of diverse functionalized tribenzo[b,d,f]azepines using readily available 2-aminobenzoic acids and cyclic hypervalent diaryliodonium reagents as starting materials under Pd(II) catalysis.[12b] In this study, they also utilized the carboxylic acid functionality both as a traceless directing group for N−H activation/arylation and as a functional handle for tandem π-extended decarboxylative annulation. This underscores the potential of π-extended decarboxylative annulation in advancing the step-economical synthesis of various types of polycyclic heteroaromatic compounds.

Therefore, the future of π-extended decarboxylative annulation holds significant promise in advancing the step-economical synthesis of diverse polycyclic heteroaromatic compounds.

1.2d. Cross-Coupling Reactions

In organic synthesis, a cross-coupling reaction takes place by combining two fragments with the assistance of metal catalysts, predominantly Cu, Pd, Ni, or Fe catalysts.[13] These reactions are employed for the creation of carbon-carbon bonds, as well as carbon-heteroatom bonds.

Carbon-carbon (C-C) bond-forming well-known coupling reactions are Suzuki reaction (organoborane & R-X),[13c] Sonogashira coupling (ArC≡CH & R-X),[13d] Heck reaction (alkene & Ar-X),[13e] Negishi coupling (R-Zn-X & R-X),[13f] Kumada Coupling (RMgBr & R-X),[13g] Cross dehydrogenative coupling (**CDC**, R-H & R'-H)[13h] etc. **Carbon-heteroatom (C-X)** bond forming cross-couplings are the Buchwald–Hartwig reaction [13i] and Ullmann reaction.[13j]

The versatility of cross-coupling reactions is evident in their widespread applications in efficient organic synthesis. Nevertheless, when it comes to the multi-step synthesis of polycyclic heteroatomic compounds, the participation of cross-coupling reactions is nearly unavoidable, often playing a crucial role in at least one step of the process.

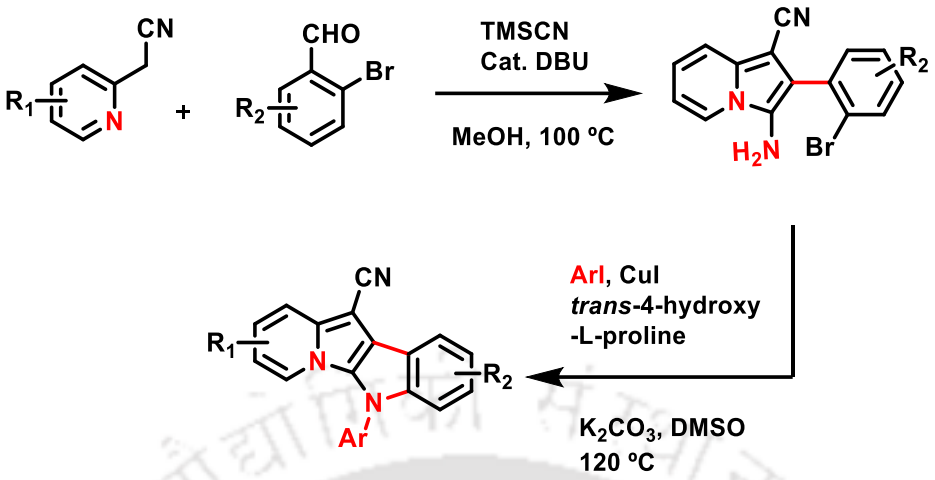

Scheme 1.5. Cu-catalyzed Ullmann-type double C−N coupling approach.

Nam *et al.* presented a method for the synthesis of a polyfunctionalized 5H-indolizino[3,2-b]indole, an indolizine−indole fused system, in a two-step procedure outlined in **Scheme 1.5**. Initially, they produced the precursor through a one-pot three-component reaction using readily available pyridine-2-acetonitrile, 2-bromobenzaldehyde, and TMSCN. Subsequently, a Cu-catalyzed Ullmann-type double C−N coupling reaction was employed to annulate the precursor, forming tetracyclic heteroaromatics. This process involves the creation of five new bonds (two C−C and three C−N) within two steps.[14a]

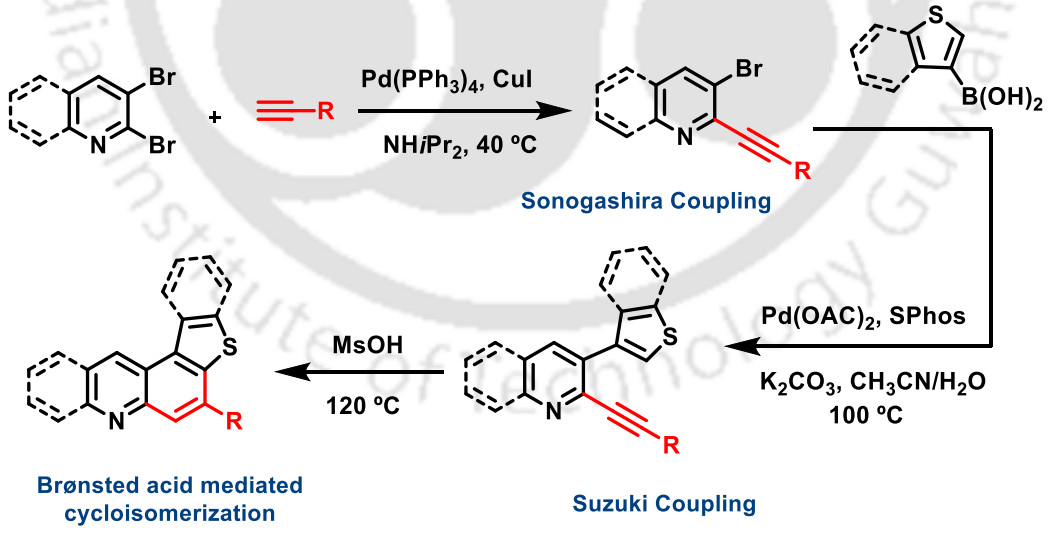

Scheme 1.6. Brønsted acid-mediated cycloisomerization reaction.

In 2020, Ponce *et al.* synthesized several thieno[2,3-*h*]-/[3,2-h]- and [2,3-f]quinolines from 2,3-dihalogenated pyridines or -quinolines following the classical methods of multi-step PHA synthesis as

shown in **Scheme 1.1**. First, the bromo functionality of the aryne-substituted fused pyridine derivatives is utilized to assemble the precursor using a Suzuki cross-coupling reaction. Then, the thiophene and pyridine-containing fused PHA are formed after Brønsted acid-mediated cyclooligomerizations as the final key step (**Scheme 1.6**).[14b]

1.2e. Palladium-Catalyzed Intramolecular Annulations

Activating C(sp2)-H bonds of aromatic compounds provides access to key scaffolds of natural products, drugs, and materials. Numerous practical methods for forming C-C, C-N, and C-O bonds through direct CH activation have been developed using transition-metal catalysis. Over the years, Pd-catalyzed intramolecular annulation strategies mainly based on C-H activation have played a leading role in the synthetic field of polyheteroaromatics.[15a-c] The direct intramolecular aromatic coupling reactions involving C-H bond cleavage are mostly done in three ways: (a) C-H/C-X coupling, (b) C-H/C-H coupling, and (c) C-H/E-H coupling (E = O, NR, S etc.). Of these, the C-H/C-H coupling reactions, as illustrated in **Scheme 1.7**.[14c]

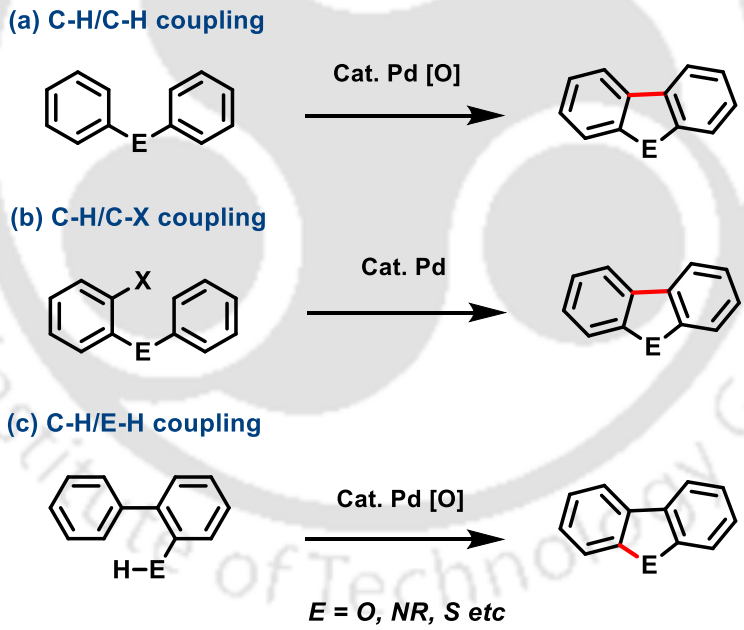

Scheme 1.7. Palladium-catalyzed intramolecular C-H/C-H biaryl coupling reactions.

Among these, the **C-H/C-H coupling reactions** (**Scheme 1.7a**) have been extensively studied for the versatile synthesis of polycyclic systems, both PAHs and PHAs.[15c-e] This type of reaction is considered to proceed via double C-H bond cleavages by Pd (II) species to provide the key six-membered palladacycle intermediates and successive reductive elimination leading to the desired products.

Jones *et al*. reported phenyl carbazole's strained oxidative dehydrogenative cyclization, which delivered the product indolo[3.2.1-*jk*]carbazole via the Pd-catalysed double C-H activation step (**Scheme 1.8**).[15d]

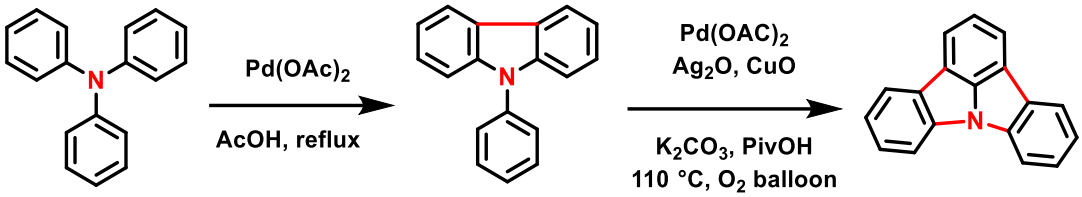

Scheme 1.8. Example of a Pd-catalyzed intramolecular C-H/C-H biaryl coupling.

In the next example, an efficient synthetic method for the preparation of heterocyclic analogues of rubicene was reported by Wudl *et al*. under the Pd-catalyzed C-H arylation (**Scheme 1.9**) following the **C-H/C-X coupling reaction** as illustrated in **Scheme 1.7b**.[15g]

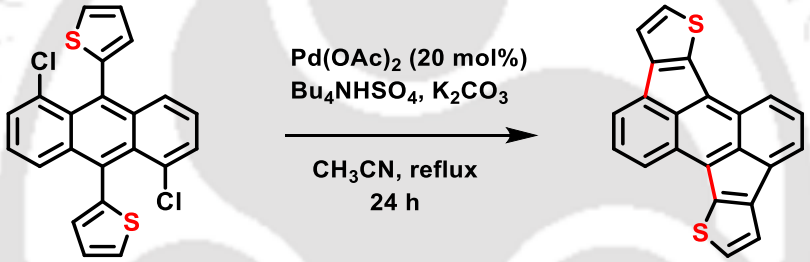

Scheme 1.9. Example of a Pd-catalyzed intramolecular C-X/C-H biaryl coupling.

The double CH activation method presents a powerful, attractive, and economical strategy for forming C-C biaryl bonds. However, prevailing methodologies frequently encounter challenges associated with selectivity in synthesizing substituted biaryls.

Numerous directing groups, including carbonyl-based and nitrogen-containing groups, have been employed to address this challenge effectively. Samanta *et al*. have introduced a highly efficient double CH activation mechanism guided by the sulfoxide group **(Scheme 1.10)**. This technique has been successfully employed to directly synthesize dibenzothiophenes from simple benzyl phenyl sulfoxides through the **C-H/E-H coupling reaction**, as illustrated in **Scheme 1.7c**.[15h]

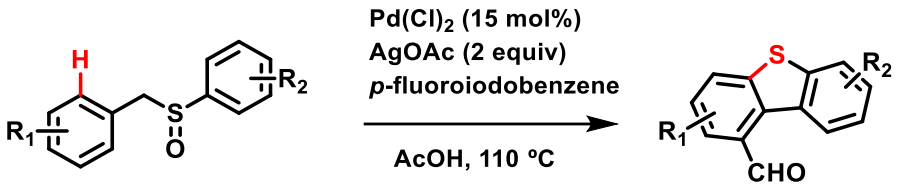

Scheme 1.10. Example of a Pd-catalyzed intramolecular C-H/C-E biaryl coupling.

1.2f. Scholl Reaction

The Scholl reaction is named after Roland Scholl (1865−1945),[16] Swiss chemist, for his pioneering work on the synthesis of polycyclic aromatic compounds in 1910 through cyclodehydrogenation under an acidic condition (**Scheme 1.11**). The Scholl reaction might be considered an example of C−H bond activation long before the term became popular.

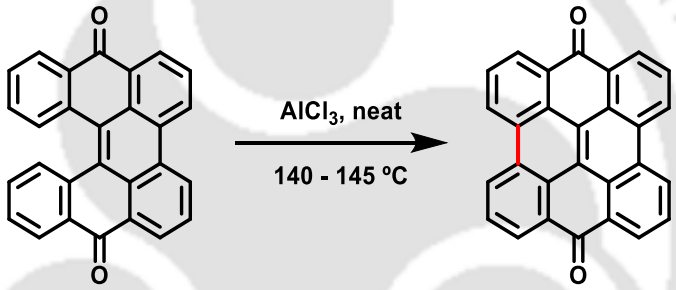

Scheme 1.11. First example of Scholl reaction.

This intramolecular dehydrocyclization reaction facilitates oxidative aryl-aryl coupling without the need for prior functionalization of the aryl groups. In the Scholl reaction, a robust acid (either a Lewis acid or Brønsted acid) and an oxidant are essential for mediating oxidative coupling between aryl groups, and a single reagent can perform both roles. An exemplary instance of such dual-role reagents is $FeCl_3$. Notably, this process differs distinctly from the dehydrogenative cross-coupling of arenes catalyzed by transition metals (such as palladium and rhodium), as the carbon-carbon bond formation in the Scholl reaction does not occur through reductive elimination on a transition metal center.

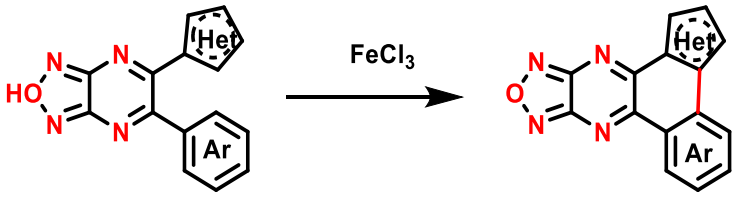

Scheme 1.12. Scholl reaction towards PHA synthesis.

Verbitskiy *et al.* reported the synthesis of [1,2,5]oxadiazolo[3,4-*b*]pyrazine scaffold, polyheteroaromatics with multiple heteroatoms *via* the $FeCl_3$-mediated intramolecular Scholl cross-coupling reaction (**Scheme 1.12**).[16b]

Besides $AlCl_3$–$CuCl_2$, $AlCl_3$–$Cu(OTf)_2$ and $FeCl_3$, reagents commonly employed in Scholl reactions include $MoCl_5$, phenyliodinebis (trifluoroacetate) (PIFA)-borontrifluoride etherate ($BF_3{\cdot}OEt_2$), VOF_3 (with $BF_3{\cdot}OEt_2$ or CF_3CO_2H), and cerium (IV) ammoniumnitrate(CAN). Nevertheless, the Scholl reaction holds substantial potential to become a potent methodology for synthesizing polycyclic heteroaromatics characterized by considerable steric hindrance or significant strain.

1.2g. Diels-Alder Reaction

The Diels–Alder (DA) reaction is arguably the most used of the pericyclic reactions. Hence, it is a powerful method for constructing six-membered cyclic systems in one stage for synthesizing both linear and angular polycyclic heteroaromatics. It can be classified as the intramolecular Diels-Alder reaction (IMDA) and intermolecular Diels-Alder reaction. The applications of these reactions in the synthesis of polycyclic aromatic systems are highlighted in a few review articles.[17a]

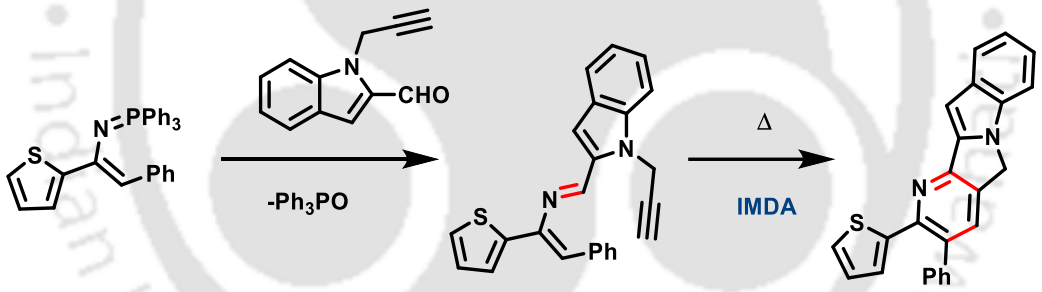

Scheme 1.13. Intramolecular Diels-Alder reaction towards PHA synthesis.

A careful execution of an intramolecular aza-Diels-Alder reaction of *N*-vinylic phosphazenes successfully provided structurally complex 5H,6H-indeno[2,1-a]indole as shown in **Scheme 1.13**.[18a]

In 2008, Yao *et al.* reported the sulfur-hetero oligoarenes based on the benzo[*k*]fluoranthene (**Scheme 1.14**) as the active materials for thin film organic field-effect transistors. The intramolecular Diels-Alder reaction between cyclopentadienone and 2,2′-(ethyne-1,2-diyl)bisthiophene followed by decarbonylation afforded fluoranthene derivative. After bromination and subsequent substitution through the Suzuki coupling reaction, the $FeCl_3$-oxidative cyclization produced sulfur-hetero benzo[*k*]fluoranthene derivatives.[18b]

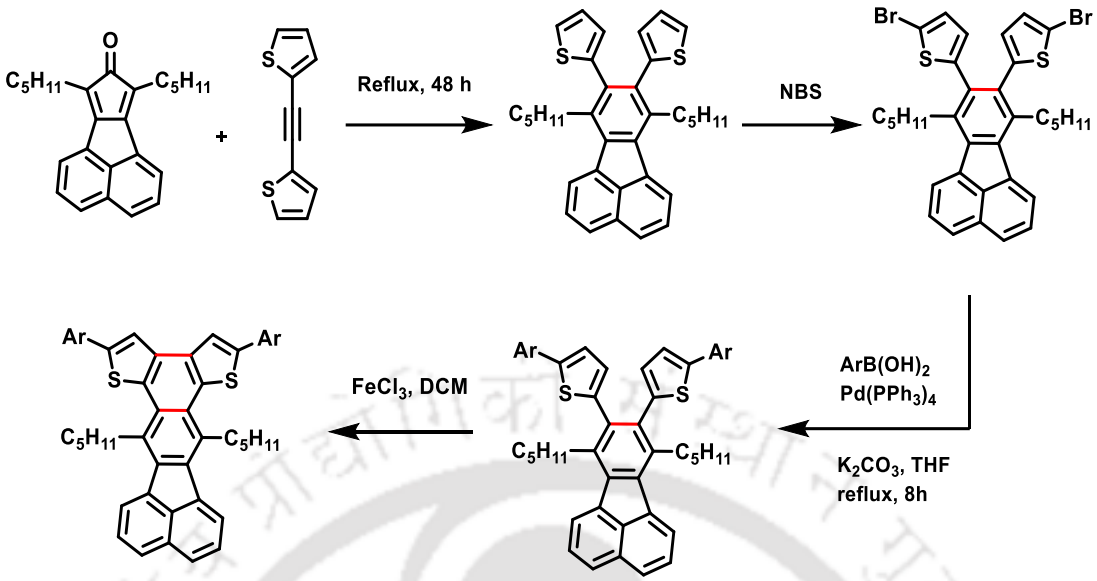

Scheme 1.14. Intermolecular Diels-Alder reaction towards PHA synthesis.

Within this class, there are other subclasses such as several subclasses: normal-, neutral- and inverse-electron-demand-, hetero-, and retro-Diels–Alder reactions which are very useful strategies for the multistep synthesis of structurally complex polyheteroaromatics.[18c]

1.2h. Mallory Reaction

The Mallory reaction involves the 6π-electronic photocyclization of the substrate followed by oxidation (formally $-H_2$) or elimination. Synthetically, the reaction forms a C−C bond between two aromatic moieties of diarylethene to give phenanthrene-type molecules. Since its discovery in 1956, this reaction has become a powerful tool for constructing complex polycyclic molecules (coronenes, helicenes, etc.) using transition-metal- and oxidant-free annulation. A simple representative example is shown in **Scheme 1.15**.[19]

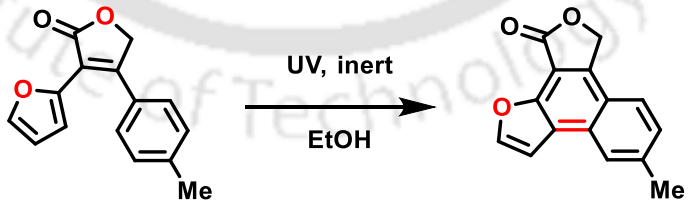

Scheme 1.15. Mallory reaction towards PHA synthesis.

1.2i. Friedel–Crafts/Bradsher Cyclization

The combination of Fridel Craft alkylation and Bradsher reaction is another very efficient method for forming various polycyclic heteroaromatics. In 2017, Bodzioch *et al*. summarized the utility of Friedel–Crafts/Bradsher cyclization in PHA synthesis in a review article. Initially, the Fridel Craft reaction helps to assemble two arene moiety. Next, the Bradsher cyclization helps in the annulation process by forming a C-C bond.

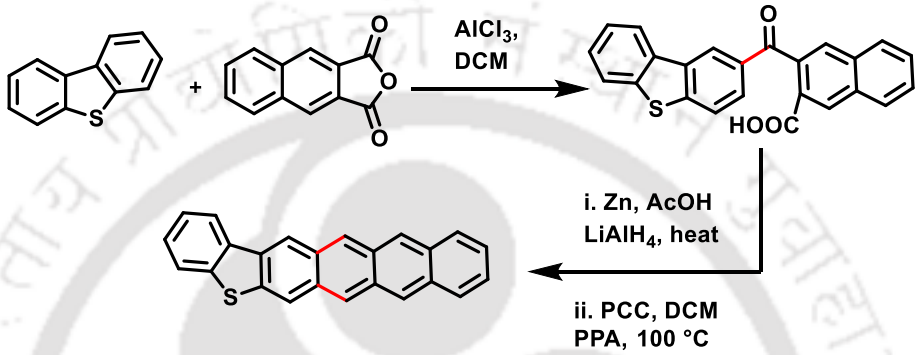

Scheme 1.16. Friedel–Crafts/Bradsher cyclization towards PHA synthesis.

For example, tetraceno[2,3-b][1]benzothiophene, a heteroacene with six fused rings, has been synthesized by the Friedel–Crafts/Bradsher aromatic cyclization of dibenzothiophene with naphtho[2,3-*c*]furan-1,3-dione as shown in **Scheme 1.16**. [20]

1.2j. Ring Closing Metathesis Reaction

Olefin metathesis is a simple but powerful C–C double bond formation tool. However, among various olefin metathesis, the ring-closing metathesis reaction (RCM) is another key catalytic step for the construction of polyheteroaromatics.[21] It provides an easy way to generate complex structures with a high atom economy that would normally take more time and resources using classical methods. Different ring-closing metathesis reactions consist of a [2+2] cycloaddition followed by a [2+2] cycloreversion between the olefin reactants on a metal catalyst. The other analogues of ring-closing olefin metathesis processes are alkyne-alkyne metathesis and alkyne-carbonyl metathesis, as shown in **Scheme 1.17**.

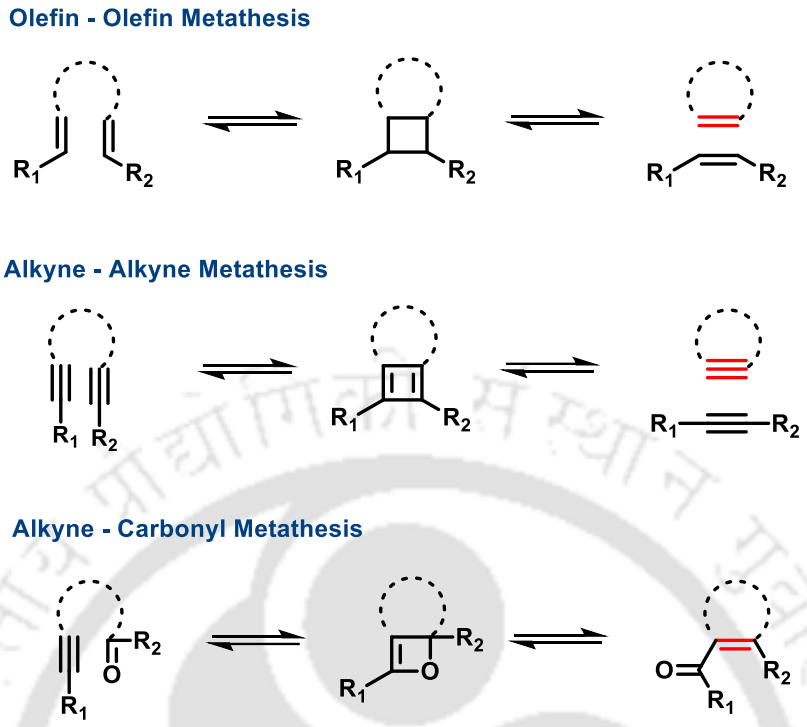

Scheme 1.17. Different types of ring closing metathesis (RCM) reactions.

In 2021, Ponce *et al*. introduced a novel method for the synthesis of pyrrolo[1,2-*a*][1,6]naphthyridines and pyrrolo[1,2-*a*][1,8]naphthyridines through Brønsted acid-mediated intramolecular alkyne-carbonyl metathesis (ACM) reactions.[21c] The initial step involved preparing the ethynyl pyrrolopyridine precursor from 3-bromopyridin-4-amine through a multi-step process (**Scheme 1.18**). Subsequently, the precursor underwent a one-pot two-step reaction, starting with electrophilic acylation, followed by an alkyne-carbonyl metathesis reaction serving as the final cyclization step to yield the tricyclic heteroaromatic compounds.

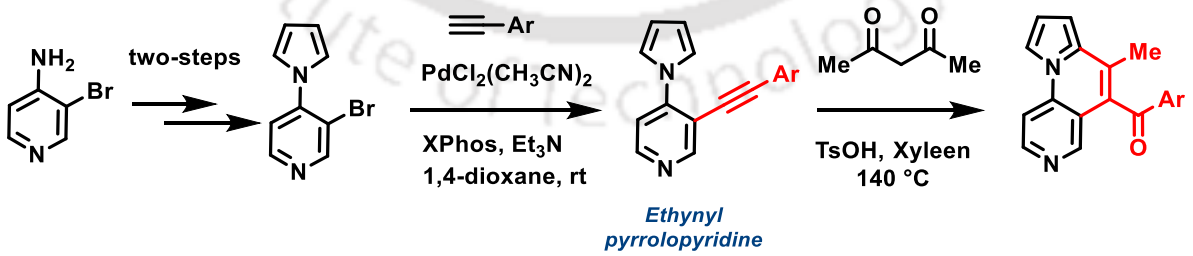

Scheme 1.18. Alkyl carbonyl metathesis towards PHA synthesis.

1.2k. Domino/Tandem/Cascade Reaction

A cascade reaction involves at least two consecutive reactions conducted in a single reaction vessel. In this scenario, each subsequent reaction takes place solely due to the chemical functionality formed in the preceding step, eliminating the necessity for isolating intermediates.[22] It is also known as a **domino reaction** or **tandem reaction**. While cascade reactions often consist of intramolecular transformations, they can also occur intermolecularly, classifying them as multicomponent reactions.

Domino reactions are efficient in constructing structurally complex polyheteroaromatics (PHAs) due to several inherent advantages over multistep syntheses, including bond-forming efficiency, time and cost-effectiveness, atom economy, and environmental friendliness.[22b-d]

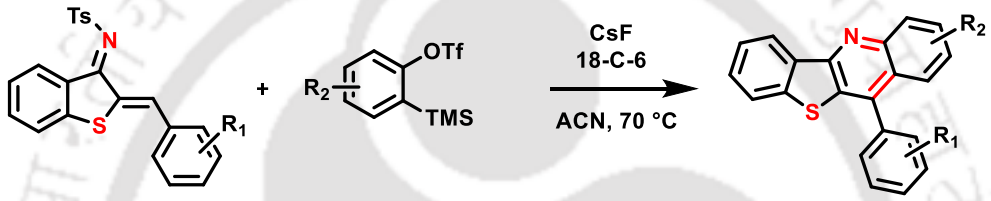

Scheme 1.19. Controllable domino reaction towards PHA synthesis.

In the previous year, Wang *et al.* disclosed a regioselective domino reaction for synthesizing benzothiophene, incorporating a range of polyheteroaromatics (PHAs) with sulfur and nitrogen heteroatoms, as illustrated in **Scheme 1.19**.[22d] This transition metal-free, base-promoted process involves the [4+2] cycloaddition reaction of azadiene and in situ generated aryne. The outcome is the formation of polycyclic heteroaromatics through the establishment of C-C and C-N bonds in a regioselective manner.

1.2l. Multicomponent Reaction

Multicomponent reactions (MCRs)[23] have acquired enormous importance in organic synthesis because structurally complex molecules and unexplored scaffolds can be synthesized in a single operation in a high atom-economic and step-economical manner. It has huge contributions to the synthesis of heterocycles. However, this strategy can be employed to obtain polycyclic heteroaromatics in a one-step and greener way conveniently.[23b]

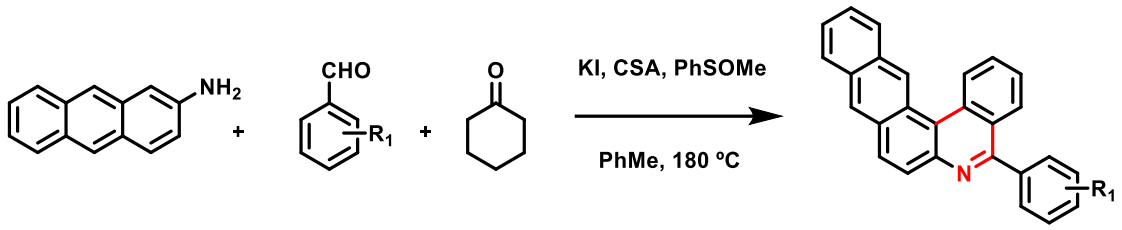

Scheme 1.20. Multicomponent reaction in the synthesis of small PHAs.

Synthesis of benzo[α]phenanthridines from aromatic aldehydes, cyclohexanones, and aromatic amines has been achieved in one step by employing the multicomponent reaction. This reaction is mediated by KI/DMSO/camphorsulfonic acid to afford a variety of functionalized benzo[α]phenanthridines in satisfactory yields, avoiding the hectic multi-step process (**Scheme 1.20**).[23c]

1.2m. Synthetic Strategies Encompassing *macro*-Annulations

Cyclic molecules containing more than 12 covalent connected atoms are called macrocycles. More than 100 drugs are approved or in clinical development, which involve macrocyclic scaffolds as the bioactive component.[24a] However, aromatic hydrocarbon macrocycles doped with have drawn the scientific community's attention due to their significant electroluminescence properties.[24b-d]

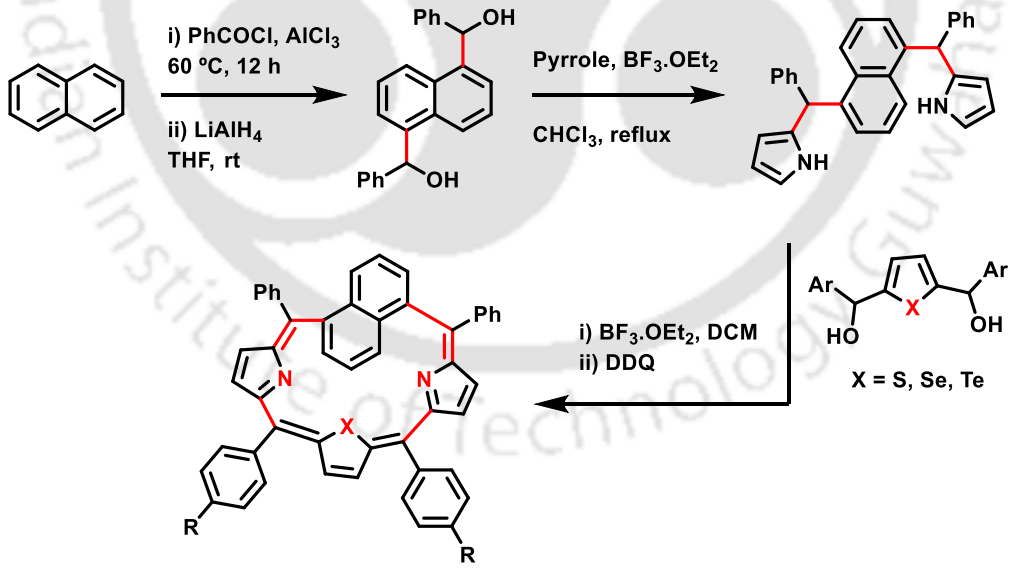

Scheme 1.21. Macrocyclization reaction for the synthesis of macrocyclic heteroaromatic compounds.

For example, Porphyrinoids in which one or two pyrrole rings are replaced with heterocycles such as naphthalene, phenanthrene, biphenyl, bipyridine, phenanthroline, etc. are a new class of polycyclic heteroaromatics containing macrocyclic structure.[24d] These types of compounds are achieved through macrocyclization reactions or macro-annulations.

Latos-Grażyński and colleagues reported the synthesis of the 1,5-naphthalene subunit incorporated heteroporphyrins, 22-hetero-1,5-naphthiporphryins, as outlined in **Scheme 1.21**. The naphthalene underwent benzoylation through Friedel-Crafts conditions, followed by reduction with $LiAlH_4$ to yield 1,5-bis(phenylhydroxymethyl)naphthalene. Subsequently, this compound was subjected to an excess of pyrrole in the presence of a catalytic amount of $BF_3.OEt_2$, resulting in tripyrrane, identified as 1,5-bis(phenyl(2-pyrrolyl)-methyl)naphthalene. In the subsequent step, the tripyrrane was condensed with 2,5-bis(arylhydroxymethyl)heteroles, employing a catalytic amount of $BF_3.OEt_2$, followed by aerobic oxidation with DDQ to produce the final macrocyclic heteroaromatic compound.

Spotlight on Selected PHA Compounds for the Thesis Work

Polyheteroaromatics (PHAs) exhibit a remarkable lack of confinement regarding structural diversity and practical applications. Structurally, PHAs can manifest as two-membered to multi-membered rings featuring linear, angular, fused, or macrocyclic configurations. Furthermore, they can be fused from two-dimensional to three-dimensional structures by incorporating electron-rich and electron-deficient heteroatoms in various permutations and combinations. Consequently, categorizing polyheteroaromatics based on their structure becomes an intricate challenge.

Following an extensive review of the literature on polyheteroaromatics (PHAs), this thesis focuses on the synthetic exploration of chromeno[4,3,2-*gh*]phenanthridine, benzophenanthridine, and fused quinolines. **Sections 1.3 to 1.6** provide a brief introduction to the significance of these compounds, along with a few synthetic explorations, leading to the objectives of the thesis.

1.3. A Short Introduction to Chromeno[4,3,2-*gh*]phenanthridine

1.3a. Importance of Chromeno[4,3,2-*gh*]phenanthridine

Advancements in natural product chemistry, particularly the discovery of pyridoacridine alkaloids, have significantly propelled research on PHAs. In 1983, two research groups, led by Schmitz and Shoolery, elucidated the structure of amphimedine, marking the first marine-derived alkaloid. Pyridoacridine is the fundamental framework for the predominantly marine-derived alkaloids found in sponges, ascidians, anemones, and tunicates, collectively called "pyridoacridines." These alkaloids exhibit notable cytotoxicity, and various compounds also demonstrate specific biological properties such as the inhibition of topoisomerase II, anti-HIV activity, Ca2+ release activity, metal chelating properties, and intercalation of DNA.[25]

Chromeno[4,3,2-*gh*]phenanthridine (I), a diheteraphenalenoid compound resembles with pyridoacridine alkaloids.[26] Methyl salt of chromeno[4,3,2-*gh*]phenanthridine (I) has also shown efficient antiproliferative activity and thereby can be used for cancer treatment. Many PHA systems, such as compounds **II** and **III** (**Figure 1.8**) containing this skeleton, also show remarkable optoelectronic properties such as lower HOMO-LUMO band gap, significant solvatochromism, higher quantum yield, red-shifted absorption and emission capacity. Hence, these compounds can be exploited in material science and the fabrication of organic devices.[27a-d]

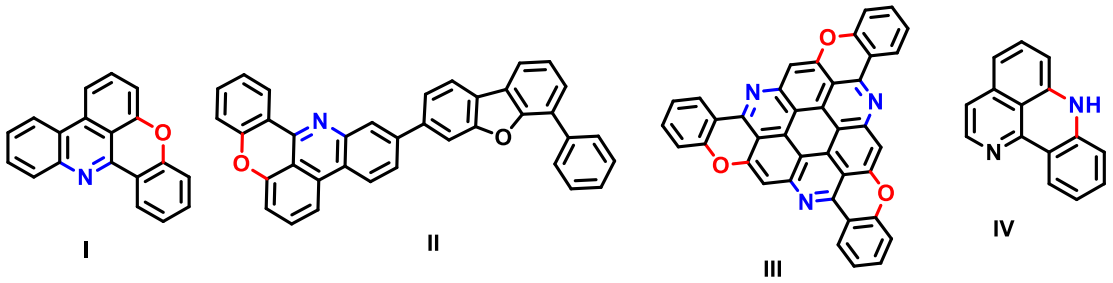

Figure 1.8. Some examples of chromeno[4,3,2-*gh*]phenanthridine containing polyheteroaromatics.

1.3b. Synthesis of Chromeno[4,3,2-*gh*]phenanthridine Derivatives

Despite having a scope of application in various scientific fields, chromeno[4,3,2-gh]phenanthridine derivatives are much less explored. A handful of syntheses of pentacyclic chromeno[4,3,2-gh]phenanthridine derivatives have been reported.

Stevens and coworkers recently synthesized 7H-pyrido[4,3,2-kfl]acridines by the Graebe-Ulmann thermolysis of triazole derivatives or via its photolysis in acetonitrile (**Scheme 1.22**). These Acridines are structurally similar to pentacyclic aza-aromatic alkaloids isolated from marine organisms. However, chromeno[4,3,2-*gh*]phenanthridine was isolated as a by-product of the coupling reaction between benzotriazole, xanthene and DDQ in refluxing toluene.[28a]

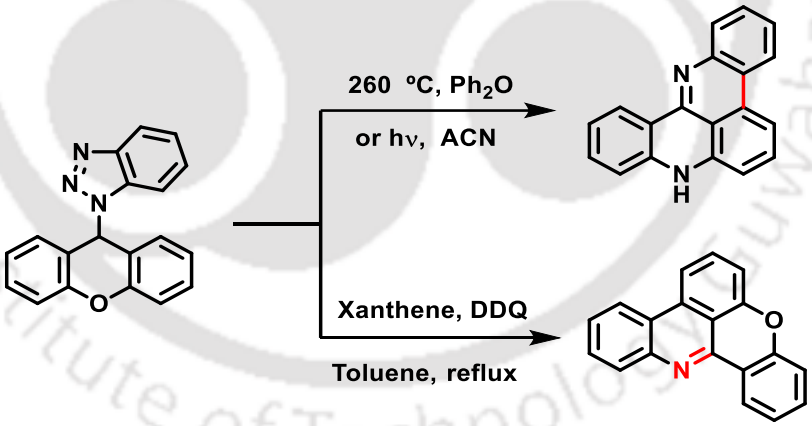

Scheme 1.22. Reaction of triazole derivative towards the synthesis of chromeno[4,3,2-*gh*]phenanthridine.

In 2003, Kristensen *et al.* reported an anionic cascade ring closure reaction to synthesize chromeno[4,3,2-*gh*]phenanthridine. Initially, Suzuki-Miyaura cross-coupling of commercially available 2-chloro-6-fluorobenzonitrile with 2-fluoroarylboronic ester gave the biaryl compound. Subsequent regioselective nucleophilic aromatic substitution of the fluorine group, ortho to the activating cyano group, by the aryl

bromide provides a triaryl compound. Next, bromine-lithium exchange using *tert*-butyllithium initiates the cascade process to accomplish chromeno[4,3,2-*gh*]phenanthridine (**Scheme 1.23**).[28b]

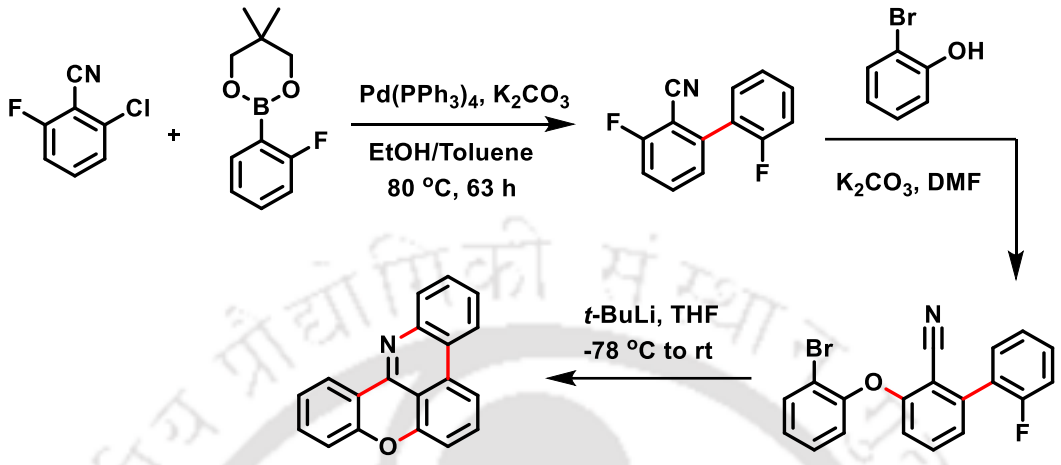

Scheme 1.23. Synthesis of chromeno[4,3,2-*gh*]phenanthridine via anionic cascade ring closure reaction.

In 2018, Elbert *et al*. used the Pictet–Spengler reaction in the syntheses of chromeno[4,3,2-*gh*] phenanthridine-containing polycyclic compounds to study their optoelectronic properties. Initially, biaryl amine was synthesized from the Suzuki cross-coupling reaction of *o*-bromoaniline and the boronic acid, which was subjected to Pictet-Spengler condensation with the biaryl amine and 3,5-di-tert-butyl-2-hydroxybenzaldehyde to deliver the phenanthridine phenol derivative. This, again, after condensation at 180 ºC, produces the final pentacyclic compound 9,11-di-*tert*-butyl-6-methoxychromeno[4,3,2-*gh*]phenanthridine (**Scheme 1.24**).[28c]

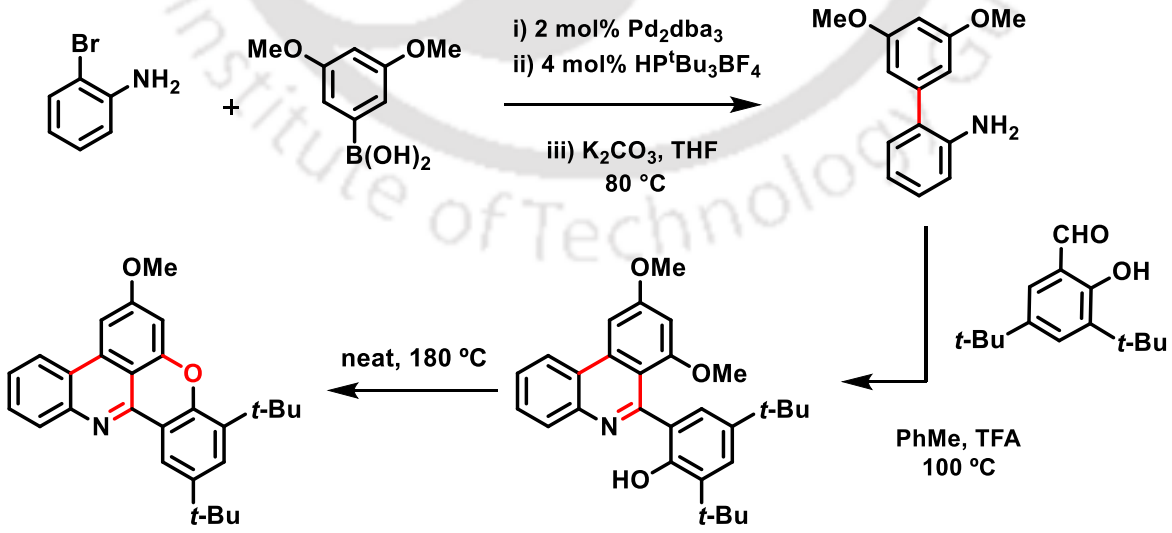

Scheme 1.24. Pictet–Spengler synthesis of chromeno[4,3,2-*gh*]phenanthridine derivatives.

1.4. A Short Introduction to Benzophenanthridines

1.4a Importance of Benzophenanthridine Derivatives

Benzophenanthridine alkaloids belong to the benzyl isoquinoline alkaloid family and are predominantly found in the Papaveraceae and Rutaceae plant families. Shang *et al.* conducted phytochemical and pharmacological investigations on Tibetan medicinal plants of Corydalis and Papaveraceae, revealing several benzophenanthridine alkaloids in 2014.[30a] Additionally, Krane et al. provided a summary of studies on isolated benzophenanthridine alkaloids and their spectral data spanning from the first half of the 19th century to 1984.[30b] Few of them are shown in **Figure 1.9**. With advancements in isolation and identification techniques, over 100 benzophenanthridine alkaloids have been reported. These compounds are gaining considerable attention due to their significant biological activities, including anti-bacterial, anti-fungal, anti-viral, anti-cancer, analgesic, anti-inflammatory, anthelminthic, and more.[30,31] In 2016, Han *et al.* highlighted the immense importance of their biological activities in a review article.[30c] Compounds such as sanguinarine, chelerythrine, and fagaronine exhibit significant potential for development as novel drugs.

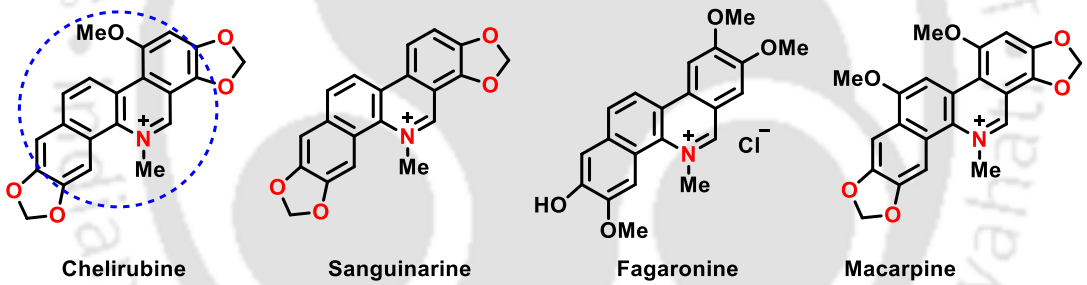

Figure 1.9. Some bioactive benzophenanthridine molecules.

1.4b. Synthesis of 6-Arylbenzophenanthridine Derivatives

To develop new drugs, synthesising various substituted benzophenanthridine is important. In this urge, the synthesis of 6-aryl/alkyl phenanthridine derivatives has been rarely investigated. In 2021, Talukdar *et al.* summarized the large synthetic developments of 6-substituted phenanthridine in a review article. Few of the synthetic methodologies have been presented schematically in **Scheme 1.25**. Most of these syntheses are metal catalyst-driven such as Pd, Cu, Fe, Rh, Mn, etc. Besides those, visible light-mediated and non-metal catalyzed synthesis are also reported.

However, there is very limited synthetic literature on 6-substituted benzophenanthridine derivatives. These limited methods have been highlighted in **Scheme 1.26** and **Scheme 1.27**.

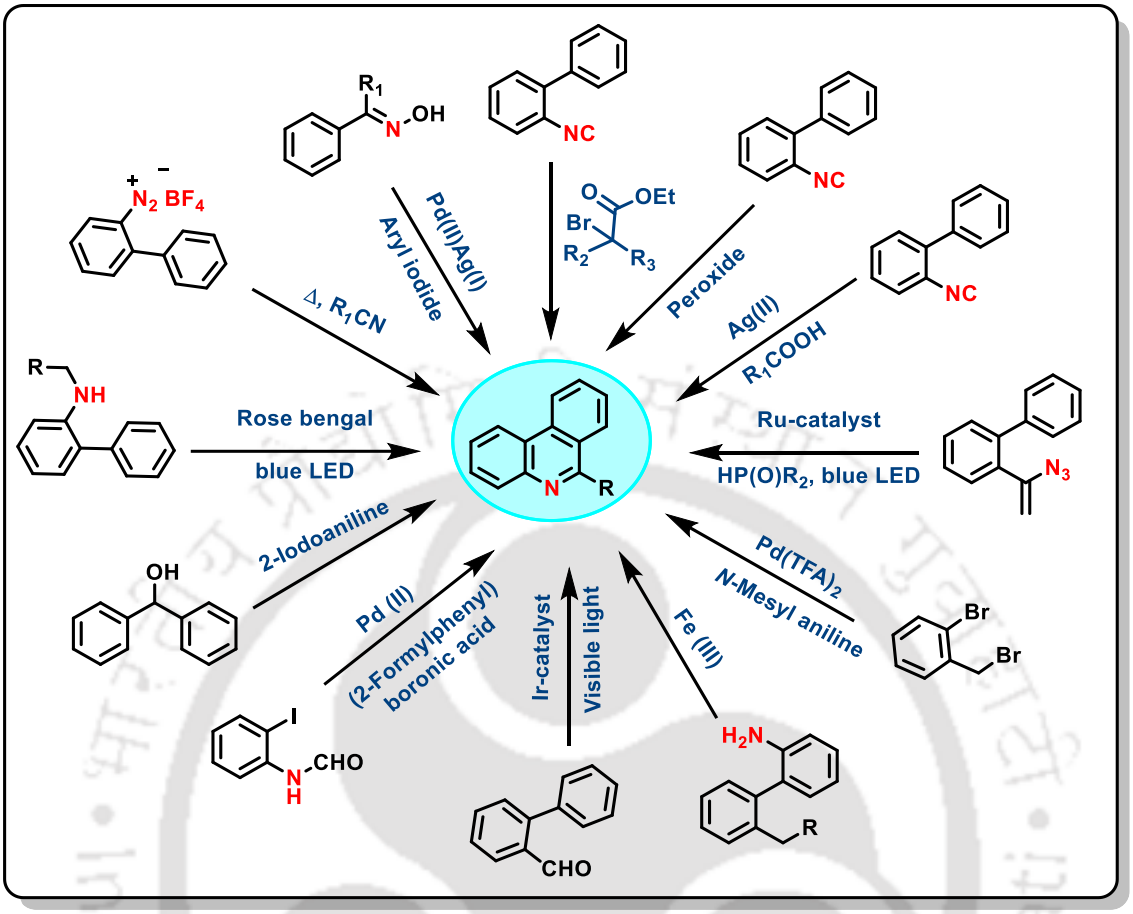

Scheme 1.25. Various synthetic strategies of 6-substituted phenanthridines.

In 2010, Maestri *et al*. reported the synthesis of phenanthridines from benzylamines and aryl iodides using a dual palladium-catalyzed process (**Scheme 1.26**). Using this methodology, they have also synthesized 6-phenylbenzo[*c*]phenanthridine from the reaction of (2-bromophenyl)(phenyl)methanamine and naphthyl iodide.[33]

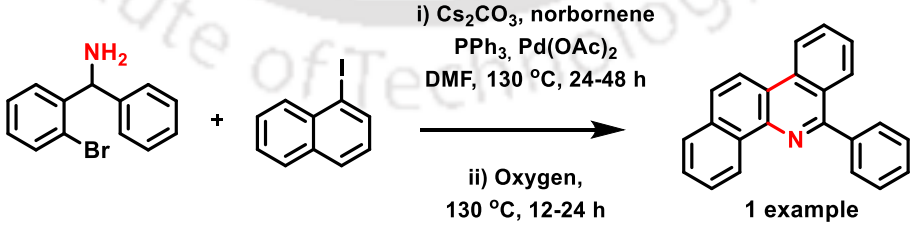

Scheme 1.26. Pd-catalyzed synthesis of 6-phenylbenzo[*c*]phenanthridine.

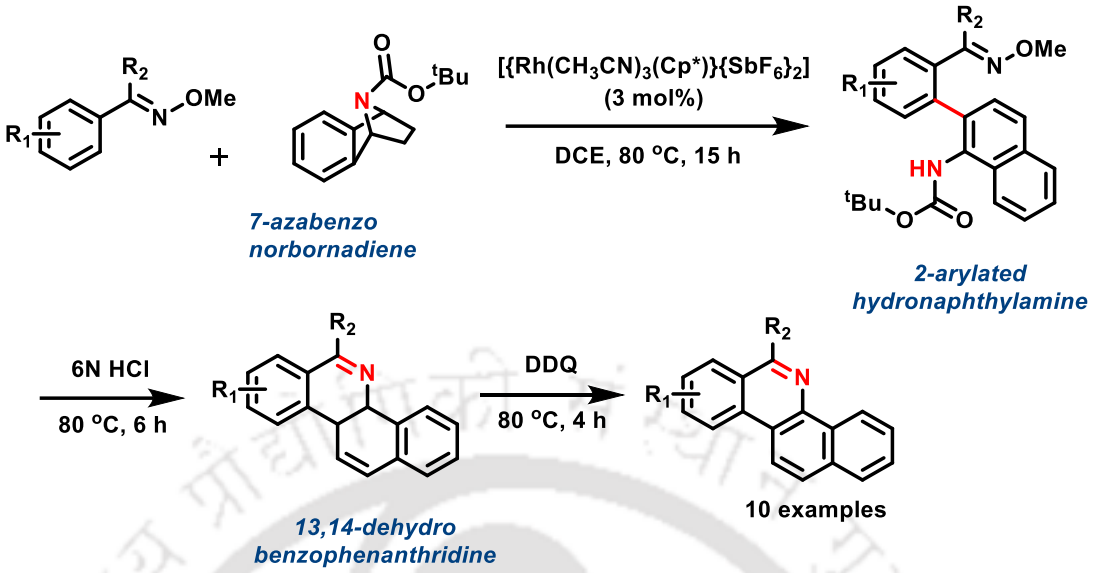

Scheme 1.27. Rh(III)-catalyzed synthesis of 6-substituted-benzo[*c*]phenanthridine derivatives.

In 2019, Vinayangam *et al*. reported a three-step synthesis of 6-substituted benzophenanthridine derivatives from aryl ketoxime (**Scheme 1.27**). A rhodium(III)-catalyzed redox-neutral ring opening of 7-azabenzonorbornadienes with aromatic ketoximes gave 2-arylated hydronaphthylamines. Later, the 2-arylated hydronaphthylamines were converted into 13,14-dihydro benzophenanthridine derivatives by HCl hydrolysis. Further, 13,14-dihydro benzophenanthridines were aromatized into 6-substituted benzophenanthridine derivatives in the presence of DDQ.[34]

1.5. A Short Introduction to Quinolines

1.5a. Importance of Quinoline Derivatives

Quinoline is considered a pioneer heterocycle in the field of organic chemistry. It is a common structural backbone of many naturally occurring alkaloids such as quinine, quinidine, etc (**Figure 1.10a**).[35] It displays a wide range of biological and pharmacological activities such as antimicrobial,[36a] anticancer,[36b] antimalarial,[36c] antifungal,[36d] anti-inflammatory,[36e] and antibacterial.[36f] Due to immense biological importance, many quinoline-containing polycyclic heteroaromatics are marketed as drugs for the treatment of cancer (Exatecan, Topotecan), malaria (Primaquine, Amodiaquinine), lowering of cholesterol (Pitavastatin), asthma (Montelukast), a local anaesthetic (Dibucaine), tuberculosis (Bedaquiline), antibacterials (Sparfloxacin, Gatifloxacin), and an antiviral agent (Saquinavir), etc. A few representative examples are given in **Figure 1.10b**.

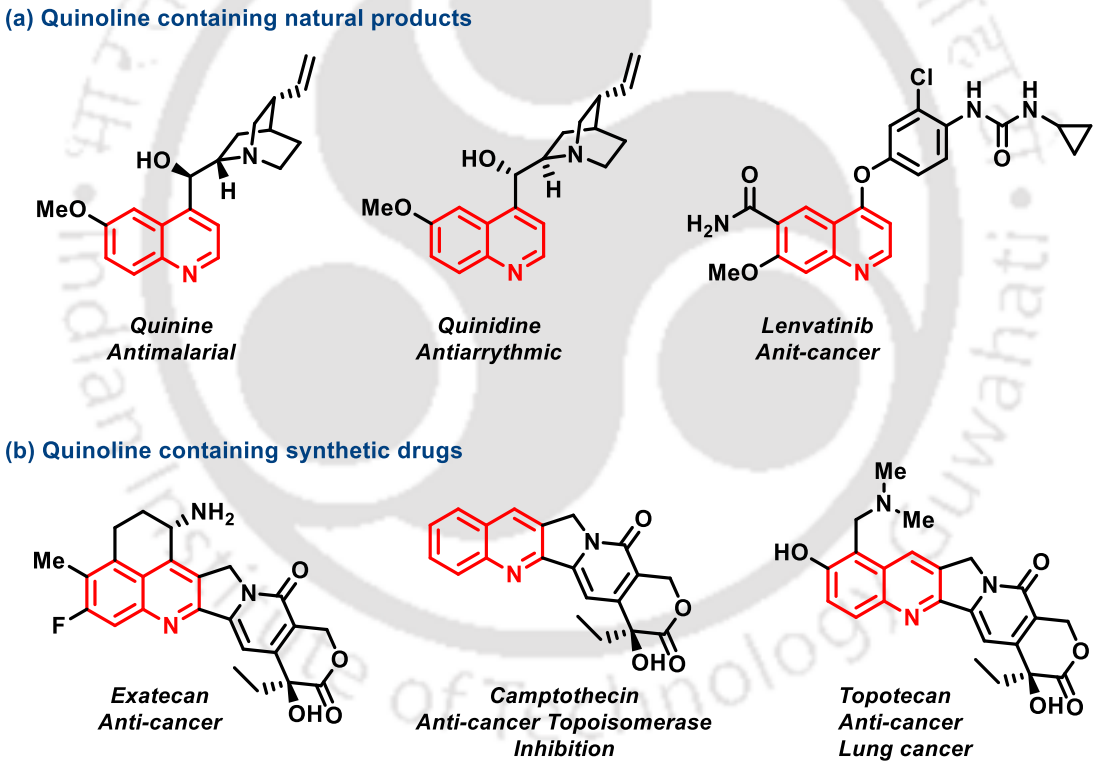

Figure 1.10. Quinoline containing bioactive PHAs.

Besides the biological and pharmaceutical applications, quinoline-containing compounds are also important in agrochemicals, material science, and industries. Polysubstituted quinoline derivatives such as 8-hydroxyquinoline and quinoline-8-thiol have been used to produce metal complexes. 2-(4-Bromo-5-ethylnylthiophen-2-yl)-6-ethynyl-4-phenylquinoline has been applied in sensors and light-emitting diodes (**Figure 1.11**).[35a,37]

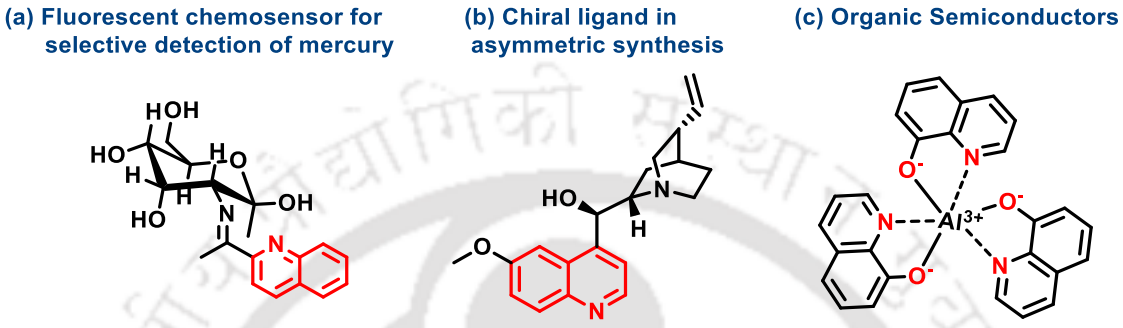

Figure 1.11. Quinoline containing important polycyclicheteroaromatics (PHAs).

Due to their tremendous pharmacological and biological importance, chemists have developed many protocols for synthesising fused tetracyclic systems comprising quinoline nuclei. A comprehensive compilation of synthetic methods of these tetracyclic ring systems, as a significant family in organic chemistry, has been done in a review article.[38]

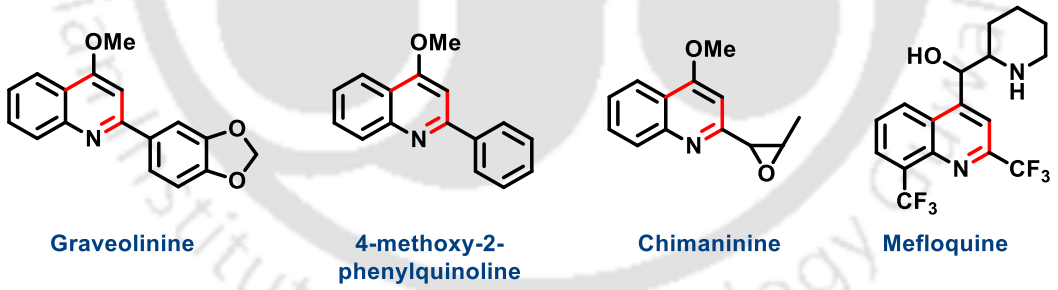

Figure 1.12. A few examples of naturally occurring 2,4-disubstituted quinoline.

It is also examined that the substitution at the C-2 and C-4 positions of the quinoline moiety effectively enhances the biological activity of the quinoline ring.[39a,b] A few examples of naturally occurring 2,4-disubstituted quinolines, such as graveolinine, mefloquine, chimaninine, etc., are shown in **Figure 1.12**.

However, benzo[*h*]quinoline and benzo[*f*]quinoline, having di-substitutions at the 2 and 4 positions in the quinoline scaffold, also exhibit anticancer and antibacterial activities.[40a] These compounds are also very useful for preparing photovoltaic cells, organic light-emitting diodes, organic field transistors, etc., due to their potential photophysical and optoelectronic properties.[40b]

1.5b. Synthesis of 2,4-Disubstituted Fused Quinoline Derivatives

Due to its abundance in natural products and extensive biological activities, significant efforts have been put to synthesize these 2,4 disubstituted quinoline derivatives. Over the years, the synthesis of 2,4-diarylquinoline was explored by the A3-coupling reaction of alkynes, aldehydes, and amines (**Scheme 1.28**).[41a] in the presence of mostly catalysts such as $Zn(OTf)_2$,[41b] AgOTf,[41c] $K_5WCo_{12}O_{40}$,[41d] AuCl–AgOTf,[41e] CuCl,[41f] CuBr–Mont,[41g] $FeCl_3$.[41h] Most of these methods involve metal catalysts, which undoubtedly brings high costs, heavy metal residues, and various side reactions.

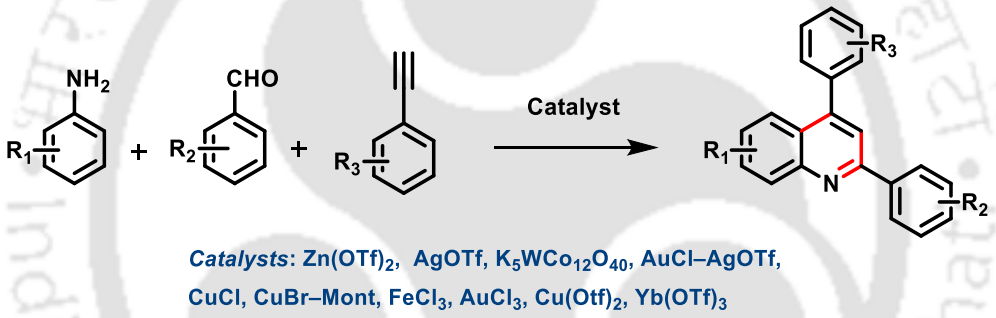

Scheme 1.28. Synthesis of 2,4-disubstituted quinoline derivatives via A3-coupling.

Unfortunately, the synthesis of fused quinolines such as benzo[*h*]quinoline, benzo[*f*]quinoline, and 3-aryl-1-methylnaphtho[2,3-*f*]quinoline derivatives with 2,4-disubstitution in the quinoline core are less explored. In 2002, Kozlov and Basalaeva reported the synthesis of 3-aryl-1-methylbenzo[*f*]quinolines from a three-component condensation of 2-aminonaphthalene, acetone, and aryl aldehydes (**Scheme 1.29**).[42a]

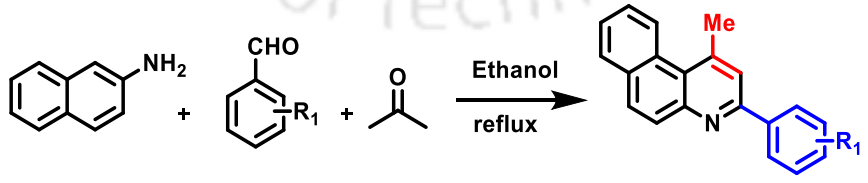

Scheme 1.29. Synthesis of 3-aryl-1-methylbenzo[*f*]quinoline derivatives.

Synthesis of few 3-aryl-1-methylnaphtho[2,3-*f*]quinoline derivatives have also been reported in 2012 from I_2 catalysed multicomponent reaction of 2-aminoanthracene, aryl aldehyde and acetone in THF (**Scheme 1.30**).[42b]

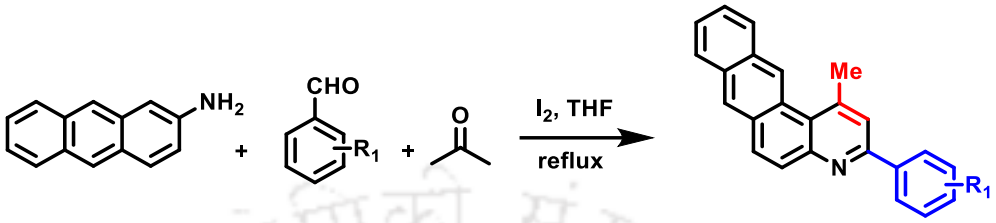

Scheme 1.30. Synthesis of a few 3-aryl-1-methylnaphtho[2,3-*f*]quinoline derivatives.

Another report of 2,4-disubstituted benzo[*h*]quinoline synthesis was disclosed by Chu *et al*. in 2017 using the condensation reaction of 1-naphthylmaine and 1,3-diketones (**Scheme 1.31**).[42c]

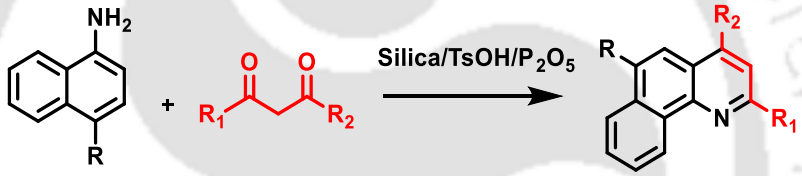

Scheme 1.31. Synthesis of 2,4-disubstituted benzo[*h*]quinoline derivatives.

1.6. Objective of the Thesis Work

Despite great efforts made in the past, the synthetic chemistry of PHAs still suffered from considerable limitations, as mentioned above. Therefore, the development of novel and efficient methodologies for the construction of PHAs is in great demand. In the last decade, our lab group has been constantly engaged in the exploration of aryl amine to accomplish various heterocycles, mostly substituted quinolines, as shown in **Figure 1.13**.[43] In 2017, we employed 1-naphthylamine in a multicomponent reaction to achieve 4-(8-(*tert*-butyl)-7,8,9,10-tetrahydrobenzo[*c*]phenanthridin-6-yl)phenol (**Scheme 5a**).[44]

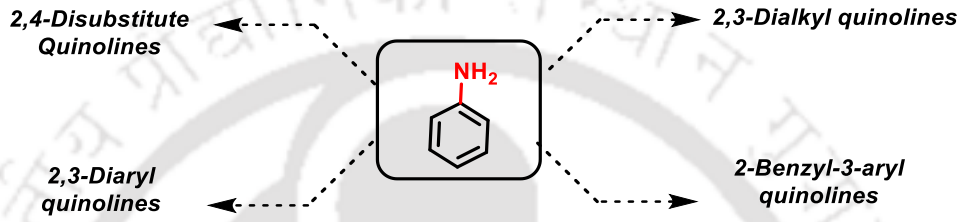

Figure 1.13. Exploration of arylamine.

From the literature survey, we anticipated that 1-naphthylamine could be explored to synthesize novel PHAS. During the last five years course of the research work, newer synthetic methodologies have been developed for hexacyclic, tetracyclic, and tricyclic fused polyheteroaromatics compounds such as benzo[*c*]chromeno[4,3,2-*gh*]phenanthridine, 7-benzo[*c*]chromeno[4,3,2-*gh*]phenanthridine, 6-aryl benzo[*c*] phenanthridin-10-ol derivatives and their precursors, and fused 2,4-disubstituted quinlines. These are mostly achieved by utilizing 1-naphthyl amine (**Figure 1.15**), and a chapter-wise synopsis of their synthetic methodologies is discussed below.

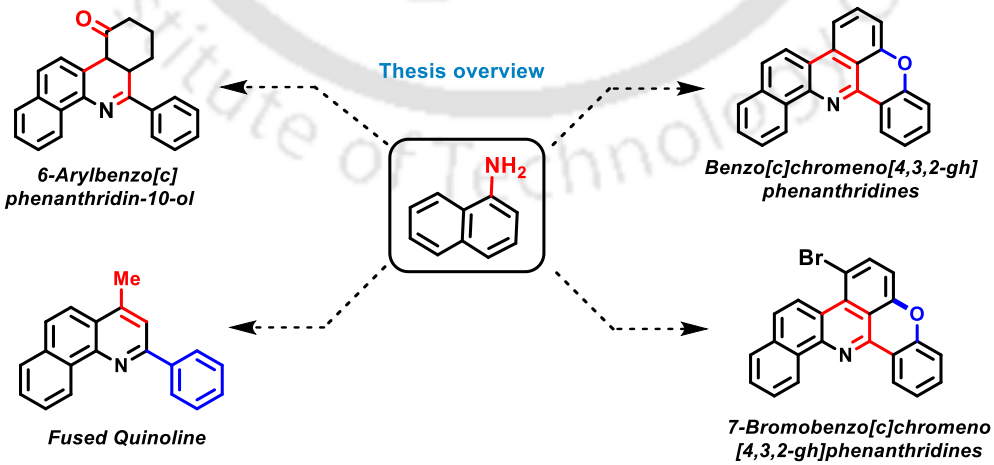

Figure 1.14. Exploration of 1-naphthylamine towards the synthesis of novel PHAs.

1.7. References

1. (a) Z. Ye, Y. Li, K. Xu, N. Chen and F. Zhang, *Org. Lett.*, 2019, **21**, 9869−9873; ***Review articles:*** (b) I. J. Keyte, R. M. Harrison and G. Lammel, *Chem. Soc. Rev.*, 2013, **42**, 9333-9391; (c) T. Jin, J. Zhao, N. Asao and Y. Yamamoto, *Chem. Eur. J*, 2014, **20**, 3554–3576; (d) R. G. Harvey, *Curr. Org. Chem.*, 2004, **8**, 303–323; (e) A. B. Patel, S. Shaikh, K. R. Jain, C. Desai and D. Madamwar, *Front. Microbiol.*, 2020, **11**, 562813.

2. (a) Q. Zhu, C. Kan, Y. Cao, Z. Tang, K. Xu, P. Hang, B. Li, Y. Yao, M. Lei and X. Yu, *Org. Lett.*, 2022, **24**, 7053–7057; ***Review articles:*** (b) M. Stępien´, E. Gon´ka, M. Zyła and N. Sprutta, *Chem. Rev.*, 2017, **117**, 3479−3716; (c) A. Borissov, Y. K. Maurya, L. Moshniaha, W.-S. Wong, M. Żyła-Karwowska and M. Stępień, *Chem. Rev.*, 2022, **122**, 565–788.

3. (a) K. P. Vijayalakshmi and C. H. Suresh, *J Comput Chem*, 2008, **29**, 1808–1817; (b) X.-Y. Wang, X. Yao and K. Müllen, *Sci. China Chem.*, 2019, **62**, 1099–1144.

4. (a) R. L. M. Allen, *Colour Chemistry*, Springer US: Boston, MA, 1971. (b) D. R. Waring, G. Hallas, Eds., *The Chemistry and Application of Dyes*, Springer: Boston, MA, 1990.

5. (a) **Review article**: M. D. Watson, A. Fechtenkötter and K. Müllen, *Chem. Rev.*, 2001, **101**, 1267–1300; (b) L. Đorđević, H. Sai, Y. Yang, N. A. Sather, L. C. Palmer and S. I. Stupp, *Angew. Chem.*, 2023, **135**, e202214997.

6. a) S. Jester, E. Sigmund, L. M. Röck and S. Höger, *Angew. Chem. Int. Ed.*, 2012, **51**, 8555–8559; (b) A. R. Yuvaraj, A. Renjith and S. Kumar, *J. Mol. Liq.*, 2018, **272**, 583–589; (c) X.-Y. Yan, M.-D. Lin, S.-T. Zheng, T.-G. Zhan, X. Zhang, K.-D. Zhang and X. Zhao, *Tetrahedron Lett.*, 2018, **59**, 592–604; (d) H. C. Menezes, S. M. R. De Barcelos, D. F. D. Macedo, A. D. Purceno, B. F. Machado, A. P. C. Teixeira, R. M. Lago, P. Serp and Z. L. Cardeal, *Anal. Chim. Acta*, 2015, **873**, 51–56; (e) Kenry and C. T. Lim, *Prog. Polym. Sci.*, 2017, **70**, 1–17.

7. (a) V. Gupta, P. Sirohi, N. Singh and R. P. Singh, *New J. Chem.*, 2020, **44**, 17714–17718; (b) S. Neidle, *The FEBS Journal*, 2010, **277**, 1118–1125.

8. (a) G. Qian, Z. Y. Wang, *Chem. - Asian J.*, 2010, **5**, 1006−1029; (b) M. Pawlicki, H. A. Collins, R. G. Denning, H. L. Anderson, *Angew. Chem., Int. Ed.*, 2009, **48**, 3244−3266; (c) S. Arai, M. Hida, A. R. Katritzky, Ed.; *Academic Press: New York*, 1992, **55**, 261−358; (d) Z. Zeng, X. Shi, C. Chi, J. T. L. Navarrete, J. Casado, J. Wu, *Chem. Soc. Rev.*, 2015, **44**, 6578−6596.

9. (a) M. Yang, I. S. Park and T. Yasuda, *J. Am. Chem. Soc.*, 2020, **142**, 19468–19472; (b) S. Kilaru, R. Gade, Y. Bhongiri, A. Tripathi, P. Chetti and S. Pola, *Mater. Sci. Semicond. Process.*, 2022, **147**, 106730; (c) V. Dávila Cerón, L. A. Illicachi and B. Insuasty, *Molecules*, 2022, **28**, 257. **Review articles**: (d) K. Dhbaibi, L. Favereau and J. Crassous, *Chem. Rev.*, 2019, **119**, 8846–8953; (e) M. Hirai, N. Tanaka, M. Sakai and S. Yamaguchi, *Chem. Rev.*, 2019, **119**, 8291−8331.

10. K. Ozaki, W. Matsuoka, H. Ito and K. Itami, *Org. Lett.*, 2017, **19**, 1930–1933.

11. (a) K. Ozaki, W. Matsuoka, H. Ito and K. Itami, *Org. Lett.*, 2017, **19**, 1930–1933; (b) B. J. Morrison and O. C. J. Musgrave, *Chem. Res.*, 2005, **2005**, 549; ***Review articles:*** (c) H. Ito, K. P. Kawahara and K. Itami, *Synthesis*, 2023, a-2169-4078; (d) H. Ito, Y. Segawa, K. Murakami and K. Itami, *J. Am. Chem. Soc.*, 2019, **141**, 3–10.

12. (a) Z. Ye, Y. Li, K. Xu, N. Chen and F. Zhang, *Org. Lett.*, 2019, **21**, 9869–9873; (b) T. Hu, Z. Ye, K. Zhu, K. Xu, Y. Wu and F. Zhang, *Org. Lett.*, 2020, **22**, 505–509.

13. **Review articles:** (a) L.-C. Campeau and N. Hazari, *Organometallics*, 2019, **38**, 3−35; (b) J. P. Sestelo and L. A. Sarandeses, *Molecules*, 2020, **25**, 4500; (c) Brijesh S. Kadu, *Catal. Sci. Technol.*, 2021, **11**, 1186–1221; (d) R. Chinchilla and C. Na´jera, *Chem. Rev.*, 2007, **107**, 874−922; (e) A. B. Dounay and L. E. Overman, *Chem. Rev*., 2003, **103**, 2945−2963; (f) N. Eiichi, *Bull. Chem. Soc. Jpn.*, 2007, **80**, 233−257; (g) M. M. Heravi and P. Hajiabbasi, *Monatsh. Chem.*, 2012, **143**, 1575–1592; (h) B. V. Varun, J. Dhineshkumar, K. R. Bettadapur, Y. Siddaraju, K. Alagiri and K. R. Prabhu, *Tetrahedron Lett.*, 2017, **58**, 803–824; (i) B. Seifinoferest, A. Tanbakouchian, B. Larijani and M. Mahdavi, *Asian. J. Org. Chem*., 2021, **10**, 1319–1344; (j) Q. Cai and W. Zhou, *Chin. J. Chem.*, 2020, **38**, 879–893.

14. (a) S. Nam and I. Kim, *J. Org. Chem.* 2023, 88, 745−754; (b) M. B. Ponce, E. T. Rodríguez, A. Flader, P. Ehlers and P. Langer, *Org. Biomol. Chem.*, 2020, **18**, 6531–6536.

15. (a) T. Jin, J. Zhao, N. Asao and Y. Yamamoto, *Chem. Eur. J.*, 2014, **20**, 3554 – 3576 and references therein; (b) P. R.-Castillo and S. L. Buchwald, *Chem. Rev.*, 2016, **116**, 12564−12649 and references therein; c) W. Hagui, H. Doucet and J.-F. Soule, *Chem*, 2007, **5**, 2006–2078; (d) Y. Nishii and M. Miura, *Catalysts*, 2023, **13**, 12 and references therein; (e) A. W. Jones, M.-L. L.-Habermeyer and F. W. Patureau, *Adv. Synth. Catal.*, 2015, **357**, 945–949; (f) P. Xi, F. Yang, S. Qin, D. Zhao, J. Lan, G. Gao, C. Hu and J. You, *J. Am. Chem. Soc.*, 2010, **132**, 1822–1824; (g) A. R. Mohebbi and F. Wudl, *Chem. Eur. J.*, 2011, **17**, 2642–2646; (h) R. Samanta and A. P. Antonchick, *Angew. Chem. Int. Ed.*, 2011, **50**, 5217–5220.

16. (b) E. V. Verbitskiy, Y. A. Kvashnin, M. V. Medvedeva, T. S. Svalova, A. N. Kozitsina, O. S. Eltsov, G. L. Rusinov*a* and V. N. Charushin*a*, *Mendeleev Commun.*, 2022, **32**, 722–725; ***Review article***: (c) Y. Zhang, S. H. Pun and Q. Miao, *Chem. Rev.*, 2022, **122**, 14554–14593.

17. (a) O. T. Dyan, G. I. Borodkin and P. A. Zaikin, *Eur. J. Org. Chem.*, 2019, **2019**, 7271–7306 and reference therein; (b) P. T. Parvatkar, H. K. Kadam and S. G. Tilve, *Tetrahedron*, 2014, *70*, 2857–2888.

18. (a) F. Palacios, C. Alonso, P. Amezua and G. Rubiales, *J. Org. Chem.*, 2002, **67**, 1941–1946; (b) Q. Yan, Y. Zhou, B. B. Ni, Y. Ma, J. Wang, J. Pei and Y. Cao, *J. Org. Chem.*, 2008, **73**, 5328–5339; (c) **Review article**: R. A. A. Foster and M. C. Willis, *Chem. Soc. Rev.*, 2013, **42**, 63-76.

19. A. G. Lvov, *J. Org. Chem.*, 2020, **85**, 8749−8759 and references therein.

20. (a) C. Du, Y. Guo, J. Chen, H. Liu, Y. Liu, S. Ye, K. Lu, J. Zheng, T. Wu, Y. Liu, Z. Shuai and G. Yu, *J. Phys. Chem. C*, 2010, **114**, 10565–10571; (b) A. Bodzioch, E. Kowalska, J. Skalik and P. Bałczewski, *Chem. Heterocycl. Compd.*, 2017, **53**, 11–20.

21. (a) **Review article**: M. C. Bonifacio, C. R. Robertson, J.-Y. Jung and B. T. King, *J. Org. Chem.*, 2005, **70**, 8522–8526; (b) A. Nuñez, B. Abarca, A. M. Cuadro, J. Alvarez-Builla and J. J. Vaquero, *Eur J Org Chem*, 2011, **2011**, 1280–1290; (c) M. B. Ponce, S. Parpart, A. Villinger, E. T. Rodríguez, P. Ehlers and P. Langer, *Synthesis*, 2021, **53**, 1237–1246.

22. (a) L. F. Tietze, *Chem. Rev.*, 1996, **96**, 115–136; (b) R. K. Maurya, D. Sharma, S. Kumari, R. Chatterjee, M. Khatravath and R. Dandela, *ChemistrySelect*, 2022, **7**, e202201408; (c) S. Nandi, U. K. Syam Kumar, H. Ila and H. Junjappa, *J. Org. Chem.*, 2002, **67**, 4916–4923; (d) B. Wang, W. Ding, L. Zhang, and X. Meng, *Org. Lett.* 2023, **25**, 140−145.

23. (a) **Review article:** B. Jiang, T. Rajale, W. Wever, S.-J. Tu and G. Li, *Chem. Asian J.*, 2010, **5**, 2318–2335; (b) W. Guan, J. Hang, Y. Qiao, C. Liu, C. Yuan, J. Chen, H. Qin, Z. Fang, D. Ji and K. Guo, *Org. Chem. Front.*, 2023, **10**, 2790–2797; (c) P. Jiang, Z. Shan, S. Chen, Q. Wang, S. Jiang, H. Zheng and G. Deng, *Chin. J. Chem.*, 2022, **40**, 365–370.

24. (a) **Review article:** K. T. Mortensen, T. J. Osberger, T. A. King, H. F. Sore and D. R. Spring, *Chem. Rev.*, 2019, **119**, 10288–10317; (b) J. Y. Xue, T. Izumi, A. Yoshii, K. Ikemoto, T. Koretsune, R. Akashi, R. Arita, H. Taka, H. Kita, S. Sato and H. Isobe, *Chem. Sci.*, 2016, **7**, 896–904; (c) K. Ikemoto, A. Yoshii, T. Izumi, H. Taka, H. Kita, J. Y. Xue, R. Kobayashi, S. Sato and H. Isobe, *J. Org. Chem.*, 2016, **81**, 662–666; (d) K. Laxman, A. Kumar and M. Ravikanth, *Asian J. Org. Chem.*, 2020, **9**, 162–180; (e) B. Szyszko, E. Pacholska-Dudziak and L. Latos-Grażyński, *J. Org. Chem.*, 2013, **78**, 5090–5095.

25. R. A. Heald, C. Modi, J. C. Cookson, I. Hutchinson, C. A. Laughton, S. M. Gowan, L. R. Kelland and M. F. G. Stevens, *J. Med. Chem.*, 2002, **45**, 590–597.

26. T. F. Molinski, *Chem. Rev.*, 1993, **93**, 1825−1838.

27. (a) R. A. Heald, C. Modi, J. C. Cookson, I. Hutchinson, C. A. Laughton, S. M. Gowan, L. R. Kelland and M. F. G. Stevens, *J. Med. Chem.*, 2002, **45**, 590–597; (b) E. Gimen´ez-Arnau, S. Missailidis and M. F. G. Stevens, *Anti-Cancer Drug Des.*, 1997, **13**, 125–143; (c) I. Hutchinson, A. J. McCarroll, R. A. Heald and M. F. G. Stevens, *Org. Biomol. Chem.*, 2004, **2**, 220–228; (d) D. Cousin, M. Frigerio and M. G. Hummersone, *World Intellectual Property Organization*, WO2012175991A1 2012-12-27.

28. (a) A. R. Katritzki, W. Du, Y. Matsukawa, I. Ghiviriga and S. N. Denisenko, *J. Heterocycl. Chem.*, 1999, **36**, 927–932; (b) J. L. Kristensen, P. Vedsø and M. Begtrup, *J. Org. Chem.*, 2003, **68**, 4091–4092; (c) S. M. Elbert, M. Reinschmidt, K. Baumgärtner, F. Rominger and M. Mastalerz, *Eur. J. Org. Chem.*, 2018, **2018**, 532–536.

29. **Review article:** B. Krane, M. O. Fagbule and M. J. Shamma, *J. Nat. Prod.*, 1984, **47**, 1–43.

30. (a) X. Yu, X. Gao, Z. Zhu, Y. Cao, Q. Zhang, P. Tu and X. Chai, *Molecules*, 2014, **19**, 13042–13060; **Review article:** (b) N. Han, Z. Yang, Z. Liu, H. Liu and J. Yin, *Nat. Prod. Commun.*, 2016, **11**, 1181–1188, and references therein.

31. (a) D. Cappoen, P. Claes, J. Jacobs, R. Anthonissen, V. Mathys, L. Verschaeve, K. Huygen and N. D. Kimpe, *J. Med. Chem.*, 2014, **57**, 2895–2290; (b) X. Xue, H. Zhang, X. Zhang, X. Liu, K. Xi, Y. Han and Z. Guo, *Nat. Prod. Commun.*, 2017, **12**, 1439–1442; (c) I. A. García, M. F. Pansa, A. D. V. Pacciaroni, M. E. García, M. L. Gonzalez, J. C. Oberti, J. L. Bocco, M. C. Carpinella, G. E. Barboza, V. E. Nicotra and G. Soria, *Front. Pharmacol.*, 2020, **11**, 593845.

32. V. Talukdar, A. Vijayan, N. Kumar Katari, K. V. Radhakrishnan and P. Das, *Adv Synth Catal*, 2021, **363**, 1202–1245.

33. G. Maestri, M.-H. Larraufie, É. Derat, C. Ollivier, L. Fensterbank, E. Lacôte and M. Malacria, *Org. Lett.*, 2010, **12**, 5692–5695.

34. V. Vinayagam, A. Mariappan, M. Jana and M. Jeganmohan, *J. Org. Chem.*, 2019, **84**, 15590−15604.

35. **Review articles:** (a) S. M. Prajapati, K. D. Patel, R. H. Vekariya, S. N. Panchal and H. D. Patel, *RSC Adv.*, 2014, **4**, 24463–24476; (b) A. Weyesa and E. Mulugeta, *RSC Adv.*, 2020, **10**, 20784–20793.

36. (a) S. Eswaran, A. V. Adhikari and N. S. Shetty, *Eur. J. Med. Chem.*, 2009, **44**, 4637–4647; (b) S. Jain, V. Chandra, P. K. Jain, K. Pathak, D. Pathak and A. Vaidya, *Arab. J. Chem.*, 2019, **12**, 4920–4946; (c) Y.-Q. Hu, C. Gao, S. Zhang, L. Xu, Z. Xu, L.-S. Feng, X. Wu and F. Zhao, *Eur. J. Med. Chem*, 2017, **139**, 22–47; (d) R. Musiol, J. Jampilek, V. Buchta, L. Silva, H. Niedbala, B. Podeszwa, A. Palka, K. M.-Maniecka, B. Oleksyn and J. Polanskia, *Bioorg. Med. Chem.*, 2006, **14**, 3592–3598; (e) M. Ratheesh, G. Sindhu and A. Helen, *Inflamm. Res.*, 2013, **62**, 367–376; (f) S. Eswaran, A. V. Adhikari, I. H. Chowdhury, N. K. Pal and K. D. Thomas, *Eur. J. Med. Chem.*, 2010, **45**, 3374–3383.

37. M. J. Mphahlele and L. G. Lesenyeho, *J. Heterocycl. Chem.*, 2013, **50**, 1–16.

38. R. A. Mekheimer, M. A. Al-Sheikh, H. Y. Medrasi and K. U. Sadek, *RSC Adv.*, 2020, **10**, 19867–19935.

39. (a) S. Naidoo and V. Jeena, *Synthesis*, 2017, **49**, 2621–2631; (b) K. Ilango, P. Valentina, K. Subhakar, and MK Kathiravan, *Austin. J. Anal. Pharm. Chem.*, 2015, **2**, 1048.

40. (a) V. Antoci, L. Oniciuc, D. A. -Mantu, C. Moldoveanu, V. Mangalagiu, A. M. Amarandei, C. N. Lungu, S. Dunca, I. I. Mangalagiu, G. Zbancioc, *Pharmaceuticals* **2021**, *14*, 335; (b) G. Lewinska, J. Sanetra, K. W. Marszalek, *J. Mater Sci: Mater Electron* **2021**, *32*, 18451–18465.

41. (a) Y. Volkova, S. Baranin and I. Zavarzin, *Adv. Synth. Catal*., 2021, **363**, 40–61 and references therein; (b) P. B. Sarode, S. P. Bahekar and H. S. Chandak, *Tetrahedron Lett.*, 2016, **51**, 5753–5756; (c) X.-S. Wang, J. Zhou, M.-M. Zhang, W. Wang and Y.-L. Li, *Monatsh. Chem.*, 2012, **143**, 935–938; (d) S. Anvar, I. M.-Baltork, S. Tangestaninejad, M. Moghadam, V. Mirkhani, A. R. Khosropour and R. Kia, *RSC Adv.*, 2012, **2**, 8713–8720; (e) Y. Kuninobu, Y. Inoue and K. Takai, *Chem. Lett.*, 2007, **36**, 1422–1423; (f) M. Rajasekar and T. M. Das, *J. Carbohydr. Chem.*, 2014, **33**, 137–151; (g) J. S. Yadav, B. V. S. Reddy, R. S. Rao, V. Naveenkumar and K. Nagaiah, *Synthesis*, 2003, **10**, 1610–1614; (h) X. Mi, J. Chen, and L. Xu, *Eur. J. Org. Chem.*, 2015, 1415–1418.

42. (a) N. G. Kozlov and L. Basalaeva, *Russ. J. Org. Chem.* 2003, **39**, 718–722; (b) W. Wang, L. Lu and X.-S. Wang, *Heterocycl. Commun.* **2012**, *18*, 17–21; (c) C. Zhu, R. Guo, Z. Sheng, Y. Li and C. Chu, *Chin. J. Chem.* **2017**, *35*, 1595–1600.

43. (a) S. Ali and A. T. Khan, *Org. Biomol. Chem.*, 2021, **19**, 8772–8782; (b) S. Ali and A. T. Khan, *Org. Biomol. Chem.*, 2021, **19**, 7041–7050; (c) S. Ali and A. T. Khan, *Org. Biomol. Chem.*, 2021, **19**, 3255–3262; (d) S. Ali and A. T. Khan, *Tetrahedron Lett.*, 2021, **70**, 152981; (e) S. Ali, R. Gattu, V. Singh, S. Mondal, A. T. Khan, G. Dubey and P. V. Bharatam, *Org. Biomol. Chem.*, 2020, **18**, 1785–1793.

44. R. Gattu, P. R. Bagdi, R. S. Basha and A. T. Khan, *J. Org. Chem.*, 2017, **82**, 12416–12429.

CHAPTER II

DMSO-Assisted Environmentally Benign Synthesis of Benzo[c]chromeno[4,3,2-gh]phenanthridines by Remote Oxidative Hetero Cross-coupling Cyclization and Aromatization Reaction

- Introduction
- Results and Discussion
- Experimental Section

2.1. Introduction

2.1a. Importance of Chromeno Phenanthridine Derivatives

Chromeno[4,3,2-*gh*]phenanthridine holds significance as a polyheteroaromatic compound bearing resemblance to the biologically important pyridoalkaloid family. Despite its importance, only a limited number of syntheses have been reported for chromeno[4,3,2-*gh*]phenanthridine. The introductory **Chapter I, Section 1.3** provides a concise overview of the potential of pentacyclic chromeno[4,3,2-*gh*]-phenanthridine derivatives, along with their very limited synthetic accounts.

Notably, benzo[*c*]chromeno[4,3,2-*gh*]phenanthridine derivatives, hexacyclic polycyclic heteroaromatic compounds, have not been reported to date. This chapter focuses on the synthetic investigation of benzo[*c*]chromeno[4,3,2-*gh*]phenanthridine, utilizing a comprehensive literature review. Detailed discussions on this topic are presented in the subsequent sections.

2.1b. Importance of *ortho*-Quinone Methide (*o*-QMs) Intermediates

ortho-Quinone methides (***o*-QMs**) represent highly reactive and transient diene entities extensively employed in organic synthesis[1a-c] and pharmaceutical applications.[1d] These *o*-QMs are characterized by a 1,3-cyclohexadiene core featuring an exocyclic methylene and a carbonyl unit inclined in an *ortho* fashion. **Figure 2.1** illustrates the similarity between *o*-QMs and *o*-quinone, as well as *o*-quinone methide, wherein the former includes two exocyclic carbonyl groups, and the latter incorporates exocyclic methylene groups attached to the 1,3-cyclohexadiene core. The existence of *o*-quinone methide was initially proposed by Fries in 1907,[2a] and later, its structure was elucidated by Gardner in 1963 through trapping experiments conducted at −100 °C.[2b]

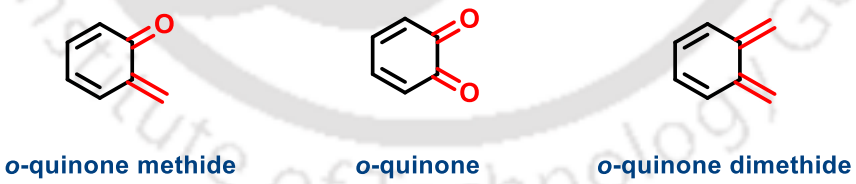

Figure 2.1. *Ortho*-quinone methide intermediate and its structural diversity.

The stability of *ortho*-quinone methides (*o*-QMs) is closely tied to the nature of their substituents. Electron-donating substituted *o*-QMs can be isolated, while those lacking such substituents must be generated *in situ* due to their high reactivity and reduced stability. Methods employed in the past for the generation of *o*-QMs can be classified as thermolysis,[3a] photolysis,[3b] and to a lesser extent, tautomerization.[3c]

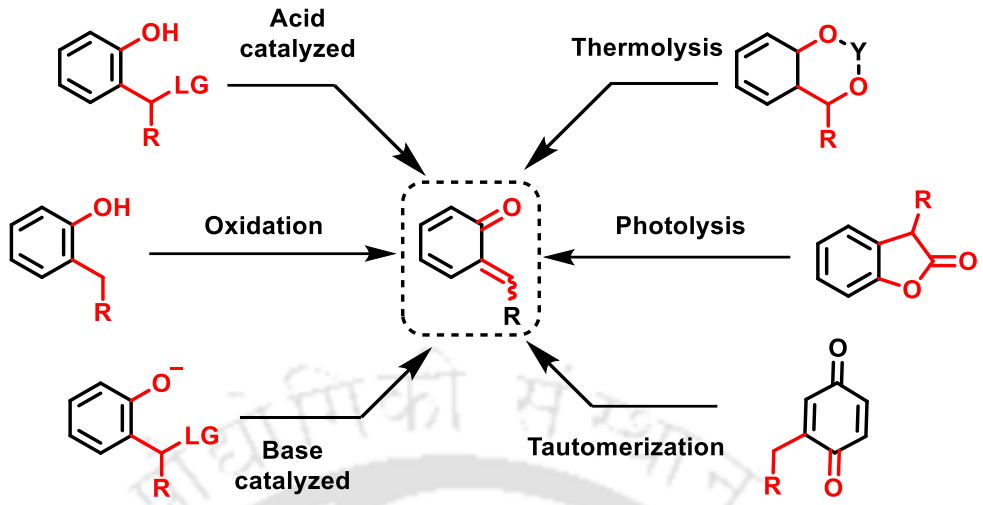

Scheme 2.1. Synthetic strategies towards *ortho*-Quinone methides (*o*-QMs).

Additionally, *o*-QMs can be produced through oxidation,[4a] acid-promoted β-elimination,[4b] and base-promoted β-elimination of *ortho*-phenol derivatives.[4c] **Scheme 2.1** provides a schematic representation of the process involved in forming *o*-QMs.

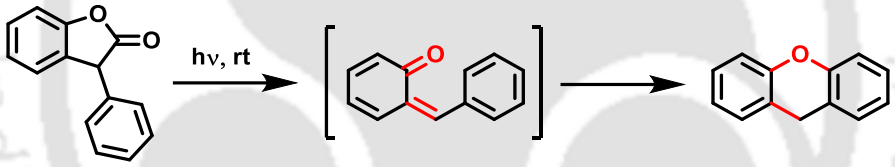

Scheme 2.2. Application of *ortho*-quinone methides in the synthesis of heterocycles.

Due to their high transience and reactivity, *ortho*-quinone methides (*o*-QMs) have proven to be a potent tool in the synthesis of heterocycles and natural products.[5,6] Serving as hetero-diene cycloaddition partners, they engage in both inter- and intramolecular Diels−Alder [4 + 2] cycloadditions with alkenes, leading to the efficient and step-economical formation of complex molecules. **Scheme 2.2** illustrates a representative example, and we anticipate that this intermediate could serve as a promising avenue for advancing the progress of the thesis work.

2.1c. Previous Reports from Our Research Group

In 2017, our research group documented a multicomponent reaction involving aryl amine, aryl aldehyde, and cyclic ketones to produce substituted fused quinoline derivatives.[7] Employing this synthetic approach, we introduced 4-(8-(*tert*-butyl)-7,8,9,10-tetrahydrobenzo[*c*]phenanthridin-6-yl)phenol (**4a'**) as part of the substrate scope, derived from the reaction of 1-naphthylamine, 4-hydroxysalicylaldehyde, and 4-*tert*-butylcyclohexanone (**Scheme 2.3a**).

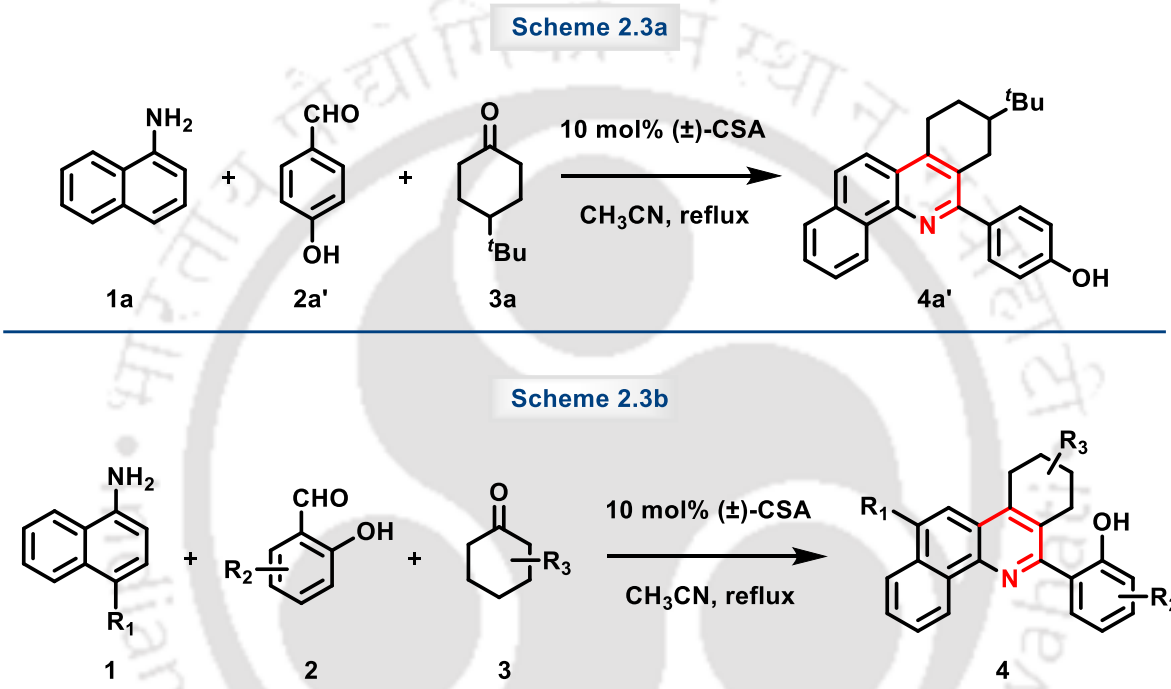

Scheme 2.3. Synthesis of (7,8,9,10-tetrahydrobenzo[*c*]phenanthridin-6-yl)phenol derivatives.

At this point, we anticipate the synthesis of 2-(7,8,9,10-tetrahydrobenzo[*c*]phenanthridin-6-yl)phenol derivatives (**4**) through this multicomponent reaction, featuring an *ortho*-directed hydroxyl (-OH) group (**Scheme 2.3b**). These phenol derivatives can ultimately be precursors for obtaining hexacyclic heteroaromatic compounds (**4**) through cyclization and aromatization reactions. However, the practical challenge is that the heteroannulation often necessitates either the robust metal-catalyzed activation of sp3-carbon or a laborious prefunctionalization for the intramolecular nucleophilic substitution by the -OH group.[8]

2.1d. Scope from the Literature Review

Following the literature mentioned above, we retrospect that this *ortho*-substituted phenolic compound can eventually be useful for the in-situ generation of ortho-quinone methide intermediate (**A1'**), as shown in **Scheme 2.4**. After that, consequent hydroxylation,[9] followed by elimination of H_2O, can form intermediate **C1'**. This intermediate can make a 6πe electrocyclic ring closure reaction feasible to form with a pyran ring **D1'**.[10]

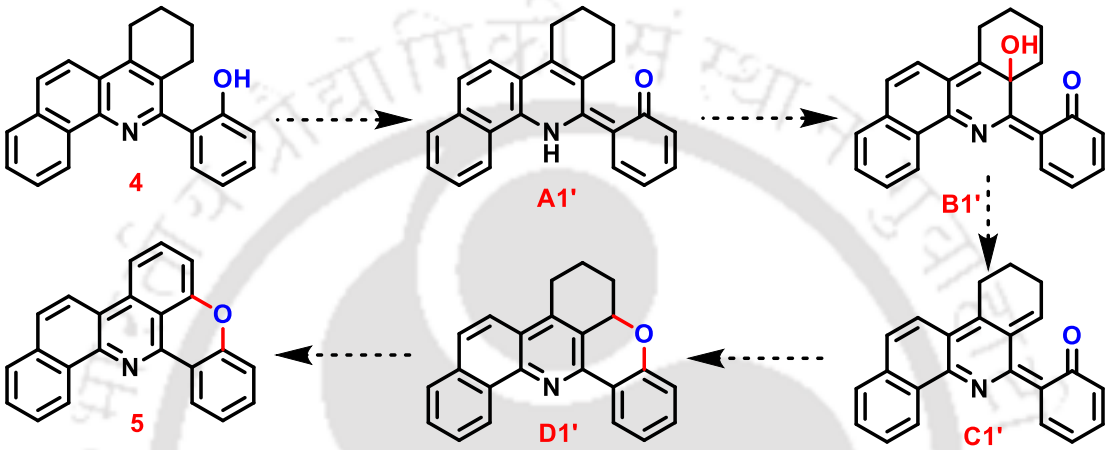

Scheme 2.4. Schematic representation of the vision for the synthesis of benzo[*c*]chromeno[4,3,2-*gh*]phenanthridine derivatives

The intermediate **D1'** can be further oxidized to fully aromatized chromenophenanthridine **5** using stoichiometric classical dehydrogenating reagents such as Pd/C, DDQ, etc.[11] This electrocyclization reaction could potentially sideline the earlier mentioned hectic cyclization process for the pyran ring formation.

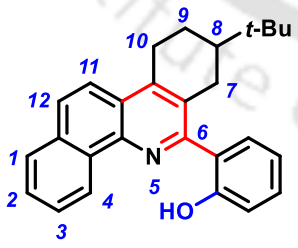

2-(8-(*tert*-butyl)-7,8,9,10-tetrahydro benzo[*c*]phenanthridin-6-yl)phenol (4a)

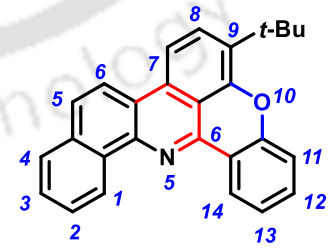

7-bromo-9-(*tert*-butyl)benzo[*c*] chromeno[4,3,2-*gh*]phenanthridine (5a)

Figure 2.2. Numbering of atoms for the naming of compounds **4a** & **5a**.

For a better understanding, the numbering pattern for the nomenclatures of the compound 2-(8-(*tert*-butyl)-7,8,9,10-tetrahydrobenzo[*c*]phenanthridin-6-yl)phenol (**4a)** and 9-(*tert*-Butyl)benzo[*c*]chromeno[4,3,2-*gh*]phenanthridine (**5a**) is illustrated in **Figure 2.2.**

2.1e. Present Work

Building upon the relevance of o-quinone methide as a reactive intermediate and drawing connections to our prior research, the inaugural thesis project has been established. **Chapter II** details a metal-free and catalyst-free synthesis of a novel category of substituted benzo[*c*]chromeno[4,3,2-*gh*]phenanthridine derivatives from 2-(7,8,9,10-tetrahydrobenzo[*c*]phenanthridin-6-yl)phenol derivatives, outlined in **Scheme 2.5**. The unique and attractive features of this procedure include i) a metal and catalyst-free intramolecular hetero annulation reaction via sp3C-H activation; ii) formation of 6-membered pyran ring through catalyst-free novel *in-situ o*-quinone methide generation and 6πe electrocyclic ring closure reaction; iii) aromatization by only DMSO is achieved for the first time; iv) exploration of electrophilic sulfur atom of DMSO for oxidation process; v) broad substrate scope.

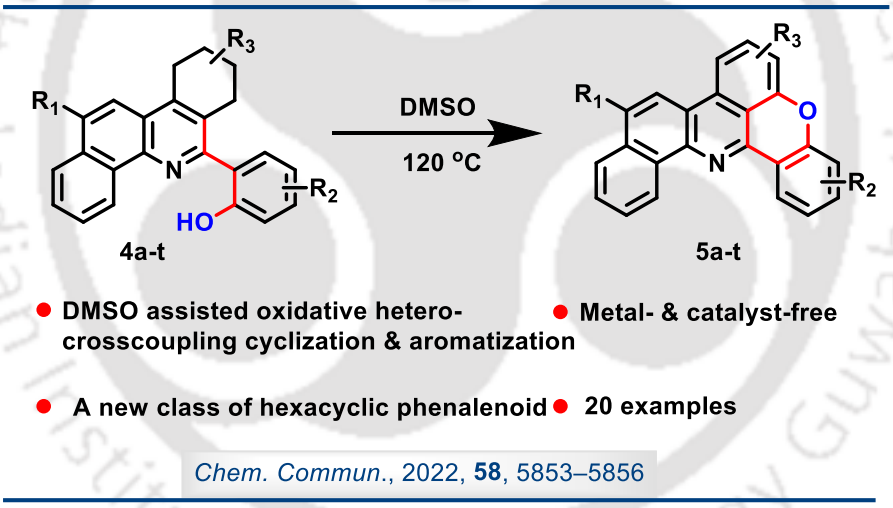

Scheme 2.5. Present work for the synthesis of benzo[*c*]chromeno[4,3,2-*gh*]phenanthridine.

2.2. Results and Discussion

2.2a. Optimization of the Methodology

As per retrosynthetic analysis (**Scheme 2.4**), we have synthesized 2-(8-(*tert*-butyl)-7,8,9,10-tetrahydrobenzo[*c*]phenanthridin-6-yl)phenol (**4a**) from 1-naphthylamine (**1a**), salicylaldehyde (**2a**), and 4-*tert*-butylcyclohexanone (**3a**). At first, we took 0.20 mmol of **4a** in DMSO solvent in a round-bottomed flask and kept it stirring at 100 ºC for 24 h to obtain the 9-(*tert*-butyl)-7,8,9,9a-tetrahydrobenzo[*c*]chromeno[4,3,2-*gh*]phenanthridine (**D1'**), according to our anticipation as shown in **Scheme 2.5**. After 24 h, we isolated a bright blue fluorescent solid compound. Very surprisingly, after characterization of the isolated compound by ^{1}H, ^{13}C NMR, and HRMS spectra, we determined that the structure of the compound was fully aromatized chromenophenanthridine. From the X-ray crystallography, we finally confirmed the compound as 9-(*tert*-butyl)benzo[*c*]chromeno[4,3,2-*gh*]phenanthridine (**5a**). XRD data of **5a** is included in **Figure 2.3 and Table 2.4**.

After structural confirmation, to establish the synthetic methodology of the hexacyclic chromeno-phenanthridine (**5**), we moved forward to optimize the reaction conditions. So, we chose 2-(8-(*tert*-butyl)-7,8,9,10-tetrahydrobenzo[*c*]phenanthridin-6-yl)phenol **4a** as a model substrate and performed a series of reactions summarized in **Table 2.1**. Initially, 0.20 mmol of **4a** was stirred at room temperature for 24 h, but no change in the reaction mixture was found (**Entry 1**). Then, the reaction was done separately at 50, 70, and 80 ºC, but the reaction did not undergo (**Entries 2-4**). Surprisingly, when the temperature was increased to 90 ºC, **4a** was obtained in 10% yields after 24 h of stirring (**Entry 5**). At 100 ºC, **5a** was isolated in 30% yield after 15 h (**Entry 6**). When the temperature was increased to 110 ºC, the yield of **5a** was increased up to 54% yield, and the reaction time was decreased to 9 h (**Entry 7**). After increasing the reaction temperature up to 120 ºC, compound **4a** was obtained in 70% yield in 6 h (**Entry 8**). But a further increase in temperature to 130 ºC provided no delightful improvement in yield of **5a** and reaction time (**Entry 9**). To find out the role of the solvent, a neat reaction was carried out at 120 ºC for 24 h; unfortunately, no desired product was found (**Entry 10**). Then, the reaction was carried out in different solvent mediums such as toluene, H_2O, and DMF, respectively (**Entries 11, 12 & 13**). Reaction in water and toluene failed, while in DMF solvent, **5a** was isolated in 30% yield at 120 ºC. Finally, we concluded that 120 ºC temperature and DMSO as a solvent were the optimum conditions for the reaction (**Entry 8**).

Table 2.1. Optimization of the Reaction Conditions[a,b]

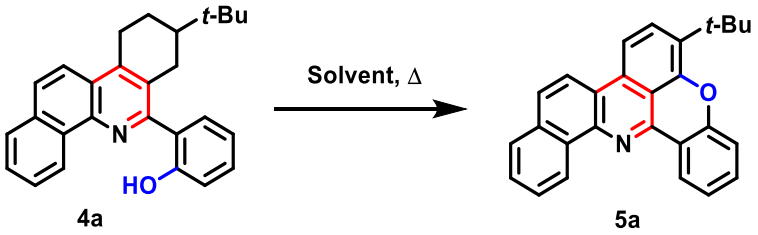

Entry	Solvent	Temperature	Time (h)	%Yield[b] (5a)
1.	DMSO	25°C	24	NR
2.	DMSO	50°C	24	NR
3.	DMSO	70°C	24	NR
4.	DMSO	80°C	24	NR
5.	DMSO	90°C	24	10
6.	DMSO	100°C	15	30
7.	DMSO	110°C	9	54
8.	**DMSO**	**120°C**	**6**	**70**
9.	DMSO	130°C	6	72
10.	Neat	120°C	24	NR
11.	Toluene	110°C	24	NR
12.	H_2O	100°C	24	NR
13.	DMF	120°C	6	30

[a]All reactions were carried out with 2-(8-(*tert*-butyl)-7,8,9,10-tetrahydrobenzo[*c*]phenanthridin-6-yl)phenol (**4a**) in 1 mL solvent. [b]Isolated yield. NR. No reaction.

2.2b. Exploration of the Substrate Scope

With the optimized reaction condition in hand, we then explored the substrate scope of this reaction. For that purpose, initially, we have synthesized various 2-(7,8,9,10-tetrahydrobenzo[*c*]phenanthridin-6-yl)phenol derivatives (**4a-4r**) from 1-naphthylamine (**1a**), salicylaldehyde (**2**), and cyclohexanone (**3**) summarized in **Table 2.2**, following the reported method. Apart from 1-naphthylamine (**1a**), **4s** and **4t** were synthesized using 4-bromo-1-napthylamine (**1b**) shown in **Table 2.2**. These compounds are then further

explored for remote cyclization to achieve substituted benzo[*c*]chromeno[4,3,2-*gh*]phenanthridine derivatives (**5a-5r**), as shown in **Table 2.3**.

Table 2.2. Scope of 2-(7,8,9,10-tetrahydrobenzo[*c*]phenanthridin-6-yl)phenol Derivatives[a,b]

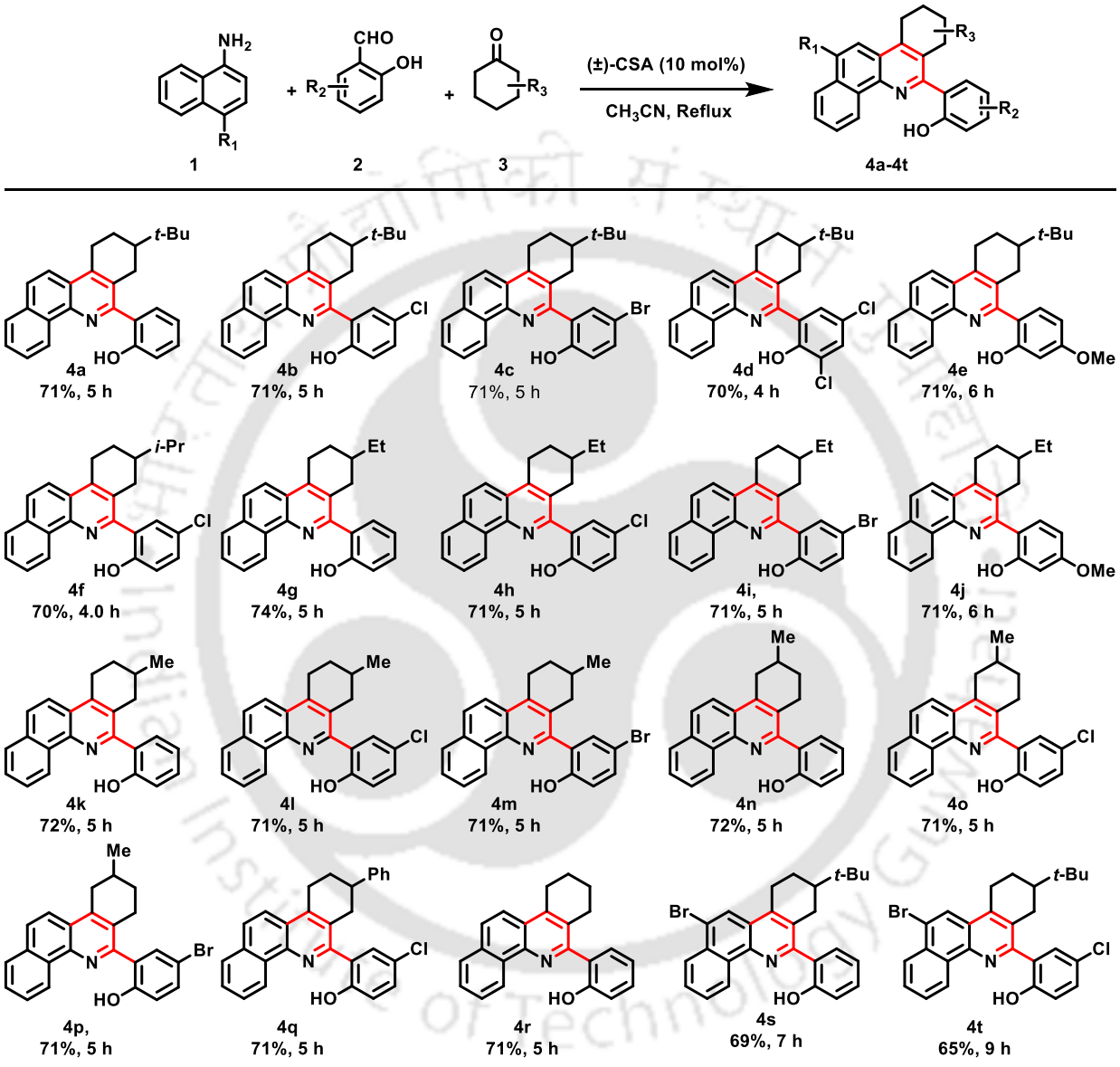

[a]All reactions were carried out with 1-naphthylamine **1** (1 mmol), salicylaldehyde **2** (1 mmol), and cyclohexanone **3** (1 mmol) derivatives in 2 mL acetonitrile solvent at 81°C. Isolated yield[b]

We took different 2-(8-(*tert*-butyl)-7,8,9,10-tetrahydrobenzo[*c*]phenanthridin-6-yl)phenol derivatives (**4b-4e)**, varying substituents at the phenol ring such as 4-Cl, 4-Br, 4,6-dichloro, 5-OMe to achieve their corresponding chromenophenanthridines (**5b-5e**) in 67-75% yield. The yield obtained for compound **5e**,

bearing electron-donating group was least among compounds **5a-5e**. Then, different 2-(7,8,9,10-tetrahydrobenzo[*c*]phenanthridin-6-yl)phenol derivatives having substituents 8-*i*Pr, 8-Et, 8-Me were subjected to the annulation aromatization reaction accomplishing final product **5f-5m** in 70-74% yield. Next, 2-(9-methyl-7,8,9,10-tetrahydrobenzo[*c*]phenanthridin-6-yl)phenols **4n-4p** provided the cyclized chhromenophenanthridine products 9-methylbenzo[*c*]chromeno[4,3,2-*gh*]phenanthridine (**5n**), and its 13-chloro (**5o**) and 13-bromo (**5p**) derivatives in 65%, 70%, and 75% respectively.

Table 2.3. Scope of Benzo[*c*]chromeno[4,3,2-*gh*]phenanthridine Derivatives[a,b]

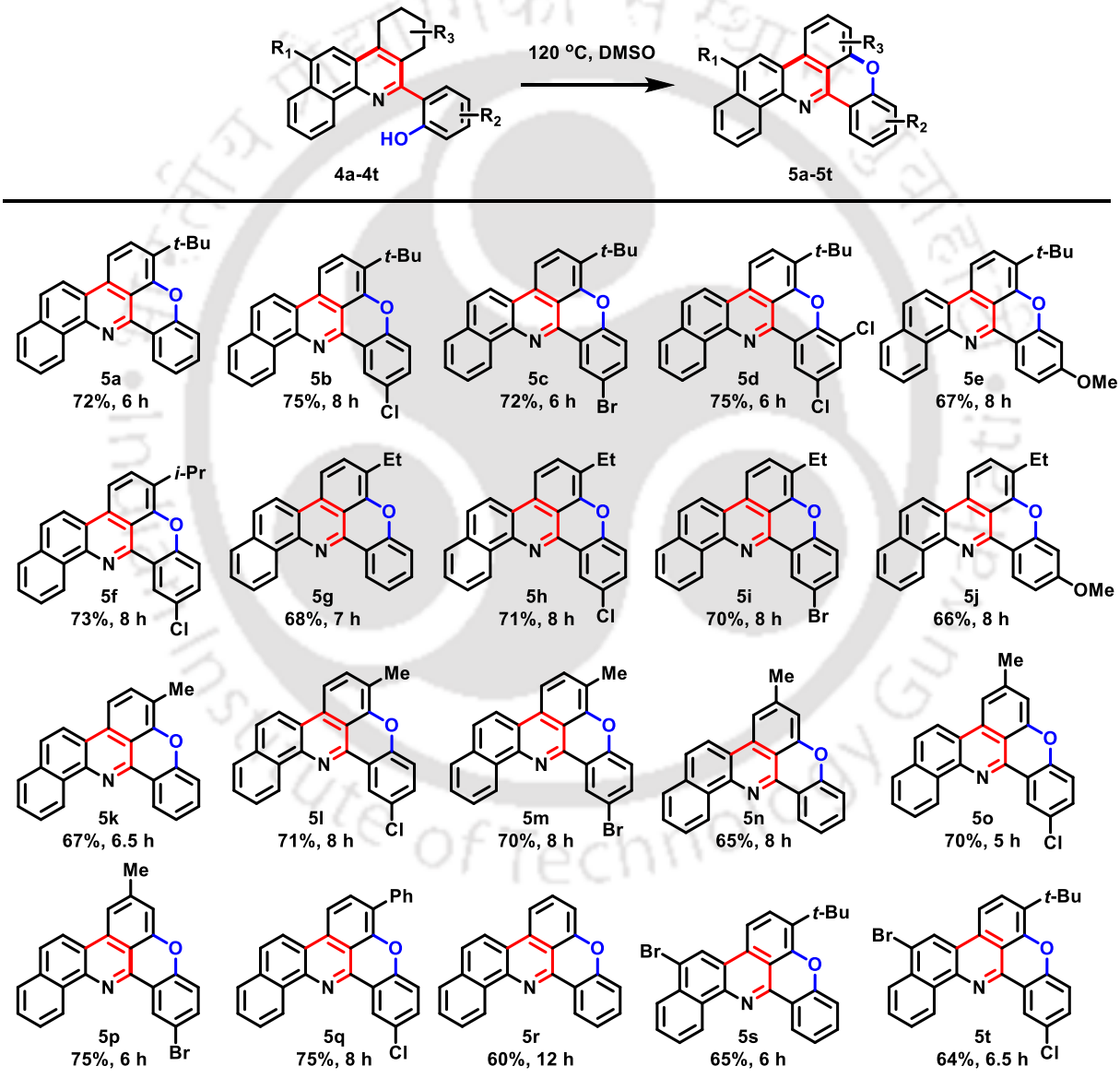

[a]All reactions were carried out with 2-(7,8,9,10-tetrahydrobenzo[*c*]phenanthridin-6-yl)phenol (0.20 mmol) derivatives in 1 mL DMSO solvent at 120 °C. Isolated yield[b]

Other than the alkyl substituent, the formation of 13-chloro-9-phenylbenzo[*c*]chromeno[4,3,2-*gh*]phenanthridine (**5q**) was also established in 75% yield. But, the unsubstituted benzo[*c*]chromeno[4,3,2-*gh*]phenanthridine (**5r**) was formed in only 60% yield. Moreover, two 2-(12-bromo-8-(*tert*-butyl)-7,8,9,10-tetrahydrobenzo[*c*]phenanthridin-6-yl)phenol compounds (**4s** and **4t**) were prepared using 4-bromo-1-naphthyl amine (**1b**) in the multicomponent reaction (**Table 2.3**). Then, the desired final products, **5s** and **5t**, were obtained in relatively lower yields (64-65%) from precursors **4s** and **4t**, respectively.

- ***All the synthesized compounds are characterized through ^{1}H, ^{13}C NMR, and HRMS spectra, and characterization data of all the compounds are given in the experimental section. A few representative spectra have also been attached in the experimental section.***

2.2c. Establishment of the Mechanism

Control Experiments

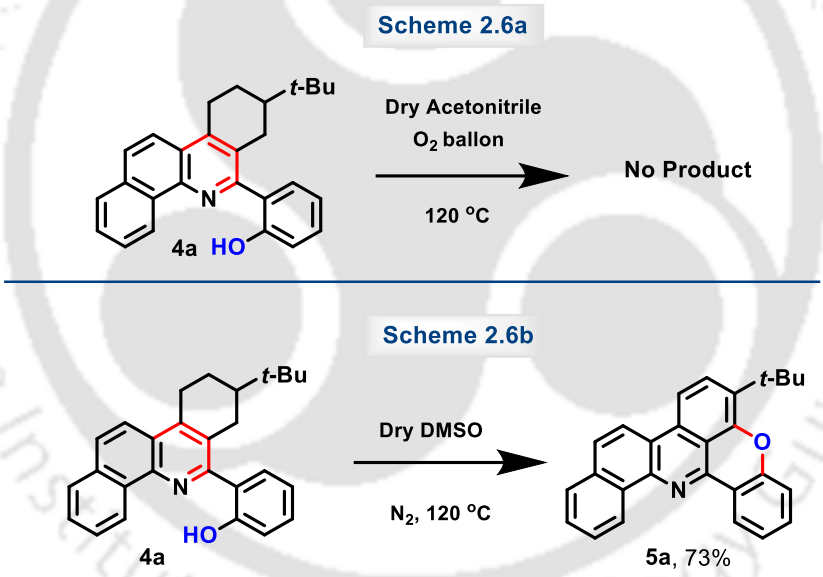

Scheme 2.6. Control experiments; [a]All Reactions were carried out with 2-(8-(*tert*-butyl)-7,8,9,10-tetrahydrobenzo[c]phenanthridin-6-yl)phenol (**4a**, 0.20 mmol) derivatives in 1 mL DMSO solvent at 120 °C.

To ascertain the mechanism of the present protocol, we performed two control experiments to verify whether product **5** is formed from **4** either by aerial oxidation or by DMSO (**Scheme S1**, ESI†). In the first experiment, compound **4a** (0.20 mmol) was refluxed in acetonitrile at 120 ºC using an oxygen balloon, and the desired product **5a** was not formed (**Scheme 2.6a**). Similarly, the second experiment was carried out with compound **4a** (0.20 mmol) in 1 mL of dry DMSO under inert atmospheric reaction conditions, and the

expected product **5a** was obtained in a 73% yield (**Scheme 2.6b**). These observations suggest that the terminal oxidant is DMSO for forming final products rather than aerial oxygen.

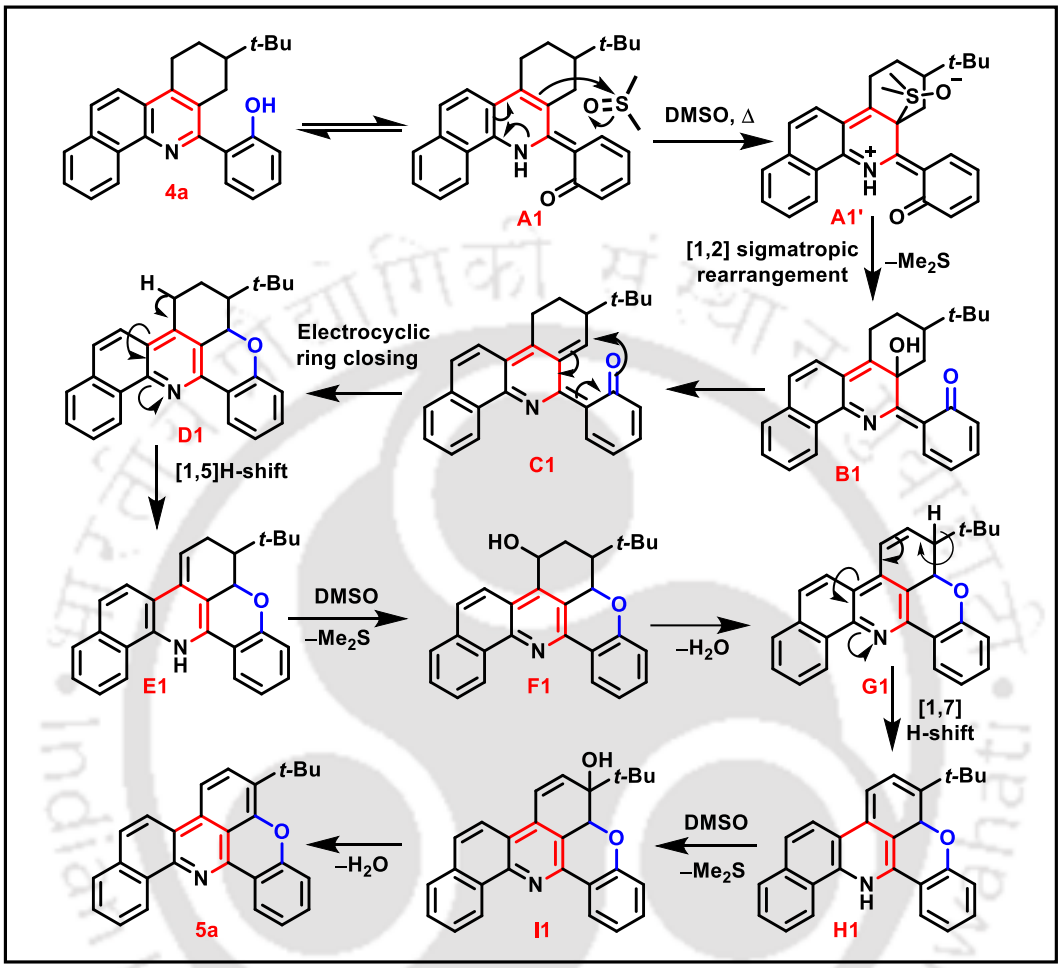

Scheme 2.7. A plausible mechanism for the synthesis of benzo[*c*]chromeno[4,3,2-*gh*]phenanthridine derivatives.

Based on the above analysis and literature reports, a plausible reaction scenario for the formation of product **5a** is outlined in **Scheme 3**. Initially, compound **4a** undergoes tautomerization in heating conditions to form the very reactive *ortho*-quinone methide intermediate **A1** by migration of hydrogen atom from the hydroxyl group to the nitrogen atom of quinoline moiety.[12] Then nucleophile **A1** reacts with electrophile DMSO to form intermediate **A1'**.[13] Then, [1,2] Sigmatropic rearrangement of **A1'** followed by Me_2S elimination generated hydroxylated intermediate **B1**,[13] which instantaneously eliminates one molecule of H_2O to generate intermediate **C1**. Thereafter, intermediate **C1** undergoes a 6πe electrocyclic ring-closing reaction to deliver the hexacyclic intermediate **D1**.[14] Subsequently, [1,5]H shift from intermediate **D1** forms intermediate **E1** which[7] then produces intermediate **F1** to **G1** by eliminating H_2O. Again, **G1** undergoes

[1,7]H shift to generate intermediate **H1**. Subsequent hydroxylation of **H1**, followed by the elimination of another molecule of H_2O, furnished the desired product **5a**.

Detection of Intermediates in HRMS

The proposed mechanism is also supported by detecting the reactive intermediates **B1**, **C1**, **D1**, **E1**, **F1**, **G1**, **H1**, and **I1** for compound **5a** in HRMS. 0.10 mmol (37 mg) of 2-(8-(*tert*-butyl)-7,8,9,10-tetrahydrobenzo[*c*]phenanthridin-6-yl)phenol **(4a)** was stirred in DMSO in a 10 mL round-bottomed flask at 120 ºC temperature. After 2.5 h, the reaction mixture was subjected to an ESI-MS mass experiment, and the intermediates **B1**, **C1**, **D1**, **E1**, **F1**, **G1**, **H1**, and **I1** were detected by HRMS values. The observed m/e values are as follows: intermediate **B1** – 398.2106 (expected 398.2115); intermediate **C1, D1, E1** – 380.2000 (expected 380.2009); intermediate **F1** – 396.1950 (expected 396.1959); intermediate **G1, H1** – 378.1853 (expected 378.1853); intermediate **I1** – 394.1795 (expected 394.1802).

2.2d. Conclusion

- We have devised a straightforward and catalyst-free synthesis of substituted and unsubstituted benzo[*c*]chromeno[4,3,2-*gh*]phenanthridine, constituting a novel category of hexacyclic 1,4-diheterophenalenoids through oxidative cross-coupling and aromatization, mediated by dimethyl sulfoxide (DMSO).
- This method generates an *o*-quinone methide intermediate *in situ* under heating conditions, eliminating the need for a metal catalyst—an achievement challenging with conventional approaches.
- The DMSO-mediated hydroxylation and elimination processes facilitate a 6πe electrocyclic ring closure reaction, forming a 6-membered pyran ring.
- Furthermore, DMSO plays a crucial role in the aromatization reaction, enabling the production of the 1,4-diheterophenalenoid product without requiring an oxidant or metal catalyst. This sequence involves hydroxylation, elimination, and H-shift reactions.
- The method offers practical advantages, including mild and straightforward conditions, environmental compatibility, cost-effectiveness, a wide substrate scope, and high yields.

This procedure will be crucial in effectively synthesizing polycyclic benzo[*c*]phenanthridines.

2.3. Experimental Section

2.3a. General procedure for the synthesis of 2-(7,8,9,10-tetrahydrobenzo[*c*]phenanthridin-6-yl)-phenol derivatives 4.

In a dry 25 mL single-necked round-bottomed flask, 1-naphthylamine **1a** (143 mg, 1.0 mmol), aromatic aldehyde **2** (1.0 mmol), and cyclohexanone derivatives **3** (154 mg, 1.0 mmol) were dissolved in acetonitrile (5.0 mL). A catalytic amount of (±)-camphor-10-sulfonic acid (CSA, 0.023 g, 0.10 mmol) was added, and the reaction mixture was allowed to stir at reflux condition on a preheated oil bath. The progress of the reaction was monitored by TLC from time to time in 30 minutes. After completion of the reaction, the reaction mixture was allowed to cool at room temperature. Precipitate, thus obtained, was filtered through a Buchner funnel, washed with acetonitrile (3 x 2.0 mL), air dried and recrystallized with acetone to obtain the desired product **4**.

2.3b. General procedure for the synthesis of benzo[*c*]chromeno[4,3,2-*gh*]phenanthridines (5).

Compound **4** (0.20 mmol) was dissolved in DMSO (1.0 mL) and taken into a 10 mL single necked-round bottomed flask. The resultant solution was stirred in a preheated oil bath (120 °C) in an air atmosphere. After the reaction (monitored on TLC) was completed, the reaction mixture was cooled to room temperature. Distilled water (10 mL) was added, extracted with ethyl acetate (3 x 10 mL), washed with distilled water (3 x 10 mL), dried over Na_2SO_4, filtered, and evaporated on the rotary evaporator under reduced pressure. The crude residue was purified through silica gel (60-120 mesh) column chromatography with hexane to obtain pure product **5**.

2.3c. Characterization Data of the Synthesized Compounds

2-(8-(*tert*-Butyl)-7,8,9,10-tetrahydrobenzo[*c*]phenanthridin-6-yl)phenol (4a)

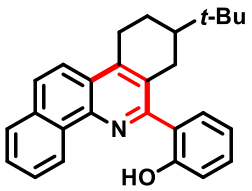

White solid (270 mg, 71%); mp 230 °C; ^{1}H NMR (400 MHz, $CDCl_3$) δ 12.65 (s, 1H), 9.19 (d, *J* = 7.9 Hz, 1H), 7.93 – 7.83 (m, 3H), 7.74 – 7.67 (m, 3H), 7.36 (t, *J* = 8.5 Hz, 1H), 7.19 (d, *J* = 7.1 Hz, 1H), 6.99 (t, *J* = 7.0 Hz, 1H), 3.54 (d, *J* = 23.8 Hz, 1H), 3.23 – 3.13 (m, 1H), 3.08 (dt, *J* = 16.3, 2.8 Hz, 1H), 2.91 – 2.84 (m, 1H), 2.27 – 2.23 (m, 1H), 1.63 – 1.58 (m, 1H), 1.30 (t, *J* = 11.5 Hz, 1H), 0.98 (s, 9H). ^{13}C NMR (100 MHz, $CDCl_3$) δ 157.6, 156.2, 145.0, 141.3, 133.3, 130.8, 130.7, 130.6, 130.2, 128.1, 128.1, 127.9, 127.6, 124.1, 124.0, 122.6, 120.6, 118.5, 118.0, 44.8, 32.5, 31.7, 28.2, 27.5, 23.9. IR (KBr)ν_{max}: 2957, 1620, 1248 cm^{-1}; HRMS (ESI) Calcd for $C_{27}H_{28}NO$ 382.2166 ($M + H^+$); Found 382.2174.

2-(8-(*tert*-Butyl)-7,8,9,10-tetrahydrobenzo[*c*]phenanthridin-6-yl)-4-chlorophenol (4b)

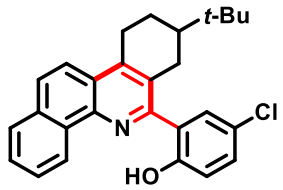

White solid (295 mg, 71%); mp 175 °C; ^{1}H NMR (600 MHz, $CDCl_3$) δ 12.71 (s, 1H), 9.04 (d, *J* = 8.1 Hz, 1H), 7.93 (d, *J* = 7.7 Hz, 1H), 7.87 – 7.83 (m, 2H), 7.73 (t, *J* = 7.0 Hz, 1H), 7.70 (t, *J* = 6.9 Hz, 1H), 7.66 (d, *J* = 2.3 Hz, 1H), 7.30 (dd, *J* = 8.7, 6.6 Hz, 1H), 7.11 (d, *J* = 8.7 Hz, 1H), 3.49 (d, *J* = 17.7 Hz, 1H), 3.16 – 3.10 (m, 1H), 3.04 (d, *J* = 15.8 Hz, 1H), 2.84 – 2.79 (m, 1H), 2.22 (s, 1H), 1.51 (d, *J* = 6.7 Hz, 1H), 1.28 (t, *J* = 12.1 Hz, 1H), 0.98 (s, 9H); ^{13}C NMR (150 MHz, $CDCl_3$) δ 156.4, 154.9, 145.4, 141.3, 133.4, 130.7, 130.5, 130.4, 129.8, 128.4, 128.3, 128.2, 127.8, 124.4, 123.9, 123.6, 123.3, 120.6, 119.4, 44.7, 32.6, 31.5, 28.2, 27.6, 23.8. IR (KBr)ν_{max}: 2958, 1614, 1248 cm^{-1}; HRMS (ESI) Calcd for $C_{27}H_{27}ClNO$ 416.1776 (M + H$^+$); Found 416.1785.

4-Bromo-2-(8-(*tert*-butyl)-7,8,9,10-tetrahydrobenzo[*c*]phenanthridin-6-yl)phenol (4c)

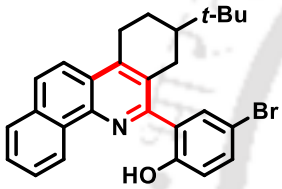

Pale yellow solid (326 mg, 71%); mp 170 °C; ^{1}H NMR (600 MHz, $CDCl_3$) δ 12.72 (s, 1H), 9.02 (d, *J* = 8.0 Hz, 1H), 7.92 (d, *J* = 7.4 Hz, 1H), 7.83 – 7.79 (m, 3H), 7.73 (t, *J* = 7.5 Hz, 1H), 7.69 (t, *J* = 7.3 Hz, 1H), 7.43 (d, *J* = 6.4 Hz, 1H), 7.05 (d, *J* = 8.7 Hz, 1H), 3.41 (d, *J* = 17.6 Hz, 1H), 3.11 – 3.05 (m, 1H), 3.01 (d, *J* = 15.8 Hz, 1H), 2.78 – 2.74 (m, 1H), 2.19 – 2.16 (m, 1H), 1.44 (dd, *J* = 12.1, 5.5 Hz, 1H), 1.29 – 1.22 (m, 1H), 0.97 (s, 9H); ^{13}C NMR (150 MHz, $CDCl_3$) δ 156.8, 154.6, 145.3, 141.1, 133.3, 133.2, 132.7, 130.6, 130.4, 128.3, 128.2, 128.1, 127.8, 124.3, 124.0, 123.8, 120.5, 119.8, 110.2, 44.6, 32.5, 31.4, 28.1, 27.5, 23.6; IR (KBr)ν_{max}: 2959, 1614, 1250 cm^{-1}; HRMS (ESI) Calcd for $C_{27}H_{27}BrNO$ 460.1271 (M + H$^+$); Found 460.1275 and 462.1258.

2-(8-(*tert*-Butyl)-7,8,9,10-tetrahydrobenzo[*c*]phenanthridin-6-yl)-4,6-dichlorophenol (4d)

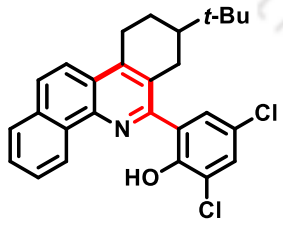

Pale yellow solid (314 mg, 70%); mp 180 °C; ^{1}H NMR (400 MHz, $CDCl_3$) δ 13.72 (s, 1H), 9.01 (d, *J* = 7.9 Hz, 1H), 7.91 (d, *J* = 7.6 Hz, 1H), 7.82 – 7.68 (m, 4H), 7.56 (d, *J* = 2.1 Hz, 1H), 7.44 (d, *J* = 2.2 Hz, 1H), 3.34 (d, *J* = 23.2 Hz, 1H), 3.07 – 2.98 (m, 1H), 2.93 (d, *J* = 15.8 Hz, 1H), 2.70 – 2.63 (m, 1H), 2.15 – 2.12 (m, 1H), 1.35 (dt, *J* = 12.2, 6.1 Hz, 1H), 1.19 (t, *J* = 11.7 Hz, 1H), 0.94 (s, 9H); ^{13}C NMR (100 MHz, $CDCl_3$) δ 154.1, 152.9, 145.6, 140.8, 133.3, 130.7, 130.4, 130.1, 128.6, 128.5, 128.4, 128.2, 128.0, 124.5, 123.9, 123.8, 123.4, 122.8, 120.3, 44.5, 32.4, 31.4, 28.1, 27.4, 23.5; IR (KBr)ν_{max}: 2957, 1614, 1251 cm^{-1}; HRMS (ESI) Calcd for $C_{27}H_{26}Cl_2NO$ 450.1386 (M + H$^+$); Found 450.1425.

2-(8-(*tert*-Butyl)-7,8,9,10-tetrahydrobenzo[*c*]phenanthridin-6-yl)-5-methoxyphenol (4e)

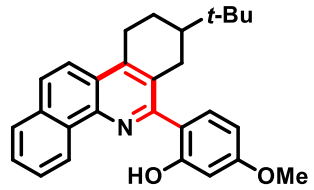

White solid (292 mg, 71%); mp 162-164 °C; ^{1}H NMR (600 MHz, $CDCl_3$) δ 13.35 (s, 1H), 8.88 (d, *J* = 7.9 Hz, 1H), 7.79 (d, *J* = 7.7 Hz, 1H), 7.77 (d, *J* = 9.1 Hz, 1H), 7.70 (d, *J* = 9.0 Hz, 1H), 7.56 (dd, *J* = 17.6, 7.6 Hz, 2H), 7.48 (d, *J* = 8.7 Hz, 1H), 6.56 (s, 1H), 6.42 (d, *J* = 8.6 Hz, 1H), 3.75 (s, 3H), 3.41 (d, *J* = 12.5 Hz, 1H), 3.05 – 3.02 (m, 1H), 2.91 (d, *J* = 16.0 Hz, 1H), 2.44 (s, 1H), 2.12 – 2.09 (m, 1H), 1.44 – 1.41 (m, 1H), 1.16 (t, *J* = 11.8 Hz, 1H), 0.84 (s, 9H); ^{13}C NMR (150 MHz, $CDCl_3$) δ 161.4, 159.6, 156.1, 152.7, 143.0, 141.8, 139.2, 136.6, 133.2, 131.0, 130.4, 128.0, 127.4, 127.4, 123.6, 123.6, 120.4, 105.2, 102.2, 55.3, 44.6, 32.3, 31.6, 28.1, 27.3, 23.6; IR (KBr)ν_{max}: 2957, 1620, 1251 cm^{-1}; HRMS (ESI) Calcd for $C_{28}H_{30}NO_2$ 412.2272 (M + H$^+$); Found 412.2329.

4-Chloro-2-(8-*iso*propyl-7,8,9,10-tetrahydrobenzo[*c*]phenanthridin-6-yl)phenol (4f)

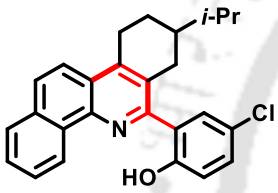

White solid (280 mg, 70%); mp 211-213 °C; ^{1}H NMR (500 MHz, $CDCl_3$) δ 9.38 (d, *J* = 7.6 Hz, 1H), 7.89 (d, *J* = 4.2 Hz, 1H), 7.81 (d, *J* = 9.1 Hz, 1H), 7.74 (d, *J* = 7.2 Hz, 1H), 7.69 – 7.63 (m, 2H), 7.55 – 7.52 (m, 2H), 7.49 – 7.46 (m, 1H), 3.53 (dd, *J* = 12.5, 5 Hz, 1H), 3.10 (td, *J* = 11.7, 6.4 Hz, 1H), 2.88 (d, *J* = 16.3 Hz, 1H), 2.71 – 2.66 (m, 1H), 2.24 – 2.20 (m, 1H), 1.51 (dq, *J* = 12.3, 6.9 Hz, 1H), 1.42 (d, *J* = 5.2 Hz, 1H), 1.40 – 1.37 (m, 1H), 0.93 (s, 6H); ^{13}C NMR (100 MHz, $CDCl_3$) δ 158.6, 143.4, 142.2, 141.7, 133.1, 132.2, 130.5, 129.6, 129.5, 129.4, 128.3, 128.1, 128.0, 127.5, 127.1, 126.7, 125.1, 124.0, 120.7, 44.6, 32.4, 30.4, 27.6, 27.4, 23.9; IR (KBr)ν_{max}: 2957, 1614, 1251 cm^{-1}; HRMS (ESI) Calcd for $C_{26}H_{25}ClNO$ 402.1620 (M + H$^+$); Found 402.1627.

2-(8-Ethyl-7,8,9,10-tetrahydrobenzo[*c*]phenanthridin-6-yl)phenol (4g)

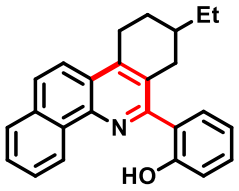

White solid (261 mg, 74%), mp 164 °C; ^{1}H NMR (500 MHz, $CDCl_3$) δ 12.57 (s, 1H), 9.09 (d, *J* = 8.0 Hz, 1H), 7.92 – 7.80 (m, 3H), 7.70 (m, 3H), 7.36 (t, *J* = 7.6 Hz, 1H), 7.19 (d, *J* = 8.1 Hz, 1H), 6.98 (t, *J* = 7.4 Hz, 1H), 3.44 (d, *J* = 17.8 Hz, 1H), 3.21 – 3.18 (m, 1H), 3.12 (d, *J* = 16.4 Hz, 1H), 2.79 – 2.75 (m, 1H), 2.19 (s, 1H), 1.57 (s, 2H), 1.46 – 1.43 (m, 2H), 0.97 (t, *J* = 6.7 Hz, 3H); ^{13}C NMR (125 MHz, $CDCl_3$) δ 157.6, 156.0, 145.0, 141.4, 133.3, 130.7, 130.6, 130.3, 130.0, 128.1, 128.0, 127.9, 127.6, 124.2, 124.0, 122.6, 120.5, 118.5, 117.9, 36.4, 35.9, 28.8, 28.1, 26.8, 11.6; IR (KBr)ν_{max}: 2956, 1614, 1252 cm^{-1}; HRMS (ESI) Calcd for $C_{25}H_{24}NO$ 354.1853 (M + H$^+$); Found 354.1841.

4-Chloro-2-(8-ethyl-7,8,9,10-tetrahydrobenzo[*c*]phenanthridin-6-yl)phenol (4h)

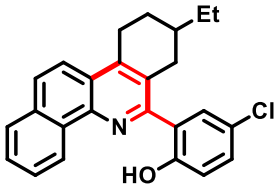

White solid (274, 71%); mp 166-168 °C; ^{1}H NMR (500 MHz, $CDCl_3$) δ 12.18 (s, 1H), 9.03 (d, *J* = 7.6 Hz, 1H), 7.91 (d, *J* = 7.2 Hz, 1H), 7.82 (s, 2H), 7.71 (t, *J* = 8.3 Hz, 2H), 7.59 (s, 1H), 7.29 (d, *J* = 8.6 Hz, 1H), 7.11 (d, *J* = 8.3 Hz, 1H), 3.34 (d, *J* = 17.6 Hz, 1H), 3.14 – 3.09 (m, 1H), 3.04 (d, *J* = 16.1 Hz, 1H), 2.70 – 2.67 (m, *J* = 15.6 Hz, 1H), 2.13 (s, 1H), 1.48 – 1.44 (m, 2H), 0.96 (s, 3H); ^{13}C NMR (125 MHz, $CDCl_3$) δ 156.0, 154.4, 141.0, 133.3, 130.5, 130.1, 129.8, 128.8, 128.4, 128.3, 128.1, 127.8, 126.2, 124.5, 123.9, 123.6, 123.4, 120.4, 119.3, 35.8, 35.6, 28.6, 27.7, 26.8, 11.5; IR (KBr)ν_{max}: 2958, 1617, 1253 cm^{-1}; HRMS (ESI) Calcd for $C_{25}H_{23}ClNO$ 388.1463 (M + H$^+$); Found 388.1462.

4-Bromo-2-(8-ethyl-7,8,9,10-tetrahydrobenzo[*c*]phenanthridin-6-yl)phenol (4i)

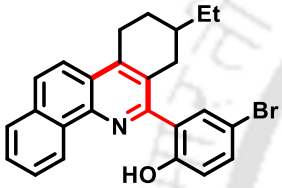

Pale yellow solid (306 mg, 71%); mp 158-160 °C; ^{1}H NMR (500 MHz, $CDCl_3$) δ 12.57 (s, 1H), 9.03 (d, *J* = 7.9 Hz, 1H), 7.92 (d, *J* = 7.5 Hz, 1H), 7.85 (q, *J* = 9.0 Hz, 2H), 7.77 (s, 1H), 7.71 (dt, *J* = 16.6, 6.8 Hz, 2H), 7.44 (d, *J* = 8.6 Hz, 1H), 7.07 (d, *J* = 8.7 Hz, 1H), 3.43 (d, *J* = 18.2 Hz, 1H), 3.22 – 3.15 (m, 1H), 3.09 (d, *J* = 16.0 Hz, 1H), 2.76 – 2.71 (m, 1H), 2.18 (s, 1H), 1.51 – 1.44 (m, 2H), 0.98 (t, *J* = 7.1 Hz, 3H); ^{13}C NMR (125 MHz, $CDCl_3$) δ 156.8, 154.6, 145.4, 141.4, 133.4, 133.2, 132.7, 130.5, 129.9, 128.3, 128.3, 128.1, 127.7, 124.5, 124.2, 123.9, 120.5, 119.8, 110.3, 36.1, 35.8, 28.6, 27.9, 26.8, 11.6; IR (KBr)ν_{max}: 2957, 1617, 1250 cm^{-1}; HRMS (ESI) Calcd for $C_{25}H_{23}BrNO$ 432.0958 (M + H$^+$); Found 432.0958 and 434.0940.

2-(8-Ethyl-7,8,9,10-tetrahydrobenzo[*c*]phenanthridin-6-yl)-5-methoxyphenol (4j)

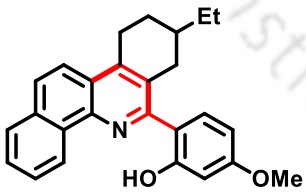

White solid (271 mg, 71%); mp 204-206 °C; ^{1}H NMR (500 MHz, $CDCl_3$) δ 13.53 (s, 1H), 9.04 (d, *J* = 8.1 Hz, 1H), 7.90 (d, *J* = 7.8 Hz, 1H), 7.85 (d, *J* = 9.1 Hz, 1H), 7.79 (d, *J* = 9.1 Hz, 1H), 7.72 (t, *J* = 7.4 Hz, 1H), 7.67 (t, *J* = 7.3 Hz, 1H), 7.62 (d, *J* = 8.7 Hz, 1H), 6.72 (s, 1H), 6.55 (d, *J* = 10.3 Hz, 1H), 3.89 (s, 3H), 3.42 (d, *J* = 22.7 Hz, 1H), 3.20 – 3.15 (m, 1H), 3.11 (d, *J* = 16.5 Hz, 1H), 2.74 (dd, *J* = 15.9, 8.9 Hz, 1H), 2.19 – 2.16 (m, 1H), 1.55 – 1.41 (m, 4H), 0.97 (t, *J* = 6.8 Hz, 3H); ^{13}C NMR (100 MHz, $CDCl_3$) δ 161.6, 160.0, 156.2, 144.8, 141.0, 133.3, 131.4, 130.4, 129.6, 128.0, 128.0, 127.5, 127.4, 123.9, 123.7, 120.5, 115.2, 105.3, 102.3, 55.4, 36.7, 36.0, 28.8, 28.0, 26.9, 11.6; IR (KBr)ν_{max}: 2950, 1620, 1251 cm^{-1}; HRMS (ESI) Calcd for $C_{26}H_{26}NO_2$ 384.1959 (M + H$^+$); Found 384.1958.

2-(8-Methyl-7,8,9,10-tetrahydrobenzo[*c*]phenanthridin-6-yl)phenol (4k)

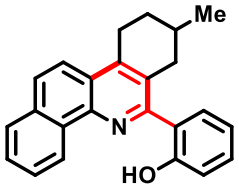

White solid (244 mg, 72%); mp 212-214 °C; ^{1}H NMR (500 MHz, $CDCl_3$) δ 12.39 (s, 1H), 9.11 – 9.08 (m, 1H), 7.91 (d, *J* = 7.6 Hz, 1H), 7.84 (q, *J* = 9.1 Hz, 2H), 7.72 (t, *J* = 7.4 Hz, 1H), 7.70 – 7.67 (m, 1H), 7.65 (d, *J* = 7.7 Hz, 1H), 7.36 (t, *J* = 7.7 Hz, 1H), 7.19 (d, *J* = 8.1 Hz, 1H), 6.98 (t, *J* = 7.5 Hz, 1H), 3.44 – 3.40 (m, 1H), 3.19 (dt, *J* = 17.8, 8.8 Hz, 1H), 3.06 (d, *J* = 16.2 Hz, 1H), 2.75 (dd, *J* = 16.0, 10.5 Hz, 1H), 2.13 – 2.09 (m, 1H), 1.70 (s, 1H), 1.63 – 1.56 (m, 1H), 1.11 (d, *J* = 6.4 Hz, 3H); ^{13}C NMR (125 MHz, $CDCl_3$) δ 157.4, 155.8, 145.0, 141.2, 133.3, 130.7, 130.4, 130.1, 128.7, 128.2, 128.0, 128.0, 127.6, 124.2, 124.0, 122.5, 120.5, 118.6, 118.0, 38.2, 30.5, 29.2, 26.9, 21.7; IR (KBr)ν_{max}: 2958, 1614, 1250 cm^{-1}; HRMS (ESI) Calcd for $C_{24}H_{22}NO$ 340.1696 (M + H$^+$); Found 340.1705.

4-Chloro-2-(8-methyl-7,8,9,10-tetrahydrobenzo[*c*]phenanthridin-6-yl)phenol (4l)

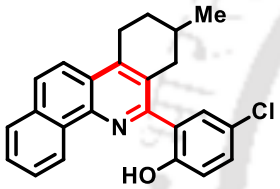

White solid (264 mg, 71%); mp 189-191 °C; ^{1}H NMR (400 MHz, $CDCl_3$) δ 12.39 (s, 1H), 9.02 (d, *J* = 7.8 Hz, 1H), 7.91 (d, *J* = 7.5 Hz, 1H), 7.81 (s, 2H), 7.75 – 7.67 (m, 2H), 7.59 (d, *J* = 2.4 Hz, 1H), 7.30 (dd, *J* = 8.7, 2.4 Hz, 1H), 7.11 (d, *J* = 8.7 Hz, 1H), 3.34 (dd, *J* = 18.1, 4.4 Hz, 1H), 3.13 (dt, *J* = 17.7, 8.5 Hz, 1H), 3.01 (d, *J* = 16.1 Hz, 1H), 2.68 (dd, *J* = 16.1, 10.3 Hz, 1H), 2.10 – 2.05 (m, 1H), 1.71 – 1.67 (m, 1H), 1.53 (dp, *J* = 17.6, 6.5 Hz, 1H), 1.11 (d, *J* = 6.5 Hz, 3H); ^{13}C NMR (125 MHz, $CDCl_3$) δ 156.1, 154.5, 145.3, 141.2, 133.4, 130.4, 129.9, 129.8, 128.4, 128.3, 128.1, 127.8, 124.5, 123.9, 123.7, 123.4, 120.4, 119.3, 37.9, 30.3, 29.0, 26.8, 21.6; IR (KBr)ν_{max}: 2957, 1614, 1251 cm^{-1}; HRMS (ESI) Calcd for $C_{24}H_{21}ClNO$ 374.1306 (M + H$^+$); Found 374.1305.

4-Bromo-2-(8-methyl-7,8,9,10-tetrahydrobenzo[*c*]phenanthridin-6-yl)phenol (4m)

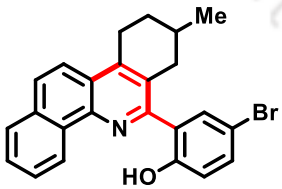

Pale yellow solid (296 mg, 71%); mp 228-230 °C; ^{1}H NMR (400 MHz, DMSO-d_6) δ 9.37 (d, *J* = 8.6 Hz, 1H), 8.30 – 8.26 (m, 2H), 8.00 – 7.94 (m, 2H), 7.76 – 7.71 (m, 2H), 7.34 (d, *J* = 7.9 Hz, 1H), 7.23 (d, *J* = 8.1 Hz, 1H), 3.45 – 3.36 (m, 1H), 2.88 (dd, *J* = 16.7, 3.8 Hz, 1H), 2.72 (s, 1H), 2.62 (dd, *J* = 16.8, 10.6 Hz, 1H), 2.26 – 2.24 (m, 1H), 2.02 – 2.00 (m, 1H), 1.74 – 1.64 (m, 1H), 1.22 (d, *J* = 6.4 Hz, 3H); ^{13}C NMR (125 MHz, $CDCl_3$) δ 155.8, 133.9, 133.9, 133.8, 133.4, 132.6, 132.6, 130.7, 129.0, 128.9, 128.8, 128.2, 126.2, 124.8, 124.1, 120.1, 111.1, 36.9, 30.0, 28.7, 27.0, 21.5; IR (KBr)ν_{max}: 2956, 1613, 1251 cm^{-1}; HRMS (ESI) Calcd for $C_{24}H_{21}BrNO$ 418.0801 (M + H$^+$); Found 418.0812 and 420.0796.

2-(9-Methyl-7,8,9,10-tetrahydrobenzo[*c*]phenanthridin-6-yl)phenol (4n)

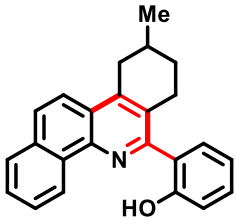

White solid (244 mg, 72%); mp 178-180 °C; ^{1}H NMR (500 MHz, $CDCl_3$) δ 12.54 (s, 1H), 9.09 (d, *J* = 8.1 Hz, 1H), 7.90 (d, *J* = 7.7 Hz, 1H), 7.88 – 7.85 (m, 1H), 7.81 (d, *J* = 8.8 Hz, 1H), 7.72 (t, *J* = 7.4 Hz, 1H), 7.69 – 7.65 (m, 2H), 7.36 (t, *J* = 7.7 Hz, 1H), 7.18 (d, *J* = 8.2 Hz, 1H), 6.97 (t, *J* = 7.5 Hz, 1H), 3.45 (d, *J* = 17.7 Hz, 1H), 3.16 (t, *J* = 13.1 Hz, 1H), 3.08 (d, *J* = 16.2 Hz, 1H), 2.7 – 2.67 (m, 1H), 2.04 (s, 1H), 1.98 (d, *J* = 13.9 Hz, 1H), 1.26 (d, *J* = 11.4 Hz, 1H), 1.22 (d, *J* = 6.5 Hz, 3H); ^{13}C NMR (100 MHz, $CDCl_3$) δ 157.5, 155.9, 145.1, 141.4, 133.3, 130.6, 130.3, 130.0, 128.1, 128.0, 127.8, 127.6, 124.2, 124.0, 122.6, 120.4, 118.5, 117.9, 35.5, 31.2, 30.1, 28.8, 22.3; IR (KBr)ν_{max}: 2956, 1617, 1251 cm^{-1}; HRMS (ESI) Calcd for $C_{24}H_{22}NO$ 340.1696 ($M + H^+$); Found 340.1696.

4-Chloro-2-(9-methyl-7,8,9,10-tetrahydrobenzo[*c*]phenanthridin-6-yl)phenol (4o)

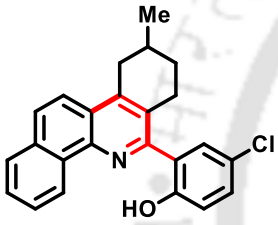

White solid (264 mg, 71%); mp 200-202 °C; ^{1}H NMR (500 MHz, $CDCl_3$) δ 12.51 (s, 1H), 9.04 (t, *J* = 6.4 Hz, 1H), 7.92 – 7.82 (m, 3H), 7.70 (dq, *J* = 14.8, 7.2 Hz, 2H), 7.64 – 7.63 (m, 1H), 7.29 (dd, *J* = 8.7, 2.2 Hz, 1H), 7.10 (d, *J* = 8.8 Hz, 1H), 3.46 (t, *J* = 17.4 Hz, 1H), 3.16 – 3.05 (m, 2H), 2.76 – 2.67 (m, 1H), 2.03 (s, 2H), 1.29 – 1.24 (m, 1H), 1.22 (d, *J* = 6.6 Hz, 3H); ^{13}C NMR (125 MHz, $CDCl_3$) δ 156.3, 154.6, 145.5, 141.5, 133.4, 130.6, 130.3, 129.9, 129.8, 128.3, 128.2, 128.1, 127.7, 124.5, 123.9, 123.7, 123.2, 120.4, 119.3, 35.5, 31.2, 29.9, 28.7, 22.3; IR (KBr)ν_{max}: 2958, 1615, 1251 cm^{-1}; HRMS (ESI) Calcd for $C_{24}H_{21}ClNO$ 374.1307 ($M + H^+$); Found 374.1308.

4-Bromo-2-(9-methyl-7,8,9,10-tetrahydrobenzo[*c*]phenanthridin-6-yl)phenol (4p)

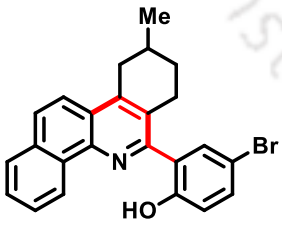

Pale yellow solid (296 mg, 71%); mp 268-270 °C; ^{1}H NMR (400 MHz, DMSO-d_6) δ 9.36 (d, *J* = 9.1 Hz, 1H), 8.29 (d, *J* = 8 Hz, 1H), 8.00 – 7.94 (m, 2H), 7.71 – 7.69 (m, 2H), 7.33 (d, *J* = 7.9 Hz, 2H), 7.21 (d, *J* = 8.7 Hz, 1H), 3.03 – 2.99 (m, 2H), 2.91 – 2.85 (m, 1H), 2.72 – 2.71 (m, 1H), 2.20 – 2.10 (m, 2H), 1.57 (dq, *J* = 16.3, 5.9, 5.3 Hz, 1H), 1.38 (d, *J* = 6.5 Hz, 3H); ^{13}C NMR (150 MHz, $CDCl_3$) δ 155.1, 151.3, 142.4, 139.4, 134.8, 133.7, 132.7, 131.8, 130.5, 130.3, 128.7, 128.6, 128.4, 126.0, 125.8, 124.1, 119.8, 119.3, 110.6, 35.8, 27.7, 26.9, 21.7, 21.1; IR (KBr)ν_{max}: 2958, 2925, 1610, cm^{-1}; HRMS (ESI) Calcd for $C_{24}H_{21}BrNO$ 418.0801 ($M + H^+$); Found 418.0806 and 420.0787.

4-Chloro-2-(8-phenyl-7,8,9,10-tetrahydrobenzo[*c*]phenanthridin-6-yl)phenol (4q)

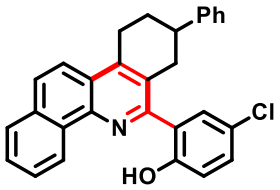

Green solid (309 mg, 71%); mp 175 °C; ^{1}H NMR (500 MHz, $CDCl_3$) δ 12.20 (s, 1H), 9.06 (d, *J* = 8.0 Hz, 1H), 7.93 (d, *J* = 7.4 Hz, 1H), 7.84 (s, 2H), 7.75 – 7.71 (m, 2H), 7.53 (s, 1H), 7.33 (d, *J* = 7.1 Hz, 2H), 7.24 (d, *J* = 5.4 Hz, 4H), 7.06 (d, *J* = 8.5 Hz, 1H), 3.44 (d, *J* = 16.9 Hz, 1H), 3.28 (d, *J* = 8.3 Hz, 1H), 3.19 (s, 2H), 2.77 (s, 1H), 2.30 (s, 1H), 2.03 (s, 1H); ^{13}C NMR (100 MHz, $CDCl_3$) δ 155.9, 154.7, 145.2, 144.8, 141.7, 133.4, 130.5, 130.4, 129.8, 129.7, 128.8, 128.5, 128.4, 128.2, 127.8, 127.0, 126.7, 124.4, 124.0, 123.7, 123.5, 120.5, 119.3, 40.5, 37.4, 29.5, 27.5; IR (KBr)ν_{max}: 2948, 1614, 1255 cm^{-1}; HRMS (ESI) Calcd for $C_{29}H_{23}ClNO$ 436.1463 ($M + H^+$); Found 436.1472.

2-(7,8,9,10-Tetrahydrobenzo[*c*]phenanthridin-6-yl)phenol (4r)

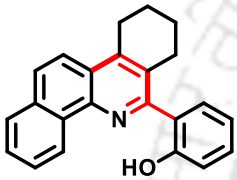

White solid (231 mg, 71%); mp 176 °C; ^{1}H NMR (400 MHz, $CDCl_3$) δ 12.44 (s, 1H), 9.14 (d, *J* = 8.0 Hz, 1H), 7.94 – 7.85 (m, 3H), 7.76 – 7.68 (m, 2H), 7.64 (d, *J* = 6.5 Hz, 1H), 7.35 (t, *J* = 7.7 Hz, 1H), 7.20 (d, *J* = 7.3 Hz, 1H), 6.98 (t, *J* = 7.5 Hz, 1H), 3.31 (t, *J* = 6.6 Hz, 2H), 3.08 (t, *J* = 5.9 Hz, 2H), 2.08 – 2.02 (m, 2H), 1.80 – 1.76 (m, 2H); ^{13}C NMR (100 MHz, $CDCl_3$) δ 157.5, 156.0, 145.1, 141.4, 133.3, 130.7, 130.6, 130.5, 130.3, 128.2, 128.0, 127.9, 127.6, 124.4, 124.0, 122.6, 120.4, 118.5, 117.9, 30.1, 26.7, 23.0, 22.5; IR (KBr)ν_{max}: 2957, 1614, 1251 cm^{-1}; HRMS (ESI) Calcd for $C_{23}H_{20}NO$ 326.1540 ($M + H^+$); Found 326.1555.

2-(12-Bromo-8-(*tert*-butyl)-7,8,9,10-tetrahydrobenzo[*c*]phenanthridin-6-yl)phenol (4s)

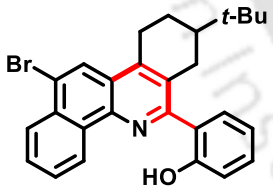

Yellow solid (317 mg, 69%); mp 162-164 °C; ^{1}H NMR (400 MHz, DMSO-d_6) δ 9.23 (d, J = 7.6 Hz, 1H), 8.16 – 8.15 (m, 3H), 7.82 (p, J = 6.6 Hz, 2H), 7.43 (d, J = 7.4 Hz, 1H), 7.10 – 7.06 (m, 1H), 7.04 (d, J = 7.6 Hz, 1H), 3.30 – 3.15 (m, 2H), 2.69 (d, J = 18.0 Hz, 1H), 2.58 (d, J = 10.2 Hz, 1H), 2.18 (d, J = 8.6 Hz, 1H), 1.49 – 1.41 (m, 2H), 0.87 (s, 9H); ^{13}C NMR (100 MHz, DMSO-d_6) δ 155.3, 135.9, 133.6, 133.2, 132.9, 131.6, 131.1, 130.5, 129.7, 129.3, 129.0, 128.1, 125.2, 124.4, 124.4, 121.2, 120.2, 119.6, 116.3, 43.3, 32.5, 28.1, 27.4, 27.3, 23.3; IR (KBr)ν_{max}: 2957, 1620, 1251 cm^{-1}; HRMS (ESI) Calcd for $C_{27}H_{27}BrNO$ 460.1271 ($M + H^+$); Found 460.1279, 462.1259.

2-(12-Bromo-8-(*tert*-butyl)-7,8,9,10-tetrahydrobenzo[*c*]phenanthridin-6-yl)-4-chlorophenol (4t)

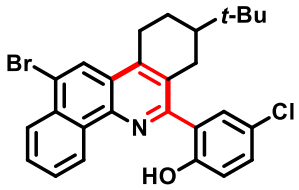

Yellow solid (320 mg, 65%); mp 174-176 °C; ^{1}H NMR (400 MHz, DMSO-d_6) δ 9.20 – 9.18 (m, 1H), 8.35 – 8.32 (m, 1H), 8.26 (d, *J* = 8.0 Hz, 1H), 8.08 (s, 1H), 7.79 – 7.78 (d, *J* = 3.8 Hz, 1H), 7.41 (d, *J* = 3.8 Hz, 1H), 7.08 (d, *J* = 9.4 Hz, 1H), 7.03 (d, *J* = 8.7 Hz, 1H), 3.07 (d, *J* = 14.1 Hz, 2H), 2.71 (d, *J* = 16.1 Hz, 2H), 2.21 – 2.19 (m, 1H), 1.48 – 1.42 (m, 2H), 0.90 (s, 9H); ^{13}C NMR (100 MHz, $CDCl_3$) δ 157.6, 156.2, 151.9, 145.0, 140.9, 132.1, 130.9, 130.7, 130.1, 127.7, 124.3, 123.4, 122.5, 121.4, 119.6, 118.6, 118.0, 116.5, 112.0, 44.7, 32.5, 31.7, 28.2, 27.5, 23.8; IR (KBr)ν_{max}: 2957, 1620, 1251 cm^{-1}; HRMS (ESI) Calcd for $C_{27}H_{26}BrClNO$ 494.0881 (M + H$^+$); Found 494.0903, 496.0886.

9-(*tert*-Butyl)benzo[*c*]chromeno[4,3,2-*gh*]phenanthridine (5a)

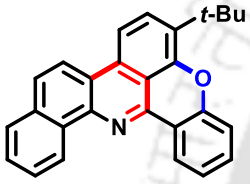

Light green solid (54 mg, 72%); mp 220-222°C; ^{1}H NMR (600 MHz, $CDCl_3$) δ 9.54 (d, *J* = 8.2 Hz, 1H), 8.92 (d, *J* = 8.1 Hz, 1H), 8.40 (d, *J* = 8.9 Hz, 1H), 8.15 (d, *J* = 8.7 Hz, 1H), 7.94 (d, *J* = 7.9 Hz, 1H), 7.91 (d, *J* = 8.5 Hz, 2H), 7.75 (t, *J* = 7.5 Hz, 1H), 7.67 (t, *J* = 6.8 Hz, 1H), 7.56 – 7.54 (m, 1H), 7.39 (t, *J* = 7.3 Hz, 2H), 1.62 (s, 9H); ^{13}C NMR (150 MHz, $CDCl_3$) δ 153.9, 150.7, 146.5, 141.5, 133.7, 132.6, 132.4, 132.1, 131.9, 130.2, 127.7, 127.3, 126.7, 126.6, 125.3, 125.1, 124.1, 121.9, 120.3, 120.1, 117.1, 116.0, 114.4, 35.1, 29.8; IR (KBr)ν_{max}: 2920, 1540, 1248 cm^{-1}; HRMS (ESI) Calcd for $C_{27}H_{22}NO$ 376.1696 (M + H$^+$); Found 376.1705.

9-(*tert*-Butyl)-13-chlorobenzo[*c*]chromeno[4,3,2-*gh*]phenanthridine (5b)

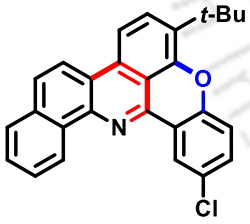

Light green solid (61 mg, 75%); mp 245-247 °C; ^{1}H NMR (600 MHz, $CDCl_3$) δ 9.43 (d, *J* = 8.2 Hz, 1H), 8.75 (d, *J* = 2.4 Hz, 1H), 8.29 (d, *J* = 8.8 Hz, 1H), 8.05 (d, *J* = 8.6 Hz, 1H), 7.90 (d, *J* = 7.9 Hz, 1H), 7.85 (dd, *J* = 12.3, 8.7 Hz, 2H), 7.74 (t, *J* = 7.4 Hz, 1H), 7.65 (t, *J* = 7.3 Hz, 1H), 7.44 (d, *J* = 8.7 Hz, 1H), 7.28 (d, *J* = 8.7 Hz, 1H), 1.61 (s, 9H); ^{13}C NMR (150 MHz, $CDCl_3$) δ 152.3, 150.3, 145.1, 141.3, 133.6, 132.5, 132.3, 131.9, 131.7, 130.3, 129.5, 127.7, 127.4, 127.0, 126.8, 125.1, 124.7, 123.1, 120.2, 120.1, 118.5, 115.6, 114.6, 35.0, 29.9; IR (KBr)ν_{max}: 2929, 1550, 1251 cm^{-1}; HRMS (ESI) Calcd for $C_{27}H_{21}ClNO$ 410.1307 (M + H$^+$); Found 410.1312.

13-Bromo-9-(*tert*-butyl)benzo[*c*]chromeno[4,3,2-*gh*]phenanthridine (5c)

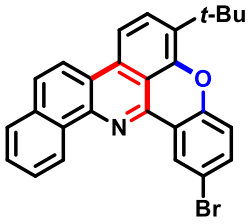

Light green solid (65 mg, 72%); mp 250 °C; ^{1}H NMR (600 MHz, $CDCl_3$) δ 9.45 (d, *J* = 8.2 Hz, 1H), 8.92 (s, 1H), 8.31 (d, *J* = 8.8 Hz, 1H), 8.08 (d, *J* = 8.5 Hz, 1H), 7.91 (d, *J* = 7.9 Hz, 1H), 7.87 (dd, *J* = 13.2, 8.7 Hz, 2H), 7.75 (t, *J* = 7.5 Hz, 1H), 7.66 (t, *J* = 7.3 Hz, 1H), 7.59 (d, *J* = 8.6 Hz, 1H), 7.23 (d, *J* = 8.6 Hz, 1H), 1.61 (s, 9H); ^{13}C NMR (150 MHz, $CDCl_3$) δ 152.8, 150.3, 145.0, 141.3, 134.6, 133.7, 132.5, 132.4, 131.9, 130.4, 127.8, 127.7, 127.5, 127.0, 126.8, 125.1, 123.6, 120.2, 120.1, 118.9, 117.0, 115.7, 114.7, 35.0, 29.9; IR (KBr)ν_{max}: 2921, 1550, 1260 cm^{-1}; HRMS (ESI) Calcd for $C_{27}H_{21}BrNO$ 454.0802 (M + H^+); Found 454.0807.

9-(*tert*-Butyl)-11,13-dichlorobenzo[*c*]chromeno[4,3,2-*gh*]phenanthridine (5d)

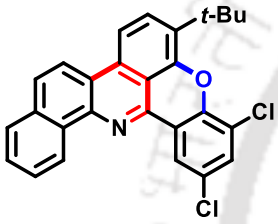

Light green solid (66 mg, 75%); mp 254-256 °C; ^{1}H NMR (600 MHz, $CDCl_3$) δ 9.43 (d, *J* = 8.1 Hz, 1H), 8.70 (s, 1H), 8.33 (d, *J* = 8.8 Hz, 1H), 8.14 (d, *J* = 8.6 Hz, 1H), 7.92 (t, *J* = 8.7 Hz, 3H), 7.76 (t, *J* = 7.3 Hz, 1H), 7.67 (t, *J* = 7.2 Hz, 1H), 7.56 (s, 1H), 1.66 (s, 9H); ^{13}C NMR (150 MHz, $CDCl_3$) δ 149.7, 148.7, 144.4, 141.3, 133.7, 133.1, 132.5, 131.9, 131.7, 130.6, 129.2, 127.7, 127.6, 127.4, 126.9, 125.0, 124.3, 123.3, 123.1, 120.4, 120.1, 115.5, 115.3, 35.1, 29.5; IR (KBr)ν_{max}: 2919, 1540, 1250 cm^{-1}; HRMS (ESI) Calcd for $C_{27}H_{20}Cl_2NO$ 444.0917 (M + H^+); Found 444.1122.

9-(*tert*-Butyl)-12-methoxybenzo[*c*]chromeno[4,3,2-*gh*]phenanthridine (5e)

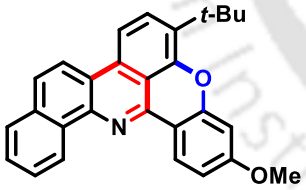

Light green solid (54 mg, 67%); mp 210-212 °C; ^{1}H NMR (600 MHz, $CDCl_3$) δ 9.50 (d, *J* = 8.1 Hz, 1H), 8.81 (d, *J* = 8.7 Hz, 1H), 8.36 (d, *J* = 8.8 Hz, 1H), 8.12 (d, *J* = 8.5 Hz, 1H), 7.93 (d, *J* = 7.8 Hz, 1H), 7.87 (d, *J* = 8.6 Hz, 2H), 7.73 (t, *J* = 7.3 Hz, 1H), 7.65 (t, *J* = 7.3 Hz, 1H), 6.96 (d, *J* = 8.6 Hz, 1H), 6.83 (s, 1H), 3.96 (s, 3H), 1.62 (s, 9H); ^{13}C NMR (150 MHz, $CDCl_3$) δ 163.0, 155.2, 150.9, 146.7, 133.7, 132.6, 132.3, 131.9, 130.0, 127.7, 127.3, 126.6, 126.5, 126.0, 125.1, 120.3, 119.5, 115.5, 115.1, 114.5, 114.2, 112.3, 100.6, 55.8, 35.0, 29.9. IR (KBr)ν_{max}: 2920, 1545, 1260 cm^{-1}; HRMS (ESI) Calcd for $C_{28}H_{24}NO_2$ 406.1802 (M + H^+); Found 406.1811.

13-Chloro-9-*iso*propylbenzo[c]chromeno[4,3,2-*gh*]phenanthridine (5f)

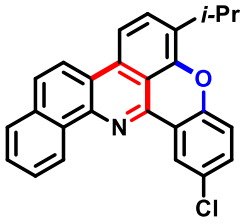

Light green solid (58 mg, 73%); mp 214-216 °C; ^{1}H NMR (500 MHz, $CDCl_3$) δ 9.47 (d, *J* = 8.2 Hz, 1H), 8.78 (d, *J* = 2.4 Hz, 1H), 8.33 (d, *J* = 8.9 Hz, 1H), 8.15 (d, *J* = 8.5 Hz, 1H), 7.92 (d, *J* = 7.9 Hz, 1H), 7.89 (d, *J* = 8.9 Hz, 1H), 7.80 (d, *J* = 8.5 Hz, 1H), 7.76 (d, *J* = 7.5 Hz, 1H), 7.67 (t, *J* = 7.4 Hz, 1H), 7.44 (dd, *J* = 8.7, 2.4 Hz, 1H), 7.25 (s, 1H), 3.68 (p, *J* = 6.9 Hz, 1H), 1.42 (d, *J* = 6.9 Hz, 6H); ^{13}C NMR (125 MHz, $CDCl_3$) δ 152.8, 148.9, 145.3, 141.6, 133.7, 132.3, 132.1, 131.8, 131.1, 129.9, 129.6, 127.7, 127.5, 127.1, 126.8, 125.2, 124.8, 123.4, 120.5, 120.2, 118.8, 115.3, 115.1, 27.0, 22.7; IR (KBr)ν_{max}: 2918, 1570, 1245 cm^{-1}; HRMS (ESI) Calcd for $C_{26}H_{19}ClNO$ 396.1150 (M + H$^+$); Found 396.1145.

9-Ethylbenzo[*c*]chromeno[4,3,2-*gh*]phenanthridine (5g)

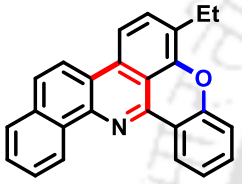

Light green solid (47 mg, 68%); mp 214-216 °C; ^{1}H NMR (500 MHz, $CDCl_3$) δ 9.54 (d, *J* = 8.3 Hz, 1H), 8.91 (d, *J* = 7.7 Hz, 1H), 8.39 (d, *J* = 8.9 Hz, 1H), 8.16 (d, *J* = 8.3 Hz, 1H), 7.94 (d, *J* = 7.9 Hz, 1H), 7.91 (d, *J* = 8.8 Hz, 1H), 7.75 (d, *J* = 8.3 Hz, 2H), 7.66 (t, *J* = 7.4 Hz, 1H), 7.54 (t, *J* = 7.6 Hz, 1H), 7.37 (t, *J* = 9.0 Hz, 2H), 3.01 (q, *J* = 7.6 Hz, 2H), 1.40 (t, *J* = 7.6 Hz, 3H); ^{13}C NMR (150 MHz, $CDCl_3$) δ 154.4, 149.9, 146.5, 141.7, 133.7, 132.7, 132.5, 132.2, 132.0, 127.7, 127.3, 126.7, 126.7, 126.6, 125.3, 125.1, 124.1, 122.1, 120.4, 120.3, 117.3, 115.5, 114.6, 23.0, 14.3; IR (KBr)ν_{max}: 2918, 1560, 1258 cm^{-1}; HRMS (ESI) Calcd for $C_{25}H_{18}NO$ 348.1383 (M + H$^+$); Found 348.1396.

13-Chloro-9-ethylbenzo[*c*]chromeno[4,3,2-*gh*]phenanthridine (5h)

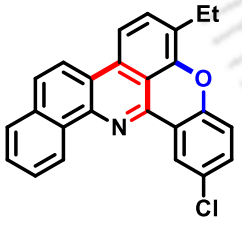

Light green solid (53 mg, 71%); mp 164-166 °C; ^{1}H NMR (500 MHz, $CDCl_3$) δ 9.32 (d, *J* = 8.2 Hz, 1H), 8.58 (d, *J* = 2.6 Hz, 1H), 8.17 (d, *J* = 8.9 Hz, 1H), 7.91 (d, *J* = 8.4 Hz, 1H), 7.87 (d, *J* = 7.8 Hz, 1H), 7.79 (d, *J* = 8.8 Hz, 1H), 7.72 – 7.69 (m, 1H), 7.65 – 7.62 (m, 1H), 7.55 (d, *J* = 8.3 Hz, 1H), 7.35 (dd, *J* = 8.7, 2.6 Hz, 1H), 7.11 (d, *J* = 8.7 Hz, 1H), 2.83 (t, *J* = 7.6 Hz, 2H), 1.34 (t, *J* = 7.6 Hz, 3H); ^{13}C NMR (125 MHz, $CDCl_3$) δ 152.6, 149.3, 144.9, 141.4, 133.6, 132.4, 132.2, 132.0, 131.5, 129.4, 127.6, 127.3, 126.9, 126.7, 126.5, 125.1, 124.6, 123.2, 120.3, 120.0, 118.6, 114.9, 114.6, 22.7, 14.1; IR (KBr)ν_{max}: 2927, 1575, 1248 cm^{-1}; HRMS (ESI) Calcd for $C_{25}H_{17}ClNO$ 382.0994 (M + H$^+$); Found 382.0993.

13-Bromo-9-ethylbenzo[*c*]chromeno[4,3,2-*gh*]phenanthridine (5i)

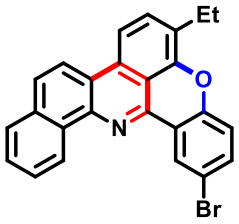

Light green solid (60 mg, 70%); mp 247-249 °C; ^{1}H NMR (500 MHz, $CDCl_3$) δ 9.46 (d, *J* = 8.3 Hz, 1H), 8.91 (s, 1H), 8.32 (d, *J* = 8.9 Hz, 1H), 8.10 (d, *J* = 8.3 Hz, 1H), 7.93 (d, *J* = 7.9 Hz, 1H), 7.89 (d, *J* = 8.9 Hz, 1H), 7.76 (t, *J* = 7.6 Hz, 1H), 7.70 – 7.66 (m, 2H), 7.58 (d, *J* = 8.7 Hz, 1H), 7.18 (d, *J* = 8.7 Hz, 1H), 2.95 (q, *J* = 7.6 Hz, 2H), 1.37 (t, *J* = 7.6 Hz, 3H); ^{13}C NMR (125 MHz, $CDCl_3$) δ 153.3, 149.5, 145.0, 141.6, 134.6, 133.7, 132.8, 132.4, 132.1, 127.8, 127.7, 127.5, 127.1, 126.8, 126.8, 125.2, 123.8, 120.5, 120.1, 119.1, 117.0, 115.2, 114.9, 22.8, 14.3; IR (KBr)ν_{max}: 2929, 1570, 1240 cm^{-1}; HRMS (ESI) Calcd for $C_{25}H_{17}BrNO$ 426.0489 (M + H$^+$); Found 426.0489 and 428.0471.

9-Ethyl-12-methoxybenzo[*c*]chromeno[4,3,2-*gh*]phenanthridine (5j)

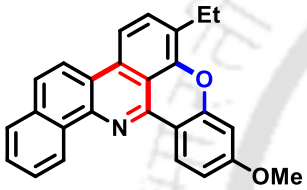

Light green solid (51 mg, 68%); mp 224 °C; ^{1}H NMR (500 MHz, $CDCl_3$) δ 9.50 (d, *J* = 8.2 Hz, 1H), 8.79 (d, *J* = 8.8 Hz, 1H), 8.36 (d, *J* = 8.9 Hz, 1H), 8.12 (d, *J* = 8.4 Hz, 1H), 7.93 (d, *J* = 7.9 Hz, 1H), 7.87 (d, *J* = 8.9 Hz, 1H), 7.72 (dd, *J* = 13.8, 8.1 Hz, 2H), 7.65 (t, *J* = 7.9 Hz, 1H), 6.95 (dd, *J* = 8.8, 2.4 Hz, 1H), 6.83 (d, *J* = 2.4 Hz, 1H), 3.95 (s, 3H), 2.99 (q, *J* = 7.6 Hz, 2H), 1.40 (t, *J* = 7.6 Hz, 3H); ^{13}C NMR (125 MHz, $CDCl_3$) δ 163.1, 155.7, 150.1, 146.7, 141.9, 133.8, 132.4, 132.2, 127.7, 127.2, 126.6, 126.6, 126.5, 126.1, 125.2, 120.3, 119.8, 115.4, 115.1, 114.7, 112.3, 100.9, 55.8, 22.9, 14.3. IR (KBr)ν_{max}: 2927, 1574, 1248 cm^{-1}; HRMS (ESI) Calcd for $C_{26}H_{20}NO_2$ 378.1489 (M + H$^+$); Found 378.1490.

9-Methylbenzo[*c*]chromeno[4,3,2-*gh*]phenanthridine (5k)

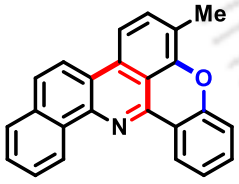

Light green solid (45 mg, 67%); mp 196-198 °C; ^{1}H NMR (500 MHz, $CDCl_3$) δ 9.54 (d, *J* = 8.2 Hz, 1H), 8.91 (d, *J* = 7.8 Hz, 1H), 8.38 (d, *J* = 8.9 Hz, 1H), 8.12 (d, *J* = 8.3 Hz, 1H), 7.94 (d, *J* = 7.9 Hz, 1H), 7.91 (d, *J* = 8.9 Hz, 1H), 7.75 (t, *J* = 7.1 Hz, 1H), 7.71 (d, *J* = 8.3 Hz, 1H), 7.67 (t, *J* = 7.4 Hz, 1H), 7.54 (t, *J* = 8.5 Hz, 1H), 7.37 (t, *J* = 7.6 Hz, 2H), 2.58 (s, 3H); ^{13}C NMR (100 MHz, $CDCl_3$) δ 154.4, 150.3, 146.4, 141.7, 134.2, 133.7, 132.5, 132.2, 132.0, 127.7, 127.3, 126.7, 125.3, 125.2, 124.1, 122.1, 120.6, 120.3, 117.3, 115.4, 114.3, 29.8; IR (KBr)ν_{max}: 2924, 1550, 1259 cm^{-1}; HRMS (ESI) Calcd for $C_{24}H_{16}NO$ 334.1227 (M + H$^+$); Found 334.1221.

13-Chloro-8-methylbenzo[*c*]chromeno[4,3,2-*gh*]phenanthridine (5l)

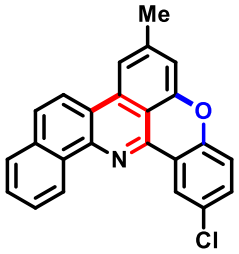

Light green solid (51 mg, 70%); mp 208-210 °C; ^{1}H NMR (500 MHz, $CDCl_3$) δ 9.49 (d, *J* = 8.3 Hz, 1H), 8.78 (d, *J* = 2.6 Hz, 1H), 8.33 (d, *J* = 8.9 Hz, 1H), 7.96 – 7.93 (m, 2H), 7.90 (d, *J* = 8.9 Hz, 1H), 7.76 (ddd, *J* = 8.2, 7.0, 1.2 Hz, 1H), 7.70 – 7.66 (m, 1H), 7.44 (dd, *J* = 8.7, 2.6 Hz, 1H), 7.22 (d, *J* = 8.8 Hz, 1H), 7.12 (s, 1H), 2.64 (s, 3H); ^{13}C NMR (125 MHz, $CDCl_3$) δ 152.7, 152.6, 145.1, 143.1, 142.5, 134.3, 133.9, 132.2, 131.8, 129.6, 127.7, 127.7, 127.0, 126.9, 125.3, 124.7, 123.4, 120.3, 120.2, 118.8, 115.2, 113.6, 112.5, 22.9; IR (KBr)ν_{max}: 2927, 1557, 1241 cm^{-1}; HRMS (ESI) Calcd for $C_{24}H_{15}ClO$ 368.0837 ($M + H^+$); Found 368.0836.

13-Bromo-9-methylbenzo[*c*]chromeno[4,3,2-*gh*]phenanthridine (5m)

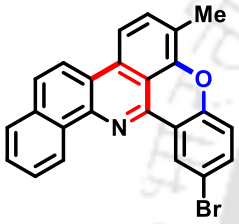

Light green solid (58 mg, 70%); mp 244-246 °C; ^{1}H NMR (500 MHz, $CDCl_3$) δ 9.32 (d, *J* = 8.2 Hz, 1H), 8.72 (d, *J* = 2.4 Hz, 1H), 8.15 (d, *J* = 8.8 Hz, 1H), 7.87 (t, *J* = 7.4 Hz, 2H), 7.79 (d, *J* = 8.8 Hz, 1H), 7.73 – 7.70 (m, 1H), 7.66 – 7.63 (m, 1H), 7.49 (d, *J* = 8.6 Hz, 2H), 7.04 (d, *J* = 8.7 Hz, 1H), 2.40 (s, 3H); ^{13}C NMR (125 MHz, $CDCl_3$) δ 153.1, 149.7, 144.6, 141.4, 134.4, 134.1, 133.6, 132.2, 132.0, 127.6, 127.4, 126.9, 126.7, 125.1, 123.6, 120.5, 120.4, 120.0, 119.0, 116.9, 114.9, 114.4, 15.5; IR (KBr)ν_{max}: 2930, 1570, 1250 cm^{-1}; HRMS (ESI) Calcd for $C_{24}H_{15}BrNO$ 412.0332 ($M + H^+$); Found 412.0332 and 414.0371.

8-Methylbenzo[*c*]chromeno[4,3,2-*gh*]phenanthridine (5n)

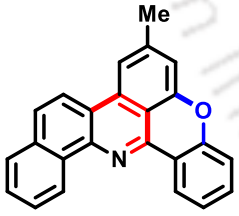

Light green solid (43 mg, 65%); mp 220-222 °C; ^{1}H NMR (500 MHz, $CDCl_3$) δ 9.51 (d, *J* = 8.2 Hz, 1H), 8.85 (d, *J* = 7.8 Hz, 1H), 8.32 (d, *J* = 8.8 Hz, 1H), 7.92 (d, *J* = 4.6 Hz, 2H), 7.87 (d, *J* = 8.8 Hz, 1H), 7.73 (t, *J* = 7.5 Hz, 1H), 7.66 (t, *J* = 7.4 Hz, 1H), 7.51 (t, *J* = 7.7 Hz, 1H), 7.35 (t, *J* = 7.5 Hz, 1H), 7.28 (d, *J* = 8.3 Hz, 1H), 7.11 (s, 1H), 2.62 (s, 3H); ^{13}C NMR (125 MHz, $CDCl_3$) δ 154.3, 152.9, 146.3, 142.8, 142.6, 134.3, 133.9, 132.3, 131.9, 127.7, 127.5, 126.6, 126.5, 125.3, 125.3, 124.0, 122.1, 120.4, 119.9, 117.2, 114.9, 113.7, 112.4, 22.8; IR (KBr)ν_{max}: 2930, 1580, 1258 cm^{-1}; HRMS (ESI) Calcd for $C_{24}H_{16}NO$ 334.1227 ($M + H^+$); Found 334.1229.

13-Chloro-9-methylbenzo[*c*]chromeno[4,3,2-*gh*]phenanthridine (5o)

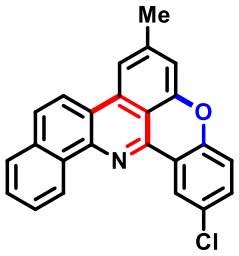

Light green solid (52 mg, 71%); mp 204-206 °C; ^{1}H NMR (500 MHz, $CDCl_3$) δ 9.39 (d, *J* = 8.2 Hz, 1H), 8.66 (s, 1H), 8.23 (d, *J* = 8.8 Hz, 1H), 7.95 (d, *J* = 8.2 Hz, 1H), 7.90 (d, *J* = 7.7 Hz, 1H), 7.84 (d, *J* = 8.8 Hz, 1H), 7.75 – 7.72 (m, 1H), 7.66 (td, *J* = 7.5, 6.9, 1.2 Hz, 1H), 7.56 (d, *J* = 8.2 Hz, 1H), 7.39 (dd, *J* = 8.7, 2.6 Hz, 1H), 7.16 (d, *J* = 8.7 Hz, 1H), 2.45 (s, 3H); ^{13}C NMR (150 MHz, $CDCl_3$) δ 152.6, 149.7, 144.9, 141.3, 134.1, 133.5, 132.2, 132.0, 131.7, 129.4, 127.7, 127.4, 126.9, 126.7, 125.0, 124.6, 123.1, 120.6, 120.4, 120.1, 118.7, 114.9, 114.4, 15.6; IR (KBr)ν_{max}: 2927, 1570, 1260 cm^{-1}; HRMS (ESI) Calcd for $C_{24}H_{15}ClNO$ 368.0837 (M + H$^+$); Found 368.0835.

13-Bromo-8-methylbenzo[*c*]chromeno[4,3,2-*gh*]phenanthridine (5p)

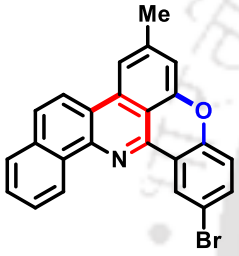

Light green solid (57 mg, 69%); mp 243-245 °C; ^{1}H NMR (400 MHz, $CDCl_3$) δ 9.46 (d, *J* = 8.2 Hz, 1H), 8.89 (d, *J* = 2.3 Hz, 1H), 8.30 (d, *J* = 8.9 Hz, 1H), 7.92 (s, 1H), 7.87 (s, 1H), 7.76 (t, *J* = 7.4 Hz, 2H), 7.68 (t, *J* = 7.5 Hz, 1H), 7.58 – 7.55 (m, 1H), 7.13 (d, *J* = 8.8 Hz, 1H), 7.09 (s, 1H), 2.62 (s, 3H); ^{13}C NMR (150 MHz, $CDCl_3$) δ 153.0, 152.4, 144.8, 143.0, 142.2, 134.5, 134.1, 133.7, 132.0, 127.7, 127.7, 127.6, 126.9, 126.8, 125.2, 123.7, 120.2, 120.0, 119.0, 116.9, 115.2, 113.4, 112.5, 22.9; IR (KBr)ν_{max}: 2937, 1520, 1260 cm^{-1}; HRMS (ESI) Calcd for $C_{24}H_{15}BrNO$ 412.0332 (M + H$^+$); Found 412.0324 and 414.0493.

13-Chloro-9-phenylbenzo[*c*]chromeno[4,3,2-*gh*]phenanthridine (5q)

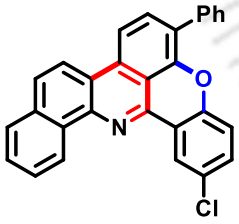

Light green solid (64 mg, 75%); mp 246-248 °C; ^{1}H NMR (500 MHz, $CDCl_3$) δ 9.49 (d, *J* = 8.2 Hz, 1H), 8.79 (d, *J* = 2.5 Hz, 1H), 8.37 (d, *J* = 8.9 Hz, 1H), 8.23 (s, 1H), 7.93 (d, *J* = 9.0 Hz, 2H), 7.90 (d, *J* = 8.5 Hz, 1H), 7.79 – 7.75 (m, 3H), 7.69 (t, *J* = 7.0 Hz, 1H), 7.55 (t, *J* = 7.5 Hz, 2H), 7.46 (t, *J* = 7.5 Hz, 1H), 7.42 (dd, *J* = 8.7, 2.6 Hz, 1H), 7.16 (d, *J* = 8.8 Hz, 1H); ^{13}C NMR (100 MHz, $CDCl_3$) δ 152.4, 148.9, 136.8, 133.8, 133.8, 133.6, 132.0, 131.9, 129.8, 129.6, 128.6, 127.8, 127.3, 127.0, 125.2, 124.7, 124.5, 123.3, 120.3, 120.2, 119.0, 115.5, 115.4; IR (KBr)ν_{max}: 2927, 1528, 1260 cm^{-1}; HRMS (ESI) Calcd for $C_{29}H_{17}ClNO$ 430.0994 (M + H$^+$); Found 430.0996.

Benzo[*c*]chromeno[4,3,2-*gh*]phenanthridine (5r)

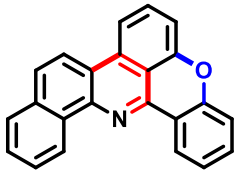

Light green solid (38 mg, 60%); mp 200-202 °C; ^{1}H NMR (500 MHz, $CDCl_3$) δ 9.55 (d, *J* = 8.2 Hz, 1H), 8.91 (d, *J* = 7.8 Hz, 1H), 8.40 (d, *J* = 8.9 Hz, 1H), 8.20 (d, *J* = 8.2 Hz, 1H), 7.94 (dd, *J* = 13.3, 8.5 Hz, 2H), 7.83 (t, *J* = 8.1 Hz, 1H), 7.76 (t, *J* = 7.5 Hz, 1H), 7.68 (t, *J* = 7.4 Hz, 1H), 7.54 (t, *J* = 7.7 Hz, 1H), 7.38 (t, *J* = 7.5 Hz, 1H), 7.33 (dd, *J* = 8.0, 4.3 Hz, 2H); ^{13}C NMR (100 MHz, $CDCl_3$) δ 154.3, 153.1, 146.5, 142.4, 134.4, 133.9, 132.2, 132.1, 131.9, 127.7, 127.6, 126.8, 126.8, 125.3, 125.3, 124.2, 122.1, 120.4, 120.2, 117.3, 115.5, 114.9, 111.2; IR (KBr)ν_{max}: 2925, 1575, 1251 cm^{-1}; HRMS (ESI) Calcd for $C_{23}H_{14}NO$ 320.1070 ($M + H^+$); Found 320.1069.

5-Bromo-9-(*tert*-butyl)benzo[*c*]chromeno[4,3,2-*gh*]phenanthridine (5s)

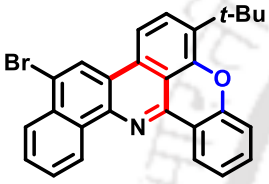

Light green solid (59 mg, 65%); mp 228-230 °C; ^{1}H NMR (500 MHz, $CDCl_3$) δ 9.55 (d, *J* = 9.2 Hz, 1H), 8.87 (d, *J* = 8.1 Hz, 1H), 8.68 (s, 1H), 8.32 (d, *J* = 9.0 Hz, 1H), 8.05 (d, *J* = 8.7 Hz, 1H), 7.90 (d, *J* = 8.6 Hz, 1H), 7.77 (t, *J* = 8.5 Hz, 2H), 7.55 (d, *J* = 8.4 Hz, 1H), 7.39 (d, *J* = 7.7 Hz, 2H), 1.63 (s, 9H); ^{13}C NMR (100 MHz, $CDCl_3$) δ 153.8, 150.6, 146.8, 141.0, 133.0, 132.9, 132.1, 131.9, 131.4, 130.4, 128.3, 127.2, 127.1, 125.3, 125.2, 124.2, 124.1, 121.5, 121.3, 120.5, 117.0, 115.9, 114.1, 35.0, 29.7; IR (KBr)ν_{max}: 2930, 1540, 1270 cm^{-1}; HRMS (ESI) Calcd for $C_{27}H_{21}BrNO$ 454.0802 ($M + H^+$); Found 454.0807, and 456.0789.

5-Bromo-9-(*tert*-butyl)-13-chlorobenzo[*c*]chromeno[4,3,2-*gh*]phenanthridine (5t)

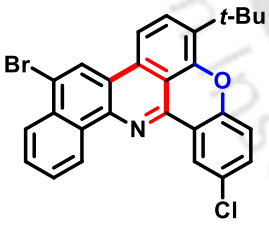

Yield 64% (62 mg), solid, light green solid (62 mg, 64%); mp 245-247 °C; ^{1}H NMR (400 MHz, $CDCl_3$) δ 9.46 (d, *J* = 8.1 Hz, 1H), 8.80 (d, *J* = 2.5 Hz, 1H), 8.36 (s, 1H), 8.17 (d, *J* = 8.8 Hz, 1H), 7.94 (t, *J* = 3.9 Hz, 2H), 7.92 (s, 1H), 7.77 (s, 1H), 7.74 (d, *J* = 2.4 Hz, 1H), 7.69 (d, *J* = 7.5 Hz, 1H), 1.69 (s, 9H); ^{13}C NMR (100 MHz, $CDCl_3$) δ 149.8, 141.1, 134.6, 133.6, 133.0, 132.4, 131.9, 131.8, 130.6, 129.6, 127.6, 127.5, 127.4, 126.8, 124.9, 124.0, 120.3, 120.0, 115.3, 111.4, 35.0, 29.4; IR (KBr)ν_{max}: 2920, 1540, 1265 cm^{-1}; HRMS (ESI) Calcd for $C_{27}H_{20}BrClNO$ 488.0412 ($M + H^+$); Found 488.0411, and 490.0425.

Table 2.4. Crystal data and structure refinement for compound 5a

Entry	Identification code	Compound 5a
01	Empirical formula	$C_{27}H_{25}NO_2$
02	Formula weight	395.48
03	Temperature	296 K
04	Wavelength	0.71073
05	Radiation type	Mo K\a
06	Radiation system	Fine-focus sealed tube
07	Crystal system	Monoclinic
08	Space group	P 21/n
09	Cell length	a=8.9415 (9) b=20.8156 (11) c=11.0217 (8)
10	Cell angle	□□90 □□109.915 (9) □□90
11	Cell volume	1928.7 (3)
12	Density	1.293
13	Completeness to theta	100
14	Absorption correction	multi-scan
15	Refinement method	Full-matrix least-squares on F2
16	Index ranges	-10<=h<=10, -24<=k<=24, -13<=l<=13
17	Reflection number	3415
18	Theta range	25.049
19	Cell formula units Z	4
20	CCDC no	2153056

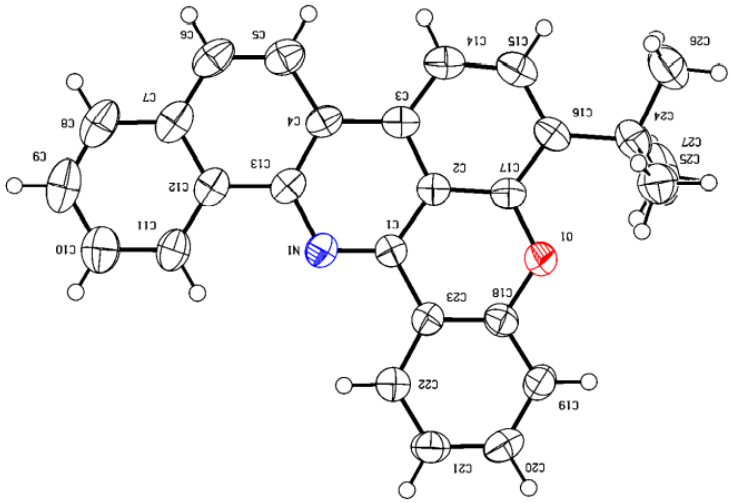

Figure 2.3. ORTEP diagrams of compound **5a**.

2.3d. Representative Characterization Spectra

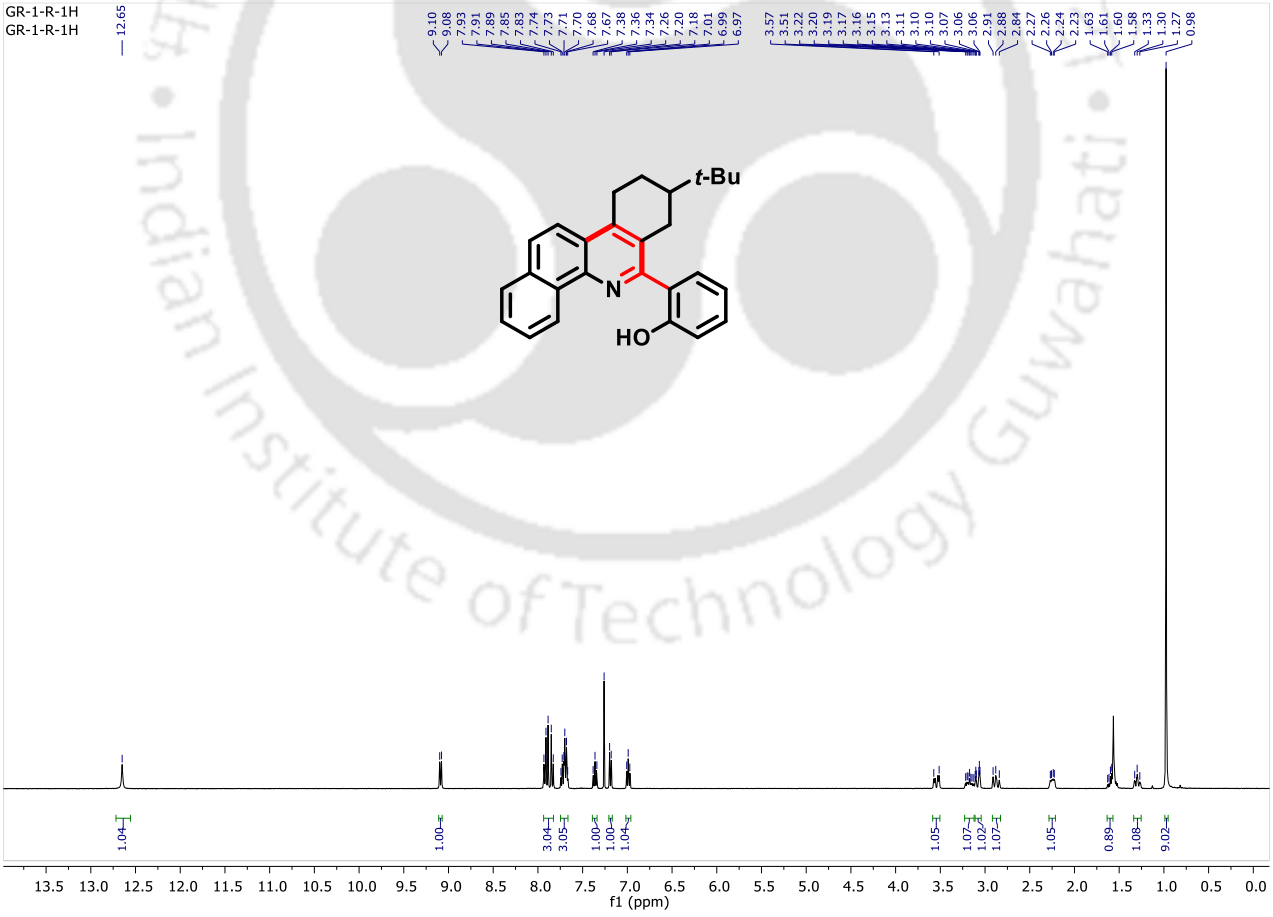

Figure 2.4. ^{1}H NMR Spectrum of 2-(8-(*tert*-butyl)-7,8,9,10-tetrahydrobenzo[*c*]phenanthridin-6-yl)phenol **(4a)**.

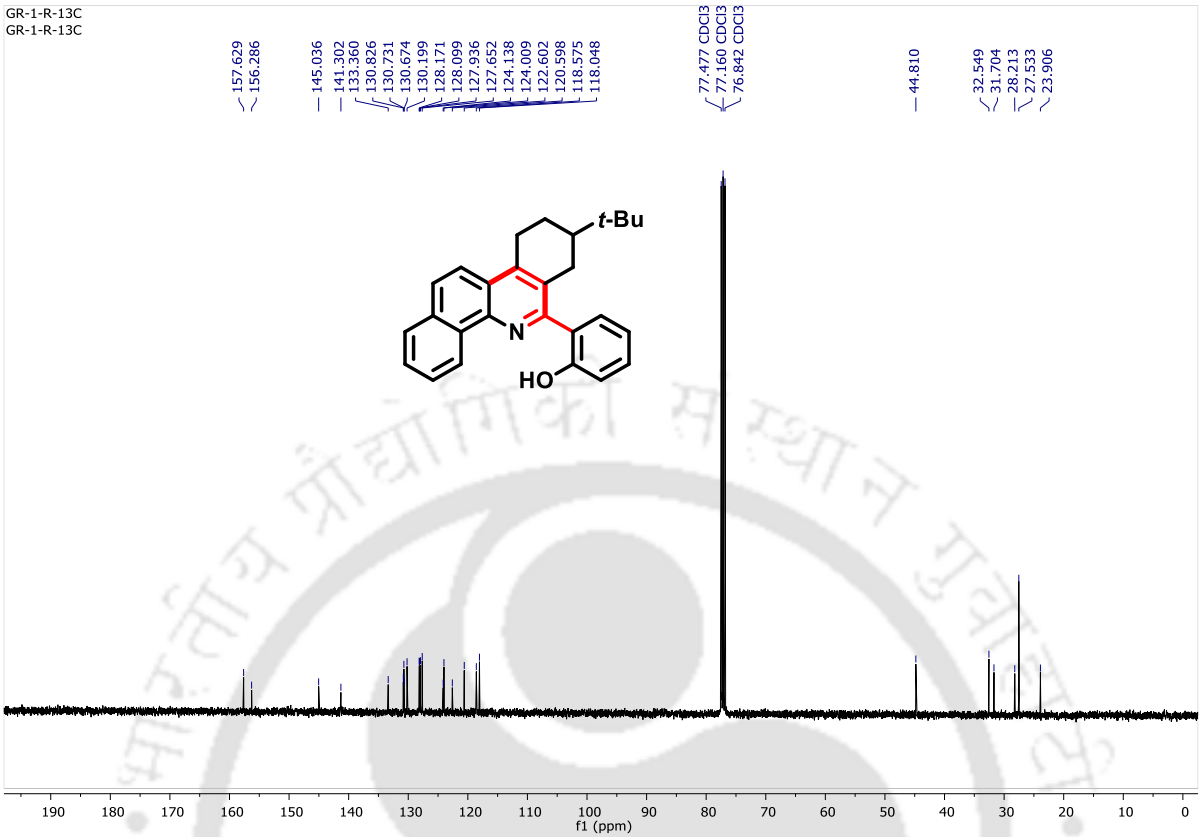

Figure 2.5. ^{13}C NMR Spectrum of 2-(8-(*tert*-butyl)-7,8,9,10-tetrahydrobenzo[*c*]phenanthridin-6-yl)phenol **(4a)**.

Sample Name	SAMPLE 3	**Position**	P2-B1	**Instrument Name**	Instrument 1	**User Name**	
Inj Vol	20	**InjPosition**		**SampleType**	Sample	**IRM Calibration Status**	Success
Data Filename	GRO-R.d	**ACQ Method**	ESI ALS 100-500.m	**Comment**		**Acquired Time**	12/26/2018 3:53:22 PM

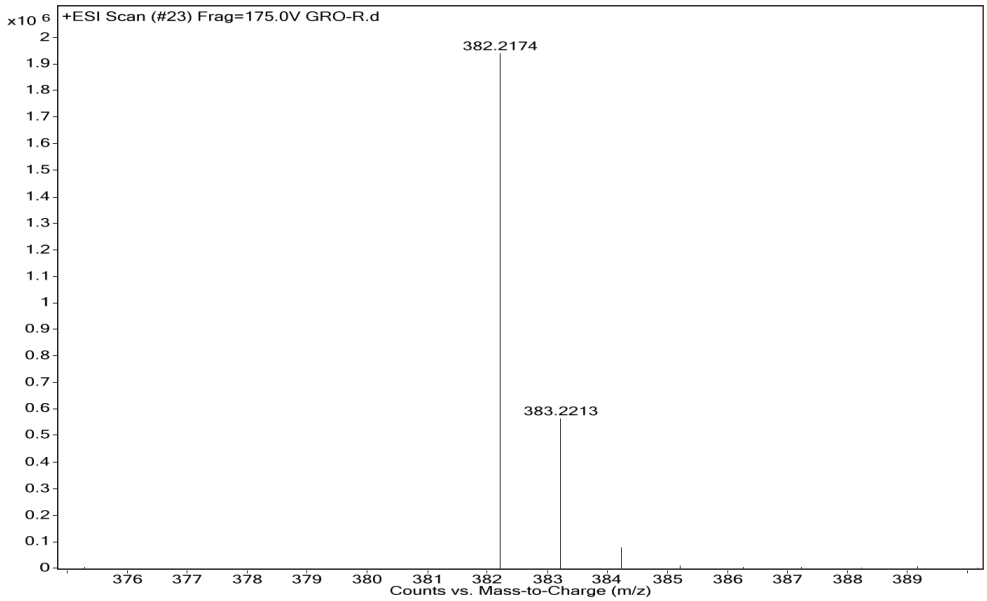

Figure 2.6. HRMS Spectrum of 2-(8-(*tert*-butyl)-7,8,9,10-tetrahydrobenzo[*c*]phenanthridin-6-yl)phenol **(4a)**.

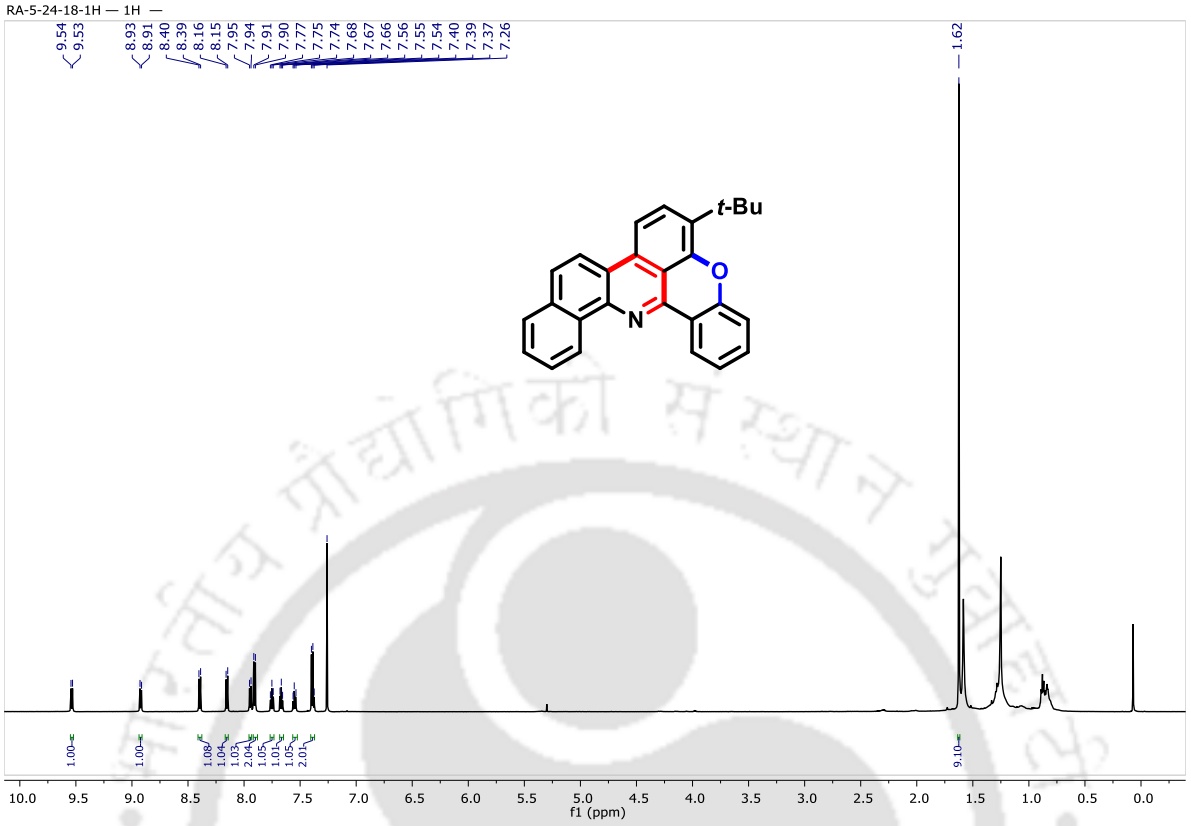

Figure 2.7. ^{1}H NMR Spectrum of 9-(*tert*-butyl)benzo[*c*]chromeno[4,3,2-*gh*]phenanthridine **(5a)**.

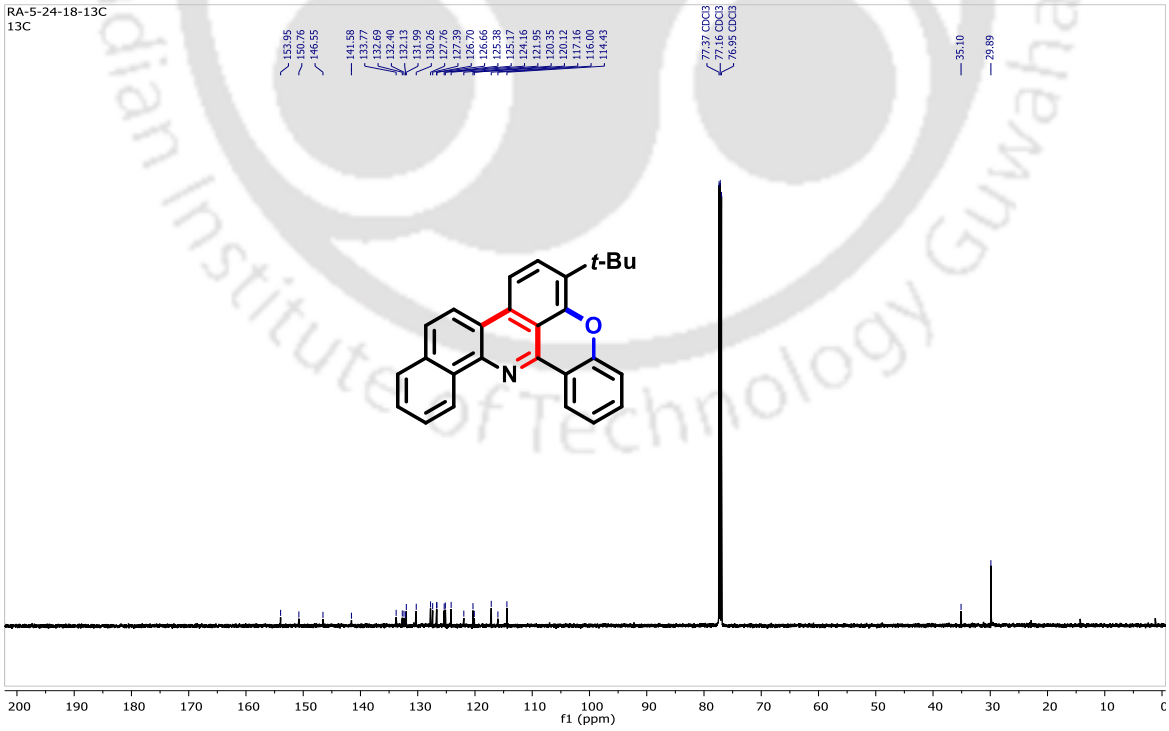

Figure 2.8. ^{13}C NMR Spectrum of 9-(*tert*-butyl)benzo[*c*]chromeno[4,3,2-*gh*]phenanthridine **(5a)**.

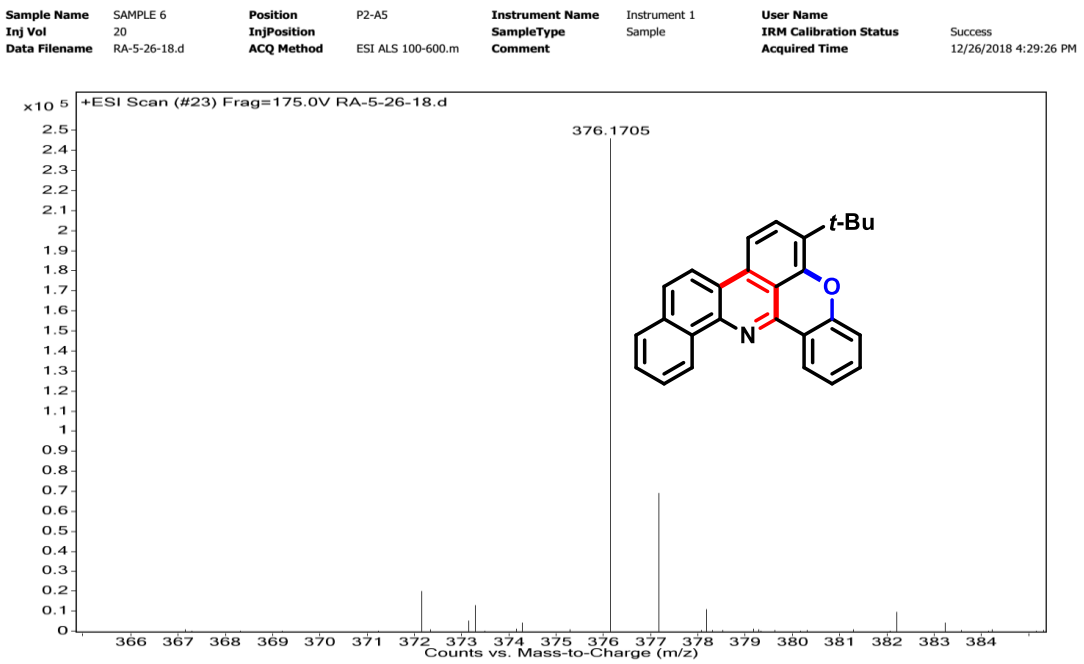

Figure 2.9. HRMS Spectrum of 9-(*tert*-butyl)benzo[*c*]chromeno[4,3,2-*gh*]phenanthridine **(5a)**.

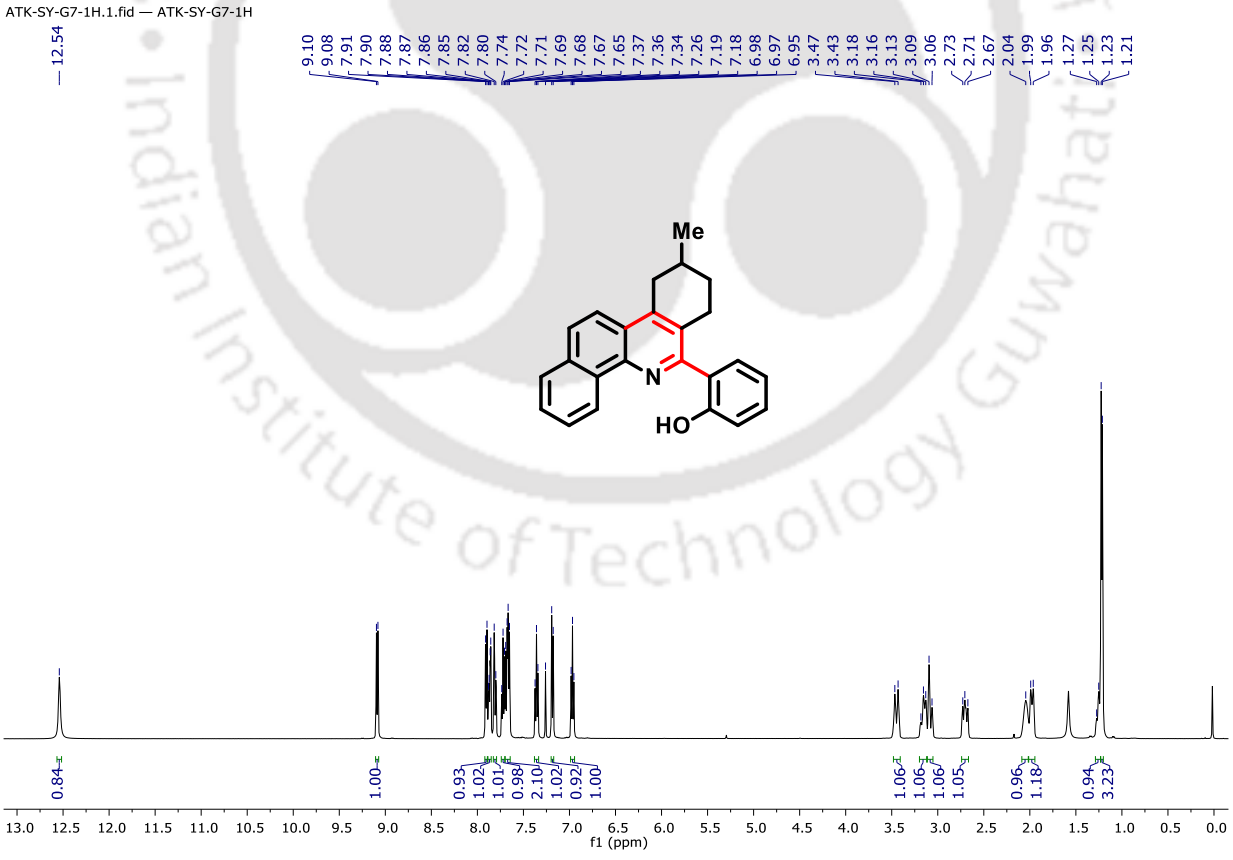

Figure 2.10. ^{1}H NMR Spectrum of 2-(9-methyl-7,8,9,10-tetrahydrobenzo[*c*]phenanthridin-6-yl)phenol **(4n)**.

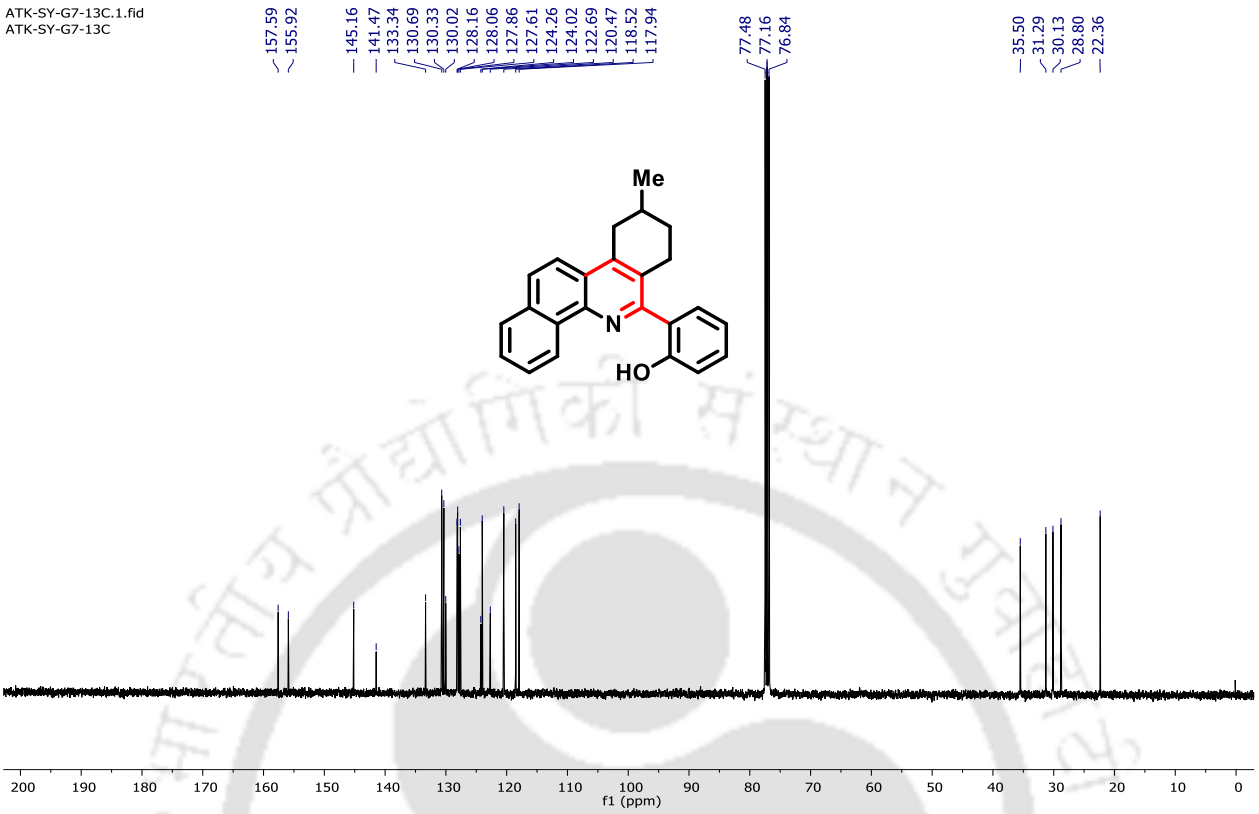

Figure 2.11. ^{13}C NMR Spectrum of 2-(9-methyl-7,8,9,10-tetrahydrobenzo[*c*]phenanthridin-6-yl)phenol **(4n)**.

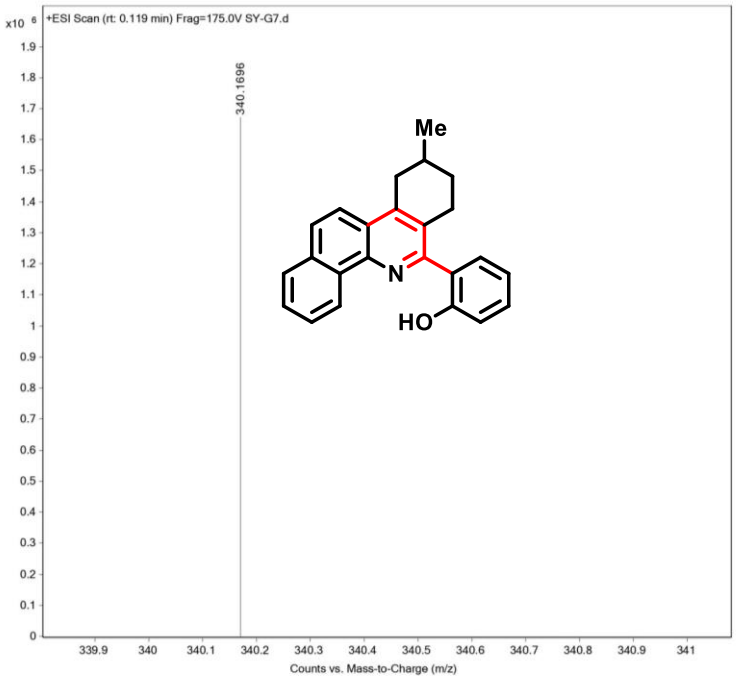

Figure 2.12. HRMS Spectra of 2-(9-methyl-7,8,9,10-tetrahydrobenzo[*c*]phenanthridin-6-yl)phenol **(4n)**.

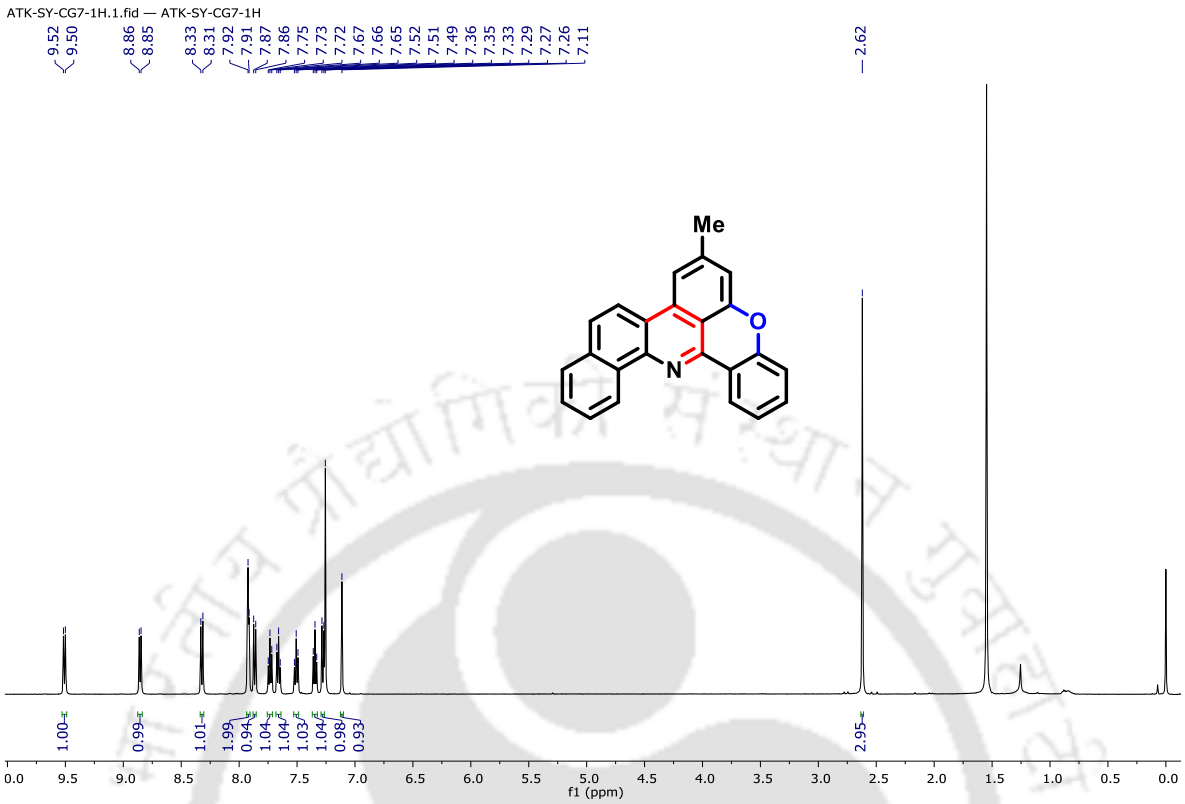

Figure 2.13. ^{1}H NMR Spectra of 8-methylbenzo[*c*]chromeno[4,3,2-*gh*]phenanthridine (**5n**).

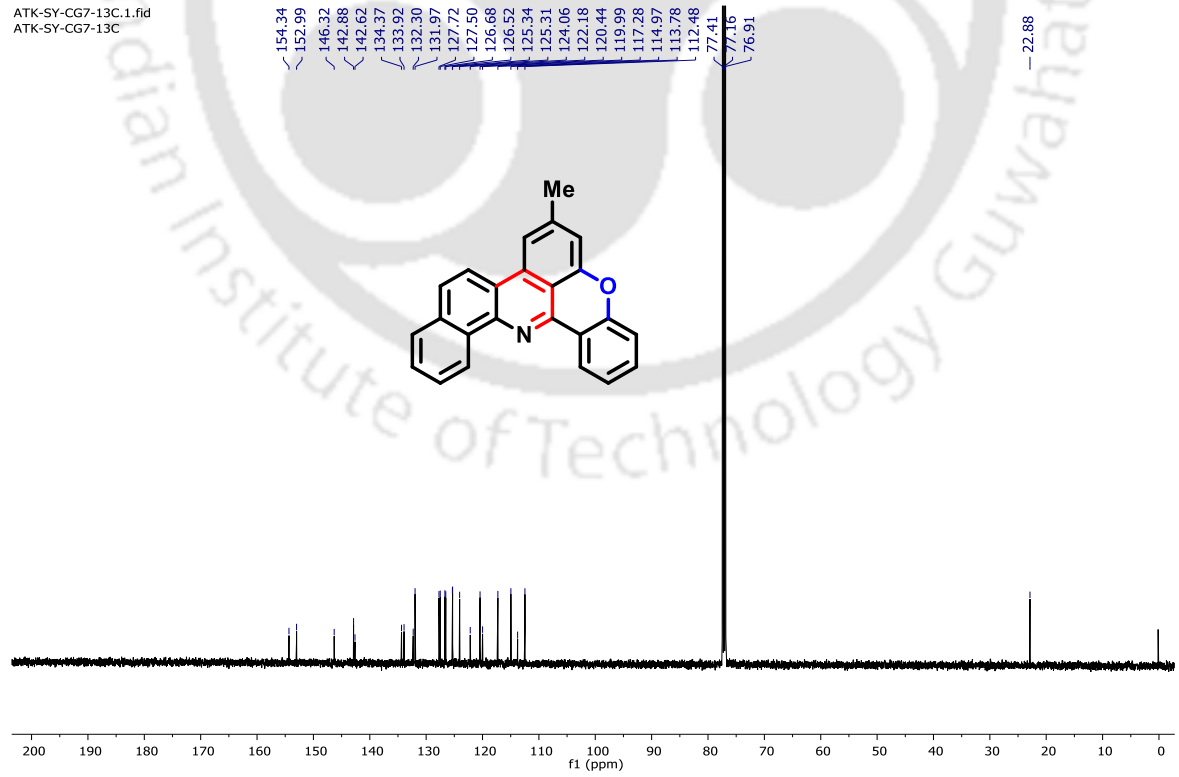

Figure 2.14. ^{13}C NMR Spectra of 8-Methylbenzo[*c*]chromeno[4,3,2-*gh*]phenanthridine (**5n**).

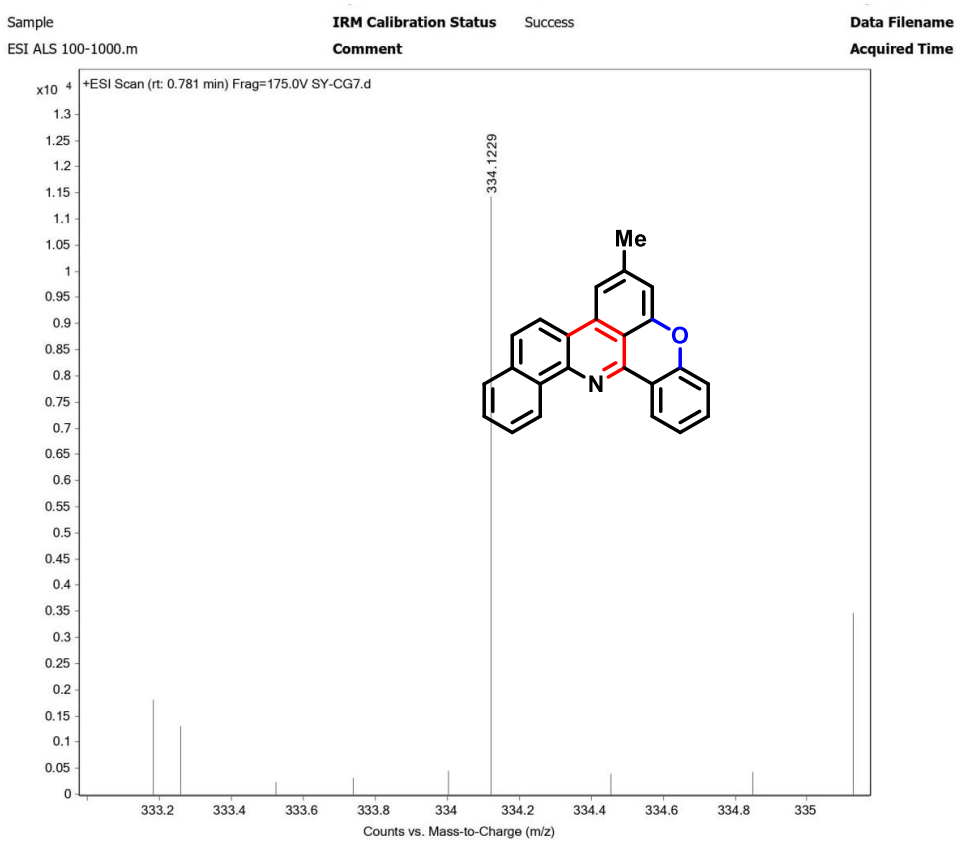

Figure 2.15. ^{13}C NMR Spectra of 8-methylbenzo[*c*]chromeno[4,3,2-*gh*]phenanthridine (**5n**).

2.4. References

1. (a) M. S. Singh, A. Nagaraju, N. Anand and S. Chowdhury, *RSC Adv.*, 2014, **4**, 55924−55959 and references therein; (b) W.-J. Bai, J. G. David, Z.-G. Feng, M. G. Weaver, K.-L. Wu and T. R. R. Pettus, *Acc. Chem. Res.*, 2014, **47**, 3655–3664 and references therein; (c) T. Hodík and C. Schneider, *Chem. Eur. J.*, 2018, **24**, 18082–18088; (d) D. C. Thompson, J. A. Thompson, M. Sugumaran and P. Moldéus, *Chem.-Biol. Interact.*, 1993, **86**, 129−162.

2. (a) K. Fries and K. I. Kann, *Liebigs Ann. Chem*., 1907, **353**, 335−356; (b) P. D. Gardner, H. Sarrafizadeh, and R. L. Brandon, *J. Am. Chem. Soc.*, 1959, **81**, 5515.

3. (a) J. T. J. Spence and J. H. B. George, *Org. Lett*., 2013, 15, 3891−3893; (b) S. Arumugam and V. V. Popik, *J. Org. Chem.*, 2010, **75**, 7338−7346; (c) J.-P. Lumb and D. Trauner, *Org. Lett.*, 2005, **7**, 5865−5868.

4. (a) D. Liao, H. Li, X. Lei, Org. Lett., 2012, **14**, 18−21; (b) J. H. George, J. H. Baldwin and R. M. Adlington, *Org. Lett.* 2010, **12**, 2394−2397; (c) A. K. Shaikh, A. J. A. Cobb and G. Varvounis, *Org. Lett.*, 2012, **14**, 584−587.

5. (a) A. Sharma, H. Hazarika and P. Gogoi, *J. Org. Chem.*, 2021, **86**, 4883–4895; (b) W.-J. Bai, J. G. David, Z.-G. Feng, M. G. Weaver, K.-L. Wu and T. R. R. Pettus, *Acc. Chem. Res.*, 2014, **47**, 3655−3664, and references therein.

6. W.-J. Bai, J. G. David, Z.-G. Feng, M. G. Weaver, K.-L. Wu and T. R. R. Pettus, *Acc. Chem. Res.*, 2014, **47**, 3655–3664.

7. R. Gattu, P. R. Bagdi, R. S. Basha and A. T. Khan, *J. Org. Chem.*, 2017, **82**, 12416−12429.

8. W. Jia, Q. Xi, T. Liu, M. Yang, Y. Chen, D. Yin and X. Wang, *J. Org. Chem.*, 2019, **84**, 5141−5149.

9. C. L.-Lopez, S. Patterson, T. Blum, A. F. Straight, J. Toth, A. M. Z. Slawin, T. J. Mitchison, J. R. Sellers and N. J. Westwood, *Eur. J. Org. Chem.*, 2005, 1736−1740.

10. J.-P. Lumb and D. Trauner, *Org. Lett.*, 2005, **7**, 5865−5868.

11. P. P. Fu and R. G. Harvey, *Chem. Rev.*, 1978, **78**, 317−36.

12. N. Basaric´ and P. Wan, Photochem. *Photobiol. Sci.*, 2006, **5**, 656–664.

13. R. Chebolu, A. Bahuguna, R. Sharma, V. K.Mishra and P. C. Ravikumar, *Chem. Commun*., 2015, **51**, 15438.

14. J.-P. Lumb and D. Trauner, *Org. Lett.*, 2005, **7**, 5865–5868.

CHAPTER III

One-step Synthesis of 7-Bromobenzo[c]chromeno[4,3,2-gh] phenanthridines through a Sequential Bromination/Cyclization/ Aromatization Reaction using N-Bromosuccinimide (NBS)

- Introduction
- Results and Discussion
- Experimental Section

3.1. Introduction

In **Chapter I, Section 1.3**, a brief overview is presented regarding the potential of pentacyclic chromeno[4,3,2-*gh*]phenanthridine derivatives, covering their synthetic aspects and the challenges encountered in their synthesis. **Chapter II** introduces the first-time demonstration of the synthesis of benzo[*c*]chromeno[4,3,2-*gh*]phenanthridine by our research group. The **Chapter III** will specifically detail the synthesis of derivatives featuring 7-bromobenzo[*c*]chromeno[4,3,2-*gh*]phenanthridine.

3.1a. NBS as a Versatile Reagent

N-Bromosuccinimide (NBS) is renowned for its effectiveness as a brominating agent.[1a,b] The discovery of NBS is credited to Ziegler, who first identified it through the bromination of succinimide using bromine under alkaline conditions.[2] Historically, NBS has found predominant use in allylic and/or benzylic bromination carried out under reflux conditions in anhydrous carbon tetrachloride (CCl_4), typically in the presence of a radical initiator such as 2,2'-azobis(*iso*butyronitrile) (AIBN) or benzoyl peroxide. This specific reaction is widely acknowledged as the Wohl-Ziegler reaction (**Scheme 3.1**).[3a-c]

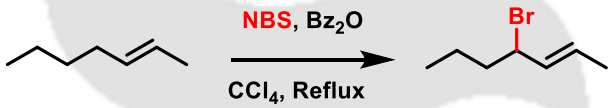

Scheme 3.1. A simple example of Wohl Ziegler reaction.

In the absence of a radical initiator, *N*-Bromosuccinimide (NBS) is capable of inducing an electrophilic aromatic ring bromination reaction. For instance, El-Wahab demonstrated this by conducting a bromination reaction on *p*-hydroxybenzoic acid using NBS in carbon tetrachloride (CCl_4) under reflux conditions. This process led to the isolation of 3,5-dibromo-4-hydroxybenzoic acid as the final product (**Scheme 3.2**).[4]

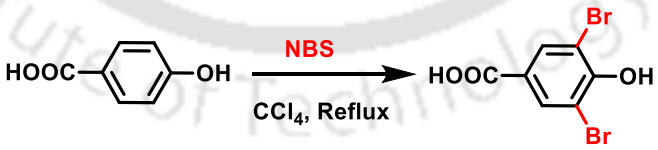

Scheme 3.2. Electrophilic aromatic ring bromination using NBS.

The significance of a radical initiator in a reaction mediated by *N*-bromosuccinimide (NBS) is highlighted by additional findings. Zhang *et al.* conducted regiospecific bromination of substituted 3-methylindoles using NBS in the presence of AIBN, leading to the formation of an allylic brominated product. Conversely, in the absence of AIBN, bromination occurred at the C-2 carbon instead, as depicted in **Scheme 3.3**.[5]

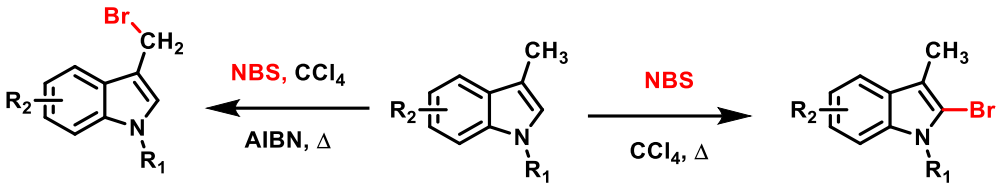

Scheme 3.3. NBS mediated reaction of 3-methylindoles.

It's worth highlighting that other than the CCl_4 solvent, *N*-Bromosuccinimide (NBS) also finds utility in the binary solvent system such as $CHCl_3$–CCl_4, or acetonitrile, toluene, DMF, etc under acidic, basic or neutral conditions.[1b,6] One example is represented in **Scheme 3.4**.

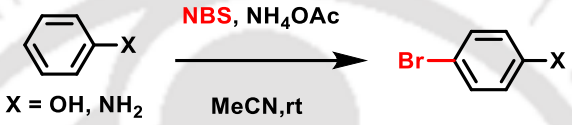

Scheme 3.4. Electrophilic bromination using NBS in acetonitrile solvent.

Other than the bromination reactions, the unique chemical reactivity of NBS also makes it a compelling additive for the execution of multiple sequential processes in a single step. It plays a facilitating role in diverse transformations such as functional group conversions, cyclization, cyclization/aromatization, annulation, haloamidation/cyclization, and more, typically in the presence of a robust base, acid, or metal catalyst.[7-9] NBS makes no direct contribution to the final product in these reactions. However, its presence as an additive is indispensable for successfully forming the desired product.

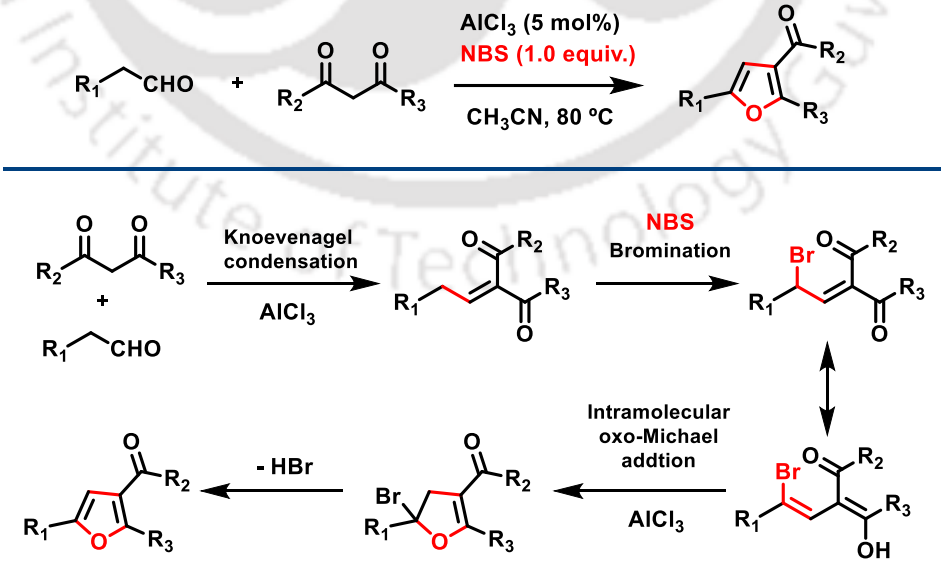

Scheme 3.5. Utilization of NBS as an additive for furan ring formation.

For example, Huang *et al* in 2017 unveiled an $AlCl_3$-catalyzed tandem reaction employing NBS as an additive for producing furan derivatives as depicted in **Scheme 3.5**. In this transformation, NBS crucially enables the intramolecular oxo-Michael addition, resulting in the formation of furan from the Knoevenagel product of aliphatic aldehydes and 1,3-dicarbonyl compounds.[8]

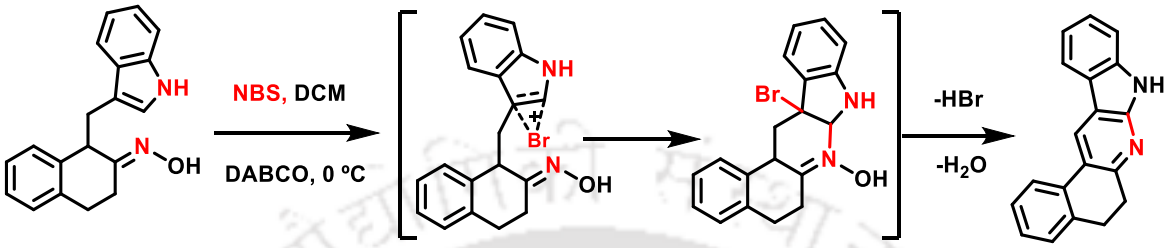

Scheme 3.6. NBS as an additive facilitating the cyclization reaction.

Likewise, in a recent study, the application of *N*-bromosuccinimide (NBS) in the treatment of 1-((1H-indol-3-yl)methyl)-3,4-dihydronaphthalen-2(1*H*)-one oxime resulted in the successful synthesis of 6,8-dihydro-5H-benzo[*f*]indolo[2,3-*b*]quinoline derivatives, as illustrated in **Scheme 3.6**.[9] In this particular reaction, NBS effectively facilitated the cyclization process without undergoing substitution of its -Br group in the final product.

3.1b. Importance of Aryl Bromides in Organic Synthesis

Aryl bromides have gained extensive application as substrates in Pd-, Ni-, and Cu-catalyzed cross-coupling reactions, including Heck, Suzuki-Miyaura, Sonogashira, Negishi, and Tsuji–Trost coupling reactions, facilitating the formation of diverse C–C, C-N, C-O, and C-S bonds.[10a-f] Additionally, aryl bromides serve as classical precursors for organolithium and Grignard reagents, as well as in benzyne generation and nucleophilic aromatic substitution.[11] Furthermore, they play a crucial role as intermediates in the synthesis of drugs, pharmaceuticals, agrochemicals, pigments, photographic materials, and various functional natural products.[11,12] Given these diverse applications, the development of regioselective electrophilic aromatic brominations is of high priority, especially for polyheteroaromatics (PHAs). One common and effective method for preparing aryl bromides is electrophilic aromatic bromination.[13] *N*-bromosuccinimide (NBS) also stands out as an economical and useful reagent for this purpose, as highlighted in **Section 3.1a.**[1b]

3.1c. Scope from the Whole Ziegler Reaction

- From the findings in the previous literature survey, the significance of incorporating a bromo functionality into an organic molecule becomes evident, given its pivotal role in subsequent organic transformations.
- Traditionally, the Wohl-Ziegler reaction, has been studied for benzylic and allylic bromination, employing the cost-effective reagent NBS in the presence of a radical initiator.
- Moreover, NBS serves as a highly convenient additive for various useful organic transformations.
- However, the application of the Wohl-Ziegler reaction for benzylic bromination, along with simultaneous cyclization and aromatization reactions in a single step using additive-like property of NBS, has not been reported until now.

In this context, the unexplored potential of the Wohl-Ziegler reaction for achieving novel Polyheteroaromatic by benzylic bromination, cyclization and aromatization reactions simultaneously, represents a substantial opportunity for advancing the second thesis work.

3.1d. Context of the Research Project

A DMSO-assisted synthesis of benzo[*c*]chromeno[4,3,2-*gh*]phenanthridine (**5**) from 2-(7,8,9,10-tetrahydrobenzo[*c*]phenanthridin-6-yl)phenol derivatives (**4**) via the *in situ* generated *o*-quinone methide intermediate is already disclosed in **Chapter II** which is also depicted in **Scheme 3.7**.[14]

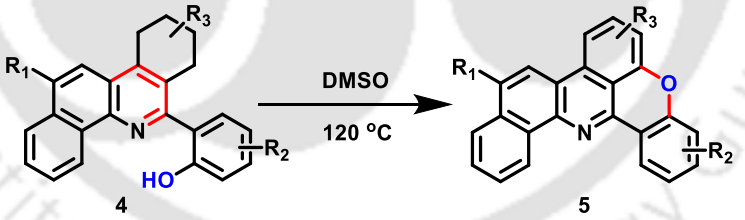

Scheme 3.7. Synthesis of benzo[*c*]chromeno[4,3,2-*gh*]phenanthridine derivatives.

Based on the existing literature and prior research,[14] we conceptualized a strategy wherein the two benzylic carbons within the phenolic compound (**4**) could be selectively harnessed in the presence of NBS/AIBN to generate intermediate **A2'** (**Scheme 3.8**). Subsequently, this intermediate could undergo O-H bond cleavage, leading to the formation of intermediate **B2'** through concurrent cyclization, creating the pyran ring. Finally, through an aromatization reaction, a hexacyclic fully aromatized heteroaromatic compound (**6**) with a bromo group selectively positioned at the C-7 position could potentially be achieved.

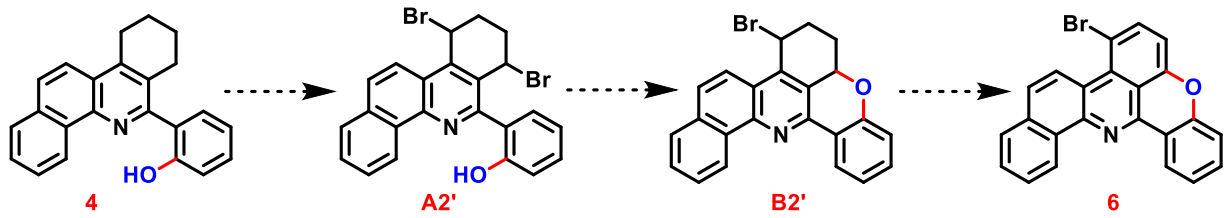

Scheme 3.8. A general schematic representation of the idea for the synthesis of 7-bromobenzo[*c*]chromeno[4,3,2-*gh*]phenanthridine derivatives.

3.1e. Present Work

Opportunely, **Chapter III** will be elaborated with the NBS-mediated radical catalyzed one-step synthesis of 7-bromobenzo[*c*]chromeno[4,3,2-*gh*]phenanthridine derivatives (**6a-r**) in CCl_4 solvent under reflux condition (**Scheme 3.9**).[14b] Sequential bromination, intramolecular ring cyclization, and aromatization without any metal catalyst, external oxidant, or harsh reaction conditions make this methodology unique and attractive. The radical-catalyzed Wohl-Ziegler reaction assists intramolecular cyclization via benzylic bromination unlike the *in situ* generated *o*-quinone methide intermediate reported in the earlier work (**Scheme 3.7**).[13] Even so, no additional electrophilic aromatic bromination reaction is required. The Bromo functionality in the molecule is exploited in the Suzuki coupling reaction using compound **6a** to obtain compound **8a** into the bargain. In addition, the photophysical properties of one of the synthesized compounds 7-bromo-9-*iso*propylbenzo[*c*]chromeno[4,3,2-*gh*]phenanthridine (**6h**) have been studied, and it showed aggregation-induced emission in THF/Hexane solvent.

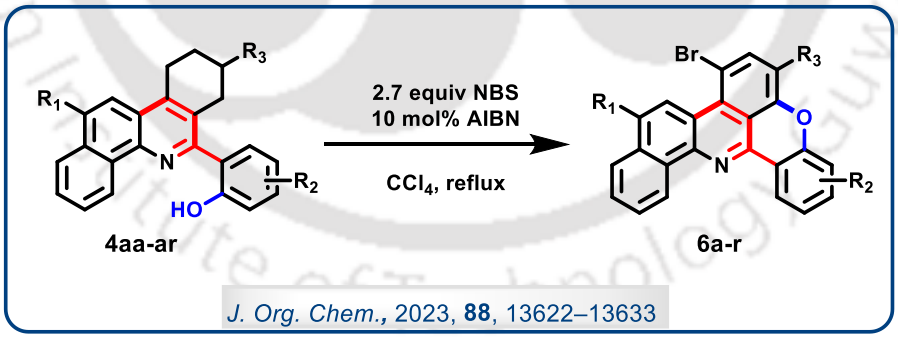

Scheme 3.9. Present methodology for the synthesis of 7-bromobenzo[*c*]chromeno[4,3,2-*gh*]phenanthridine derivatives.

3.2. Results and Discussion

3.2a. Optimization of the Methodology

Our initial efforts focused on establishing optimal reaction conditions for synthesizing derivatives of 7-bromobenzo[*c*]chromeno[4,3,2-*gh*]phenanthridine. We began by synthesizing 2-(8-(*tert*-butyl)-7,8,9,10-tetrahydrobenzo[c]phenanthridin-6-yl)phenol (**4aa**) through a previously reported multicomponent reaction involving 1-naphthyl amine, salicylaldehyde, and 4-*tert*-butylcyclohexanone.[14a,15] For a better understanding of the naming of the compounds **4aa** and **6a,** the numbering of the atoms in their basic skeleton is shown in **Figure 3.1**.

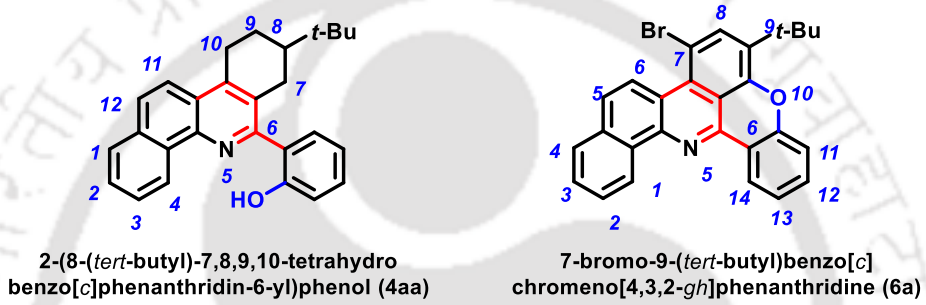

2-(8-(*tert*-butyl)-7,8,9,10-tetrahydro benzo[*c*]phenanthridin-6-yl)phenol (4aa)

7-bromo-9-(*tert*-butyl)benzo[*c*] chromeno[4,3,2-*gh*]phenanthridine (6a)

Figure 3.1. Numbering of atoms for the naming of compounds **4aa** & **6a**.

Subsequently, we used **4aa** as a model substrate (0.10 mmol scale) for optimization of the reaction conditions, and the results are summarized in **Table 3.1**. In the initial attempt, 0.10 mmol of **4aa** (38 mg) and 1.4 equiv. of NBS were stirred in carbon tetrachloride solvent (CCl_4). After 12 hours, the desired product, 7-bromo-9-(*tert*-butyl)benzo[*c*]chromeno[4,3,2-*gh*]phenanthridine (**6a**), was obtained in 18% yield (**Entry 1**). After adding 10 mol% AIBN, the yield increased to 35% (**Entry 2**), and the NBS amount increased to 2 equiv. led to a 50% yield (**Entry 3**). An optimal yield of 70% was achieved with 2.7 equiv. of NBS in 7 hours (**Entry 4**), while a slight decrease in yield to 60% was observed with 3.1 equiv. of NBS (**Entry 5**).

Exploring different catalysts, such as hydrogen peroxide (H_2O_2), *tert*-butyl hydroperoxide (TBHP), and benzoyl peroxide (Bz_2O), with 2.7 equiv. NBS in CCl_4 resulted in varying outcomes (**Entries 6**, **7**, & **8**). Notably, TBHP and Bz_2O yielded the desired product **6a** in 50% and 55%, respectively.

Testing different solvents, including chloroform, acetic acid, ethanol, water, and toluene, revealed that product **5a** could be obtained in fair yields with chloroform, acetic acid, ethanol, and toluene, but not in water (**Entries 9-13**). However, reaction conducted with 2.7 equiv. NBS and 10 mol% AIBN without solvent did not yield the expected product (**Entry 14**).

Table 3.1. Optimization of the Reaction Conditions[a,b]

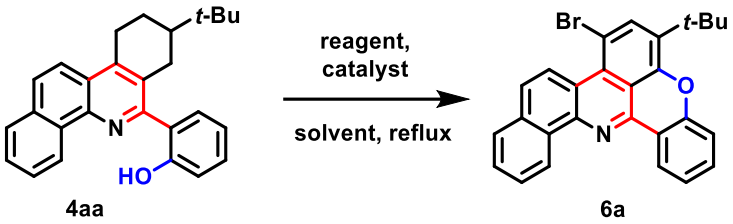

4aa 6a

Sl No.	Reagent (equiv.)	Catalyst (mol%)	Solvent	Time (h)	Yield (%)
1	NBS (1.4 equiv.)	-	CCl_4	12	18
2	NBS (1.4 equiv.)	AIBN (10)	CCl_4	12	35
3	NBS (2.0 equiv.)	AIBN (10)	CCl_4	12	50
4	**NBS (2.7 equiv.)**	**AIBN (10)**	**CCl_4**	**7**	**70**
5	NBS (3.1 equiv.)	AIBN (10)	CCl_4	7	60
6	NBS (2.7 equiv.)	H_2O_2 (10)	CCl_4	7	NR
7	NBS (2.7 equiv.)	TBHP (10)	CCl_4	7	50
8	NBS (2.7 equiv.)	Bz_2O (10)	CCl_4	7	55
9	NBS (2.7 equiv.)	AIBN (10)	$CHCl_3$	7	45
10	NBS (2.7 equiv.)	AIBN (10)	CH_3COOH	7	30
11	NBS (2.7 equiv.)	AIBN (10)	EtOH	7	42
12	NBS (2.7 equiv.)	AIBN (10)	H_2O	7	NR
13	NBS (2.7 equiv.)	AIBN (10)	Toluene	7	60
14	NBS (2.7 equiv.)	AIBN (10)	-	7	NR

[a]All reactions were done with 2-(8-(*tert*-butyl)-7,8,9,10-tetrahydrobenzo[*c*]phenanthridin-6-yl)phenol (**4aa,** 0.10 mmol) in 1 mL solvent in reflux condition. [b]Yield based on starting material recovery. NR-No reaction.

In conclusion, the optimized reaction conditions for the synthesis of 7-bromobenzo[*c*]chromeno[4,3,2-*gh*]phenanthridine derivatives involve 2.7 equiv. of NBS, 10 mol% AIBN, and CCl_4 solvent at its boiling temperature (**Entry 4**).

3.2b. Exploration of the Substrate Scope

Table 3.2. Scope of 2-(7,8,9,10-Tetrahydrobenzo[*c*]phenanthridin-6-yl)phenol Derivatives[a,b]

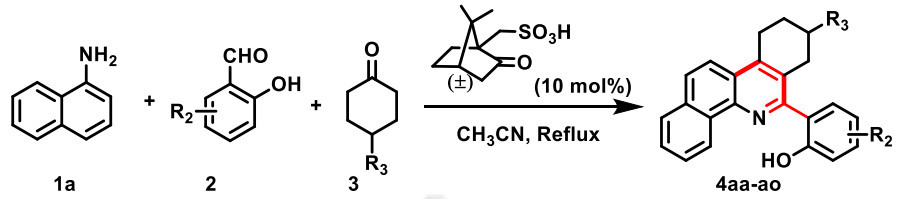

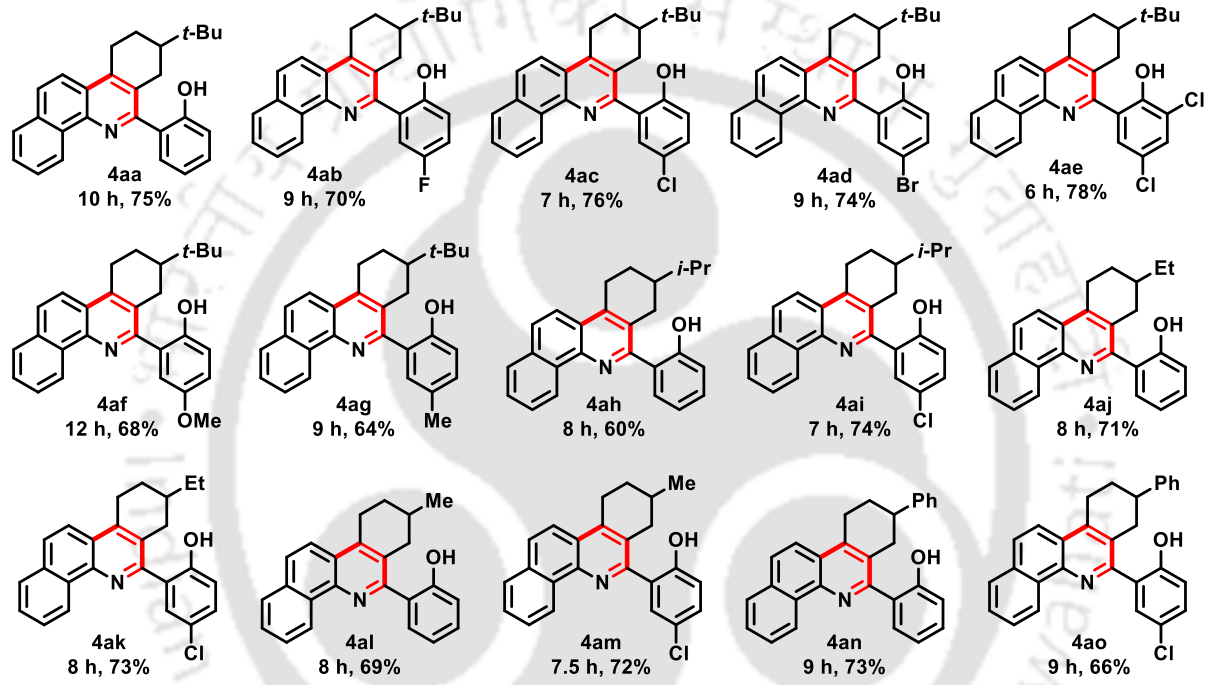

[a]All reactions were carried out with 1-naphthylamine **1a** (1 mmol), salicylaldehyde **2** (1 mmol), and cyclohexanone **3** (1 mmol) derivatives in 5 mL acetonitrile solvent at 81°C. Isolated yield[b]

Finishing the optimization of the reaction conditions, we synthesized a wide variety of (7,8,9,10-tetrahydrobenzo[*c*]phenanthridin-6-yl)phenol derivatives (**4ab**-**4ao**) employing the same multicomponent reaction of 1-naphthylamine (**1a**), salicylaldehyde (**2**) and cyclohexanone derivatives, listed in **Table 3.2**. Three of the 2-(12-bromo-8-(*tert*-butyl)-7,8,9,10-tetrahydrobenzo[*c*]phenanthridin-6-yl)phenol (**4ap**-**4ar**) were also prepared using 4-bromo-1-naphthylamine (**1b**) as shown in **Table 3.3**.

Table 3.3. Scope of 2-(12-Bromo-8-(*tert*-butyl)-7,8,9,10-tetrahydrobenzo[*c*]phenanthridin-6-yl)phenol Derivatives[a,b]

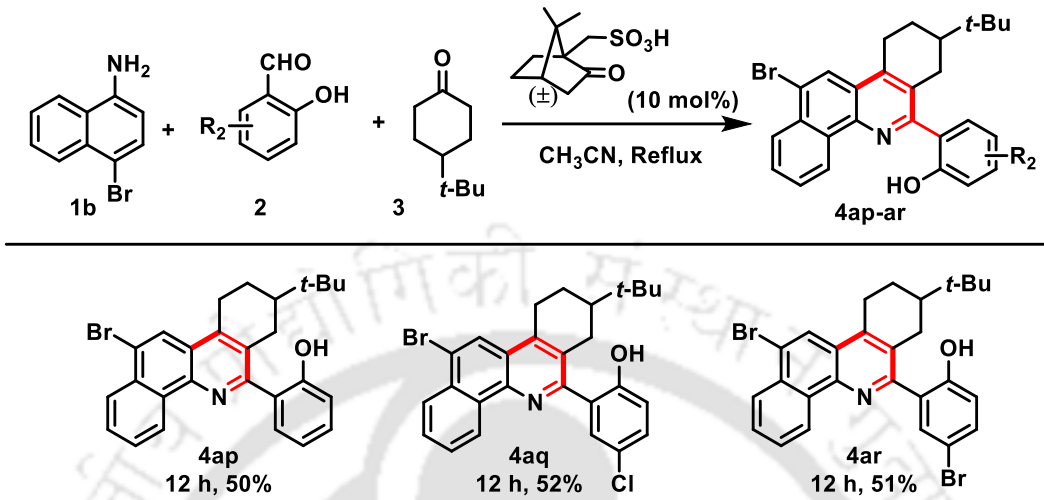

[a]All reactions were carried out with 1-amino-4-bromonaphthalene **1b** (1 mmol), salicylaldehyde **2** (1 mmol), and cyclohexanone **3** (1 mmol) derivatives in 5 mL acetonitrile solvent at 81°C. Isolated yield[b]

With these starting materials in hand, we started exploring the substrate scopes of the present methodology for the synthesis of 7-bromobenzo[*c*]chromeno[4,3,2-*gh*]phenanthridines (**6a-o**, **Table 3.4**). Initially, 2-(8-(*tert*-butyl)-7,8,9,10-tetrahydrobenzo[*c*]phenanthridin-6-yl)phenol (**4ab-4ag**) were subjected to the NBS catalyzed cascade reaction bearing both electron-withdrawing and electron-donating groups. For example, compounds having 4-F, 4-Cl, 4-Br, and 2,4-dichloro groups in the phenol ring (**4ab-4ae**) gave the desired 7-bromo-9-(*tert*-butyl)benzo[*c*]chromeno[4,3,2-*gh*]phenanthridine derivatives (**6b-e**) in 67-70% yield. 13-Methoxy and 13-methyl-7-bromo-9-(*tert*-butyl)benzo[*c*]chromeno[4,3,2-*gh*]phenanthridines (**6f** & **6g**) with the electron-donating group are isolated successfully from the reaction of compounds **4af** & **4ag**.

Phenol derivatives having other alkyl groups such as 8-*iso*propyl, 8-ethyl, and 8-methyl in its tetrahydrophenanthridine backbone (**4ah-4am**) also delivered 7-bromo-9-alkylchromenophenanthridines (**6h-6m**) in a good yield. At the same time, 7-bromo-8-phenylchromenophenanthridine derivatives **6n** & **6o** were also successfully achieved in 65% and 67% yields.

Table 3.4. Scope of 7-Bromobenzo[*c*]chromeno[4,3,2-*gh*]phenanthridine Derivatives[a,b]

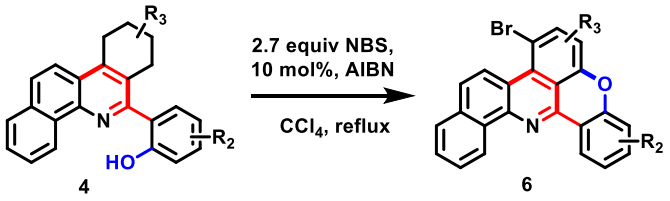

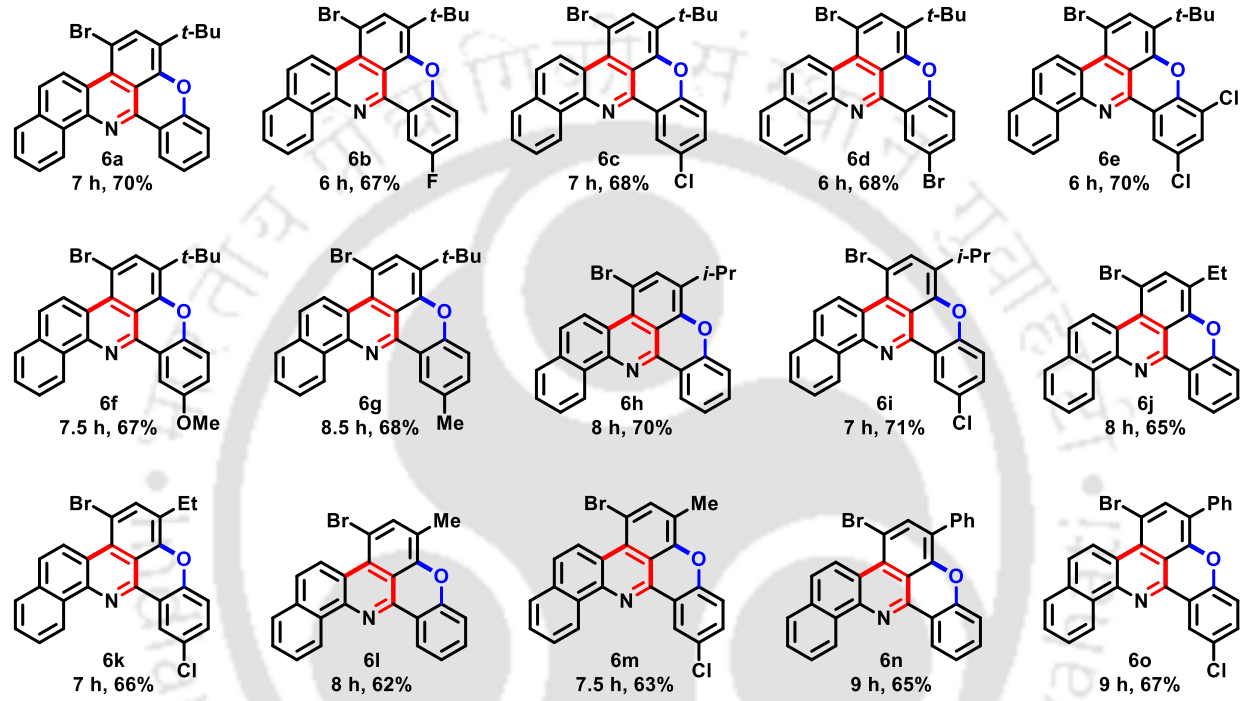

[a]All reactions were done with 0.10 mmol of compound **4aa-ao** in 1 mL CCl_4 solvent. [b]The yield based on starting material recovery.

The NBS catalyzed reaction was also employed for the 2-(12-bromo-8-(*tert*-butyl)-7,8,9,10-tetrahydrobenzo[*c*]phenanthridin-6-yl)phenol derivatives (**4ap-ar**), shown in **Table 3.5**. As a result, the corresponding desired product 5,7-dibromo-9-(*tert*-butyl)benzo[*c*]chromeno[4,3,2-*gh*]phenanthridine derivatives (**6p-r)** was achieved in 55-58% yield relatively in less time.

Table 3.5. Scope of 5,7-Dibromobenzo[*c*]chromeno[4,3,2-*gh*]phenanthridine Derivatives[a,b]

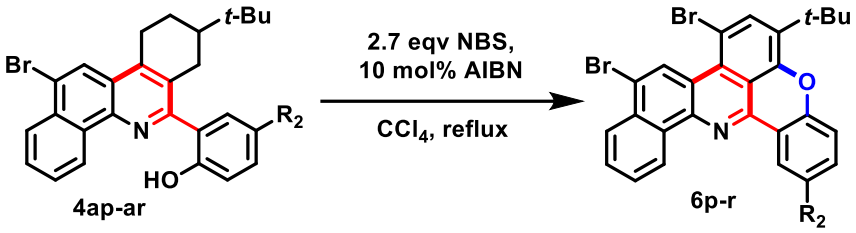

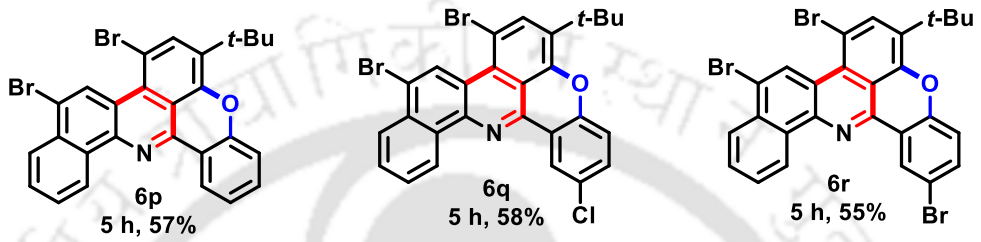

[a]All reactions were done with 0.10 mmol of compound **4ap-ar** in 1 mL CCl_4 solvent. [b]Yield based on starting material recovery.

Table 3.6. Failed Reactions for the Synthesis of 7-Bromobenzo[*c*]chromeno[4,3,2-*gh*]phenanthridine Derivatives.[a]

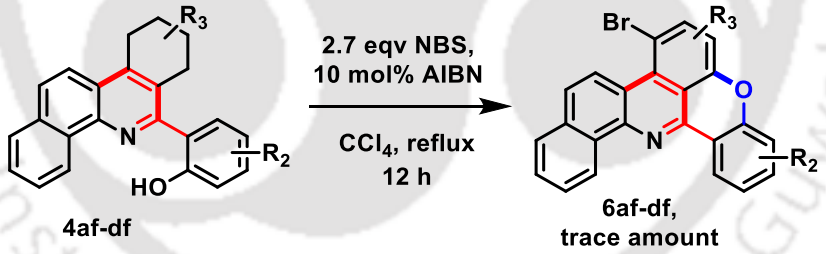

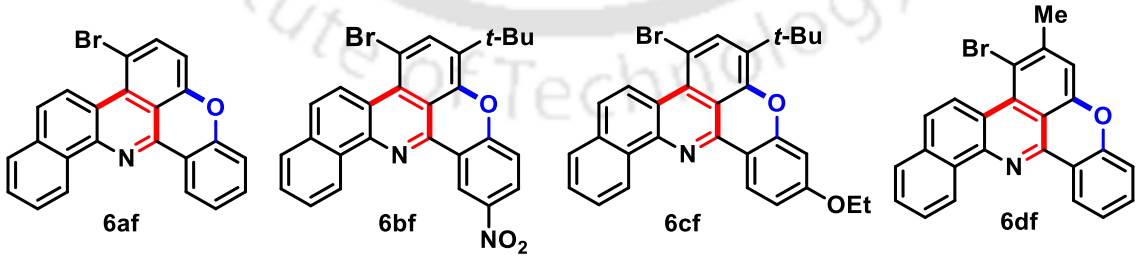

[a]All the reactions were done with 0.10 mmol of **4af-df** derivatives in 5 mL CCl_4 solvent.

It was noticed that the reaction underwent better with the increase in the density of the alkyl group at the 9th position of the chromenophenanthridine derivatives. Unfortunately, a few of the 7-bromochromenophenanthridines (**6af-df**) could not be characterized due to the formation of the products in a very low yield. These products are listed in **Table 3.6**.

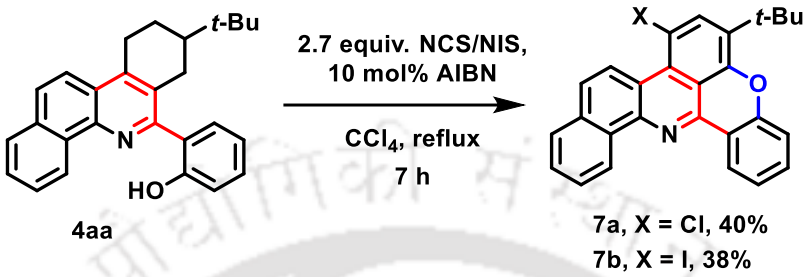

Scheme 3.10. Synthesis of 7-chloro/7-iodo-9-(*tert*-butyl)-benzo[*c*]chromeno[4,3,2-*gh*]phenanthridine. [a]Both reactions were done with 0.10 mmol of **4aa** derivatives in 1 mL CCl_4 solvent. [b]Yield based on starting material recovery.

Another two reactions of compound **4aa** were performed with *N*-chlorosuccinimide (NCS) and *N*-iodosuccinimide (NIS) in CCl_4 solvent under reflux conditions (**Scheme 3.10**). However, expected products 7-chloro/7-iodo-9-(*tert*-butyl)benzo[*c*]chromeno[4,3,2-*gh*]phenanthridine (**7a** & **7b**) were also isolated in relatively poor yield.

Large-Scale Reaction

To verify the scalability of the present protocol, the reaction was carried out with 2-(8-(*tert*-Butyl)-7,8,9,10-tetrahydrobenzo[*c*]phenanthridin-6-yl)phenol (**4aa**, 381 mg, 1 mmol) and *N*-bromosuccinimide (477 mg, 2.7 mmol) in the presence of 10 mol% AIBN (16 mg, 0.10 mmol) in 25 mL of CCl_4 in a pre-heated oil-bath under reflux condition. After 24 h of the reaction, the desired product **6a** was isolated 131 mg along with 0.200 g of unreacted starting material after column chromatography purification. The yield is 60% based on the starting material recovery. From this observation, we inferred that the present protocol is not practically viable for a large-scale reaction.

- ***All the synthesized compounds are characterized through ^{1}H, ^{13}C NMR, and HRMS spectra, and characterization data of all the compounds are given in the experimental section. A few of the representative spectra have also been attached in the experimental section.***

3.2c. Establishment of the Reaction Mechanism

To examine whether the brominated product **5a** can be obtained or not from the earlier reported cyclized products **9a**,[6c] the bromination reaction was carried out overnight using NBS under room temperature (**Scheme 3.11**). Unfortunately, the expected mono-brominated product (**6a**) was not obtained. From this observation, we may conclude that the present methodology is efficient for producing the mono-brominated benzo[*c*]chromeno[4,3,2-*gh*]phenanthridine product regioselectively at 7th position of the molecule.

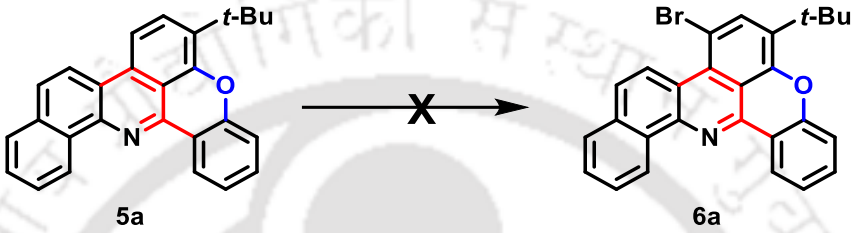

Scheme 3.11. Regioselective aromatic electrophilic ring bromination of benzo[*c*]chromeno[4,3,2-*gh*]phenanthridine (**6a**).

Control Experiments

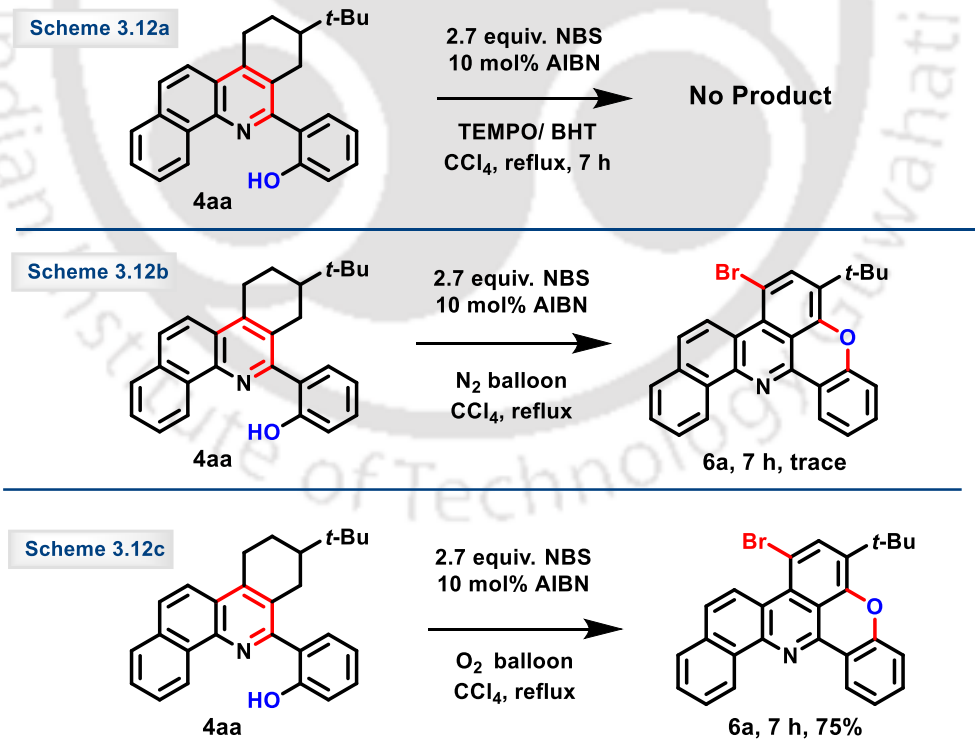

Scheme 3.12. Control experiments. Reactions were carried out with 2-(8-(*tert*-butyl)-7,8,9,10-tetrahydrobenzo[*c*]phenanthridin-6-yl)phenol (**4a**, 0.10 mmol) derivatives in 1 mL CCl_4 solvent at reflux temperature.

To propose a probable reaction mechanism, a series of control experiments were performed (**Scheme 3.12**). To verify, whether the reaction is following the radical pathway or not, compound **4aa** was examined in the presence of TEMPO and BHT under similar reaction conditions respectively. The formation of the product (**6a**) was not observed (**Scheme 3.12a**). This observation implied that the reaction is following the radical pathway.

Another reaction was performed in CCl_4 with 2.7 equivalents NBS and 10 mol% AIBN under a nitrogen atmosphere (**Scheme 3.12b**). Surprisingly, the desired product **6a** was obtained in a trace amount. After this observation, a third reaction was carried out in the presence of O_2 balloon which led to the isolation of compound **6a** in 75% yield (**Scheme 3.12c**). The yield was increased from 70 to 75%. From these two observations, we may propose that atmospheric O_2 is responsible for the aromatization.

Benzylic Bromination and Role of Free -OH Group

Initially, the phenolic hydroxyl group of compound 2-(8-(*tert*-butyl)-7,8,9,10-tetrahydrobenzo[*c*]phenan thridin-6-yl)phenol (**4aa**) has been protected with methyl iodide to get product 8-(*tert*-butyl)-6-(2-methoxyphenyl)-7,8,9,10-tetrahydrobenzo[*c*]phenanthridine (**5ab**). When compound **5ab** was subjected to a NBS mediated bromination reaction, a fully aromatized compound (**5ac**) was isolated as shown in **Scheme 3.13**. Compounds **5ab** and **5ac** were characterized through NMR and HRMS spectra. We also have detected the 7,10-dibromo-8-(*tert*-butyl)-6-(2-methoxyphenyl)-7,8,9,10-tetrahydrobenzo[*c*]phenanthridine (**5ac'**) in HRMS from the reaction mixture of NBS bromination of **5ab**. HRMS (ESI) of **5ac'** Calcd for $C_{28}H_{28}Br_2NO$ 554.0512 ($M + H^+$); Found 554.0512 and 552.0530 (isotopic peak). From this observation, we may conclude that the formation of compound **5ac** is facilitated by the di-bromination at the two benzylic carbon followed by the elimination of two molecules of HBr. It indirectly proves the proposed mechanism (**Scheme 3.14**).

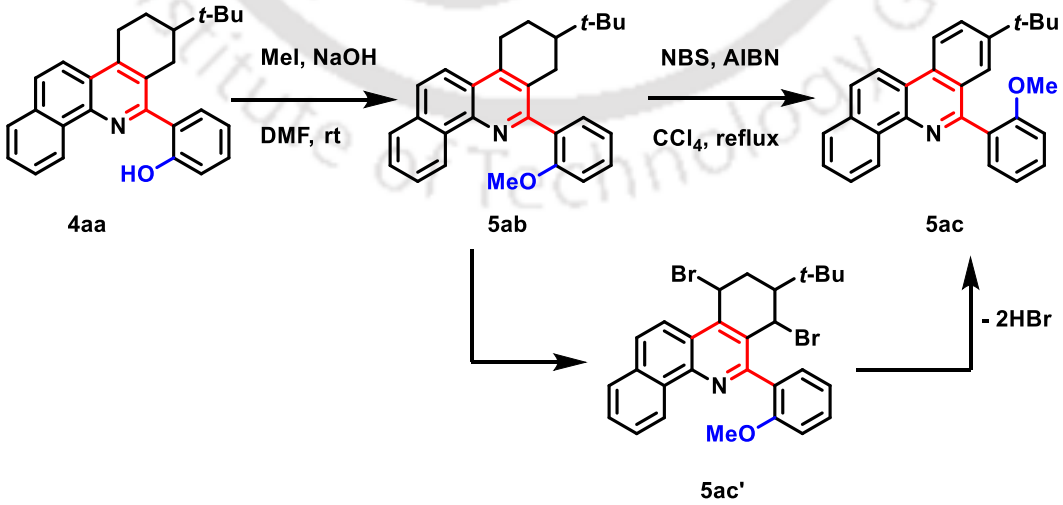

Scheme 3.13. Control experiment to prove the benzylic di-bromination.

Proposed Mechanism

Based on the results of the controlled experiments, we are proposing the probable reaction mechanism in **Scheme 3.14**. The formation of compound **6a** from the starting material **4aa** has been considered as the model reaction for the proposition of the reaction mechanism. Here, azoisobutyronitrile (AIBN) acts as a radical initiator.

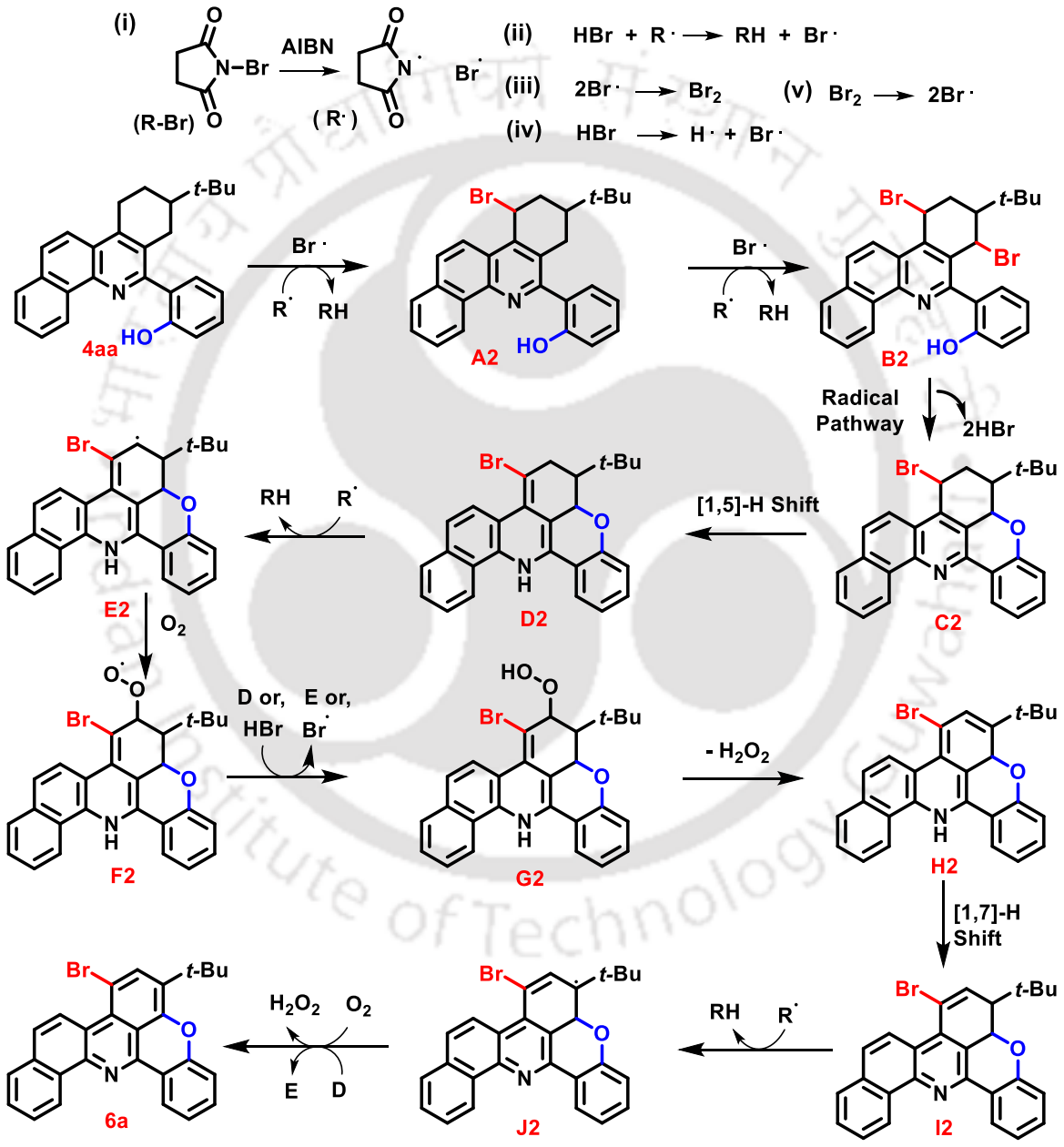

Scheme 3.14. A plausible mechanism for the synthesis of 7-bromobenzo[*c*]chromeno[4,3,2-*gh*]phenanthridines

It cleaves NBS and forms succinimide ($R^{\cdot}$) and $Br^{\cdot}$ radical. This succinimide radical abstracts $H^{\cdot}$ from the 10th carbon of the phenolic compound (**4**) and helps the bromination in the presence of $Br^{\cdot}$ radical to form mono-brominated intermediate **A2**. Our previous work can support bromination at this particular benzylic carbon.[15a] Next, intermediate **A2** again undergoes radical bromination at another benzylic carbon (7th C of starting material **4**) to give di-brominated intermediate **B2**. Intermediate **B2** undergoes intramolecular cyclization via a radical pathway to form intermediate **C2**. Then, [1,5]-H shift of intermediate **C2** leads to the formation of **D2**, which eventually forms radical intermediate **E2**. Then it can react with aerobic oxygen and form hydroperoxide intermediate **G2** by abstracting one $H^{\cdot}$ from the medium. Next, eliminating H_2O_2 from **G2** provides intermediate **H2,** which consecutively forms intermediate **I2** through [1,7]-H shift. Finally, the desired product **6** is obtained by the radical-mediated aerobic oxidation of intermediate **I2**.

Detection of Intermediates in HRMS

0.10 mmol (37 mg) of 2-(8-(*tert*-butyl)-7,8,9,10-tetrahydrobenzo[*c*]phenanthridin-6-yl)phenol **(4aa**), 2.7 equiv. of NBS and 10 mol% of AIBN were taken in a 25 ml r.b flask. Then, the mixture was stirred in CCl_4 solvent under reflux conditions. After 4 h, the reaction mixture was subjected to an ESI-MS mass experiment, and the intermediates **A2**, **B2**, **C2**, **G2**, and **H2** were detected by HRMS values along with their isotopic values for the presence of bromine atoms. The observed m/z values ($M+H^+$) are as follows:

Intermediate A2 – Expected m/z calculated for **$C_{27}H_{27}BrNO$** 460.1271 ($M + H^+$); **Found** 460.1252 and 462.1251. **Intermediate B2** – Expected m/z calculated for **$C_{27}H_{26}Br_2NO$** 540.0356 ($M + H^+$); **Found** 540.0363 & 538.0376. **Intermediate C2, D2** – Expected m/z calculated for **$C_{27}H_{25}BrNO$** 458.1115 ($M + H^+$); **Found** 458.0960 & 460.1252. **Intermediate H2, I2** – Expected m/z calculated for $C_{27}H_{23}BrNO$ 456.0958 ($M + H^+$); **Found** 456.0959 & 458.0960.

DFT Calculations

To understand how the cyclization intermediate (**C2**) forms from the intermediate **B2**, we have performed calculations using Density Functional Theory (DFT) using the model system of starting material **4al** and presented the resulting free energy profile in **Figure 3.2**. Alongside the mono-brominated intermediate **A2**, the experimental HRMS spectra also reveal the notable presence of a di-brominated intermediate **B2**. We consider this di-brominated intermediate **B2** as the initial point for calculating the reaction energy profile of the reaction. During the ring cyclization process, two potential routes are foreseeable: (i) The transfer of a Br radical from the di-brominated intermediate generates **IM1**, which then reacts with an OH group, resulting in the formation of the ring cyclization intermediate **IM2** (intermediate **C2**); (ii) A pathway resembling S_N2 transition state, where an OH group attacks the 7th carbon atom of intermediate **B2** of

compound **4al**, leading to the formation of **IM2** which is the intermediate **C2** *via* the ring cyclization. However, this S_N2-like route can be disregarded due to a substantial energy barrier of 17.3 kcal/mol to reach the **TS'**. On the contrary, the radical coupling pathway emerges as more feasible, featuring an exceptionally low energy barrier. In this pathway, **IM1** forms with an energy release of -17.8 kcal/mol, accompanied by generation of one equiavalent of HBr. The calculated energy barrier for the radical coupling between the OH group and the carbon radical at the 7th position of starting material **4al** is very low of 7.2 kcal/mol to form **TS1**. This is eventually leading the ring cyclization with a release of -6.3 kcal/mol. Hence, the radical coupling pathway serves as the driving force for the subsequent cyclisation for the formation of the pyran ring which is shown in the proposed mechanism (**Scheme 3.14**).

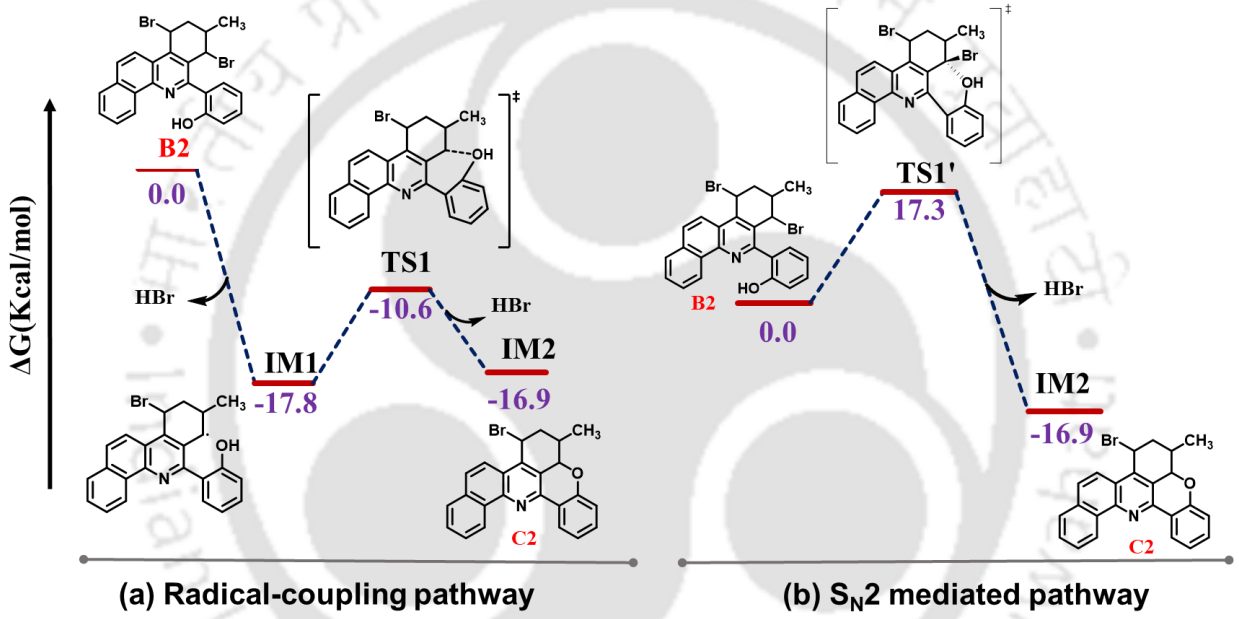

Figure 3.2. Computed free energy (ΔG, in kcal/mol) profiles for the formation of intermediate **C2** by (a) radical-coupling pathway, and (b) S_N2 mediated pathway. Relative free energies (in kcal/mol) are computed based on PBE0-D3/Def2-TZVP single point energies, and gas-phase free energies corrections obtained at the PBE-D3/Def2-SVP level of theory.

3.2d. Application

Post-Synthetic Application: It should be noted that the presence of the bromo functionality in the chromenophenanthridines can be beneficial in further synthetic organic conversions to accomplish new organic compounds through various cross-coupling reactions such as Suzuki-Miyaura, Sonogashira cross-coupling reaction. As an example, compound **6a** was used in the Suzuki cross-coupling reaction with *p*-tolyl boronic acid to get the cross-coupled product **8a** (**Scheme 3.15**).

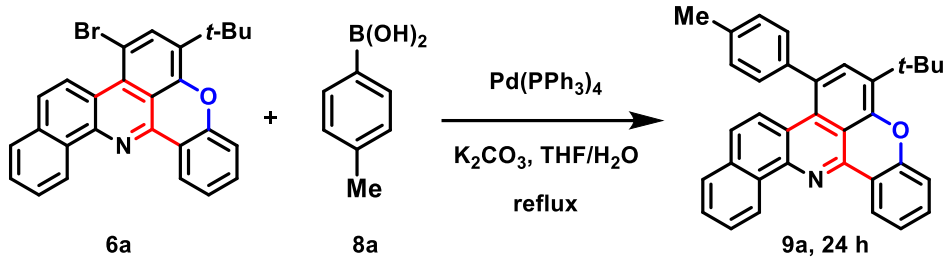

Scheme 3.15. Application of compound **6a** in Suzuki cross-coupling reaction.

Photophysical Study

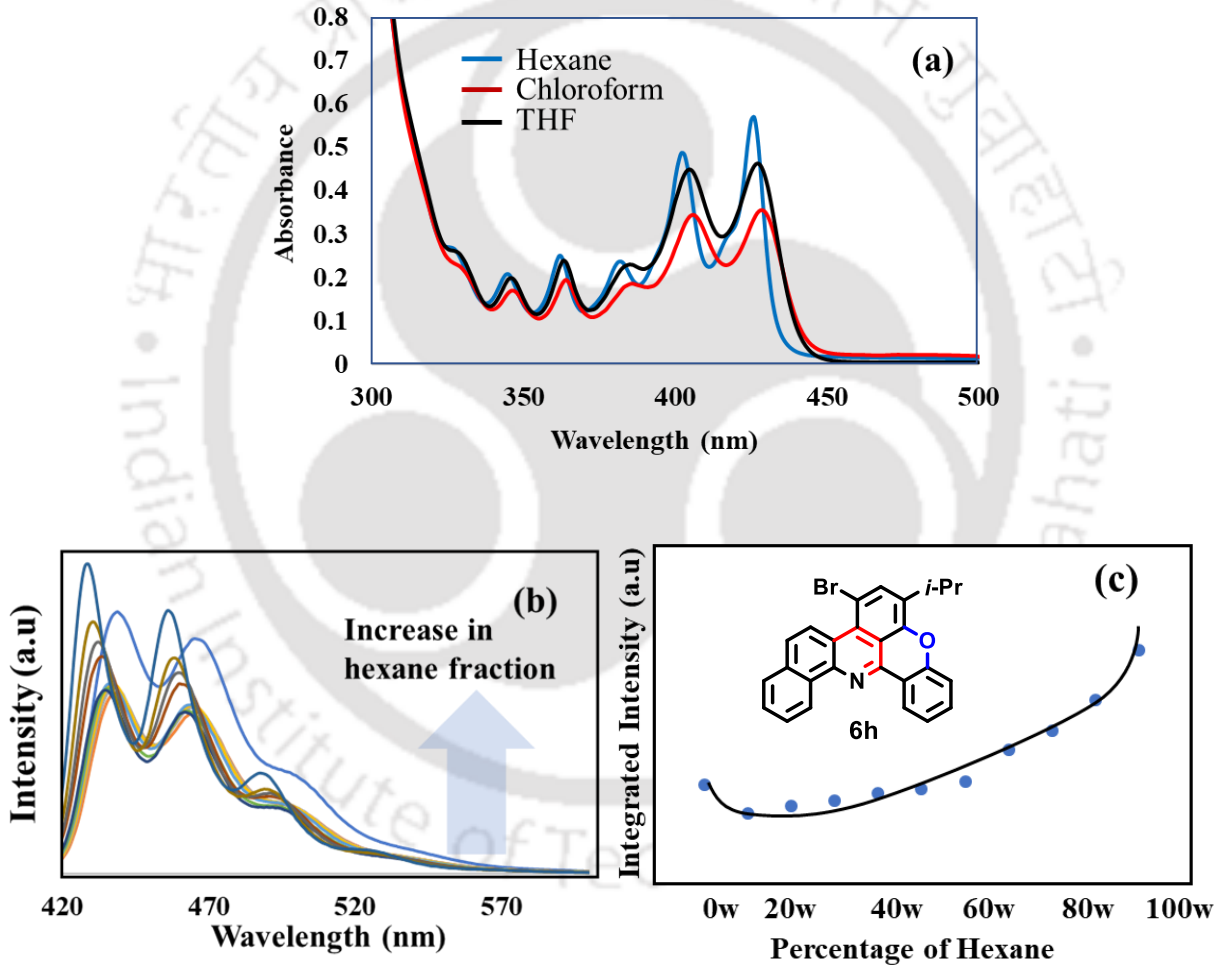

Figure 3.3. (**a**) Absorption Spectra of compound **6h** (1 μM) in different solvents at 298 K; (**b**) Emission Spectra (λex= 385 nm) of compound **6h** (1 μM) is recorded by adding a different percentage of hexane in THF at 298 K; (**c**) Plot of Integrated Emission Intensity against the percentage of hexane.

Hence, the polycyclic aromatic compounds are highly luminescent and explored for various photophysical studies, such as aggregation-induced emission (AIE).[16] To begin with photophysical studies, we carried out absorption spectra of the compound **6h** in different solvents in 1 μM concentration. The absorption maxima of the compound lies between 320 nm and 450 nm in the case of all the solvents (**Figure 3.3a**). Emission Spectroscopy was carried out to further detail the photophysical properties exciting the compound at 400 nm and their aggregating behaviour in the THF-Hexane binary mixture solvent system (**Figure 3.3b** & **3.3c**). The increase in the percentage of hexane in THF showed a rise in emission intensity. This indicates aggregation-induced emission and the compound proves to be AIEgen. The compound remains solvated in THF, exhibiting weaker fluorescence. On increasing the percentage of poor solvent, the compound starts to aggregate. Below 40% of hexane content, the solvating power of the solution is enough to dissolve the luminogens; when the percentage of hexane rises above 60%, the compound fairly aggregates, and the fluorescence intensity is enhanced. The highest emission intensity is observed at 100% hexane, where the compound exists as emissive aggregates.

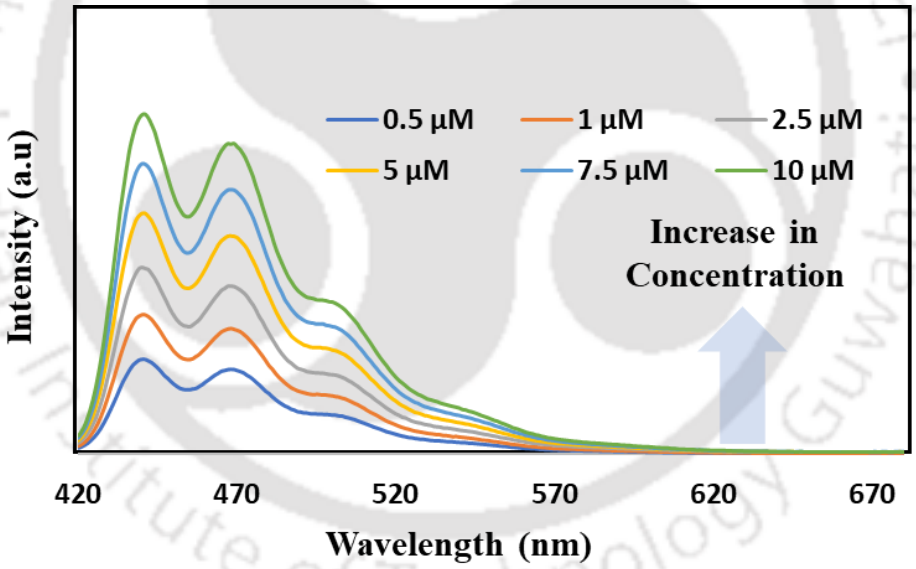

Figure 3.4. Fluorescence emission spectra (λex= 385 nm) in different concentrations of the compound **6h** in THF solvent in 298K.

The AIE factor (αAIE) can be measured by comparing the quantum yields of the respective states, which can provide a quantitative idea about the fluorescence enhancement by the formation of aggregates. In THF, the quantum yields of compound **6h** in solution were calculated to be 0.54, whereas, in the aggregated states, it was 0.64, resulting in AIE factors, and αAIE values being 1.25.

The concentration-dependent emission spectroscopy of compound **6h** was also recorded at room temperature in THF solvent (**Figure 3.4**). The emission intensity increases with an increase in the concentration of the probe in the solution from 0.5 μM to 10 μM. This elucidates the potential-stacking interaction leading to the aggregation-induced emission.

3.2e. Conclusions

In summary, we have synthesized 7-bromobenzo[*c*]chromeno[4,3,2-*gh*]phenanthridine derivatives (**6a-r**) in the presence of 2.7 equiv. NBS and 10 mol% AIBN in CCl_4 solvent under reflux condition. The advantages of this procedure are:

i) Utilization of Whol-Ziegler reaction for regioselective bromination, intramolecular ring cyclization, and subsequent aromatization are happening in a single step for the first time;

ii) All the synthesized 7-bromobenzo[*c*]chromeno[4,3,2-*gh*]phenanthridine derivatives are completely new.

iii) A DFT study has been done to prove the radical-mediated pathway for the cyclization rather than the S_N2 pathway;

iv) The introduction of bromine atom selectively at the C-7 is achieved without an additional aromatic electrophilic bromination reaction;

v) *In-situ* radical-catalyzed benzylic bromination propagates the intramolecular pyran ring formation;

vi) The non-requirement of transition metal catalyst, oxidant, or dehydrogenation reagent and the use of cheap reagent NBS;

vii) The utilization of the bromo group at the C-7 position is demonstrated in the Suzuki cross-coupling reaction for the compound **6a**;

viii) However, a brief photo-physical study of one compound **6h** among all the synthesized compounds has also been investigated, and it displayed aggregation-induced emission in the THF/Hexane mixture. Thus, we affirm that the synthesized compound has good optical properties and emissive features and can be applied to the material and supramolecular chemistry.

3.3. Experimental Section

3.3a. General Procedure for Synthesizing 2-(7,8,9,10-Tetrahydrobenzo[*c*]phenanthridin-6-yl)-phenol Derivatives 4.

In a dry 25 mL single-necked round-bottomed flask, 1-naphthylamine **1** (143 mg, 1.0 mmol), aromatic aldehyde **2** (1.0 mmol), and cyclohexanone derivatives **3** (154 mg, 1.0 mmol) were dissolved in acetonitrile (5.0 mL). A catalytic amount of (±)-camphor-10-sulfonic acid (CSA, 0.023 g, 0.10 mmol) was added to it, and the same reaction mixture was refluxed with constant stirring on a preheated oil bath. The progress of the reaction was monitored by checking TLC from time to time at intervals of 30 minutes. After completion of the reaction, the reaction mixture was allowed to cool at room temperature. The precipitate was filtered through a Büchner funnel, washed with acetonitrile (3 x 2.0 mL), and air-dried to get the desired product **4**.

3.3b. General Procedure for the Synthesis of 7-Bromobenzo[*c*]chromeno[4,3,2-*gh*]phenanthridine 6

In a dry 25 mL single-necked round-bottomed flask, phenol derivative **4** (0.10 mmol), *N*-bromosuccinimide/NBS (2.7 equiv, 48 mg), and azobisisobutyronitrile/AIBN (1.5 mg, 10 mol%) were mixed in 5 mL tetrachloromethane/CCl_4 solvent. Then, the reaction mixture was refluxed with constant stirring in a preheated oil bath. The progress of the reaction was scrutinized by checking TLC from time to time at intervals of 30 minutes. After the product formation, the excess solvent was removed under a rotary evaporator. Workup was done using a dichloromethane water mixture. Then the organic layer was collected and dried over anhydrous Na_2SO_4. Finally, the reaction mixture was purified through silica gel using hexane to obtain the desired light green colored solid product **6**.

3.3c. General Procedure for the Synthesis of 7-Chloro-9-(*tert*-butyl)benzo[*c*]chromeno[4,3,2-*gh*]phenanthridine (7a) and 7-Iodo-9-(*tert*-butyl)benzo[*c*]chromeno[4,3,2-*gh*]phenanthridine (7b).

In a dry 25 mL single-necked round-bottomed flask, phenol derivative **4** (0.10 mmol), *N*-chlorosuccinimide/NCS (2.7 equiv, 36 mg) or *N*-iodosuccinimide/NIS (2.7 equiv, 60 mg) were taken in CCl_4 solvent to achieve compound **7a** or **7b** respectively. Then, azobisisobutyronitrile/AIBN (1.5 mg, 10 mol%) was added to the reaction mixture and stirred under reflux conditions in a preheated oil bath. The progress of the reaction was scrutinized by checking TLC. After the product formation, the excess solvent was removed under a rotary evaporator. The crude was dissolved in dichloromethane and washed with water. For NIS, the reaction mixture was quenched with Na_2SO_3 solution and then washed with water. Then, the organic layer was collected and dried over anhydrous Na_2SO_4. Finally, the reaction mixture was purified through silica gel to obtain the desired products **7a** and **7b**.

3.3d. General Procedure for the Synthesis of 9-(*tert*-Butyl)-7-(*p*-tolyl)benzo[*c*]chromeno[4,3,2-*gh*]phenanthridine (9a).

An oven-dried 25 mL two-necked round-bottomed flask containing a magnetic stir bar was charged with compound **6a** (15 mg, 0.033 mmol), the *p*-tolylboronic acid (**8a**, 6 mg, 1.5 equiv.), $Pd(PPh_3)_4$ (1 mg, 10.0 mol%), and anhydrous K_2CO_3 (14 mg, 4.0 equiv.). The r.b was capped with a rubber septum and adapter. Then it was evacuated and backfilled with nitrogen (this sequence was repeated three times). After that, THF (5.0 mL) and water (1 mL) were added through the septum via syringe, and the resulting mixture was stirred at reflux condition for 24 h. The reaction mixture was then allowed to cool to room temperature, diluted with dichloromethane (5 mL), filtered through a filter paper, and washed with water. The organic layer was dried over anhydrous sodium sulfate and purified by column chromatography on silica gel using pure hexane to obtain compound **9a**.

3.3e. Characterization Data of all the Synthesized Compounds

The characterization data for the compounds **4aa**, **4ac-af**, **4ai-am**, and **4ao-aq** are already given in **Chapter II, Section 3**.

2-(8-(*tert*-Butyl)-7,8,9,10-tetrahydrobenzo[*c*]phenanthridin-6-yl)-4-fluorophenol (4ab)

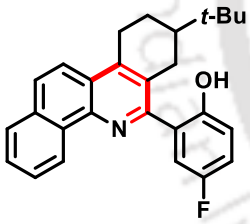

White solid (279 mg, 70%); mp 267-269 °C; ^{1}H NMR (500 MHz, $CDCl_3$) δ 12.27 (s, 1H), 9.07 (d, *J* = 7.9 Hz, 1H), 7.94 – 7.85 (m, 3H), 7.75 – 7.68 (m, 2H), 7.40 (dd, *J* = 9.9, 2.9 Hz, 1H), 7.13 (dd, *J* = 8.9, 5.1 Hz, 1H), 7.08 (td, *J* = 8.9, 8.4, 3.0 Hz, 1H), 3.56 (dd, *J* = 17.9, 5.7 Hz, 1H), 3.22 – 3.15 (m, 1H), 3.08 (d, *J* = 15.9 Hz, 1H), 2.88 – 2.82 (m, 1H), 2.28 – 2.25 (m, 1H), 1.63 – 1.58 (m, 1H), 1.32 (t, *J* = 11.9 Hz, 1H), 0.99 (s, 9H); ^{13}C NMR (125 MHz, $CDCl_3$) δ 156.4, 155.1, 154.5, 153.6, 145.3, 141.4, 133.4, 130.7, 130.6, 128.3 (d, *J* = 1.1 Hz), 127.9 (d, *J* = 49.1 Hz), 124.4, 123.9, 123.0 (d, *J* = 7.0 Hz), 120.5, 118.7 (d, *J* = 7.7 Hz), 117.2 (d, *J* = 22.7 Hz), 116.2 (d, *J* = 24.3 Hz), 116.1, 44.8, 32.5, 31.5, 28.22, 27.5, 23.8; ^{19}F NMR (471 MHz, $CDCl_3$) δ -125.39; IR (KBr)ν_{max}: 2951, 2920, 2852, 1621 cm^{-1}; HRMS (ESI) Calcd for $C_{27}H_{27}FNO$ 400.2072 ($M + H^+$); Found 400.2084.

2-(8-(*tert*-Butyl)-7,8,9,10-tetrahydrobenzo[*c*]phenanthridin-6-yl)-4-methylphenol (4ag)

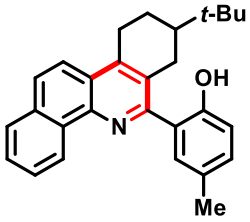

White solid (252 mg, 64%); mp 238 °C; ^{1}H NMR (400 MHz, $CDCl_3$) δ 12.19 (s, 1H), 9.09 (d, *J* = 7.7 Hz, 1H), 7.93 – 7.89 (m, 2H), 7.84 (d, *J* = 9.1 Hz, 1H), 7.74 – 7.66 (m, 2H), 7.49 (s, 1H), 7.16 (dd, *J* = 8.3, 1.8 Hz, 1H), 7.08 (d, *J* = 8.2 Hz, 1H), 3.54 (dd, *J* = 18.0, 5.8 Hz, 1H), 3.22 – 3.09 (m, 1H), 3.11 (d, *J* = 16.6 Hz, 1H), 2.88 (t, *J* = 16.0 Hz, 1H), 2.37 (s, 3H), 2.28 – 2.23 (m, 1H), 1.64 – 1.56 (m, 1H), 1.34 (d, *J* = 11.2 Hz, 1H), 0.98 (s, 9H); ^{13}C NMR (125 MHz, $CDCl_3$) δ 156.3, 155.1, 144.9, 141.4, 133.3, 131.2, 130.7, 130.6, 128.1, 128.0, 127.8, 127.6, 127.5, 124.0, 122.4, 120.6, 117.7, 44.7, 32.5, 31.6, 28.1, 27.5, 23.9, 20.9. IR (KBr)ν_{max}: 2952, 2923, 2855, 1624 cm^{-1}; HRMS (ESI) Calcd for $C_{28}H_{30}NO$ 396.2322 (M + H^+); Found 396.2313.

2-(8-Isopropyl-7,8,9,10-tetrahydrobenzo[*c*]phenanthridin-6-yl)phenol (4ah)

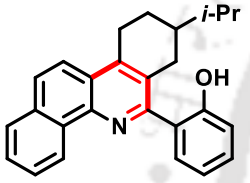

White solid (220 mg, 60%); mp 254 °C; ^{1}H NMR (500 MHz, $CDCl_3$) δ 12.54 (s, 1H), 9.09 (d, *J* = 8.0 Hz, 1H), 7.93 – 7.90 (m, 2H), 7.85 (d, *J* = 9.1 Hz, 1H), 7.74 – 7.67 (m, 3H), 7.38 – 7.34 (m, 1H), 7.19 (d, *J* = 8.1 Hz, 1H), 6.98 (t, *J* = 7.1 Hz, 1H), 3.53 (dd, *J* = 18.1, 5.0 Hz, 1H), 3.25 – 3.17 (m, 1H), 3.08 (d, *J* = 16.2 Hz, 1H), 2.92 – 2.87 (m, 1H), 2.23 – 2.17 (m, 1H), 1.69 – 1.61 (m, 2H), 1.42 – 1.35 (m, 1H), 0.98 (dd, *J* = 16.3, 6.8 Hz, 6H); ^{13}C NMR (125 MHz, $CDCl_3$) δ 157.6, 157.0, 156.2, 145.1, 141.4, 133.3, 130.7, 130.4, 130.3, 128.1, 128.1, 127.9, 127.6, 124.2, 124.0, 122.6, 120.5, 118.5, 118.0, 40.7, 33.9, 32.0, 27.4, 25.6, 20.2, 19.8. IR (KBr)ν_{max}: 2955, 2922, 2851, 1620 cm^{-1}; HRMS (ESI) Calcd for $C_{26}H_{26}NO$ 368.2009 (M + H^+); Found 368.2036.

2-(8-Phenyl-7,8,9,10-tetrahydrobenzo[*c*]phenanthridin-6-yl)phenol (4an)

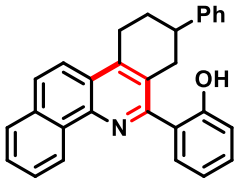

White solid (264 mg, 66%); mp 224 °C; ^{1}H NMR (500 MHz, $CDCl_3$) δ 12.44 (s, 1H), 9.13 (d, *J* = 8.1 Hz, 1H), 7.95 (d, *J* = 7.8 Hz, 1H), 7.92 – 7.86 (m, 2H), 7.76 (t, *J* = 7.3 Hz, 1H), 7.72 (t, *J* = 7.4 Hz, 1H), 7.59 (d, *J* = 7.5 Hz, 1H), 7.37 – 7.31 (m, 3H), 7.30 – 7.25 (m, 3H), 7.17 (d, *J* = 8.0 Hz, 1H), 6.91 (t, *J* = 7.5 Hz, 1H), 3.59 (t, *J* = 19.9 Hz, 1H), 3.38 – 3.33 (m, 1H), 3.31 – 3.21 (m, 2H), 2.84 – 2.82 (m, 1H), 2.40 – 2.38 (m, 1H), 2.17 (s, 1H); ^{13}C NMR (125 MHz, $CDCl_3$) δ 157.1, 155.6, 145.4, 133.4, 131.0, 130.2, 128.8, 128.6, 128.4, 128.2, 128.0, 127.0, 126.7, 124.3, 124.2, 122.3, 120.4, 119.1, 118.3, 40.5, 37.7, 29.2, 27.7. IR (KBr)ν_{max}: 2956, 2925, 2853, 1621 cm^{-1}; HRMS (ESI) Calcd for $C_{29}H_{24}NO$ 402.1853 (M + H^+); Found 402.1852.

4-Bromo-2-(12-bromo-8-(*tert*-butyl)-7,8,9,10-tetrahydrobenzo[c]phenanthridin-6-yl)phenol (4ar)

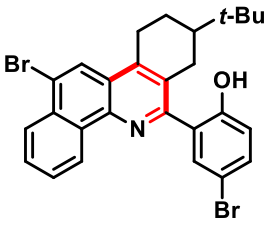

Brown solid (273 mg, 51%); mp 320-322 °C; ^{1}H NMR (500 MHz, Methanol-d_4) δ 9.13 (d, *J* = 8.1 Hz, 1H), 8.28 (s, 1H), 8.22 (d, *J* = 8.5 Hz, 1H), 7.98 – 7.91 (m, 2H), 7.75 (d, *J* = 2.4 Hz, 1H), 7.70 (dd, *J*=8.8, 2.4 Hz, 1H), 7.08 (d, *J* = 8.8 Hz, 1H), 3.87 (d, *J* = 17.6 Hz, 1H), 3.44 (dt, *J* = 18.4, 9.1 Hz, 1H), 2.84 (d, *J* = 18.9 Hz, 1H), 2.70 – 2.65 (m, 1H), 2.37 (t, *J* = 8.1 Hz, 1H), 1.64 – 1.58 (m, 2H), 0.96 (s, 9H); ^{13}C NMR (125 MHz, Methanol-d_4) δ 157.4, 155.9, 151.9, 136.7, 136.2, 135.8, 135.6, 134.1, 132.3, 132.0, 130.5, 130.1, 128.0, 124.6, 124.0, 122.2, 121.3, 119.1, 112.4, 44.5, 33.1, 30.2, 29.3, 27.3, 24.0. IR (KBr)ν_{max}: 2952, 2923, 2855, 1624 cm^{-1}; Calcd for $C_{27}H_{26}Br_2NO$ 540.0356 (M + H$^+$); Found 540.0352 & 538.0361.

7-Bromo-9-(*tert*-butyl)benzo[*c*]chromeno[4,3,2-*gh*]phenanthridine (6a)

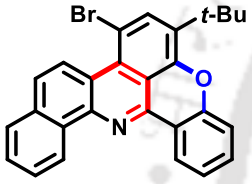

Light green solid (22 mg, 70%); mp 295 °C; ^{1}H NMR (500 MHz, $CDCl_3$) δ 9.43 (d, *J* = 8.1 Hz, 1H), 8.91 (d, *J* = 2.4 Hz, 1H), 8.34 (d, *J* = 8.9 Hz, 1H), 8.15 (d, *J* = 8.7 Hz, 1H), 7.95 – 7.88 (m, 4H), 7.86 (d, *J* = 2.4 Hz, 1H), 7.76 (t, *J* = 7.6 Hz, 1H), 7.68 (d, *J* = 8.0 Hz, 1H), 1.69 (s, 9H); ^{13}C NMR (150 MHz, $CDCl_3$) δ 150.2, 149.8 144.1, 141.2, 137.3, 133.6, 133.0, 132.4, 131.8, 130.6, 127.7, 127.6, 127.4, 127.1, 126.9, 125.0, 124.7, 120.3, 120.0, 116.8, 115.4, 115.3, 111.7, 35.1, 29.5. IR (KBr)ν_{max}: 2951, 2921, 2852, 1728, 1621 cm^{-1}; HRMS (ESI) Calcd for $C_{27}H_{21}BrNO$ 454.0802 (M + H$^+$); Found 454.0799 and 456.0781.

7-Bromo-9-(*tert*-butyl)-13-flurobenzo[*c*]chromeno[4,3,2-*gh*]phenanthridine (6b)

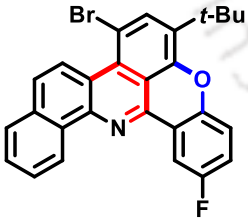

Light green solid (22 mg, 67%); mp 204-206 °C; ^{1}H NMR (500 MHz, $CDCl_3$) δ 9.46 (d, *J* = 8.2 Hz, 1H), 8.55 (dd, *J* = 8.6, 3.0 Hz, 1H), 8.38 (d, *J* = 8.9 Hz, 1H), 8.19 (d, *J* = 8.7 Hz, 1H), 7.95 – 7.93 (m, 3H), 7.76 (t, *J* = 7.0 Hz, 1H), 7.68 (t, *J* = 7.4 Hz, 1H), 7.52 (dd, *J* = 7.3, 3.0 Hz, 1H), 1.69 (s, 9H); ^{13}C NMR (125 MHz, $CDCl_3$) δ 159.5, 157.6, 150.1, 147.8, 144.8, 141.3, 133.7, 133.1, 132.5, 131.9, 130.7, 127.8, 127.6, 127.4, 126.9, 125.0, 123.1, 122.9 (d, *J* = 27.0 Hz), 120.4, 120.1, 115.2, 111.2 (d, *J* = 9.5 Hz), 110.2 (d, *J* = 24.2 Hz), 35.1, 29.5. ^{19}F NMR (471 MHz, $CDCl_3$) δ -116.99. IR (KBr)ν_{max}: 2957, 2922, 2850, 1614 cm^{-1}; HRMS (ESI) Calcd for $C_{27}H_{20}BrFNO$ 472.0707 (M + H$^+$); Found 472.0707 & 474.0689.

7-Bromo-9-(*tert*-butyl)-13-chlorobenzo[*c*]chromeno[4,3,2-*gh*]phenanthridine (6c)

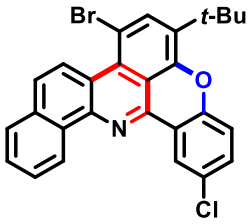

Light green solid (33 mg, 68%); mp 275 °C; ^{1}H NMR (500 MHz, $CDCl_3$) δ 9.40 (d, *J* = 8.2 Hz, 1H), 8.73 (d, *J* = 2.5 Hz, 1H), 8.31 (d, *J* = 8.9 Hz, 1H), 8.11 (d, *J* = 8.7 Hz, 1H), 7.91 – 7.88 (m, 3H), 7.74 (t, *J* = 7.05 Hz, 1H), 7.71 (d, *J* = 2.5 Hz, 1H), 7.66 (t, *J* = 6.9 Hz, 1H), 1.69 (s, 9H); ^{13}C NMR (100 MHz, $CDCl_3$) δ 149.9, 149.8, 144.3, 141.2, 134.7, 133.7, 133.1, 132.5, 131.9, 130.6, 129.6, 127.7, 127.6, 127.4, 126.9, 125.0, 124.3, 124.0, 120.3, 120.0, 115.4, 115.3, 111.5, 35.1, 29.5. IR (KBr)ν_{max}: 2957, 2922, 2855, 1620 cm^{-1}; HRMS (ESI) Calcd for $C_{27}H_{20}BrClNO$ 488.0412 ($M + H^+$); Found 488.0406 and 490.0399.

7,13-Dibromo-9-(*tert*-butyl)benzo[*c*]chromeno[4,3,2-*gh*]phenanthridine (6d)

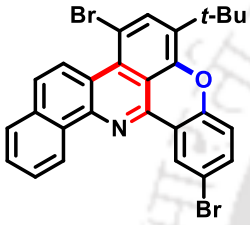

Light green solid (25 mg, 68%); mp 267-269 °C; ^{1}H NMR (400 MHz, $CDCl_3$) δ 9.45 (d, *J* = 8.4 Hz, 1H), 8.94 (d, *J* = 2.3 Hz, 1H), 8.36 (d, *J* = 8.8 Hz, 1H), 8.17 (d, *J* = 8.7 Hz, 1H), 7.94 – 7.92 (m, 3H), 7.87 (d, *J* = 2.3 Hz, 1H), 7.77 (t, *J* = 7.3 Hz, 1H), 7.68 (t, *J* = 7.4 Hz, 1H), 1.69 (s, 9H); ^{13}C NMR (100 MHz, $CDCl_3$) δ 150.3, 149.9, 144.3, 141.4, 137.4, 133.7, 133.2, 132.6, 132.0, 130.7, 127.8, 127.7, 127.5, 127.2, 127.0, 125.1, 124.9, 120.4, 120.1, 116.9, 115.6, 115.4, 111.8, 35.1, 29.5. IR (KBr)ν_{max}: 2958, 2915, 2852, 1614 cm^{-1}; HRMS (ESI) Calcd for $C_{27}H_{20}Br_2NO$ 533.9886 ($M + H^+$); Found 533.9883 and 531.9891.

7-Bromo-9-(*tert*-butyl)-11,13-dichlorobenzo[*c*]chromeno[4,3,2-*gh*]phenanthridine (6e)

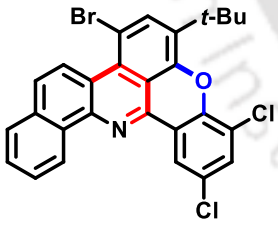

Light green solid (25 mg, 70%); mp 207-209 °C; ^{1}H NMR (400 MHz, $CDCl_3$) δ 9.47 (d, *J* = 8.0 Hz, 1H), 8.76 (d, *J* = 2.5 Hz, 1H), 8.38 (d, *J* = 8.9 Hz, 1H), 8.19 (d, *J* = 8.8 Hz, 1H), 7.95 – 7.93 (m, 2H), 7.77 (t, *J* = 7.2 Hz, 1H), 7.69 (t, *J* = 7.4 Hz, 1H), 7.58 (d, *J* = 2.5 Hz, 1H), 1.67 (s, 9H); ^{13}C NMR (125 MHz, $CDCl_3$) δ 149.8, 148.7, 144.4, 141.3, 133.7, 133.2, 132.5, 131.9, 131.7, 130.7, 129.2, 127.8, 127.6, 127.5, 127.0, 125.0, 124.4, 123.4, 123.2, 120.4, 120.1, 115.6, 115.4, 35.1, 29.5. IR (KBr)ν_{max}: 2956, 2921, 2852, 1617 cm^{-1}; HRMS (ESI) Calcd for $C_{27}H_{19}BrCl_2NO$ 522.0022 ($M + H^+$); Found 522.0025 and 523.9994.

7-Bromo-9-(*tert*-butyl)-13-methoxybenzo[*c*]chromeno[4,3,2-*gh*]phenanthridine (6f)

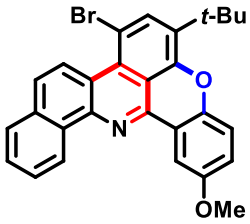

Light green solid (22 mg, 67%); mp 227 °C; ^{1}H NMR (500 MHz, $CDCl_3$) δ 9.21 (d, *J* = 8.2 Hz, 1H), 8.70 (s, 1H), 8.05 (d, *J* = 8.9 Hz, 1H), 7.84 (d, *J* = 8.6 Hz, 1H), 7.79 – 7.71 (m, 4H), 7.66 (t, *J* = 7.4 Hz, 1H), 7.57 (t, *J* = 7.4 Hz, 1H), 4.03 (s, 3H), 1.69 (s, 9H); ^{13}C NMR (100 MHz, $CDCl_3$) δ 156.8, 151.3, 150.0, 143.8, 141.0, 133.4, 132.8, 132.1, 131.6, 130.3, 128.0, 127.5, 127.4, 126.8, 126.6, 124.9, 120.4, 119.8, 115.2, 115.0, 112.9, 107.3, 61.0, 35.1, 29.5. IR (KBr)ν_{max}: 2955, 2925, 2855, 1619 cm^{-1}; HRMS (ESI) Calcd for $C_{28}H_{23}BrNO_2$ 484.0907 ($M + H^+$); Found 484.0901 and 486.0884.

7-Bromo-9-(*tert*-butyl)-13-methylbenzo[*c*]chromeno[4,3,2-*gh*]phenanthridine (6g)

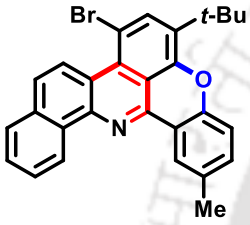

Light green solid (21 mg, 68%); mp 205-207 °C; ^{1}H NMR (500 MHz, $CDCl_3$) δ 9.49 (d, *J* = 8.3 Hz, 1H), 8.64 (s, 1H), 8.36 (d, *J* = 8.9 Hz, 1H), 8.13 (d, *J* = 8.7 Hz, 1H), 7.94 – 7.89 (m, 3H), 7.74 (t, *J* = 8.1 Hz, 1H), 7.66 (t, *J* = 6.9 Hz, 1H), 7.59 (s, 1H), 2.52 (s, 3H), 1.70 (s, 9H); ^{13}C NMR (100 MHz, $CDCl_3$) δ 150.3, 149.1, 145.8, 141.4, 136.2, 134.6, 133.7, 133.0, 132.5, 132.0, 130.4, 127.7, 127.4, 126.9, 126.7, 125.1, 124.4, 123.1, 120.2, 120.1, 115.7, 114.8, 110.4, 35.1, 29.5, 20.9. IR (KBr)ν_{max}: 2956, 2908, 2872, 1619 cm^{-1}; HRMS (ESI) Calcd for $C_{28}H_{23}BrNO$ 468.0958 ($M + H^+$); Found 468.0952 and 470.0942.

7-Bromo-9-*iso*propylbenzo[*c*]chromeno[4,3,2-*gh*]phenanthridine (6h)

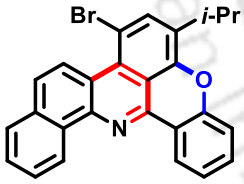

Light green solid (21 mg, 70%); mp 232-234 °C; ^{1}H NMR (400 MHz, $CDCl_3$) δ 9.30 (d, *J* = 8.2 Hz, 1H), 8.72 (d, *J* = 2.3 Hz, 1H), 8.22 (d, *J* = 8.9 Hz, 1H), 8.05 (d, *J* = 8.5 Hz, 1H), 7.88 – 7.82 (m, 3H), 7.78 (d, *J* = 2.3 Hz, 1H), 7.75 (d, *J* = 8.5 Hz, 1H), 7.71 (t, *J* = 7.4 Hz, 1H), 7.63 (t, *J* = 7.2 Hz, 1H), 3.67 (p, *J* = 6.9 Hz, 1H), 1.46 (d, *J* = 6.9 Hz, 6H); ^{13}C NMR (125 MHz, $CDCl_3$) δ 150.0, 148.4, 144.2, 141.4, 137.1, 133.6, 132.1, 131.9, 131.5, 130.0, 127.7, 127.5, 127.4, 127.0, 126.9, 125.0, 124.7, 120.5, 119.9, 116.7, 115.5, 114.8, 112.1, 27.6, 22.3. IR (KBr)ν_{max}: 2958, 2920, 2850, 1609 cm^{-1}; HRMS (ESI) Calcd for $C_{26}H_{19}BrNO$ 440.0645 ($M + H^+$); Found 440.0645 and 442.0611.

7-Bromo-13-chloro-9-*iso*propylbenzo[*c*]chromeno[4,3,2-*gh*]phenanthridine (6i)

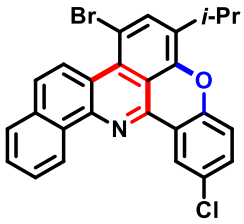

Light green solid (23 mg, 71%); mp 212-214 °C; ^{1}H NMR (400 MHz, $CDCl_3$) δ 9.32 (d, *J* = 8.1 Hz, 1H), 8.60 (d, *J* = 2.4 Hz, 1H), 8.23 (d, *J* = 8.9 Hz, 1H), 8.06 (d, *J* = 8.6 Hz, 1H), 7.88 (d, *J* = 7.8 Hz, 1H), 7.84 (d, *J* = 8.8 Hz, 1H), 7.76 (d, *J* = 8.5 Hz, 1H), 7.71 (t, *J* = 7 Hz, 1H), 7.66 – 7.64 (m, 2H), 3.68 (p, *J* = 6.9 Hz, 1H), 1.46 (s, 6H); ^{13}C NMR (100 MHz, $CDCl_3$) δ 149.5, 148.4, 144.4, 141.4, 134.5, 133.6, 132.1, 131.9, 131.5, 130.1, 129.5, 127.7, 127.5, 127.4, 126.9, 125.0, 124.2, 124.0, 120.5, 119.9, 115.5, 114.8, 111.8, 27.6, 22.3. IR (KBr)ν_{max}: 2960, 2924, 2853, 1623 cm^{-1}; HRMS (ESI) Calcd for $C_{26}H_{18}BrClNO$ 474.0255 (M + H$^+$); Found 474.0258 and 476.0281.

7-Bromo-9-ethylbenzo[*c*]chromeno[4,3,2-*gh*]phenanthridine (6j)

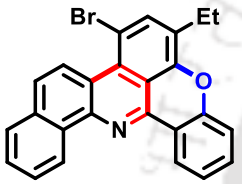

Light green solid (19 mg, 65%); mp 240-242 °C; ^{1}H NMR (400 MHz, $CDCl_3$) δ 9.40 (d, *J* = 8.2 Hz, 1H), 8.83 (d, *J* = 2.3 Hz, 1H), 8.31 (d, *J* = 9.0 Hz, 1H), 8.11 (d, *J* = 8.4 Hz, 1H), 7.92 (t, *J* = 8.6 Hz, 2H), 7.83 (d, *J* = 2.3 Hz, 1H), 7.76 (t, *J* = 8 Hz, H), 7.72 (d, *J* = 8.4 Hz, 1H), 7.68 (t, *J* = 8 Hz, 1H) 3.00 (q, *J* = 7.6 Hz, 2H), 1.41 (d, *J* = 7.5 Hz, 3H); ^{13}C NMR (100 MHz, $CDCl_3$) δ 150.0, 149.0, 144.2, 141.5, 137.1, 133.6, 132.9, 132.3, 132.0, 127.7, 127.6, 127.5, 127.4, 127.0, 126.9, 125.1, 124.7, 120.6, 120.0, 116.7, 115.4, 114.9, 112.2, 23.1, 14.0; IR (KBr)ν_{max}: 2958, 2920, 2851, 1733, 1619 cm^{-1}; HRMS (ESI) Calcd for $C_{25}H_{17}BrNO$ 426.0489 (M + H$^+$); Found 426.0468 and 428.0481.

7-Bromo-13-chloro-9-ethylbenzo[*c*]chromeno[4,3,2-*gh*]phenanthridine (6k)

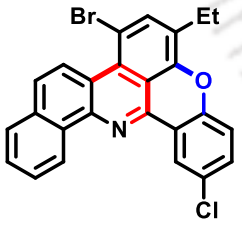

Light green solid (21 mg, 66%); mp 194 °C; ^{1}H NMR (400 MHz, $CDCl_3$) δ 9.27 (d, *J* = 8.1 Hz, 1H), 8.52 (d, *J* = 2.4 Hz, 1H), 8.18 (d, *J* = 8.9 Hz, 1H), 7.97 (d, *J* = 8.4 Hz, 1H), 7.88 (d, *J* = 8.0 Hz, 1H), 7.82 (d, *J* = 8.8 Hz, 1H), 7.70 (t, *J* = 7 Hz, 1H), 7.65 (d, *J* = 8.04 Hz, 1H), 7.62 – 7.60 (m, 2H), 2.92 (q, J = 7.5 Hz, 2H), 1.39 (t, J = 7.6 Hz, 3H); ^{13}C NMR (100 MHz, $CDCl_3$) δ 149.4, 148.9, 144.2, 141.3, 134.4, 133.6, 132.7, 132.1, 131.9, 129.5, 127.7, 127.5, 127.4, 127.2, 126.8, 125.0, 124.1, 123.9, 120.5, 119.9, 115.2, 114.6, 111.8, 23.0, 13.9; IR (KBr)ν_{max}: 2960, 2922, 2853, 1620 cm^{-1}; HRMS (ESI) Calcd for $C_{25}H_{16}BrClNO$ 460.0099 (M + H$^+$); Found 460.0107 and 462.0084.

7-Bromo-9-methylbenzo[*c*]chromeno[4,3,2-*gh*]phenanthridine (6l)

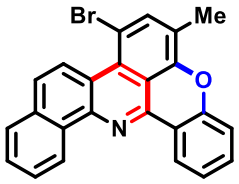

Light green solid (14 mg, 62%); mp 287 °C; ^{1}H NMR (400 MHz, $CDCl_3$) δ 9.38 (d, 1H), 8.81 (d, *J* = 2.1 Hz, 1H), 8.29 (d, *J* = 8.9 Hz, 1H), 8.06 (d, *J* = 8.5 Hz, 1H), 7.94 – 7.89 (m, 3H), 7.82 (d, *J* = 2.2 Hz, 1H), 7.75 (t, *J* = 7.5 Hz, 1H), 7.69 – 7.66 (m, 2H), 2.56 (s, 3H); ^{13}C NMR (125 MHz, $CDCl_3$) δ 144.2, 141.6, 137.2, 134.4, 133.7, 132.3, 132.0, 127.8, 127.6, 127.5, 127.1, 127.0, 125.1, 124.8, 121.4, 120.7, 120.0, 116.8, 115.2, 114.9, 112.2, 15.5. IR (KBr)ν_{max}: 2957, 2920, 2854, 1614 cm^{-1}; HRMS (ESI) Calcd for $C_{24}H_{15}BrNO$ 412.0332 (M + H$^+$); Found 412.0333 and 414.0317.

7-Bromo-13-chloro-9-methylbenzo[*c*]chromeno[4,3,2-*gh*]phenanthridine (6m)

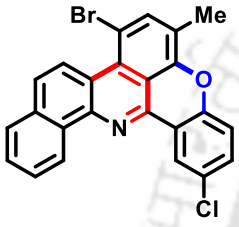

Light green solid (19 mg, 63%); mp 265 °C; ^{1}H NMR (400 MHz, $CDCl_3$) δ 9.37 (d, *J* = 8.2 Hz, 1H), 8.64 (d, *J* = 2.5 Hz, 1H), 8.28 (d, *J* = 8.9 Hz, 1H), 8.04 (d, *J* = 8.3 Hz, 1H), 7.92 (d, *J* = 8.0 Hz, 1H), 7.89 (d, *J* = 8.9 Hz, 1H), 7.73 (t, *J* = 7.1 Hz, 1H), 7.69 – 7.64 (m, 3H), 2.55 (s, 3H); ^{13}C NMR (100 MHz, $CDCl_3$) δ 141.5, 134.5, 134.4, 133.7, 132.2, 132.0, 129.6, 127.7, 127.6, 127.5, 126.9, 125.0, 124.2, 124.0, 121.3, 120.6, 120.0, 116.3, 115.1, 111.9, 15.4. IR (KBr)ν_{max}: 2952, 2921, 2852, 1625 cm^{-1}; HRMS (ESI) Calcd for $C_{24}H_{14}BrClNO$ 445.9942 (M + H$^+$); Found 445.9938 and 447.9908.

7-Bromo-9-phenylbenzo[*c*]chromeno[4,3,2-*gh*]phenanthridine (6n)

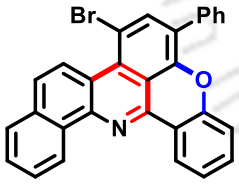

Light green solid (21 mg, 65%); mp 270 °C; ^{1}H NMR (400 MHz, $CDCl_3$) δ 9.42 (d, *J* = 8.1 Hz, 1H), 8.85 (d, *J* = 2.4 Hz, 1H), 8.35 (d, *J* = 9.0 Hz, 1H), 8.25 (d, *J* = 8.6 Hz, 1H), 7.96 – 7.92 (m, 4H), 7.87 (d, *J* = 7.4 Hz, 2H), 7.80 (d, *J* = 2.3 Hz, 1H), 7.76 (t, *J* = 7.1 Hz, 1H), 7.69 (t, *J* = 8.0 Hz, 1H), 7.55 (t, *J* = 7.6 Hz, 2H), 7.46 (t, *J* = 7.4 Hz, 1H); ^{13}C (125 MHz, $CDCl_3$) δ 150.0, 148.4, 144.4, 142.0, 137.4, 136.0, 133.8, 133.5, 131.9, 130.0, 129.6, 128.6, 128.5, 128.0, 127.9, 127.8, 127.8, 127.1, 127.0, 125.1, 124.8, 120.5, 120.0, 117.1, 116.0, 115.3, 112.1; IR (KBr)ν_{max}: 2955, 2915, 2842, 1617 cm^{-1}; HRMS (ESI) Calcd for $C_{29}H_{17}BrNO$ 474.0489 (M + H$^+$); Found 474.0484 and 476.0465.

7-Bromo-13-chloro-9-phenylbenzo[*c*]chromeno[4,3,2-*gh*]phenanthridine (6o)

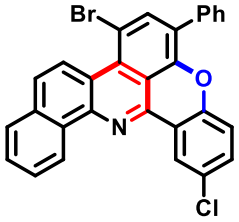

Light green solid (23 mg, 67%); mp 248-250 °C; ^{1}H NMR (400 MHz, $CDCl_3$) δ 9.32 (d, *J* = 8.1 Hz, 1H), 8.60 (d, *J* = 2.3 Hz, 1H), 8.25 (d, *J* = 9.0 Hz, 1H), 8.14 (d, *J* = 8.6 Hz, 1H), 7.90 – 7.84 (m, 4H), 7.76 – 7.64 (m, 3H), 7.61 (d, *J* = 2.3 Hz, 1H), 7.54 (t, *J* = 2.3 Hz, 2H), 7.45 (t, *J* = 7.4 Hz, 1H); ^{13}C NMR (125 MHz, $CDCl_3$) δ 149.5, 148.4, 144.4, 141.9, 136.0, 134.8, 133.8, 133.7, 133.4, 131.9, 130.0, 129.9, 129.6, 128.6, 128.5, 127.9, 127.8, 127.8, 127.7, 127.0, 125.1, 123.9, 120.4, 120.0, 115.9, 115.2, 111.8; IR (KBr)ν_{max}: 3052, 2957, 2922, 2853, 1619 cm^{-1}; HRMS (ESI) Calcd for $C_{29}H_{16}BrClNO$ 508.0099 (M + H$^+$); Found 508.0088 and 510.0074.

5,7-Dibromo-9-(*tert*-butyl)benzo[*c*]chromeno[4,3,2-*gh*]phenanthridine (6p)

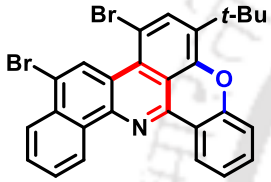

Light green solid (21 mg, 57%); mp 286 °C; ^{1}H NMR (500 MHz, $CDCl_3$) δ 9.43 (d, *J* = 8.2 Hz, 1H), 8.90 (s, 1H), 8.33 (d, *J* = 8.9 Hz, 1H), 8.14 (d, *J* = 8.8 Hz, 1H), 7.92 – 7.90 (m, 3H), 7.86 (s, 1H), 7.76 (t, *J* = 7.7 Hz, 1H), 7.67 (t, *J* = 7.1 Hz, 1H), 1.69 (s, 9H); ^{13}C NMR (125 MHz, $CDCl_3$) δ 150.3, 149.9, 144.3, 141.3, 137.4, 133.7, 133.2, 132.6, 131.9, 130.7, 127.8, 127.6, 127.5, 127.1, 127.0, 125.1, 124.9, 120.4, 120.1, 116.9, 115.6, 115.4, 111.8, 35.1, 29.5; IR (KBr)ν_{max}: 2957, 2920, 2855, 1621 cm^{-1}; HRMS (ESI) Calcd for $C_{27}H_{20}Br_2NO$ 533.9886 (M + H$^+$); Found 533.9882 and 531.9895.

5,7-Dibromo-9-(*tert*-butyl)-13-chlorobenzo[*c*]chromeno[4,3,2-*gh*]phenanthridine (6q)

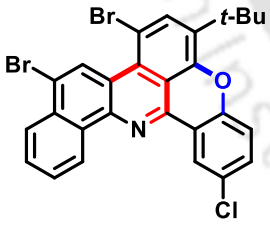

Light green solid (23 mg, 58%); mp 222-224 °C; ^{1}H NMR (400 MHz, $CDCl_3$) δ 9.41 (d, *J* = 8.2 Hz, 1H), 8.73 (d, *J* = 2.4 Hz, 1H), 8.31 (d, *J* = 8.9 Hz, 1H), 8.11 (d, *J* = 8.7 Hz, 1H), 7.92 – 7.88 (m, 2H), 7.75 (t, *J* = 2.4 Hz, 1H), 7.71 (d, *J* = 2.4 Hz, 1H), 7.66 (t, *J* = 7.3 Hz, 1H), 1.69 (s, 9H); ^{13}C NMR (100 MHz, $CDCl_3$) δ 149.9, 149.8, 144.4, 141.3, 134.7, 133.7, 133.1, 132.5, 131.9, 130.6, 129.7, 127.7, 127.6, 127.4, 126.9, 125.1, 124.4, 124.1, 120.4, 120.0, 115.5, 115.4, 111.5, 35.1, 29.5; IR (KBr)ν_{max}: 2957, 2920, 2850, 1619 cm^{-1}; HRMS (ESI) Calcd for $C_{27}H_{19}Br_2ClNO$ 567.9496 (M + H$^+$); Found 567.9496.

5,7,13-Tribromo-9-(*tert*-butyl)benzo[*c*]chromeno[4,3,2-*gh*]phenanthridine (6r)

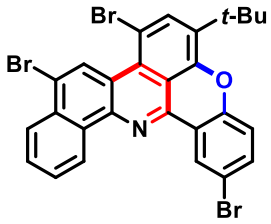

Light green solid (23 mg, 55%); mp 233-235 °C; ^{1}H NMR (500 MHz, $CDCl_3$) δ 9.47 (d, *J* = 8.3 Hz, 1H), 8.96 (s, 1H), 8.38 (d, *J* = 9.0 Hz, 1H), 8.19 (d, *J* = 8.6 Hz, 1H), 7.94 (d, *J* = 8.7 Hz, 1H), 7.88 (s, 1H), 7.78 (t, *J* = 7.5 Hz, 1H), 7.68 (t, *J* = 7.3 Hz, 1H), 1.69 (s, 9H); ^{13}C NMR (100 MHz, $CDCl_3$) δ 150.4, 149.9, 137.4, 133.8, 133.3, 132.0, 132.0, 130.7, 130.7, 127.8, 127.7, 127.5, 127.2, 127.0, 125.1, 120.5, 120.1, 116.9, 115.4, 112.2, 111.9, 35.1, 29.5. IR (KBr)ν_{max}: 2957, 1614 cm^{-1}; HRMS (ESI) Calcd for $C_{27}H_{19}Br_3NO$ 611.8991 ($M + H^+$); Found 611.8987 and 613.9006.

9-(*tert*-Butyl)-7-chlorobenzo[*c*]chromeno[4,3,2-*gh*]phenanthridine (7a)

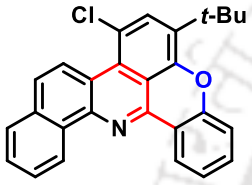

Light green solid (11 mg, 40%); mp 220-222 °C; ^{1}H NMR (500 MHz, $CDCl_3$) δ 9.46 (d, *J* = 8.4 Hz, 1H), 8.51 (dd, *J* = 8.6, 3.0 Hz, 1H), 8.39 (d, *J* = 8.9 Hz, 1H), 8.20 (d, *J* = 8.7 Hz, 1H), 7.97 – 7.94 (m, 4H), 7.77 (t, *J* = 7.3 Hz, 1H), 7.69 (t, *J* = 7.1 Hz, 1H), 7.38 (dd, *J* = 7.5, 3.0 Hz, 1H), 1.67 (s, 9H); ^{13}C NMR (125 MHz, $CDCl_3$) δ 133.8, 133.2, 132.5, 132.0, 130.7, 127.8, 127.6, 127.5, 127.0, 125.0, 120.5, 120.1, 120.0, 119.8, 115.4, 115.2, 109.7, 109.5, 35.1, 29.5; IR (KBr)ν_{max}: 2956, 2924, 2854, 1614 cm^{-1}; HRMS (ESI) Calcd for $C_{27}H_{21}ClNO$ 410.1307 ($M + H^+$); Found 410.1303.

9-(*tert*-Butyl)-7-iodobenzo[*c*]chromeno[4,3,2-*gh*]phenanthridine (7b)

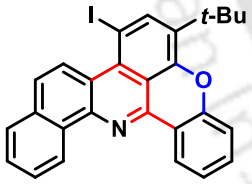

Light green solid (13 mg, 38%); mp 250-252 °C; ^{1}H NMR (400 MHz, $CDCl_3$) δ 9.54 (d, *J* = 8.3 Hz, 1H), 8.93 (d, *J* = 7.8 Hz, 1H), 8.40 (d, *J* = 8.9 Hz, 1H), 8.16 (d, *J* = 8.7 Hz, 1H), 7.95 (d, *J* = 8.0 Hz, 1H), 7.91 (d, *J* = 8.6 Hz, 2H), 7.75 (t, *J* = 7.2 Hz, 1H), 7.67 (t, *J* = 6.9 Hz, 1H), 7.56 (t, *J* = 8.4 Hz, 1H), 7.40 (d, *J* = 7.8 Hz, 1H), 1.63 (s, 9H); ^{13}C NMR (100 MHz, $CDCl_3$) δ 153.9, 150.7, 146.5, 141.6, 133.7, 132.7, 132.4, 132.1, 132.0, 130.2, 127.7, 127.4, 126.6, 125.3, 125.1, 124.1, 121.9, 120.3, 120.1, 117.1, 116.0, 114.4, 35.1, 29.9; IR (KBr)ν_{max}: 2957, 2921, 2850, 1614 cm^{-1}; HRMS (ESI) Calcd for $C_{27}H_{21}INO$ 502.0663 ($M + H^+$); Found 502.0635.

9-(*tert*-Butyl)-7-(*p*-tolyl)benzo[*c*]chromeno[4,3,2-*gh*]phenanthridine (9a)

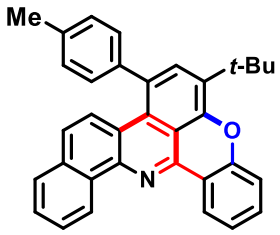

Light green solid (10 mg, 60%); mp 212-214 °C; ^{1}H NMR (400 MHz, $CDCl_3$) δ 9.55 (d, *J* = 8.0 Hz, 1H), 9.05 (d, *J* = 2.5 Hz, 1H), 8.39 (d, *J* = 8.9 Hz, 1H), 8.15 (d, *J* = 8.8 Hz, 1H), 7.94 (t, *J* = 9.3 Hz, 3H), 7.85 (d, *J* = 8.7 Hz,1H), 7.80 (t, *J* = 6.4 Hz, 1H), 7.69 (t, *J* = 6.4 Hz, 1H), 7.57 (d, *J* = 2.5 Hz, 1H), 7.40 (d, *J* = 7.9 Hz, 2H), 7.30 (t, *J* = 7.8 Hz, 2H), 2.47 (s, 3H), 1.20 (s, 9H); ^{13}C NMR (125 MHz, $CDCl_3$) δ 150.8, 150.4, 145.4, 141.4, 138.0, 135.8, 133.9, 133.7, 133.4, 132.9, 132.6, 132.0, 130.5, 129.9, 129.0, 127.8, 127.5, 127.1, 127.0, 126.9, 125.2, 123.9, 120.3, 120.2, 116.7, 114.7, 34.6, 29.3, 21.4; IR (KBr)ν_{max}: 2956, 2924, 2853, 1614 cm^{-1}; HRMS (ESI) Calcd for $C_{34}H_{28}NO$ 466.2166 (M + H^{+}); Found 466.2166.

3.3f. Representative Characterization Spectra

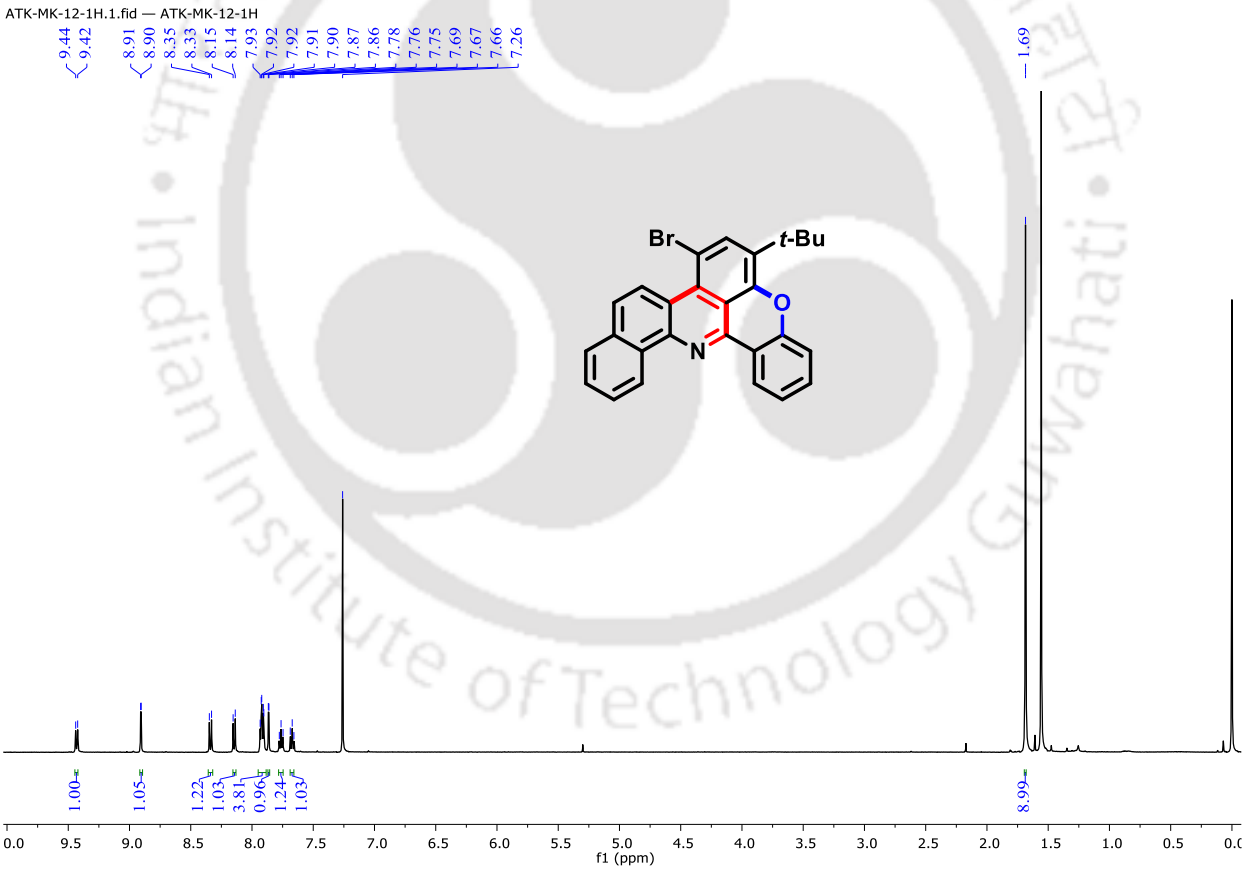

Figure 3.5. ^{1}H NMR spectrum of 7-bromo-9-(*tert*-butyl)benzo[*c*]chromeno[4,3,2-*gh*]phenanthridine (**6a**).

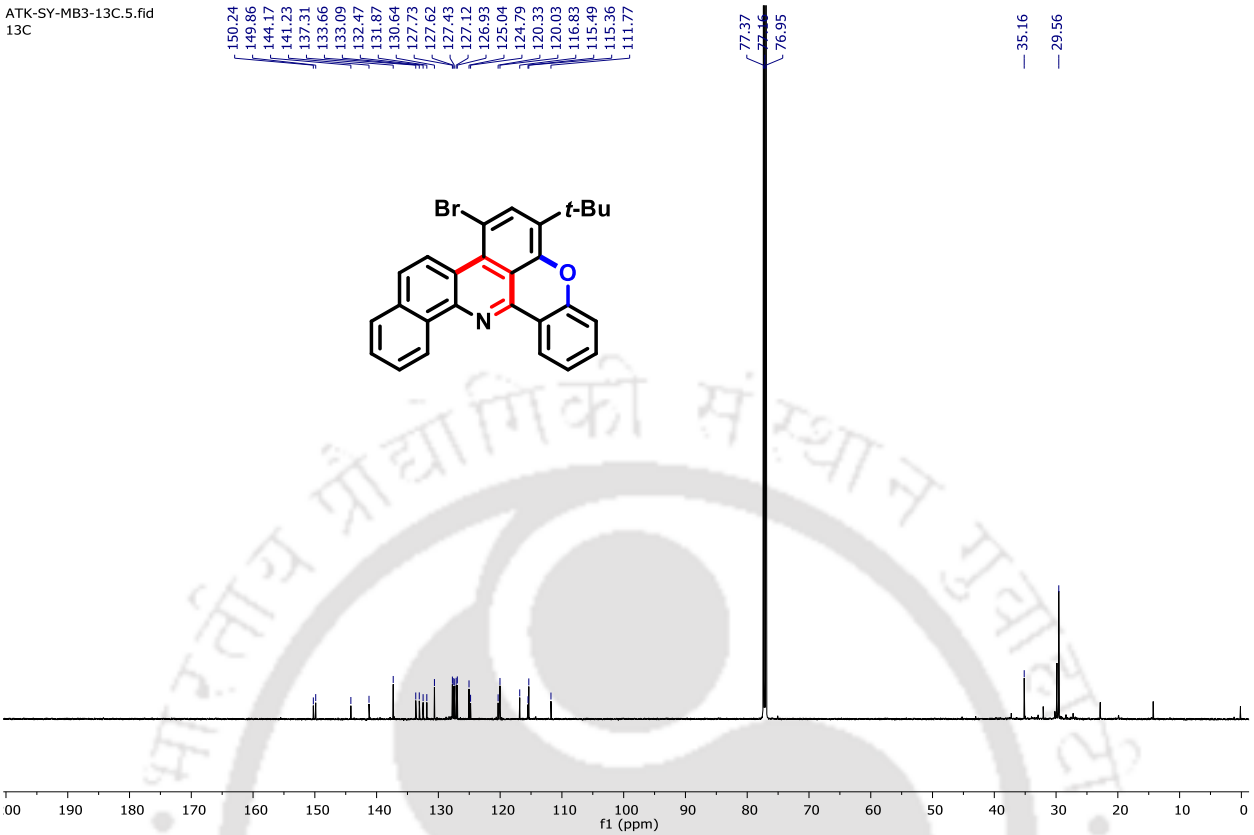

Figure 3.6. ^{13}C NMR spectrum of 7-bromo-9-(*tert*-butyl)benzo[*c*]chromeno[4,3,2-*gh*]phenanthridine (**6a**).

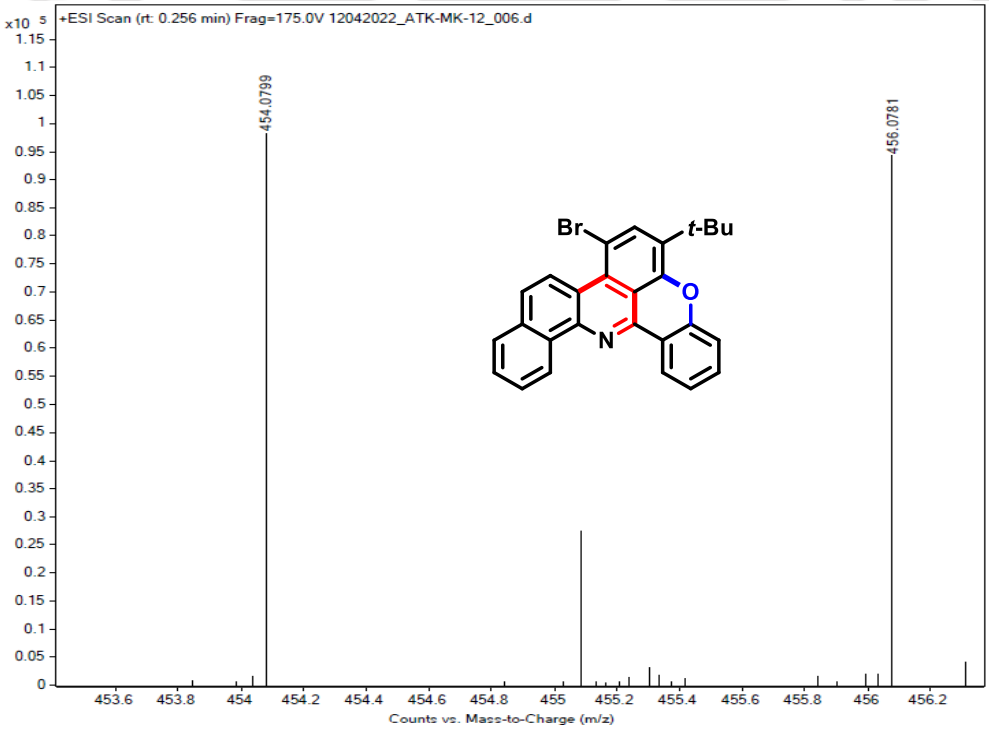

Figure 3.7. HRMS spectrum of 7-bromo-9-(*tert*-butyl)benzo[*c*]chromeno[4,3,2-*gh*]phenanthridine (**6a**).

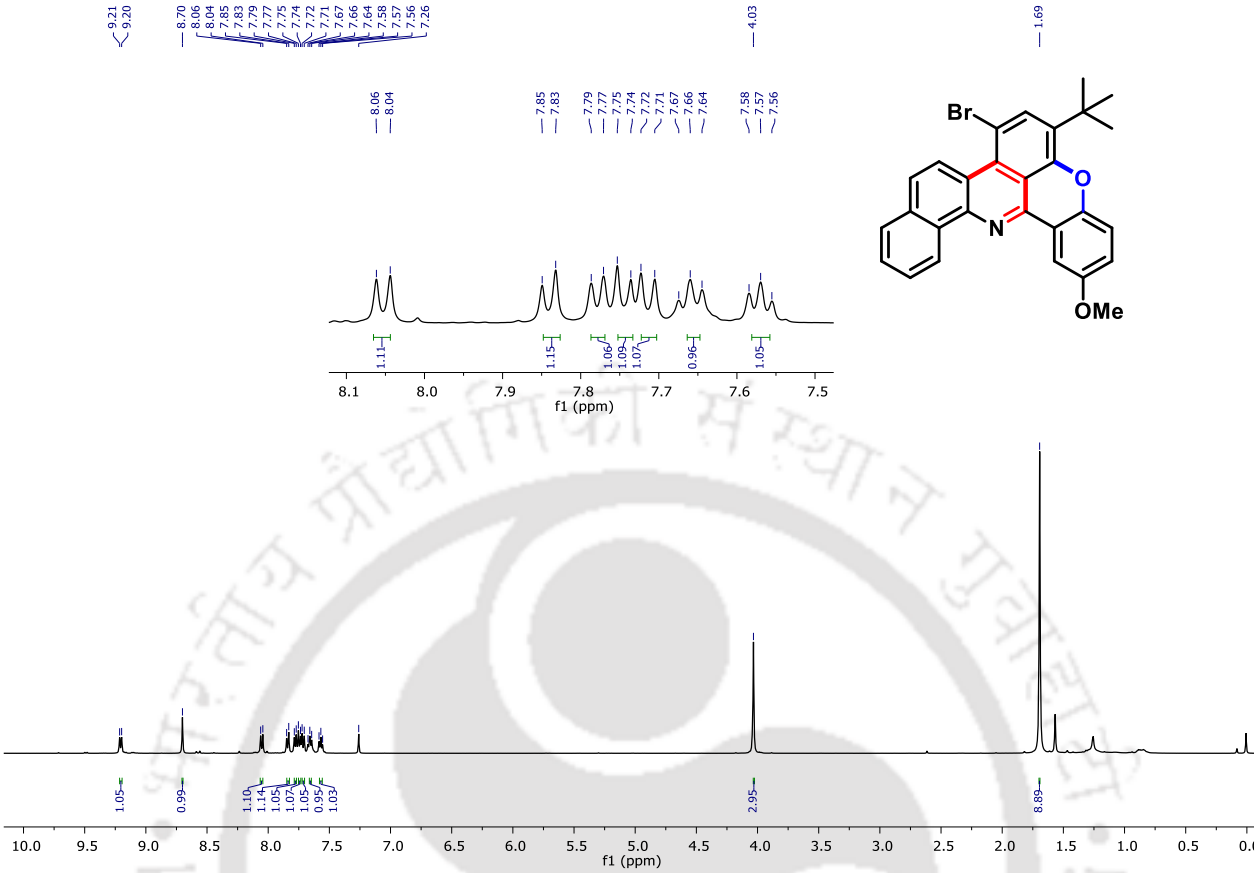

Figure 3.8. ^{1}H NMR spectrum of 7-bromo-9-(*tert*-butyl)-13-methoxybenzo[*c*]chromeno[4,3,2-*gh*]phenanthridine (**6f**).

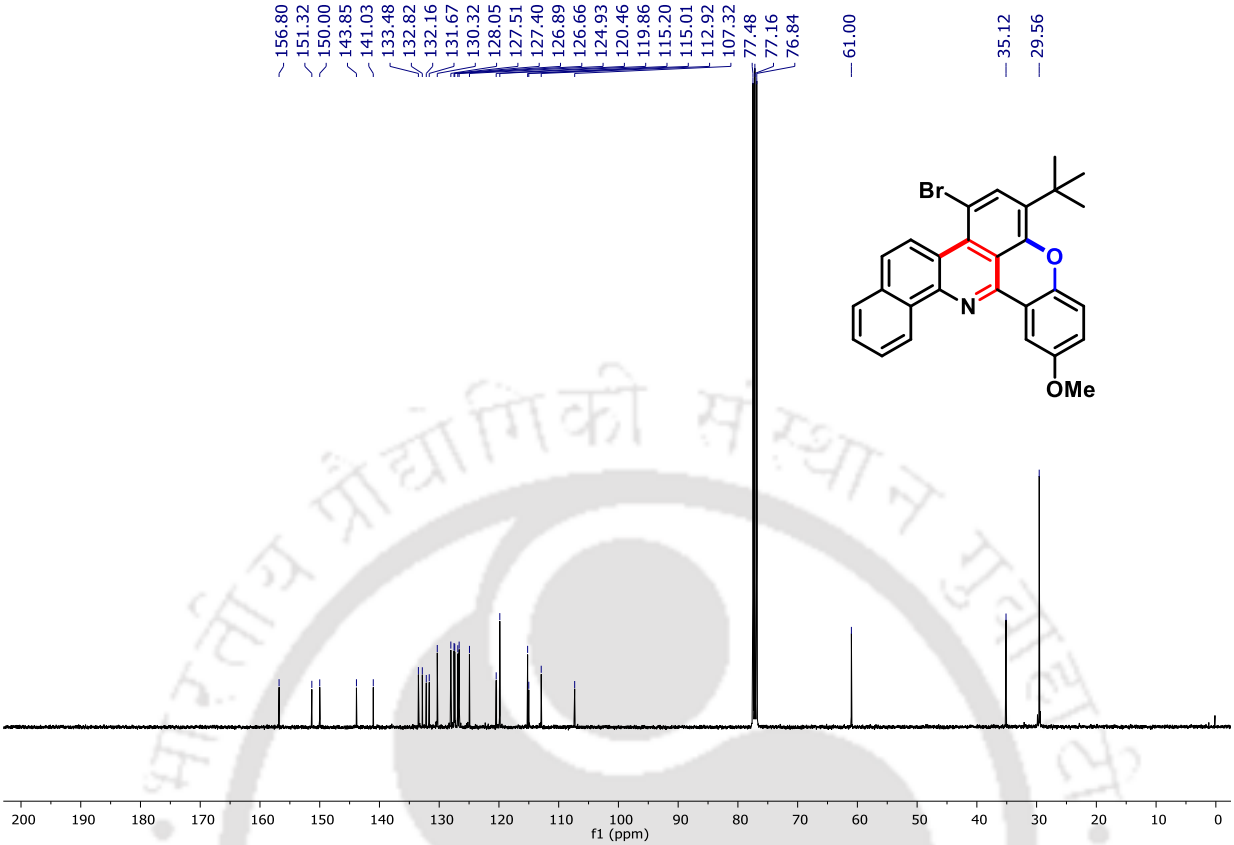

Figure 3.9. ^{13}C NMR spectrum of 7-bromo-9-(*tert*-butyl)-13-methoxybenzo[*c*]chromeno[4,3,2-*gh*]phenanthridine **6f**.

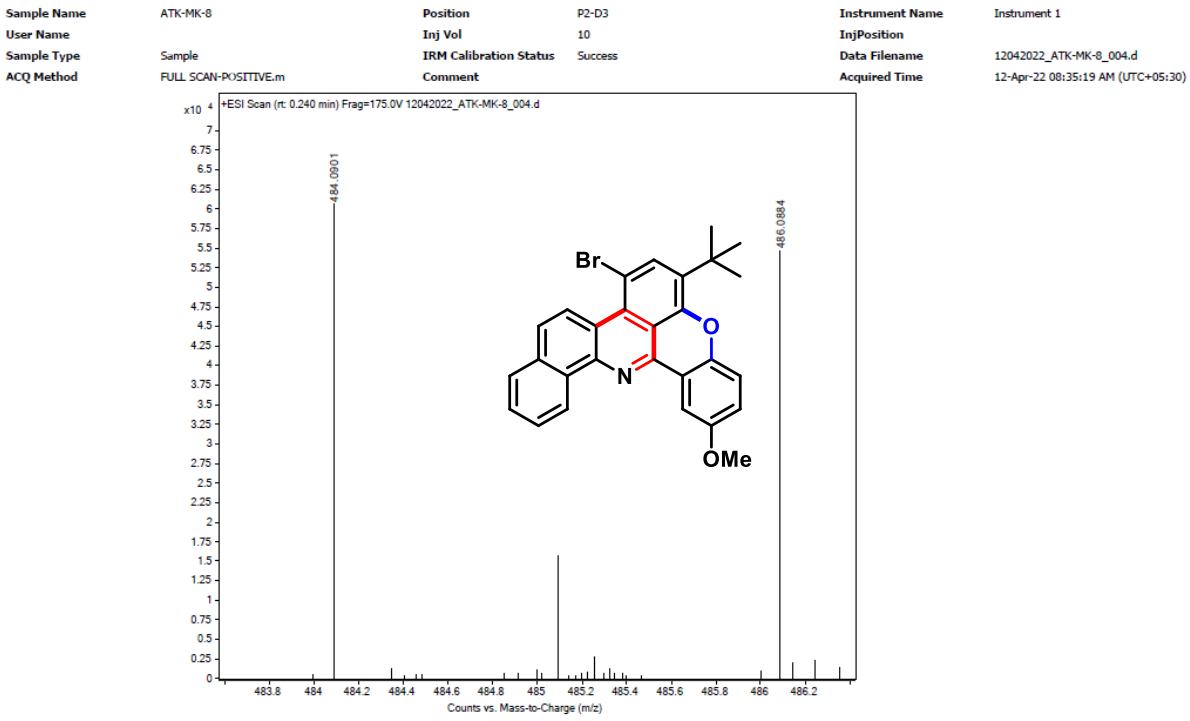

Figure 3.10. HRMS spectrum of 7-bromo-9-(*tert*-butyl)-13-methoxybenzo[*c*]chromeno[4,3,2-*gh*]phenanthridine (**6f**).

3.3g. Experimental Details for the Photophysical Studies

The stock solutions of the probe **6h** was prepared in chloroform at 10^{-2} mol L−1 (M) and the solutions were further diluted to as per experimental requirements. Various spectra for the study of aggregation behavior were recorded in 10^{-6} mol L−1 (M) concentration. The absorption measurements were recorded on a PerkinElmer Lamda-365+ UV−Vis spectrophotometer using 10 mm path-length quartz cuvettes in the wavelength range of 300−700 nm. The fluorescence spectra were recorded on a Horiba Fluoromax-4 Spectrofluorometer using 10 mm path length quartz cuvettes with at 298 K.

3.3h. Computational Details

All computational calculations presented in this study were performed using the ORCA 5.0.1 software.[17,18] For all geometry optimizations in the gas phase, we employed the PBE density functional, the Def2-SVP basis set and included atom-pairwise dispersion corrections with Becke-Johnson (D3BJ) damping.[19-21] Additionally, frequency calculations were calculated to confirm the absence of imaginary frequencies in the optimized local minima. Each transition state geometry was validated based on the presence of a single imaginary frequency. We conducted single-point calculations using a higher-level theory using PBE0-D3/Def2-TZVP in the CPCM solvation (Chloroform) model to further refine the reaction energy profile.[22] All the coordinates for the optimized structures are available in the supporting information of the published article (https://doi.org/10.1021/acs.joc.3c01329).[14b]

3.4. References

1. (a) I. V. Koval', *Russ. J. Org. Chem.*, 2002, **38**, 301–337; (b) I. Saikia, A. J. Borah and P. Phukan, *Chem. Rev.*, 2016, **116**, 6837–7042 and references therein.

2. K. Ziegler, A. Späth, E. Schaaf, W. Schumann and E. Winkelmann, *Ann. Chem.*, 1942, **551**, 80–119.

3. (a) Y. Apeloig and R. Schreiber, *J. Am. Chem. Soc.*, 1980, **102**, 6144–6146; (b) M. S. Anson, J. G. Montana, *Synlett* 1994, **1994**, 219–220; (c) S. Chandrappa, M. Umashankara, K. Vinaya, C. S. A. Kumar and K. S. Rangappa, *Tetrahedron Lett.*, 2012, **53**, 2632–2635.

4. M. F. Abd El-Wahab and M. Z. Barakat, *Monatsh. Chem.*, 1957, **88**, 692–701.

5. P. Zhang, R. Liu and J. M. Cook, *Tetrahedron Lett.*, 1995, **36**, 3103–3106.

6. B. Das, K. Venkateswarlu, A. Majhi, V. Siddaiah and K. R. Reddy, *J. Mol. Catal. A: Chem.*, 2007, **267**, 30–33.

7. S. Chen, R. Bai, M. Li, P. Liu and Y. Gu, *Chem. Rec.*, **2021**, *21*, 87–115, and references therein.

8. W. Huang, C. Liu and Y. Gu, *Adv. Synth. Catal.* **2017**, *359*, 1811–1818.

9. Y. Jiang, S.-W. Yu, Y. Yang, Y.-L. Liu, X.-Y. Xu, X.-M. Zhang and W.-C. Yuan, *Org. Biomol. Chem.*, 2018, **16**, 9003–9010.

10. (a) I. P. Beletskaya and A. V. Cheprakov, *Chem. Rev.*, 2000, **100**, 3009–3066; (b) F. Alonso, I. P. Beletskaya and M. Yus, *Tetrahedron*, 2005, **61**, 11771–11835; (c) F. Alonso, I. P. Beletskaya and M. Yus, *Tetrahedron*, 2008, **64**, 3047–3101; (d) R. Martin and S. L. Buchwald, *Acc. Chem. Res.*, 2008, **41**, 1461–1473; (e) M. Lamblin, L. N.-Hardy, J. C. Hierso, E. Fouquet and F. X. Felpin, *Adv. Synth. Catal.*, 2010, **352**, 33–79; (f) R. Narayanan, *Molecules*, 2010, **15**, 2124–2138.

11. (a) H. Pellissier and Santelli, *Tetrahedron*, 2003, **59**, 701–730; (b) P. M. Tadross and B. M. Stoltz, *Chem. Rev.*, 2012, **112**, 3550–3577.

12. (a) k. Smith and D. Bahzad, *Chem. Commun.*, 1996, **1996**, 467–468; (b) J. Wang, W. Wang and J. H. Li, *Green Chem.*, 2010, **12**, 2124–2126; (c) H.-J. Li, Y.-C. Wu, J.-H. Dai, Y. Song, R. Cheng and Y. Qiao, *Molecules*, 2014, **19**, 3401–3416.

13. (a) S. C. Roy, C. Guin, K. K. Rana and G. Maiti, *Tetrahedron Lett.*, 2001, **42**, 6941–6942; (b) J. S. Yadav, B. V. S. Reddy, P. S. R. Reddy, A. K. Basak and A. V. Narsaiah, *Adv. Synth. Catal.*, 2004, **346**, 77–

82; (c) D. Pla, F. Albericio and M. Alvarez, *Eur. J. Org. Chem.*, 2007, **2007**, 1921–1924; (d) G. Majetich, R. Hicks and S. Reister, *J. Org. Chem.*, 1997, **62**, 4321–4326; (e) J. Kong, B. Galabov, G. Koleva, J. J. Zou, H. F. Schaefer III and P. V. R. Schleyer, *Angew. Chem. Int. Ed.*, **2011**, *50*, 6809–6813; (f) G. K. S. Prakash, T. Mathew, D. Hoole, P. M. Esteves, Q. Wang, G. Rasul and G. A. Olah, *J. Am. Chem. Soc.*, 2004, **126**, 15770–15776.

14. (a) S. Yashmin, R. Ali, S. Mondal and A. T. Khan, *Chem. Commun.*, 2022, **58**, 5853–5856; (b) S. Yashmin, A. T. Khan, S. J. Akula, R. P and K. Bhattacharyya, *J. Org. Chem.*, 2023, **88**, 13622–13633.

15. (a) R. Gattu, P. R. Bagdi, R. S. Basha and A. T. Khan, *J. Org. Chem.*, 2017, **82**, 12416–12429; (b) S. Yashmin, S. Mondal, R. Das, P. Banerjee and A. T. Khan, *Org. Biomol. Chem.*, 2022, **20**, 7302–7315.

16. N. Baig, S. Shetty, R. Tiwari, S. K. Pramanik and B. Alameddine, *ACS Omega*, 2022, **7**, 45732–45739.

17. F. Neese, *WIREs Comput. Mol. Sci.*, 2012, **2**, 73–78.

18. F. Neese, F. Wennmohs, U. Becker and C. Riplinger, *J. Chem. Phys*., 2020, **152**, 224108.

19. J. P. Perdew, *Phys. Rev. B: Condens. Matter Mater. Phys.*, 1986, **33**, 8822–8824.

20. A. D. Becke, *Phys. Rev. A: At., Mol., Opt. Phys.*, 1988, **38**, 3098−3100.

21. F. Weigend and R. Ahlrichs, *Phys. Chem. Chem. Phys.*, 2005, **7**, 3297–3305

22. R. Cammi, B. Mennucci and J. Tomasi, *J. Phys. Chem. A*, 2000, **104**, 5631–5637.

CHAPTER IV

Regioselective Synthetic Approach for key Precursors of 6-Aryl Benzo[c]phenanthridin-10-ol Derivatives: A Useful Compound for Selective Chromogenic Recognition of Fluoride

- Introduction
- Results and Discussion
- Experimental Section

4.1. Introduction

4.1a. Importance of Benzophenanthridine Derivatives

Benzophenanthridine serves as a pivotal structural component within the naturally occurring benzophenanthridine alkaloids family. These alkaloids exhibit a diverse array of biological applications, significantly impacting the realm of organic synthesis. A brief overview of their extensive importance and synthetic methods is provided in **Chapter I, Section 1.4**. Inspired by the literature review, our research is driven by exploring a novel pathway for synthesizing 6-arylbenzophenanthridine derivatives. The insights gained from the literature survey, which are discussed below, have played a crucial role in shaping the content of **Chapter IV** of this thesis.

4.1b. DMSO as a Reagent

Dimethyl sulfoxide (DMSO), an economical organosulfur compound, is a colourless, odourless, and tasteless liquid that acquires a pungent garlic-like smell due to the presence of DMS (dimethyl sulfide) as an impurity. Alexander Zaytsev first synthesized DMSO in 1867.[1] This polar and aprotic liquid can dissolve both polar and non-polar compounds, making it a widely utilized reaction medium in organic synthesis and analytical applications over the decades.[2] In recent years, there has been growing scientific interest in exploring DMSO's potential as a reagent in chemical reactions. Due to its low cost, high abundance, and environmental benignity, DMSO has been widely used in various greener organic transformations, which have been summarized in a few review articles.[3]

DMSO is a versatile oxygen, carbon, or sulfur source in a broad spectrum of organic reactions. It facilitates the transfer of units such as methyl (–CH_3),[4a] methylene (–CH_2–, =CH_2),[4b,c] methine (=CH),[4d] methyl sulfoxide (–CH_2SOMe),[5a] (–CH_2SMe),[5b] methylthio (–SMe),[5c] methylsulfonyl (–SOMe),[5d] oxygen (OH, –O–, =O)[6a-c] and even the intact DMSO molecule into the target molecules.[5e]

4.1c. DMSO as a Source of Oxygen

DMSO incorporates the -OH, -O-, =O group in many organic reactions by exchanging its oxygen atom. In 2015, Jiao *et al*. utilized DMSO as an oxygen source for the synthesis of α-hydroxy carbonyl compounds catalyzed by I_2 or NBS, as shown in **Scheme 4.1**.[6a]

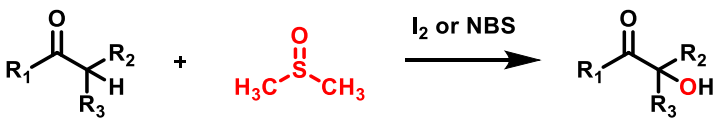

Scheme 4.1. Utilization of DMSO as a source of **-OH** group.

In 2019, Cao *et al.* reported an efficient strategy via the multicomponent annulation of readily available ketones and ammonium persulfate to afford 2,4-disubstituted oxazoles. In this methodology, DMSO transfers -O- moiety for the regioselective assembly of 2,4-disubstituted oxazoles (**Scheme 4.2**).[6b]

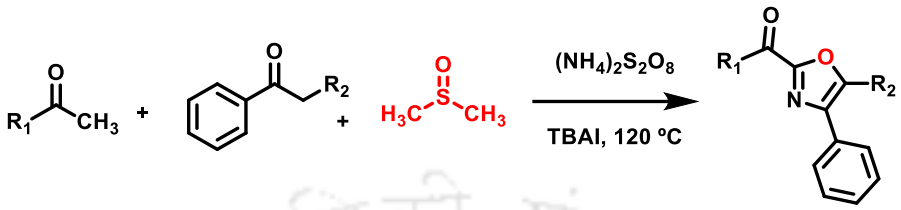

Scheme 4.2. Synthesis of oxazoles using DMSO as a source of **-O-** group.

In 2016, Xiao *et al.* reported the oxidative reaction of *N*-sulfonylaziridines with DMSO in the presence of 2-methylquinoline at room temperature to afford the corresponding α-amino aryl ketones (**Scheme 4.3**). In this reaction, DMSO acts not only as a solvent but also as an oxidant and oxygen donor (=O).[6c]

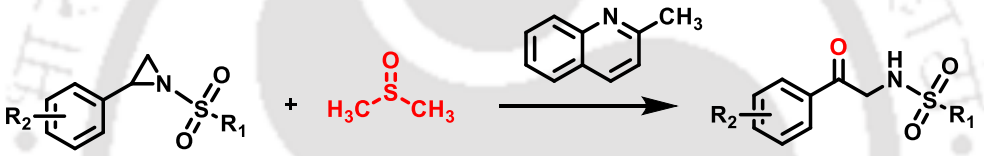

Scheme 4.3. The synthesis of α-amino aryl ketones using DMSO as a source of **=O** group.

The oxygen atom of DMSO is nucleophilic to hard electrophile, and this property makes DMSO an oxygen source. The general key intermediate in these reactions is an alkoxy sulfonium intermediate, which can be formed through conventional activation of sulfoxide, i.e. Swern oxidation (**Scheme 4.4a**),[7a] Kornblum oxidation (**Scheme 4.4b**),[7b] or by activation of the substrate, i.e. electrochemical oxidation.[7c]

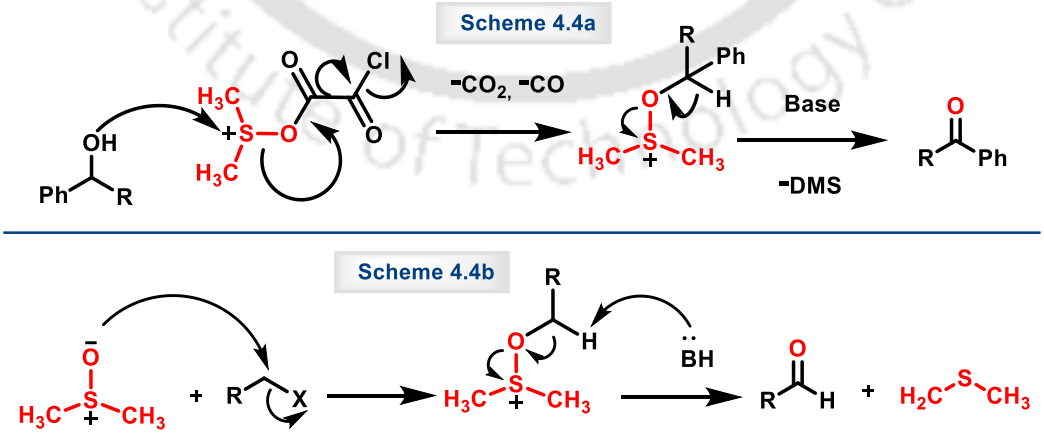

Scheme 4.4. (a) Mechanism of Swern Oxidation using DMSO as an oxidant; **(b)** Mechanism of Kornblum Oxidation using DMSO as a 'O' source.

Nevertheless, in 2015, Chebolu *et al.* showcased the oxidation of active methylenes and benzhydrols by employing DMSO as an oxygen source, utilizing a distinct mechanistic approach (**Scheme 4.5a**). This protocol harnessed the electrophilic centre of DMSO for oxidation, representing a concept of reverse polarity of DMSO that had not been explored before (**Scheme 4.5b**).[8]

Scheme 4.5a

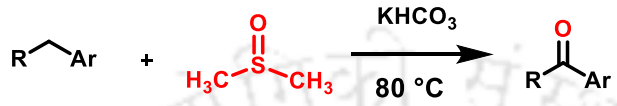

Scheme 4.5b

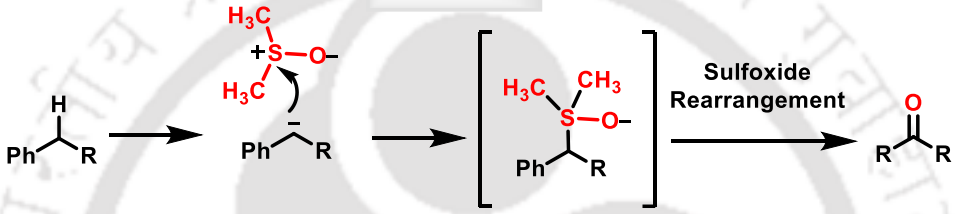

Scheme 4.5. Utilization of DMSO as a source of oxygen using reverse polarized conditions.

4.1d. Emerging Role of Green Oxidant I_2/DMSO

Meanwhile, the I_2/DMSO oxidative system has garnered significant attention due to its applications in diverse oxidative transformations, including C-C and C-X bond formation reactions.[9] In these processes, iodine serves as a mild Lewis acid catalyst, while DMSO is an oxidant, solvent, and source of oxygen. Examples of these reactions include the oxidation of alkenes and alkynes (**Scheme 4.6**),[10a] dehydrogenation reactions,[10b] and aromatization.[11a-b] These systems offer the advantages of being environmentally friendly, efficient, atom-economical, cost-effective, and operating under mild conditions, aligning with sustainable chemistry principles.

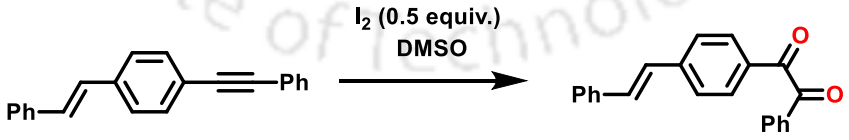

Scheme 4.6. Utilization of I_2/DMSO for oxygenation reaction.

Lokhande *et al.* demonstrated a new protocol for the aromatization of tetrahydrocarbazoles using a catalytic amount of iodine in DMSO with high yield. A 25 mol% iodine aromatization process in DMSO at 100 °C was achieved, and the corresponding carbazole was isolated with an excellent yield (**Scheme 4.7)**.

Scheme 4.7. Utilization of I_2/DMSO in aromatization reaction.

4.1e. Fluoride Sensing

The selective recognition of anions has emerged as a burgeoning research focus in supramolecular chemistry, driven by their potential significance in various physiological and environmental processes.[13a-e] Among the diverse array of anions, fluoride (F-) has gained particular attention as a crucial target for detection, notably in dental care.[14] Adequate fluoride levels in drinking water protect against dental caries and promote mineral deposition in bones.[15] However, excessive fluoride exposure can lead to fluorosis, urolithiasis, and even cancer.[16] Consequently, the excess presence of F- in water sources is a cause for concern. The World Health Organization (WHO) has set the maximum permissible level of fluoride in drinking water at 1.5 ppm, necessitating continuous monitoring of fluoride levels.[17]

Various analytical techniques, such as ion chromatography, voltammetry, and atomic absorption spectroscopy, are currently available for fluoride detection.[18a-c] However, these methods suffer from high costs, lack of portability, time consumption, and specialized expertise requirements. In this context, simple colourimetric chemosensors are highly favoured for their straightforward 'naked eye' colourimetric read-out, rapid response, portability, and cost-effectiveness. Nevertheless, many of the developed probes face challenges related to selectivity and sensitivity, limiting their ability to detect targeted F^- among its other congeners selectively.

4.1f. Previously Reported Work from our Lab Group

In 2020, our lab group also successfully utilized DMSO as a solvent as well as a source of 'O' atom in the synthesis of 2-aryl-10*H*-thiochromeno[3,2-*b*][1,4]oxathiin-10-one derivatives from arylacetylenes and 4-hydroxydithiocoumarins in the presence of 10 mol% CuI and K_2CO_3 in an oil-bath at 70 °C (**Scheme 4.9**).[19]

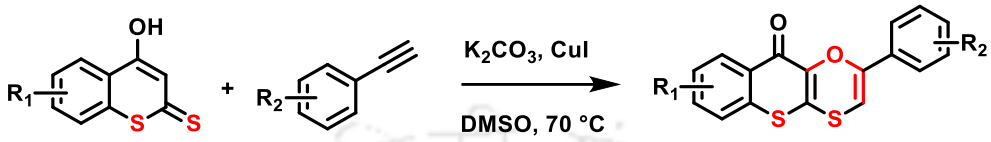

Scheme 4.8. Exploitation of DMSO as a solvent cum reactant for -O- source.

In **Chapters II** and **III**, the synthesis of (7,8,9,10-tetrahydrobenzo[*c*]phenanthridin-6-yl)phenol derivatives have already been demonstrated employing the multicomponent reaction of 1-naphthylamine, aromatic aldehyde, and cyclic ketone in acetonitrile solvent as shown in **Scheme 4.9**.[20a-c]

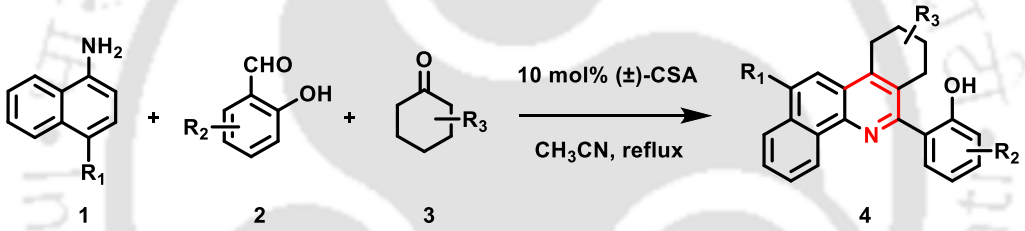

Scheme 4.9. Utilization of the multicomponent reaction.

4.1g. Scope from the Literature Review

Through a comprehensive review of the literature and our previously documented laboratory work, we have identified significant opportunities, including:

- The utilization of DMSO as both a solvent and a reactant for extracting its oxygen atom in the desired product.
- The application of the reverse polarity mechanism of DMSO, as illustrated in **Scheme 4.5**, for the transposition of the keto (=O) group at the benzylic carbon of compound **4**, as demonstrated in **Scheme 4.9**.
- The achievement of this phenomenon in a single step by substituting the acetonitrile solvent with DMSO in the multicomponent reaction outlined in **Scheme 4.9**.
- The employment of I_2/DMSO for the aromatization process.
- The utilization of the dangling -OH group for fluoride sensing.

4.1h. Present Work

In this chapter, we present the synthesis of 6-aryl-8,9-dihydrobenzo[c]phenanthridin-10(7H)-ones (**10**) through a one-pot process involving 1-naphthylamine, aryl aldehyde, cyclohexanones, and DMSO, facilitated by 20 mol% (±)-camphor-10-sulfonic acid (CSA) and fine-tuning of the reaction temperature (see **Scheme 4.10a**). Notably, DMSO serves a dual role as solvent and reactant, leveraging its electrophilic sulfur atom for '=O' bond transposition in the multicomponent reaction—a hitherto unreported phenomenon, to our knowledge. The oxygenation step proceeds without needing an external catalyst, base, or activator. Subsequently, the ketone derivatives (**10**) are readily transformed into the corresponding 6-arylbenzo[*c*]phenanthridin-10-ol compounds (**12**) using 10 mol% I_2/DMSO.

Furthermore, compounds **10s**, **10u**, **10x**, and **10z**, featuring dangling –OH functionality, exhibit noteworthy colourimetric fluoride sensing behaviour with detection limits of 0.65 ppm, 0.6 ppm, 0.34 ppm, and 2.2 ppm, respectively (**Scheme 4.10b**). This sensing mechanism operates through strong hydrogen bonding interactions, leading to a prominent and easily observable 'naked eye' chromogenic change from pale yellow to orange. The observed chromogenic alterations are also evident in the solid state. The sensing mechanism was evident from ^{1}H NMR spectroscopic analysis.

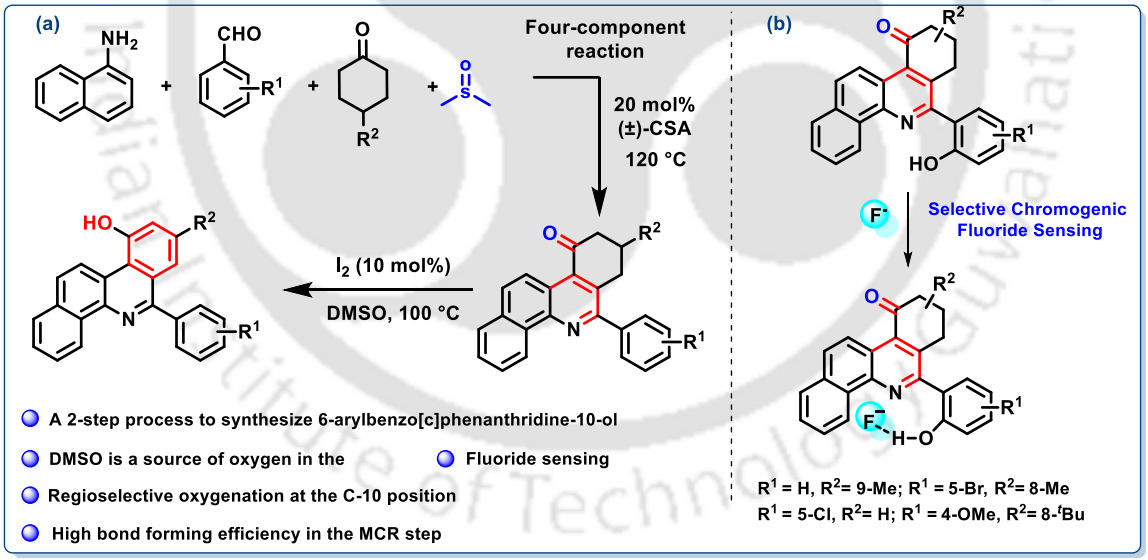

Scheme 4.10. (a) Present synthetic methodology of 6-arylbenzo[*c*]phenanthridin-10-ol derivatives (**7**); and **(b)** selective chromogenic fluoride sensing of compound **10s**, **10u**, **10x**, and **10z**.

4.2. Results and Discussion

4.2a. Optimization of the Methodology

To identify optimal reaction conditions for the synthesis of 6-aryl-8,9-dihydrobenzo[*c*]phenanthridine-10(7*H*)one derivatives, numerous reactions were investigated using 1-naphthylamine (**1a**), benzaldehyde (**2b**), and cyclohexanone (**3b**) as model substrates. The summarized results are presented in **Table 4.1**. Drawing inspiration from our previous work, the reaction was conducted on a 1 mmol scale with the aforementioned model substrates, utilizing 10 mol% CSA as a catalyst in DMSO solvent at a temperature of 80 °C within a preheated oil bath (**Entry 1**). The isolated yield of the product 6-phenyl-7,8,9,10-tetrahydrobenzo[*c*]phenanthridine (**4b'**) was 20%.

Upon elevating the reaction temperature to 100 °C (**Entry 2**), the anticipated product 6-phenyl-8,9-dihydrobenzo[*c*]phenanthridine-10(7*H*)one (**10a**) was obtained in a 25% yield, accompanied by a reduced yield of **4b'** to 10%. To enhance the yield of **10a**, the reaction temperature was gradually increased from 100 °C to 120 °C (**Entry 3**), resulting in an improved yield from 25% to 45% for the desired compound, with **4b'** yielding 5%.

Next, reactions were performed varying the concentration of CSA. A reaction was conducted with 20 mol% CSA, leading to an increased yield of the desired product from 45% to 65%, with a negligible amount of **4b'** (**Entry 4**). However, no further improvement was observed when the catalyst loading was increased to 30 mol% (**Entry 5**). The yield did not improve further while carrying out the reaction at 130 °C (**Entry 6**).

To assess alternative catalysts, reactions were performed with various protic acid catalysts such as *p*-TSA, TFA, triflic acid, AcOH, and L-proline under the optimized catalyst concentration (**Entries 7-11**). The yields of the desired product **10a** were 50% with *p*-TSA, 12% with TFA, and 20% with triflic acid. Unfortunately, AcOH and L-proline did not yield **10a**. Furthermore, reactions were conducted with H_2O and DMF (**Entries 12 & 13**), revealing that only DMF effectively produced **10a**.

Considering all observations, it has been established that the optimal reaction conditions involve a 20 mol% CSA catalyst at 120 °C in DMSO solvent in the synthesis of 6-aryl-8,9-dihydrobenzo[*c*]phenanthridine-10(7*H*)one derivative (**Entry 4**).

Table 4.1. Optimization of the Reaction Conditions.[a,b]

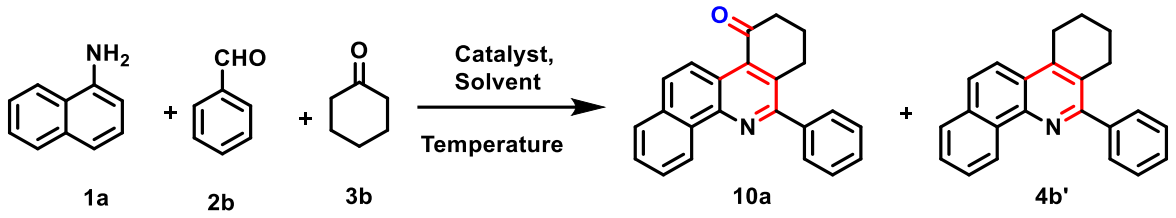

Entry	Catalyst	Mol%	Solvent	Temperature	Time (h)	%Yield (10a)	%Yield (4b')
1.	(±)-CSA	10	DMSO	80 °C	15	-	20
2.	(±)-CSA	10	DMSO	100 °C	10	25	10
3.	(±)-CSA	10	DMSO	120 °C	7	45	05
4.	**(±)-CSA**	**20**	**DMSO**	**120 °C**	**2.5**	**65**	**01**
5.	(±)-CSA	30	DMSO	120 °C	2.5	66	01
6.	(±)-CSA	20	DMSO	130 °C	2.5	65	01
7.	*p*-TSA	20	DMSO	120 °C	12	50	-
8.	TFA	20	DMSO	120 °C	24	12	-
9.	TfOH	20	DMSO	120 °C	24	20	-
10.	Acetic acid	20	DMSO	120 °C	12	-	-
11.	L-Proline	20	DMSO	120 °C	12	-	-
12.	(±)-CSA	20	H_2O	100 °C	24	-	-
13.	(±)-CSA	20	DMF	120 °C	8	40	-

[a]All reactions were carried out with 1-naphthylamine **1a** (0.143 g, 1 mmol), benzaldehyde **2b** (0.106 g, 1 mmol), and cyclohexanone **3b** (0.098 g, 1 mmol) in 1 mL of solvent at different temperatures mentioned above. [b]Yield of the isolated product.

4.2b. Exploration of the Substrate Scope

After obtaining the optimized reaction conditions, we performed the reaction with various substrates to generalize the present protocol (**Table 4.2**). Initially, we have done the reaction with various substituted aldehydes. Aldehydes with electron-donating and electron-withdrawing substituents provided the desired products in high yields (**10a-f**).

Table 4.2. Scope of 6-Aryl-8,9-dihydrobenzo[*c*]phenanthridine-10(7*H*)one Derivatives from 1-Naphthylamine, Cyclohexanone, and Aryl Aldehydes.[a,b]

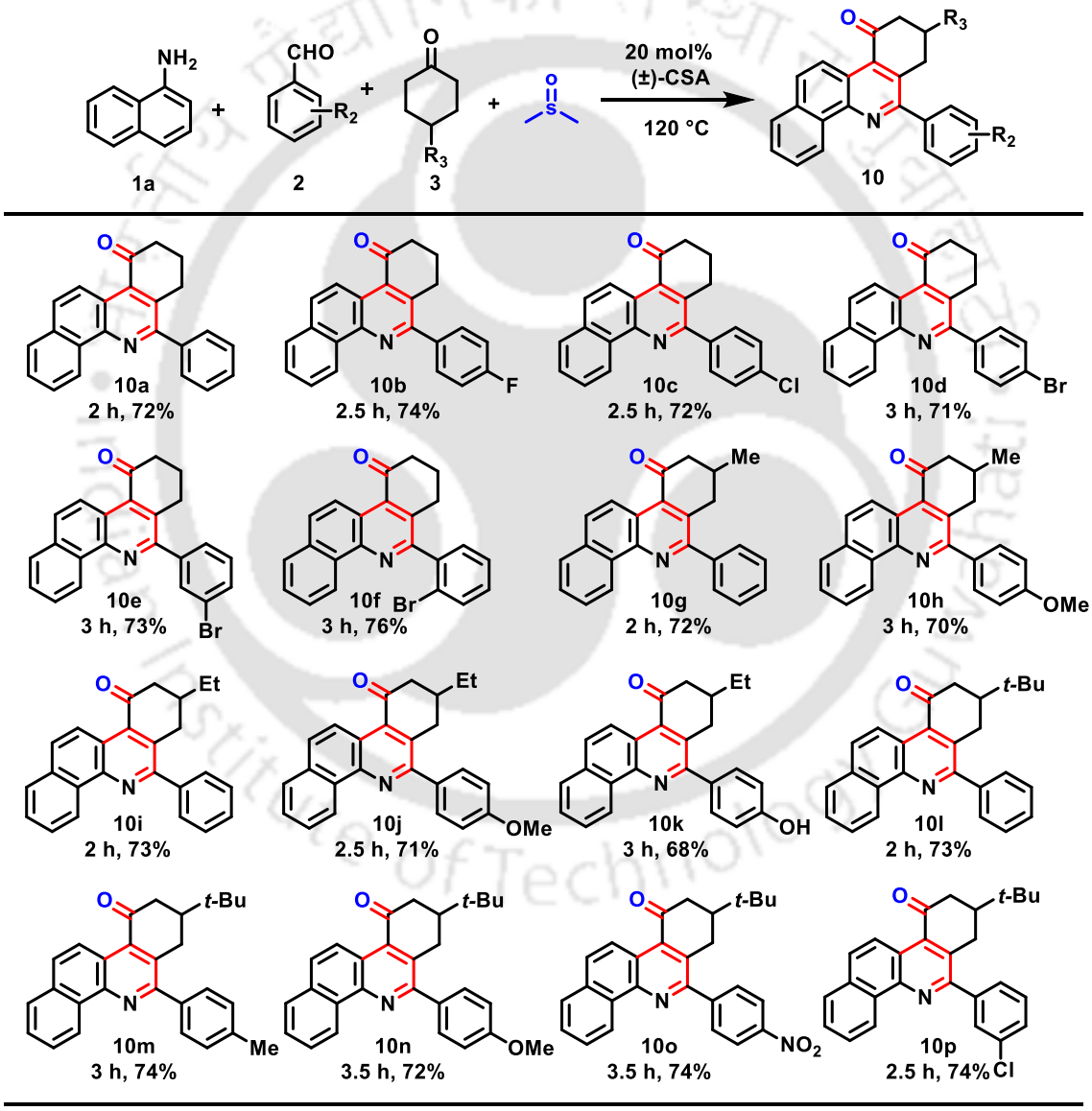

[a]All reactions were carried out using 1-naphthylamine (1 mmol), aryl aldehyde (1 mmol), and cyclohexanone (1 mmol), in the presence of 20 mol% CSA in 1 mL DMSO in 120 °C. [b]Yield of the isolated product.

Interestingly, various substituted cyclohexanone derivatives, such as methyl, ethyl, and *tert*-butyl at the 4th position, also formed the desired products in 72-74% yields (**10g-p**). Then, we carried out reactions with several salicylaldehyde derivatives, and the products were achieved in a moderate to good yields under the optimized reaction conditions (**10q-10z** and **10aa**, **Table 4.3**). Furthermore, the structure of compound **10t** is ascertained by a single X-ray crystallographic data (**Table 4.6 & Fig. 4.2**). However, heteroaryl aldehydes such as furfural, 2-pyridine carboxaldehyde, and indole-3-carboxaldehyde failed to give the expected outcomes.

Table 4.3. Scope of 6-Aryl-8,9-dihydrobenzo[*c*]phenanthridine-10(7*H*)one Derivative from 1-Naphthylamine, Cyclohexanone, and Salicylaldehyde Derivatives.[a,b]

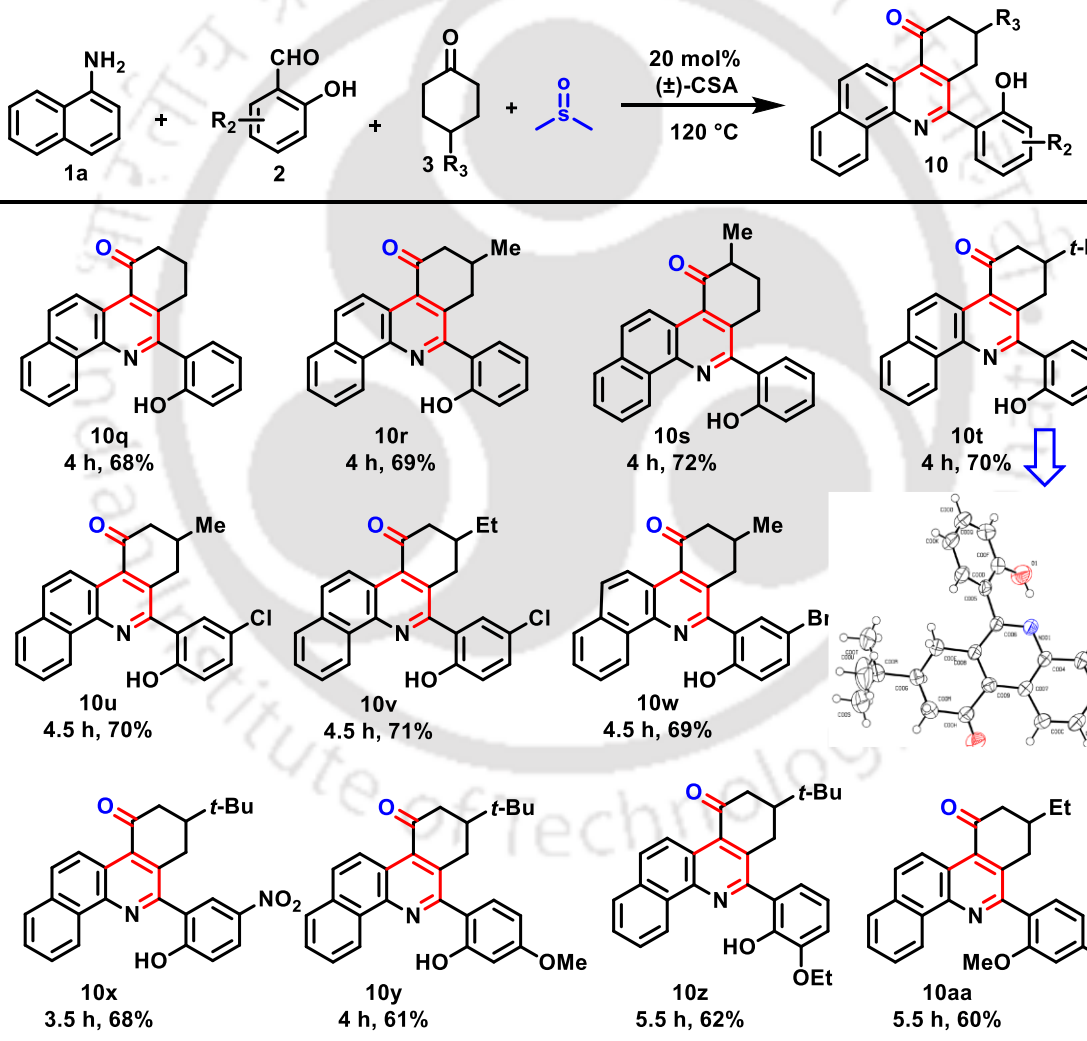

[a]All reactions were carried out using 1-naphthylamine (1 mmol), salicylaldehyde (1 mmol), and cyclohexanones (1 mmol), in the presence of 20 mol% CSA in 1 mL DMSO in 120 °C. [b]Yield of the isolated product.

Table 4.4. Scope of 6-Aryl-8,9-dihydrophenanthridine-10(7*H*)one Derivatives.[a,b]

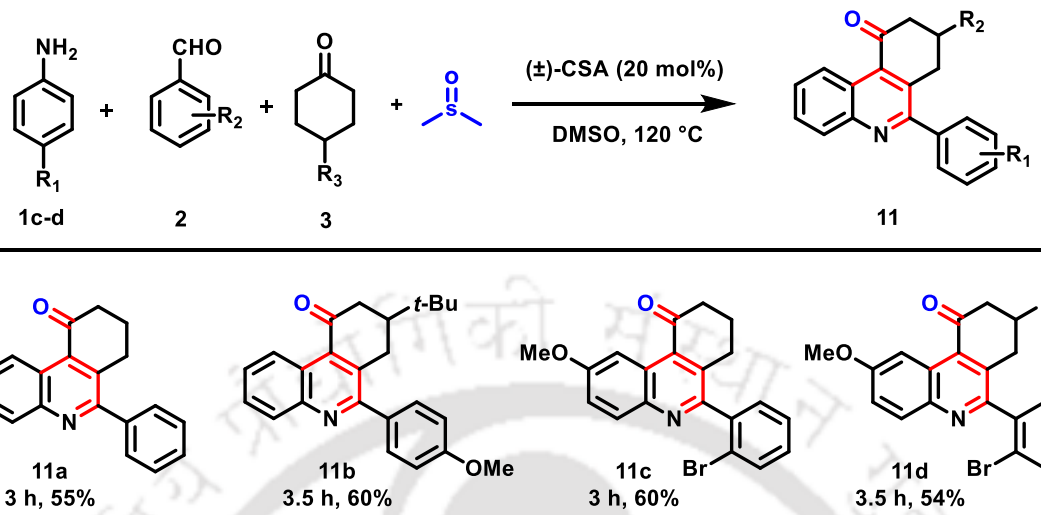

[a]All reactions were carried out using anilines (1 mmol), aryl aldehydes (1 mmol), and cyclohexanones (1 mmol), in the presence of 20 mol% CSA and 1 mL DMSO at 120 °C. [b]Yield of the isolated product.

Though the reaction proceeded well with various cyclohexanone derivatives, it failed with other cyclic ketones, such as cyclopentanone, cycloheptanone, and cyclooctanone.

Apart from 1-naphthylamine, aniline and 4-methoxy aniline provided the desired products in fairly good yields under the same reaction conditions (**Table 4.4**, **11a-d**). Unfortunately, the substituted aniline derivatives having electron-withdrawing groups, such as 4-flouroaniline and 4-chloroaniline, did not provide the desired product under identical reaction conditions.

4.2c. Establishment of the Mechanism

Control Experiment

Three control experiments were conducted to elucidate the proposed mechanism and are depicted in **Scheme 4.11**. Initially, to confirm whether the formation of the desired product **10a** is directly from **4b'** or not, 0.10 mmol of compound **4b'** was heated with 20 mol% CSA in DMSO (**Scheme 4.11a**) at 120 ºC for 2.5 hours. No observable change in the starting material was noted, indicating that the generation of product **10a** does not occur directly from the intermediate **4b'**.

To investigate whether oxygen incorporation arises from H_2O present in DMSO or directly from DMSO, a second reaction was performed using **1a** (1 mmol), **2b** (1 mmol), and **3b** (1 mmol) under optimized conditions in an inert atmosphere with dry DMSO (**Scheme 4.11b**). The isolation of product **10a** in 63%

yield suggests that the oxygen atom at the C-10 position is exclusively derived from DMSO rather than H_2O.

To further confirm whether oxygen incorporation occurs from aerobic oxygen, a similar reaction was carried out in dry acetonitrile in the presence of an oxygen balloon under reflux conditions (**Scheme 4.11c**). Interestingly, the product **4b'** was isolated in 75% yield instead of the desired product **10a**. This indicates that no aerial oxidation occurs for the oxidation at the C-10 position of product **10a**.

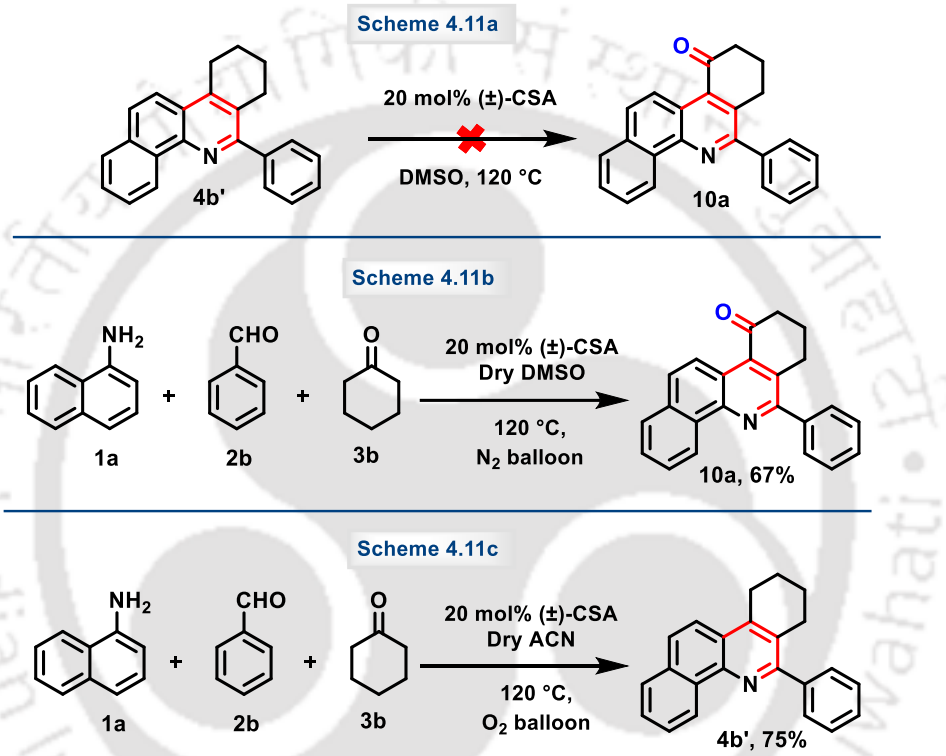

Scheme 4.11. Control experiment to establish reaction mechanism for the formation of **10** or **11**.

Proposed Mechanism

From the earlier literature and our results, we have proposed the mechanism for the formation of the products in **Scheme 4.12**, which can be described as follows: Initially, 1-naphthylamine **1a** or aniline **5** and aryl aldehyde **2** react in presence of CSA to give imine **A3**.[21] Again, CSA assisted the enolization of cyclohexanone derivatives to form intermediate **B3**.[22] Intermediate imine is activated by the CSA and reacts with enol **B3** to give intermediate **C3**, which immediately cyclizes to intermediate **D3**, having a *tertiary* -OH group. Then intermediate **D3** eliminates one molecule of H_2O to give intermediate **E3**. Then, **E3** undergoes [1,5]-H shift to form reactive dihydropyridine intermediate **F3**. The formation of intermediate **F3** is supported by our previous work,[20c] and then it reacts with the electrophilic sulfur atom of DMSO for

the oxygenation process at 120 °C temperature and generates intermediate **G3**.[8] It can undergo [1,2] sigmatropic shift and elimination of one molecule of dimethyl sulfide (DMS) to give intermediate **H3**. Then, it reacts again with another DMSO molecule and provides intermediate **I3**. Thereafter, the intermediate **I3** abstracts a proton to generate carbanion intermediate **J3**, which eliminates another molecule of DMS and H_2O to produce intermediate **K3**. After oxidation, the intermediate **K3** forms the final product, either **10** or **11**.

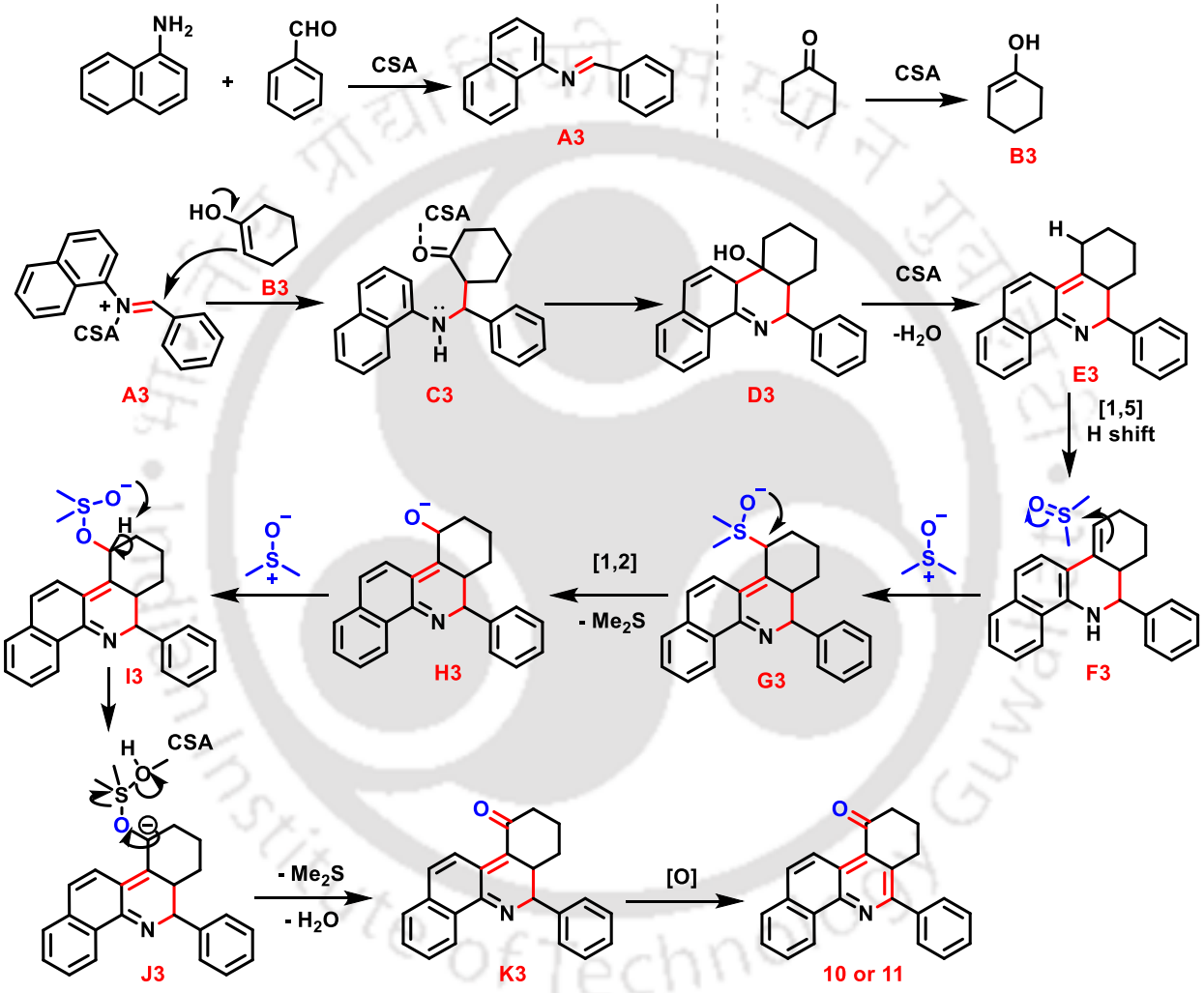

Scheme 4.12. A plausible mechanism for the synthesis of compounds **10** and **11**.

Detection of intermediates in HRMS

The proposed mechanism is also supported by detecting the intermediates through HRMS. 1-Naphthylamine (1 mmol), benzaldehyde (1 mmol), and 4-*tert*butylcyclohexanone (1 mmol), 20 mol% CSA (46 mg) were taken in a round-bottomed flask and dissolved in 1 mL DMSO. The reaction mixture was stirred at 120 °C temperature in a preheated oil bath. After 2 h, a very small amount of it was subjected to

ESI-MS mass experiment, and HRMS values detected the intermediates **E3**, **F3**, **H3**, and **K3**. Observed m/z values ($M+H^+$) are as follows:

i) **E3** or **F3** - 368.2302 (Calcd for $C_{27}H_{30}N$ 368.2373);

ii) **H3** - 383.2218 (Calcd for $C_{27}H_{29}NO$ 383.2249);

iii) **K3** - 382.2174 (Calcd for $C_{27}H_{28}NO$ 382.2166).

4.2d. Conversion to Phenol Derivatives

Then, we moved forward to aromatize the 6-aryl-8,9-dihydrobenzo[*c*]phenanthridine-10(7*H*)one derivative to form the compounds containing the benzophenanthridine core unit. When **10i** was heated at 100 ºC in 10 mol% I_2 and 1 mL DMSO, 6-phenylbenzo[*c*]phenanthridin-10-ol (**12i**) was isolated after 2 h. Further, the reaction was explored with five different 6-aryl-8,9-dihydrobenzo[*c*]phenanthridine-10(7*H*)one derivative to obtain 6-arylbenzo[*c*]phenanthridin-10-ol derivatives **12j**, **12q**, **12t**, **12v**, and **12w** in 64-68% yield (**Table 4.5**).

Table 4.5. Scope of 6-Arylbenzo[*c*]phenanthridin-10-ol Derivatives.[a,b]

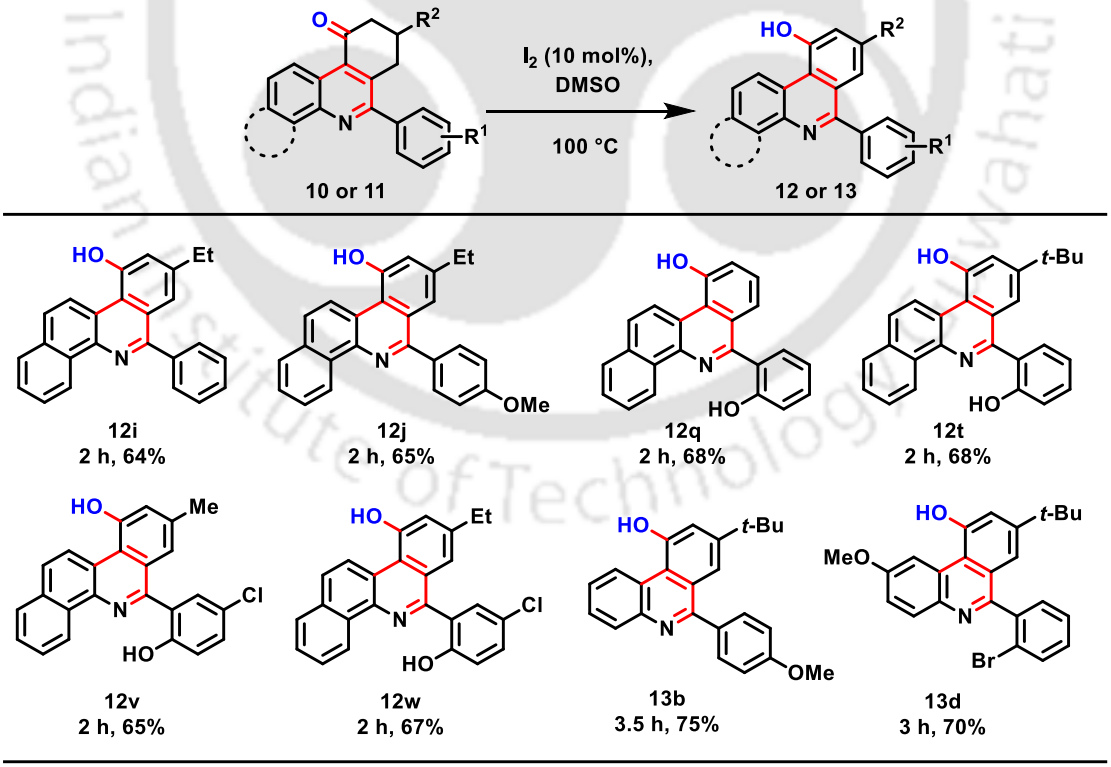

[a]All reactions were carried out using compound **10** or **11** (0.25 mmol), 10 mol% I_2, and 1 mL DMSO in 100 °C. [b]Yield of the isolated product.

Two of the 6-aryl-8,9-dihydro-phenanthridine-10(7*H*)one derivative, **11b** and **11d**, were also converted to their phenolic compounds **13b** and **13d** in 75% and 70% yield, respectively (**Table 4.5**). The possible mechanism for converting the ketone derivatives to phenol derivatives (**12** & **13**) is illustrated in **Scheme 4.13**. At first, iodination occurs at the α-position to form intermediate **L3**, which undergoes an elimination reaction to form intermediate **M3**.[23] Subsequently, intermediate **M3** tautomerizes to form the final product **12** or **13**.

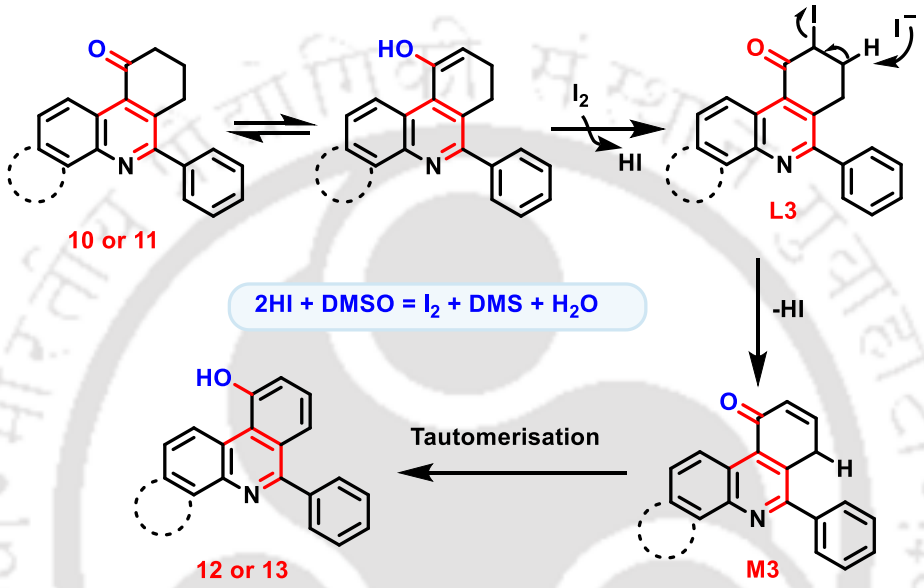

Scheme 4.13. A plausible mechanism for the synthesis of 6-arylbenzo[*c*]phenanthridin-10-ol & 6-arylphenanthridin-10-ol derivatives.

- ***All the synthesized compounds are characterized through ^{1}H, ^{13}C NMR, and HRMS spectra, and characterization data of all the compounds are given in the experimental section. A few representative spectra have also been attached in the experimental section.***

4.2e. Photophysical characterization and selective colorimetric fluoride sensing, evidenced from UV-Vis spectroscopic studies.

The presence of a dangling hydroxyl group in the synthesized compounds, which may act as a favourable anion binding site, has instigated us to check the propensity of the compounds toward selective interactions with anions. Now to evaluate the anion sensitivity of the developed compounds (**10s**, **10u**, **10x**, and **10z**) bearing hydroxyl group (**Scheme 4.14**), at first the selectivity of the designed sensory probes towards various anions like F^-, CN^-, Br^-, Cl^-, HSO_4^-, BF_4^-, ClO_4^-, AcO^-, *etc.* with their tetrabutylammonium salts has been checked separately *via* '*naked eye*' detection approach.

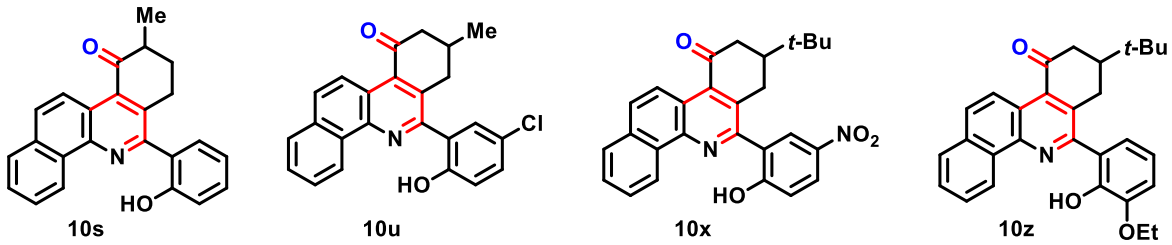

Scheme 4.14. Selected compounds for photophysical studies.

All the chemosensors, **10s**, **10u**, **10x**, and **10z** exhibited distinct colourimetric alteration from pale yellow to orange only in the presence of F^- in DMSO/H_2O (v/v 7/3) (**Figure 4.1**). This visual experimentation indicates the immense selectivity of the chemosensors towards F^-.

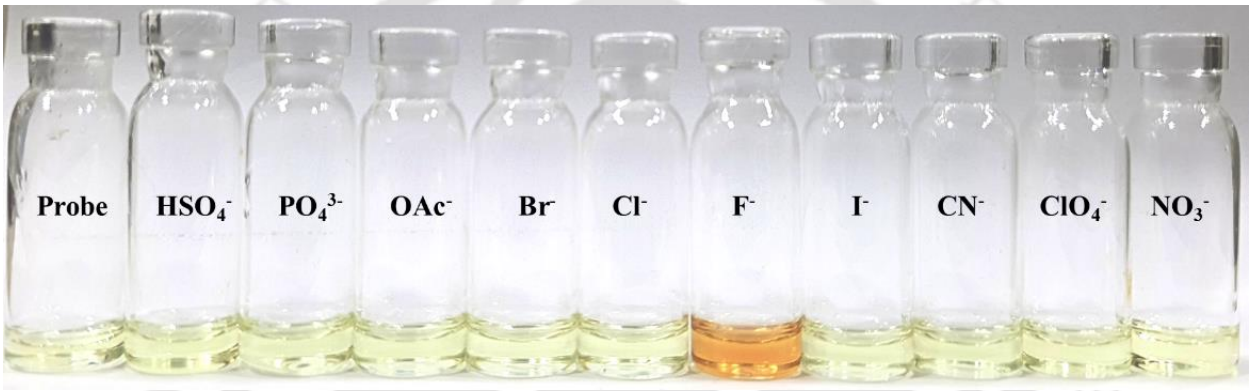

Figure 4.1. Selectivity of Probe (**10u**) in the presence of different anions in 0.5 mM DMSO/H_2O (v/v 7/3)**.**

The compounds **10s**, **10u**, **10x,** and **10z** in DMSO exhibited two major absorption bands at 295 nm and 375 nm, with an additional band at 320 nm for **10x**. The bands of the chemosensors at 295 and 320 nm may be ascribed to the π→π* transitions, while the band at 375 nm may be due to the n→π* transitions throughout the molecule. Moreover, to check the solvent-dependent spectral behaviour of the chemosensors, the absorption and emission spectral data were recorded in different organic solvents. From the optical data shown in Table 4.6 and Figure 4.2, it has been observed that the emission peak moved to the red-shifted region with increasing the solvent polarity from hexane to DMSO. However, the UV-Vis absorption spectral data in different solvents exhibited subtle spectral variation (**Figure 4.3**).

Table 4.6. Optical Data of 10s, 10x, and 10u in Different Organic Solvents.

Solvents	λ_{Em} /nm		
	10s	**10x**	**10u**
Hexane	430	434	440
Dichloromethane (DCM)	435	434	448
Methanol (MeOH)	448	438	460
Acetonitrile (MeCN)	437	438	447
Dimethyl sulfoxide (DMSO)	442	450	454

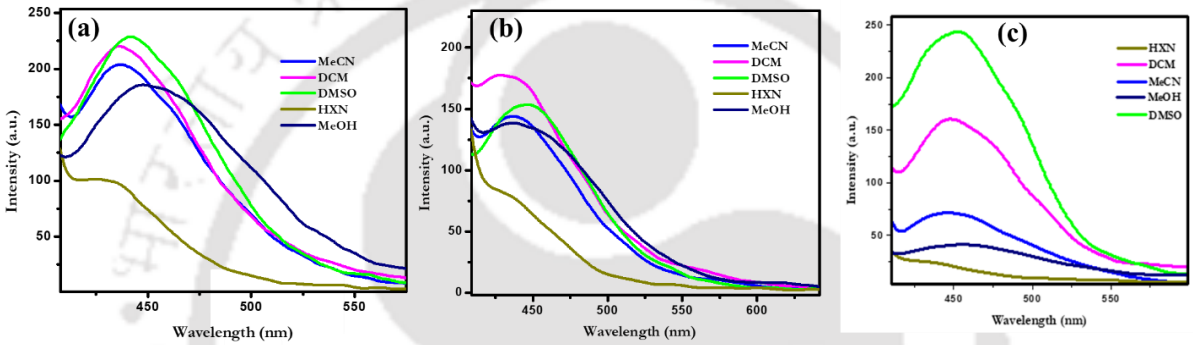

Figure 4.2. Emission spectral changes of **(a) 10s, (b) 10x** and **(c) 10u** in different organic solvents.

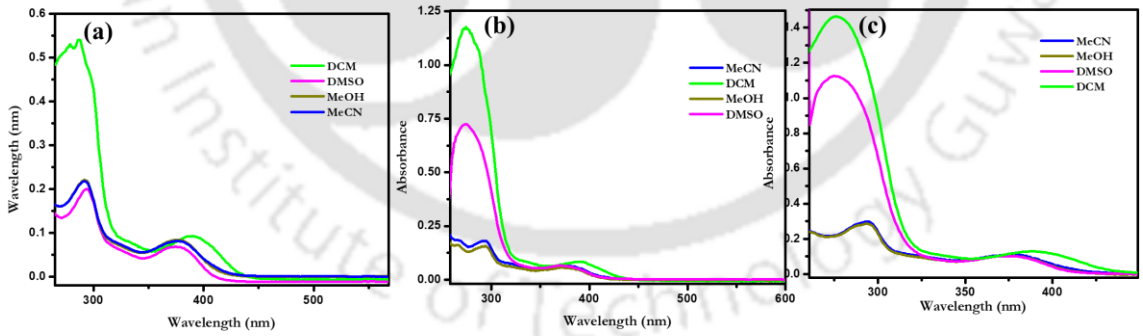

Figure 4.3. UV-Vis absorption spectral changes of **(a) 10s, (b) 10x,** and **(c) 10u** in different organic solvents.

Next, to understand the mode of binding interaction of the chemosensors towards F^-, typical UV-Vis spectral studies of all four compounds, **10s**, **10x**, **10u,** and **10z** (100 μM in DMSO) were carried out with the gradual addition of 0.5 mM F^- in DMSO/H_2O (v/v 7/3). In the presence of F^-, there occurs similar hypsochromic shifting of the low energy absorption band at 375 nm in all three compounds (**10s**, **10x,** and

10u) with the gradual emergence of a new ICT band at 460 nm, leading to visible chromogenic modulation from pale yellow to orange. For **10z** a new broad ICT band appeared at ~480 nm. The absorbance of the peak at 460 nm (for **10s**, **10x**, and **10u**) and 480 nm (for **10z**) gradually increased and reached maximum up to the addition of ~1 equivalent of F^- (Figure **4.4a,b** and **Figure 4.5a,b**).

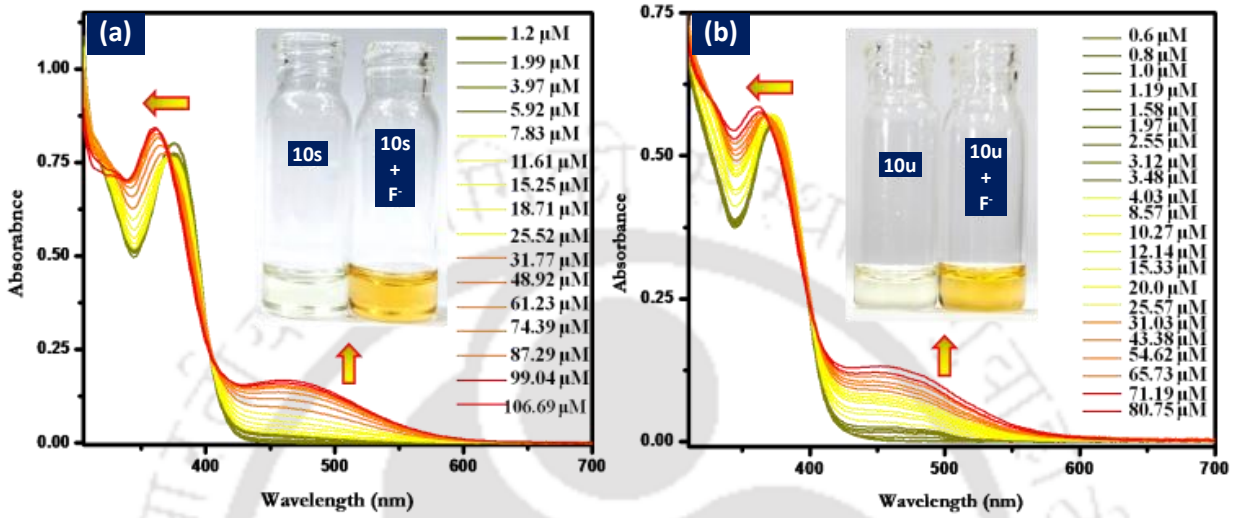

Figure 4.4. UV-Vis titration of **(a) 10s** and **(b) 10u** (100 µM in DMSO) in the presence of 60 µL F^- in 0.5 mM DMSO/H_2O (v/v 7/3) (Inset: the corresponding colorimetric changes).

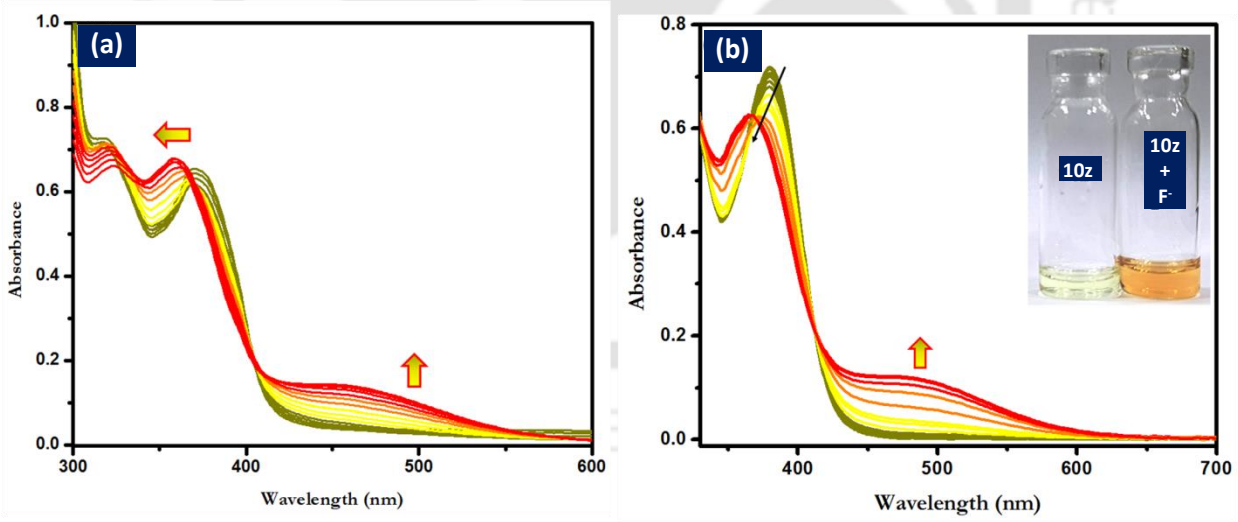

Figure 4.5. UV-Vis titration of **(a) 10x** and **(b) 10z** (100 µM in DMSO) in the presence of 60 µL and 100 µL F^- in 0.5 mM DMSO/H_2O (v/v 7/3) respectively.

The detectable chromogenic changes and the generation of a new ICT band may have originated from the facile ICT transition in the chemosensors upon interaction with F^- due to F^- induced strong H-bonding interaction of the chemosensors.[24] Upon interaction with F^-, the electron density of the hydroxyl oxygen

was largely increased, which was mainly responsible for the facile ICT. Interestingly, two major isosbestic points appeared at 370 and 400 nm (415 nm for **10z**) for all the chemosensors, which indicates that there is a formation of a single species in all the cases and there is equilibrium between the chemosensors and the corresponding adducts.

From the UV-Vis spectral studies, it has been observed that there is a good correlation between the absorbance of the chemosensors at 460 nm (480 nm for **10z**) as the function of F^- concentration with the linear regression equation of $A\text{-}A_0 = -7.14\times10^{-5}+4.58\times10^{-4}[F^-]\times5\times10^{-7}$, $A\text{-}A_0 = -0.00031+0.00954[F^-]\times5\times10^{-7}$, $A\text{-}A_0 = -0.0092+0.00579[F^-]\times5\times10^{-7}$, $A\text{-}A_0 = -5.9\times10^{-5}+7.4\times10^{-5}[F^-]\times5\times10^{-7}$ for **10s**, **10u, 10x** and **10z** respectively. Accordingly, the detection limits of the chemosensors towards F^- were acquired to be 2.5 μM (corresponding to 0.65 ppm), 1.3 μM (corresponding to 0.34 ppm), 2.3 μM (corresponding to 0.6 ppm), and 6.9 μM (corresponding to 2.2 ppm) respectively, which are much lower than the safe limit of fluoride in drinking water (1.5 ppm), set by World Health Organization (WHO)[17] (**Figure 4.6**).

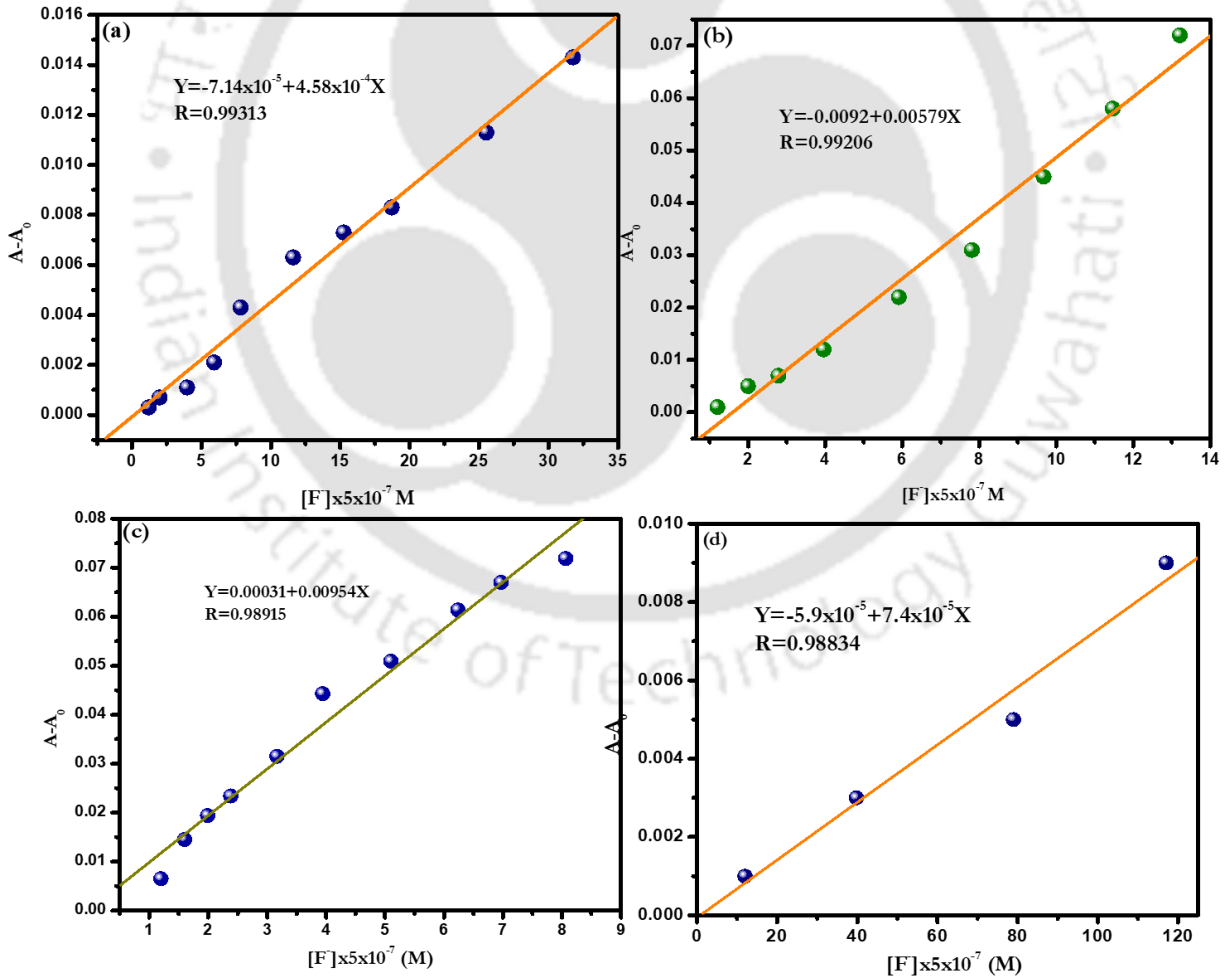

Figure 4.6. Calculation of LOD of **(a) 10s, (b) 10x, (c) 10u** and **(d) 10z** towards F^-.

However, the order of magnitude of K_a for **10z** is lower than those of the other three chemosensors (**10s**, **10u**, and **10x**), which probably suggests the decreased acidity of the interacting phenolic proton of **10z** due to the presence of electron-donating methoxy substituent on the same ring, thereby reducing its hydrogen bond-donating character. Moreover, to establish our assumption, control sensing experiments were carried out using two compounds (**10i** and **10j**), which do not contain any –OH group. However, no chromogenic change and UV-Vis spectral alteration of **10i** and **10j** were perceived in the presence of F^- (**Figure 4.7**). This designates that the incoming guest analyte, F^- interacts through the –OH site of the chemosensors to form the corresponding adducts *via* H-bonding interaction.

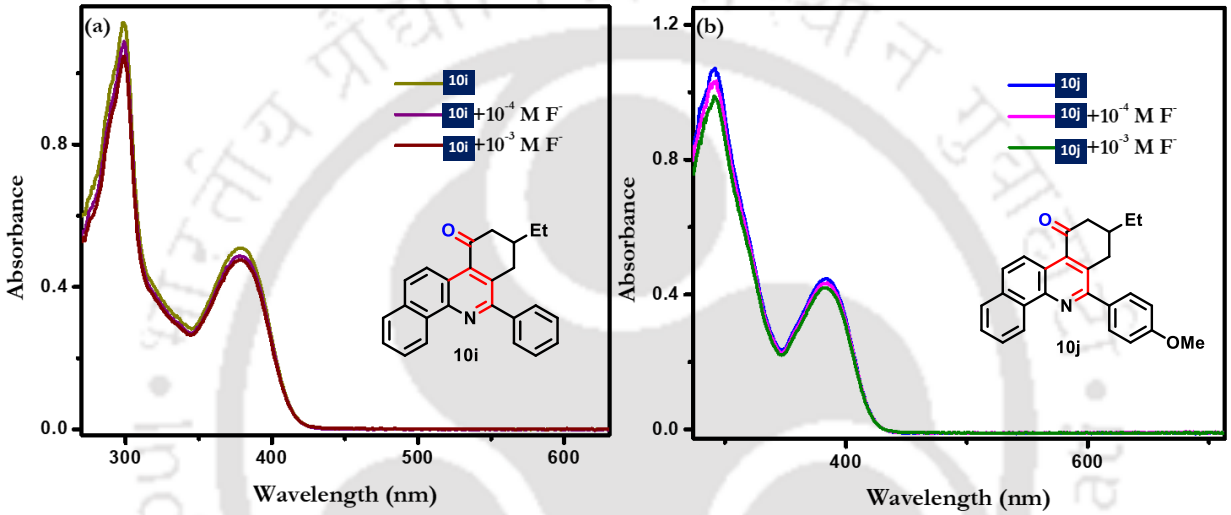

Figure 4.7. UV-Vis spectral data of **(a) 10i** (100 μM in DMSO); **(b) 10j** (100 μM in DMSO) in the presence of F^- in DMSO/H_2O (v/v 7/3).

Insight into the Sensing Mechanism by ^{1}H NMR spectroscopic investigation

To better understand the intermolecular sensing mechanism, ^{1}H NMR spectral studies have been carried out with the chemosensors upon incremental addition of F^-. It has been observed that the hydroxyl proton signal of **10u** in CD_3Cl (1.5×10^{-4} M) appeared as a singlet at δ 11.8 ppm. Upon gradual addition of F^-, it has been observed that the –OH proton signal gradually upfield shifted from 11.8 to ~10.6 ppm, broadening, and ultimately disappearing (**Figure 4.8**).

The peak broadening and disappearance of the –OH proton signal may be ascribed to the strong intermolecular H-bonding interaction between the hydroxyl –OH and F^-. This incoming analyte increased the electron density on the chemosensor skeleton, deshielded the –OH proton, and led to the observed downfield shifting. The other aromatic proton signals at 8.95 and 9.0 ppm also experienced slight upfield shifting (Δδ= ~0.1 and~0.2 ppm, respectively) due to the increase of electron density *via* the bond-

propagation effect.[25] Thus, the observed experimental outcomes suggest the strong intermolecular H-bonding interaction of the hydroxyl proton of the chemosensors with the incoming analyte, F^-. Based on this, the plausible mechanistic course of interaction has been schematized in the inset of **Figure 4.8**.

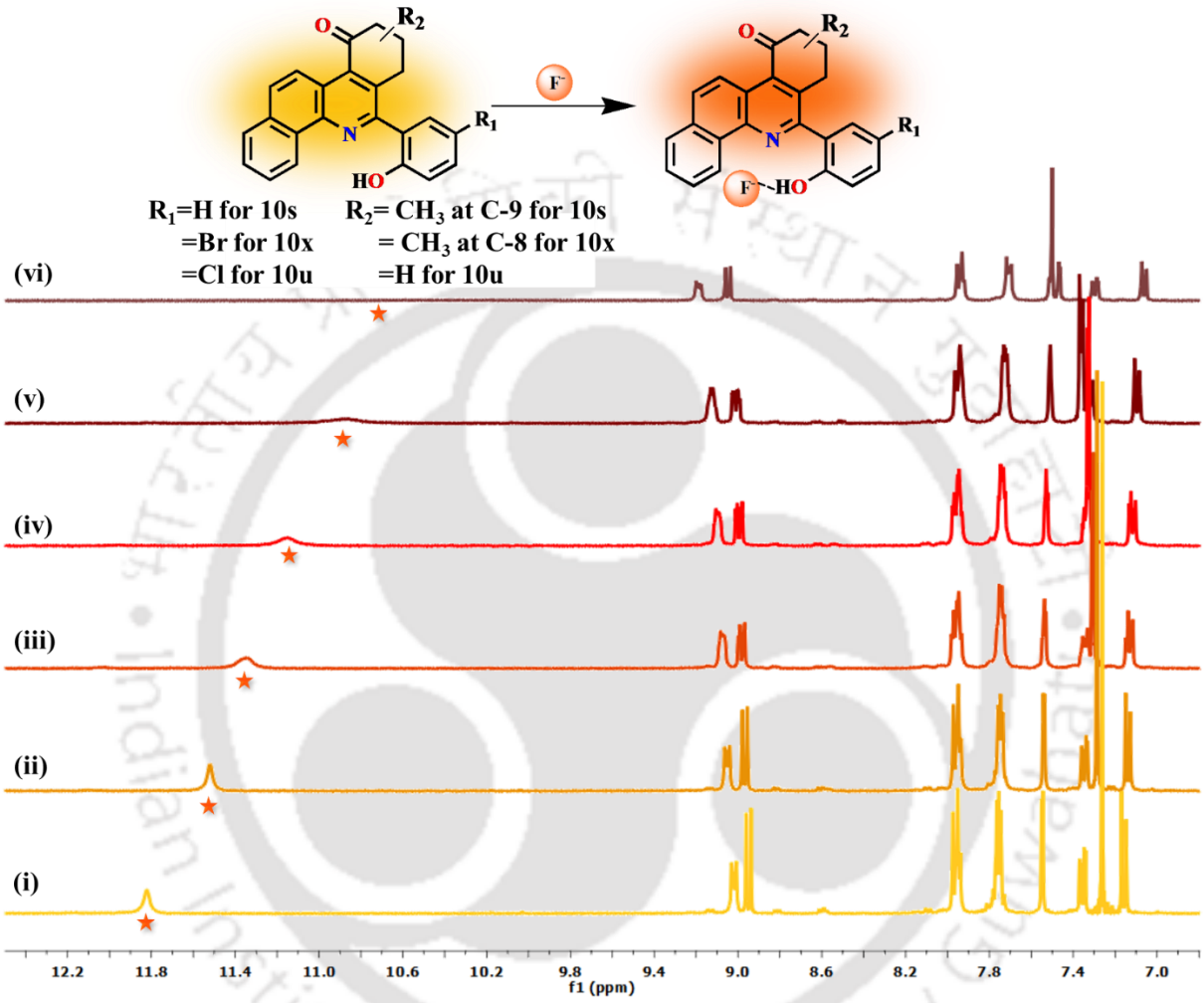

Figure 4.8. ^{1}H NMR titration of **10u** with the gradual addition of F^- (i: 0, ii: 0.01, iii: 0.02, iv=0.05, v: 0.2, and vi: 1.1 equivalents) (Inset: plausible mechanistic course of interaction.

Solid-state detection of Fluoride by spot TLC test

To explore the solid-state sensitivity of the compounds, the spot TLC assay was performed due to cost-effectiveness, ease of use, portability, low sample consumption, *etc*. At first, the TLC plate made of silica gel was spotted with **10u** (1 mM in DMSO). After proper air-drying, 1 mM F^- in DMSO/H_2O (v/v 7/3) was dropped onto it. This led to a clear '*naked eye*' chromogenic change from pale yellow to yellowish-orange

(**Figure 4.9**). Thus, by this simple '*naked eye*' TLC test, the presence of the targeted analyte can be determined.

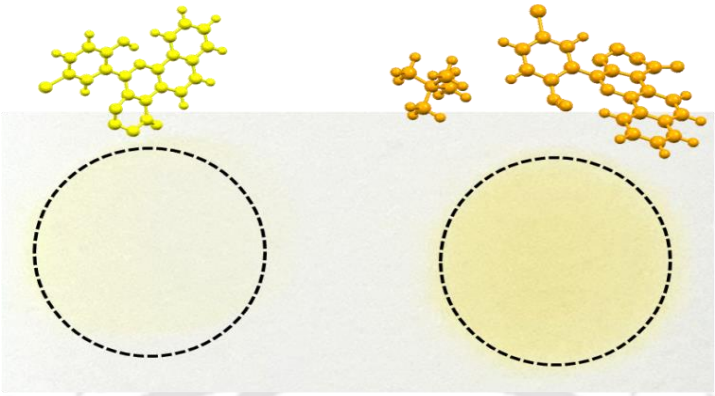

Figure 4.9. Naked eye solid state chromogenic recognition of F^- by **10u** (left: only **10u**, right: **10u** in the presence of F^-).

4.2f. Conclusions

- In summary, we have accomplished a one-pot, four-component synthetic route for the synthesis of 6-aryl-8,9-dihydrophenanthridine-10(7*H*)-ones from readily available starting materials 1-napthylamine/ aniline, aryl aldehydes, cyclohexanones, and dimethyl sulfoxide.
- DMSO acts as a solvent-cum-reactant for the regioselective oxygenation at the C-10 position of the tetrahydrobenzophenanthridine scaffold.
- The other features of the protocol are broad substrate scopes, shorter reaction time, good yields, high bond-forming efficiency, and atom economy.
- Moreover, some ketone derivatives were efficiently converted into 6-aryl-8-alkylbenzo[*c*]phenanthridin-10-ol derivatives under metal-free conditions.
- Every compound produced is novel and has not been synthesized before.
- The compounds containing phenolic –OH groups are efficient enough to detect F^- ion selectively in trace levels (LOD of **10s**, **10u, 10x,** and **10z** are 0.65 ppm, 0.6 ppm, 0.34 ppm, and 2.2 ppm, respectively) with a prompt response (~18 s). The sensitivity was checked in the solid state using a spot TLC test. Thus, the present work will be a considerable footstep in synthesizing new organic compounds with their promising optochemical sensing applications.

4.3. Experimental Section

4.3a. General Procedure for the Synthesis of 6-Aryl-8,9-dihydrobenzo[*c*]phenanthridine-10(7*H*)one (10), and 6-aryl-8,9-dihydrophenanthridine-10(7*H*)one derivatives (11).

1-naphthylamine **1** (1.0 mmol), aromatic aldehyde **2** (1.0 mmol), cyclic ketone **3** (1.0 mmol), and 20 mol% camphor sulfonic acid (46 mg) were taken into a 25 mL round-bottomed flask, and 1 mL dimethyl sulfoxide (DMSO) was added to it. Then, the reaction mixture was placed in a preheated oil bath at 120 °C with constant stirring. The progress of the reaction was monitored by TLC. After complete consumption of the starting material, the reaction mixture was brought to room temperature, and then it was extracted with DCM (2 × 10 mL) and washed with water (2 x 5 mL). Finally, the organic layer was dried over anhydrous sodium sulfate and concentrated in a rotatory evaporator. Then, the crude residue was purified through a silica gel (60−120 mesh) column chromatography, and the desired products, 6-aryl-8,9-dihydrobenzo[*c*]phenanthridine-10(7*H*)one derivative (**10**), were eluted with a mixture of *n*-hexane and ethyl acetate (9.7:0.3, v/v). A similar procedure was followed for the synthesis of 6-aryl-8,9-dihydrophenanthridine-10(7*H*)one derivative (**11**).

4.3b. General Procedure for the Synthesis of 6-Arylbenzo[*c*]phenanthridin-10-ol Derivatives (12), and 6-Arylphenanthridin-10-ol Derivatives (13).

A mixture of 6-Aryl-8,9-dihydrobenzo[*c*]phenanthridine-10(7*H*)one derivative (**10**) or 6-aryl-8,9-phenanthridine-10(7*H*)one (**11**, 0.25 mmol) and 10 mol% molecular iodine (8 mg) were taken in 1 mL of dimethyl sulfoxide in a 10 mL round-bottomed flask. Then, the reaction mixture was stirred in a preheated oil bath at 100 °C. When the reaction was over, as monitored by TLC, it was brought to room temperature. Then, it was extracted with DCM (2 × 5 mL) and washed with 10% sodium thiosulfate solution (5 mL) to remove unreacted iodine. Finally, it was washed with water (2 x 5 mL). Then, the organic extract was dried over anhydrous Na_2SO_4, and the solvent was evaporated in a rotary evaporator. Then, the crude reaction mixture was purified through silica gel (60−120 mesh) column chromatography (eluent: *n-hexane/ethyl* acetate = 9.5:0.5) to obtain the desired product (**12** or **13**).

4.3c Characterization Data

6-Phenyl-8,9-dihydrobenzo[*c*]phenanthridin-10(7*H*)-one (10a)

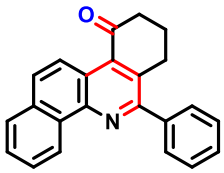

Yellow solid (210 mg, 65%); mp 188-190 °C; ^{1}H NMR (600 MHz, $CDCl_3$) δ 9.34 (dd, *J* = 6.0, 3.5 Hz, 1H), 9.06 (d, *J* = 9.3 Hz, 1H), 7.94 (d, *J* = 9.4 Hz, 1H), 7.91 (dd, *J* = 5.8, 3.3 Hz, 1H), 7.75 (d, *J* = 7.0 Hz, 2H), 7.70 – 7.68 (m, 2H), 7.56 (t, *J* = 7.3 Hz, 2H), 7.51 (t, *J* = 7.3 Hz, 1H), 3.13 (t, *J* = 6 Hz, 2H), 2.87 (t, *J* = 6.7 Hz, 2H), 2.12 (quin, *J* = 6.5 Hz, 2H); ^{13}C NMR (150 MHz, $CDCl_3$) δ 201.3, 158.0, 145.5, 140.5, 135.9, 134.5, 133.0, 131.4, 130.0, 129.7, 128.7, 128.4, 128.3, 127.4, 127.09, 125.0, 123.1, 122.0, 40.7, 29.0, 23.1; IR (KBr)ν_{max}: 1685 cm^{-1}; HRMS (ESI) Calcd for $C_{23}H_{18}NO$ 324.1383 ($M + H^+$); Found 324.1385.

6-(4-Fluorophenyl)-8,9-dihydrobenzo[*c*]phenanthridin-10(7*H*)-one (10b)

Yellow solid (252 mg, 74%); mp 130 °C; ^{1}H NMR (400 MHz, $CDCl_3$) δ 9.32 – 9.30 (m, 1H), 9.05 (d, *J*= 8 Hz, 1H), 7.94 (d, *J* = 8 Hz, 1H), 7.92 – 7.90 (m, 1H), 7.75 (d, *J* = 3.5 Hz, 2H), 7.71 – 7.69 (m, 2H), 7.27 (s, 1H), 7.23 (d, *J* = 12 Hz, 1H), 3.12 (t, *J* = 4 Hz, 2H), 2.88 (t, *J* = 4 Hz, 2H), 2.17 – 2.10 (m, 2H); ^{13}C NMR (100 MHz, $CDCl_3$) δ 201.2, 164.4, 161.9, 156.9, 145.6, 136.5, 135.7, 134.7, 133.1, 131.6, 131.5, 131.4, 130.2, 128.4, 127.5, 127.1, 124.9, 123.1, 122.1, 115.5, 115.3, 40.7, 29.1, 23.1; IR (KBr)ν_{max}: 1685 cm^{-1}; HRMS (ESI) Calcd for $C_{23}H_{17}FNO$ 342.1289 ($M + H^+$); Found 342.1289.

6-(4-Chlorophenyl)-8,9-dihydrobenzo[*c*]phenanthridin-10(7*H*)-one (10c)

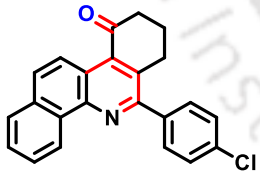

Yellow solid (257 mg, 72%); mp 129 °C; ^{1}H NMR (400 MHz, $CDCl_3$) δ 9.29 (dd, *J* = 6.1, 3.5 Hz, 1H), 9.05 (d, *J* = 9.4 Hz, 1H), 7.94 (d, *J* = 9.4 Hz, 1H), 7.91 – 7.90 (m, 1H), 7.70 – 7.68 (m, 4H), 7.53 (d, *J* = 8.4 Hz, 2H), 3.12 – 3.09 (m, 2H), 2.87 (t, *J* = 6.7 Hz, 2H), 2.16 – 2.10 (m, 2H); ^{13}C NMR (150 MHz, $CDCl_3$) δ 201.0, 156.7, 145.6, 138.9, 135.6, 134.9, 134.6, 133.1, 131.4, 131.1, 130.3, 128.6, 128.4, 127.5, 127.2, 124.9, 123.1, 122.2, 40.7, 29.0, 23.1; IR (KBr)ν_{max}: 1686 cm^{-1}; HRMS (ESI) Calcd for $C_{23}H_{17}ClNO$ 358.0993 ($M + H^+$); Found 358.0996.

6-(4-Bromophenyl)-8,9-dihydrobenzo[*c*]phenanthridin-10(7*H*)-one (10d)

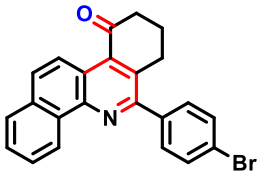

Yellow solid (284 mg, 71%); mp 207 °C; ^{1}H NMR (400 MHz, $CDCl_3$) δ 9.30 – 9.28 (m, 1H), 9.05 (d, *J* = 9.4 Hz, 1H), 7.94 (d, *J* = 9.3 Hz, 1H), 7.91 – 7.89 (m, 1H), 7.72 – 7.68 (m, 4H), 7.63 (d, *J* = 8.5 Hz, 2H), 3.11 – 3.08 (m, 2H), 2.87 (t, *J* = 6.7 Hz, 2H), 2.16 – 2.10 (m, 2H); ^{13}C NMR (100 MHz, $CDCl_3$) δ 201.1,

156.8, 145.6, 139.3, 135.6, 134.6, 133.1, 131.6, 131.4, 130.3, 128.5, 127.5, 127.2, 124.90, 123.1, 123.0, 122.2, 40.7, 29.0, 23.1; IR (KBr)ν_{max}: 1685 cm^{-1}; HRMS (ESI) Calcd for $C_{23}H_{17}BrNO$ 402.0488 ($M + H^+$); Found 402.0490 and 404.0466.

6-(3-Bromophenyl)-8,9-dihydrobenzo[*c*]phenanthridin-10(7*H*)-one (10e)

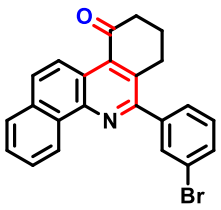

Yellow solid (292 mg, 73%); mp 207 °C; ^{1}H NMR (500 MHz, $CDCl_3$) δ 9.32 – 9.30 (m, 1H), 9.06 (d, *J* = 9.5 Hz, 1H), 7.95 (d, *J* = 10.0 Hz, 1H), 7.92 – 7.90 (m, 2H), 7.72 – 7.70 (m, 2H), 7.66 – 7.63 (m, 2H), 7.44 – 7.41 (m, 1H), 3.11 (t, *J* = 5 Hz, 2H), 2.88 (t, *J* = 5 Hz, 2H), 2.15 (quin, *J* = 5 Hz, 2H); ^{13}C NMR (100 MHz, $CDCl_3$) δ 201.0, 156.4, 145.6, 142.5, 135.7, 134.6, 133.1, 132.7, 131.7, 131.4, 130.5, 129.9, 128.5, 128.3, 127.5, 127.2, 124.9, 123.0, 122.6, 122.3, 40.7, 28.9, 23.1; IR (KBr)ν_{max}: 1685 cm^{-1}; HRMS (ESI) Calcd for $C_{23}H_{17}BrNO$ 402.0488 ($M + H^+$); Found 402.0487 and 404.0448.

6-(2-Bromophenyl)-8,9-dihydrobenzo[*c*]phenanthridin-10(7*H*)-one (10f)

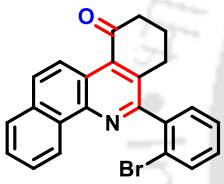

Yellow solid (280 mg, 70%); mp 210 °C; ^{1}H NMR (500 MHz, $CDCl_3$) δ 9.27 – 9.25 (m, 1H), 9.14 (d, *J* = 9.5 Hz, 1H), 7.97 (d, 1H), 7.91 – 7.89 (m, 1H), 7.74 (d, *J* = 1.2 Hz, 1H), 7.68 – 7.65 (m, 2H), 7.51-7.48 (m, 1H), 7.47-7.45 (m, 1H), 7.39 – 7.34 (m, 1H), 3.04 – 2.98 (m, 1H), 2.89 – 2.84 (m, 2H), 2.79 – 2.73 (m, 1H), 2.24 – 2.15 (m, 2H); ^{13}C NMR (125 MHz, DMSO-d_6) δ 201.2, 158.0, 145.5, 141.7, 136.5, 133.9, 133.1, 132.9, 131.5, 130.7, 130.4, 130.0, 128.3, 127.8, 127.4, 127.1, 125.2, 123.1, 122.9, 122.6, 40.9, 27.6, 22.8; IR (KBr)ν_{max}: 1684 cm^{-1}; HRMS (ESI) Calcd for $C_{23}H_{17}BrNO$ 402.0488 ($M + H^+$); Found 402.0491 and 404.0437.

8-Methyl-6-phenyl-8,9-dihydrobenzo[*c*]phenanthridin-10(7*H*)-one (10g)

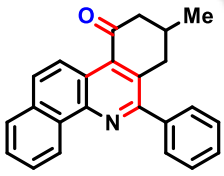

Yellow solid (242 mg, 72%); mp 248 °C; ^{1}H NMR (600 MHz, $CDCl_3$) δ 9.33 (d, *J* = 9.5 Hz, 1H), 9.10 (d, *J* = 9.4 Hz, 1H), 7.94 (d, *J* = 9.4 Hz, 1H), 7.91 (dd, *J* = 5.7, 3.4 Hz, 1H), 7.75 (d, *J* = 8.3 Hz, 2H), 7.69 (d, *J* = 6.1 Hz, 2H), 7.57 (t, *J* = 7.4 Hz, 2H), 7.53 (d, *J* = 7.3 Hz, 1H), 3.14 (ddd, *J* = 16.6, 3.6, 2.0 Hz, 1H), 2.93 (ddd, *J* = 16.7, 4.0, 1.9 Hz, 1H), 2.85 (dd, *J* = 16.6, 10.8 Hz, 1H), 2.55 (dd, *J* = 16.7, 12.5 Hz, 1H), 2.33 – 2.26 (m, 1H), 1.14 (d, *J* = 6.5 Hz, 3H); ^{13}C NMR (150 MHz, $CDCl_3$) δ 201.6, 158.1, 145.5, 140.5, 135.1, 134.1, 133.1, 131.4, 130.1, 129.7, 128.6, 128.4, 128.3, 127.4, 127.1, 125.0, 123.0, 122.0, 48.8, 37.3, 30.6, 21.4 ; IR (KBr)ν_{max}: 1685 cm^{-1}; HRMS (ESI) Calcd for $C_{24}H_{20}NO$ 338.1539 ($M + H^+$); Found 338.1542.

6-(4-Methoxyphenyl)-8-methyl-8,9-dihydrobenzo[*c*]phenanthridin-10(7*H*)-one (10h)

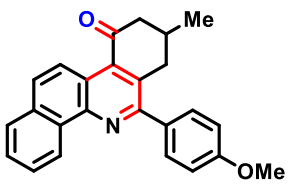

Yellow solid (257 mg, 70%); mp 186 °C; ^{1}H NMR (400 MHz, $CDCl_3$) δ 9.35 – 9.33 (m, 1H), 9.08 (d, *J* = 9.3 Hz, 1H), 7.93 – 7.87 (m, 2H), 7.72 (d, *J* = 8.6 Hz, 2H), 7.69 – 7.67 (m, 2H), 7.09 (d, *J* = 8.6 Hz, 2H), 3.92 (s, 3H), 3.16 (dd, *J* = 14.7, 2.8 Hz, 1H), 2.92 (d, *J* = 13.1 Hz, 1H), 2.84 (dd, *J* = 16.7, 10.8 Hz, 1H), 2.52 (dd, *J* = 16.8, 12.4 Hz, 1H), 2.30 – 2.23 (m, 1H), 1.14 (d, *J*= 6.6 Hz, 3H);^{13}C NMR (100 MHz, $CDCl_3$) δ 201.6, 160.1, 157.7, 145.5, 135.1, 134.1, 133.1, 133.0, 131.4, 131.1, 129.8, 128.2, 127.4, 127.0, 125.0, 123.1, 121.7, 113.8, 55.5, 48.8, 37.4, 30.6, 21.3; IR (KBr)ν_{max}: 1684 cm^{-1}; HRMS (ESI) Calcd for $C_{25}H_{22}NO_2$ 368.1645 (M + H$^+$); Found 368.1645.

8-Ethyl-6-phenyl-8,9-dihydrobenzo[*c*]phenanthridin-10(7*H*)-one (10i)

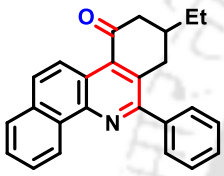

Yellow solid (256 mg, 73%); mp 201 °C; ^{1}H NMR (600 MHz, $CDCl_3$) δ 9.33 (d, *J* = 9.5 Hz, 1H), 9.09 (d, *J* = 9.3 Hz, 1H), 7.94 (d, *J* = 9.4 Hz, 1H), 7.91 (dd, *J* = 6.2, 2.9 Hz, 1H), 7.75 (d, *J* = 7.0 Hz, 2H), 7.69 (dd, *J* = 6.0, 3.3 Hz, 2H), 7.57 (t, *J* = 7.3 Hz, 2H), 7.52 (t, *J* = 7.4 Hz, 1H), 3.17 (ddd, *J* = 16.6, 3.4, 1.8 Hz, 1H), 2.99 (ddd, *J* = 16.6, 3.9, 1.7 Hz, 1H), 2.86 (dd, *J* = 16.6, 10.7 Hz, 1H), 2.56 – 2.51 (m, 1H), 2.13 –2.05 (m, 1H), 1.58 – 1.44 (m, 2H), 0.93 (t, *J* = 7.4 Hz, 3H); ^{13}C NMR (150 MHz, $CDCl_3$) δ 201.7, 158.2, 145.5, 140.5, 135.1, 134.3, 133.1, 131.4, 130.1, 129.6, 128.7, 128.4, 128.3, 127.5, 127.1, 125.0, 123.0, 121.9, 46.6, 37.0, 35.2, 28.6, 11.2; IR (KBr)ν_{max}: 1685 cm^{-1}; HRMS (ESI) Calcd for $C_{25}H_{22}NO$ 352.1696 (M + H$^+$); Found 352.1708.

8-Ethyl-6-(4-methoxyphenyl)-8,9-dihydrobenzo[*c*]phenanthridin-10(7*H*)-one (10j)

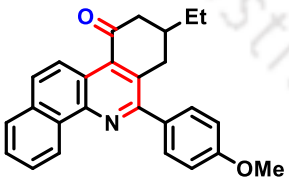

Yellow solid (270 mg, 71%); mp 159 °C; ^{1}H NMR (400 MHz, $CDCl_3$) δ 9.35 – 9.32 (m, 1H), 9.07 (d, *J* = 9.4 Hz, 1H), 7.92-7.88 (m, 2H), 7.72 (d, *J* = 8.7 Hz, 2H), 7.68 (dd, *J* = 5.6, 3.6 Hz, 2H), 7.08 (d, *J* = 8.6 Hz, 2H), 3.92 (s, 3H), 3.19 (dd, *J* = 16.3, 2.9 Hz, 1H), 2.97 (dd, *J* = 15.5, 3.6 Hz, 1H), 2.85 (dd, *J* = 16.6, 10.8 Hz, 1H), 2.51 (dd, *J* = 16.8, 12.3 Hz, 1H), 2.06 (dt, *J* = 11.3, 7.4 Hz, 1H), 0.92 (d, *J* = 7.4 Hz, 3H); ^{13}C NMR (100 MHz, $CDCl_3$) δ 201.8, 160.1, 157.8, 145.4, 135.1, 134.3, 133.1, 133.0, 131.4, 131.1, 129.8, 128.2, 127.4, 127.0, 125.0, 123.1, 121.7, 113.8, 55.5, 46.6, 37.0, 35.3, 28.6, 11.2; IR (KBr)ν_{max}: 1685 cm^{-1}; HRMS (ESI) Calcd for $C_{26}H_{24}NO_2$ 382.1802 (M + H$^+$); Found 382.1802.

8-Ethyl-6-(4-hydroxyphenyl)-8,9-dihydrobenzo[*c*]phenanthridin-10(7*H*)-one (10k)

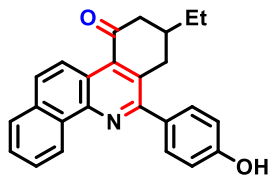

Yellow solid (250 mg, 68%); mp 239 °C; ^{1}H NMR (400 MHz, $CDCl_3$) δ 9.34 – 9.31 (m, 1H), 9.07 (d, *J* = 9.4 Hz, 1H), 7.93 – 7.89 (m, 2H), 7.70 – 7.66 (m, 4H), 7.02 (d, *J* = 8.3 Hz, 2H), 5.38 (s, bs, 1H), 3.19 (d, *J* = 17.5 Hz, 1H), 2.99 (d, *J* = 16 Hz, 1H), 2.88 – 2.82 (m, 1H), 2.53 (dd, *J* = 16.9, 12.3 Hz, 1H), 2.10 – 2.06 (m, 1H), 1.53 – 1.45 (m, 2H), 0.93 (t, *J* = 7.4 Hz, 3H); ^{13}C NMR (100 MHz, $CDCl_3$) δ 202.0, 157.8, 156.2, 145.5, 135.1, 134.4, 133.1, 131.4, 131.3, 129.9, 128.3, 127.5, 127.0, 125.0, 123.0, 121.7, 115.3, 46.6, 37.0, 35.3, 28.6, 11.2; IR (KBr)ν_{max}: 3300, 1680 cm^{-1}; HRMS (ESI) Calcd for $C_{25}H_{22}NO_2$ 368.1645 (M + H$^+$); Found 368.1644.

8-(*tert*-Butyl)-6-phenyl-8,9-dihydrobenzo[*c*]phenanthridin-10(7*H*)-one (10l)

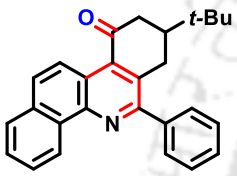

Yellow solid (276 mg, 73%); mp 220 °C; ^{1}H NMR (600 MHz, $CDCl_3$) δ 9.33 – 9.32 (m, 1H), 9.07 (d, *J* = 9.3 Hz, 1H), 7.94 (d, *J* = 9.3 Hz, 1H), 7.91 (dd, *J* = 6.3, 2.8 Hz, 1H), 7.75 (d, *J* = 7.0 Hz, 2H), 7.69 (dd, *J* = 5.9, 3.5 Hz, 2H), 7.57 (t, *J* = 7.4 Hz, 2H), 7.51 (t, *J* = 7.4 Hz, 1H), 3.20 – 3.17 (m, 1H), 2.95 (dd, *J* = 13.7, 3.5 Hz, 1H), 2.84 (dd, *J* = 16.4, 12.2 Hz, 1H), 2.60 (dd, *J* = 16.4, 14.0 Hz, 1H), 1.97 – 1.91 (m, 1H), 0.94 (s, 9H); ^{13}C NMR (150 MHz, $CDCl_3$) δ 202.4, 158.3, 145.4, 140.5, 135.8, 134.1, 133.1, 131.5, 130.1, 129.6, 128.7, 128.4, 128.3, 127.5, 127.1, 125.0, 123.0, 121.9, 45.5, 42.9, 32.6, 30.6, 27.1; IR (KBr)ν_{max}: 1684 cm^{-1}; HRMS (ESI) Calcd for $C_{27}H_{26}NO$ 380.2009 (M + H$^+$); Found 380.2014.

8-(*tert*-Butyl)-6-(*p*-tolyl)-8,9-dihydrobenzo[*c*]phenanthridin-10(7*H*)-one (10m)

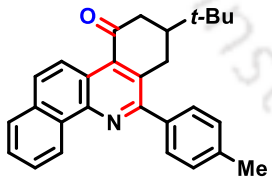

Yellow solid (291 mg, 74%); mp 238 °C; ^{1}H NMR (500 MHz, $CDCl_3$) δ 9.33 (s, 1H), 9.07 (d, *J* = 9.3 Hz, 1H), 7.92 (d, *J* = 10.1 Hz, 2H), 7.68 (d, *J* = 5.9 Hz, 2H), 7.65 (d, *J* = 7.9 Hz, 2H), 7.37 (d, *J* = 7.4 Hz, 2H), 3.21 (d, *J* = 16.3 Hz, 1H), 2.95 (d, *J* = 16.5 Hz, 1H), 2.86 – 2.80 (m, 1H), 2.59 (t, *J* = 15.2 Hz, 1H), 2.49 (s, 3H), 1.93 (t, *J* = 12.8 Hz, 1H), 0.95 (s, 9H);^{13}C NMR (100 MHz, $CDCl_3$) δ 202.5, 158.4, 145.4, 138.6, 137.7, 135.8, 134.1, 133.1, 131.5, 129.9, 129.5, 129.1, 128.2, 127.4, 127.0, 125.0, 123.0, 121.7, 45.5, 42.9, 32.6, 30.7, 27.1, 21.5; IR (KBr)ν_{max}: 1684 cm^{-1}; HRMS (ESI) Calcd for $C_{28}H_{28}NO$ 394.2165 (M + H$^+$); Found 394.2165.

8-(*tert*-Butyl)-6-(4-methoxyphenyl)-8,9-dihydrobenzo[*c*]phenanthridin-10(7*H*)-one (10n)

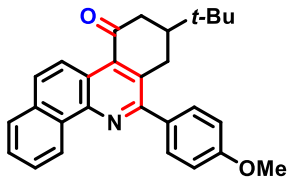

Yellow solid (294 mg, 72%); mp 213 °C; ^{1}H NMR (400 MHz, $CDCl_3$) δ 9.34 – 9.32 (m, 1H), 9.05 (d, *J* = 9.4 Hz, 1H), 7.92 – 7.89 (m, 2H), 7.72 (d, *J* = 8.5 Hz, 2H), 7.69 – 7.67 (m, 2H), 7.09 (d, *J* = 8.6 Hz, 2H), 3.93 (s, 3H), 3.22 (dd, *J*= 16.3, 2.6 Hz, 1H), 2.97 – 2.93 (m, 1H), 2.88 – 2.81 (m, 1H), 2.62 – 2.54 (m, 1H), 1.96 – 1.87 (m, 1H), 0.95 (s, 9H);^{13}C NMR (100 MHz, $CDCl_3$) δ 202.5, 160.0, 157.9, 145.4, 135.8, 134.1, 133.1, 133.0, 131.4, 131.1, 129.8, 128.2, 127.5, 127.0, 125.0, 123.0, 121.6, 113.8, 55.5, 45.5, 42.8, 32.6, 30.8, 27.1; IR (KBr)ν_{max}: 1682 cm^{-1}; HRMS (ESI) Calcd for $C_{28}H_{28}NO_2$ 410.2115 (M + H$^+$); Found 410.2115.

8-(*tert*-Butyl)-6-(4-nitrophenyl)-8,9-dihydrobenzo[*c*]phenanthridin-10(7*H*)-one (10o)

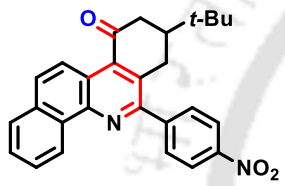

Yellow solid (314 mg, 74%); mp 163 °C; ^{1}H NMR (400 MHz, $CDCl_3$) δ 9.28 – 9.25 (m, 1H), 9.08 (d, *J* = 9.4 Hz, 1H), 8.44 (d, *J* = 8.7 Hz, 2H), 7.98 (d, *J* = 9.4 Hz, 2H), 7.94 (d, *J* = 8.7 Hz, 2H), 7.73 – 7.71 (m, 2H), 3.12 – 3.07 (m, 1H), 3.01 – 2.96 (m, 1H), 2.90 – 2.83 (m, 1H), 2.66 – 2.58 (m, 1H), 2.01 – 1.94 (m, 1H), 0.95 (s, 9H); ^{13}C NMR (100 MHz, $CDCl_3$) δ 201.8, 155.7, 148.0, 146.9, 145.8, 135.2, 134.5, 133.2, 131.3, 131.1, 130.7, 128.7, 127.7, 127.4, 124.8, 123.7, 122.9, 122.6, 45.6, 42.8, 32.7, 30.5, 27.1; IR (KBr)ν_{max}: 1688, 1550, 1330 cm^{-1}; HRMS (ESI) Calcd for $C_{27}H_{25}N_2O_3$ 425.1860 (M + H$^+$); Found 425.1861.

8-(*tert*-Butyl)-6-(3-chlorophenyl)-8,9-dihydrobenzo[*c*]phenanthridin-10(7*H*)-one (10p)

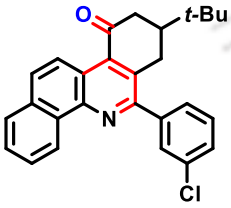

Yellow solid (306 mg, 74%); mp 163 °C; ^{1}H NMR (500 MHz, $CDCl_3$) δ 9.31 – 9.29 (m, 1H), 9.07 (d, *J* = 9.4 Hz, 1H), 7.95 (d, *J* = 9.3 Hz, 1H), 7.92 – 7.90 (m, 1H), 7.77 (s, 1H), 7.71 – 7.60 (m, 2H), 7.60 – 7.58 (m, 1H), 7.50 – 7.49 (m, 2H), 3.17 – 3.12 (m, 1H), 2.98 – 2.94 (m, 1H), 2.85 – 2.79 (m, 1H), 2.63 – 2.56 (m, 1H), 1.98 – 1.91 (m, 1H), 0.95 (s, 9H); ^{13}C NMR (125 MHz, $CDCl_3$) δ 202.1, 156.8, 145.5, 142.3, 135.5, 134.5, 134.3, 133.2, 131.4, 130.5, 129.9, 129.6, 128.8, 128.5, 127.7, 127.6, 127.2, 125.0, 122.9, 122.2, 45.6, 42.9, 32.6, 30.5, 27.1; IR (KBr)ν_{max}: 1686 cm^{-1}; HRMS (ESI) Calcd for $C_{27}H_{25}ClNO$ 414.1619 (M + H$^+$); Found 414.1619.

6-(2-Hydroxyphenyl)-8,9-dihydrobenzo[*c*]phenanthridin-10(7*H*)-one (10q)

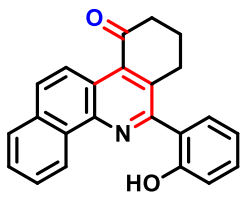

Yellow solid (230 mg, 68%); mp 180 – 182 °C; ^{1}H NMR (600 MHz, $CDCl_3$) δ 11.91 (s, 1H), 9.05 (d, *J* = 9.2 Hz, 1H), 8.94 (d, *J* = 9.3 Hz, 1H), 7.94 (d, *J* = 9.1 Hz, 2H), 7.77 – 7.73 (m, 2H), 7.57 (dd, *J* = 7.8, 1.4 Hz, 1H), 7.42 – 7.39 (m, 1H), 7.23 – 7.21 (m, 1H), 7.04 – 7.01 (m, 1H), 3.29 (t, *J* = 5.0 Hz, 2H), 2.91 (t, *J* = 6.7 Hz, 2H), 2.09 (quint, *J* = 6.6 Hz, 2H); ^{13}C NMR (150 MHz, $CDCl_3$) δ 200.8, 157.2, 155.9, 143.7, 136.8, 136.8, 133.4, 131.3, 130.6, 130.5, 130.0, 128.9, 128.0, 127.9, 123.8, 122.8, 122.2, 121.8, 119.0, 118.1, 40.3, 29.7, 23.1; IR (KBr)ν_{max}: 3300 (bs), 1687 cm^{-1}; HRMS (ESI) Calcd for $C_{23}H_{18}NO_2$ 340.1332 (M + H$^+$); Found 340.1333.

6-(2-Hydroxyphenyl)-8-methyl-8,9-dihydrobenzo[*c*]phenanthridin-10(7*H*)-one (10r)

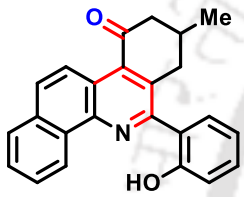

Yellow solid (244 mg, 69%); mp 165 °C; ^{1}H NMR (600 MHz, $CDCl_3$) δ 11.85 (s, 1H), 9.05 (d, *J* = 9.0 Hz, 1H), 8.99 (d, *J* = 9.3 Hz, 1H), 7.95 – 7.93 (m, 2H), 7.76 – 7.72 (m, 2H), 7.57 (dd, *J*= 7.8, 1.3 Hz, 1H), 7.43 – 7.40 (m, 1H), 7.23 – 7.22 (m, 1H), 7.05 – 7.02 (m, 1H), 3.32 (dt, *J*= 16.2, 2.8 Hz, 1H), 3.01 – 2.97 (m, 2H), 2.55 (dd, *J* = 17.8, 12.5 Hz, 1H), 2.24 – 2.17 (m, 1H), 1.17 (d, *J* = 6.5 Hz, 3H); ^{13}C NMR (150 MHz, $CDCl_3$) δ 201.2, 157.2, 156.0, 143.7, 136.4, 136.0, 133.4, 131.3, 130.6, 130.6, 130.0, 128.9, 128.0, 127.9, 123.9, 122.8, 122.1, 121.9, 119.1, 118.2, 48.4, 37.9, 31.1, 21.2; IR (KBr)ν_{max}: 3300 (bs), 1687 cm^{-1}; HRMS (ESI) Calcd for $C_{24}H_{20}NO_2$ 354.1489 (M + H$^+$); Found 354.1494.

6-(2-Hydroxyphenyl)-9-methyl-8,9-dihydrobenzo[*c*]phenanthridin-10(7*H*)-one (10s)

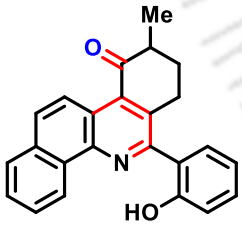

Yellow solid (254 mg, 72%); mp 165 °C; ^{1}H NMR (400 MHz, $CDCl_3$) δ 11.72 (s, 1H), 9.05 – 9.03 (m, 1H), 8.89 (d, *J* = 9.4 Hz, 1H), 7.94 – 7.90 (m, 2H), 7.76 – 7.70 (m, 2H), 7.58 (dd, *J* = 7.8, 1.3 Hz, 1H), 7.42 – 7.38 (m, 1H), 7.21 (d, *J* = 8.1 Hz, 1H), 7.01 (t, *J* = 7.5 Hz, 1H), 3.30 (dd, *J* = 7.4, 4.4 Hz, 2H), 2.85 (dq, *J* = 12.1, 6.9, 6.1 Hz, 1H), 2.25 (dq, *J* = 13.6, 4.5 Hz, 1H), 1.82 – 1.72 (m, 1H), 1.39 (d, *J* = 6.9 Hz, 3H); ^{13}C NMR (125 MHz, $CDCl_3$) δ 203.8, 157.2, 155.9, 143.8, 136.9, 136.5, 133.4, 131.3, 130.4, 130.3, 130.1, 128.8, 128.0, 127.8, 123.9, 122.9, 122.4, 122.0, 119.0, 118.2, 44.2, 31.4, 28.6, 16.4; IR (KBr)ν_{max}: 3300 (bs), 1687 cm^{-1}; HRMS (ESI) Calcd for $C_{24}H_{20}NO_2$ 354.1489 (M + H$^+$); Found 354.1488.

8-(*tert*-Butyl)-6-(2-hydroxyphenyl)-8,9-dihydrobenzo[*c*]phenanthridin-10(7*H*)-one (10t)

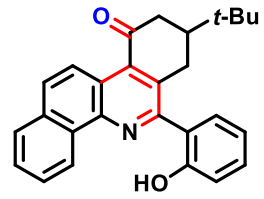

Yellow solid (276 mg, 70%); mp 165 °C; ^{1}H NMR (500 MHz, $CDCl_3$) δ 11.87 (s, 1H), 9.02 (d, *J* = 8.8 Hz, 1H), 8.94 (d, *J* = 9.3 Hz, 1H), 7.93 – 7.90 (m, 2H), 7.75 – 7.71 (m, 2H), 7.55 (d, *J* = 7.8 Hz, 1H), 7.40 (t, *J* = 7.7 Hz, 1H), 7.22 (d, *J* = 8.2 Hz, 1H), 7.03 (t, *J* = 7.5 Hz, 1H), 3.34 (d, *J* = 16.0 Hz, 1H), 2.97 – 2.89 (m, 2H), 2.60 – 2.54 (m, 1H), 1.83 – 1.78 (m, 1H), 0.97 (s, 9H); ^{13}C NMR (150 MHz, $CDCl_3$) δ 201.9, 157.2, 156.2, 143.5, 136.6, 136.3, 133.3, 131.3, 130.5, 130.4, 130.0, 128.8, 128.0, 127.8, 123.8, 122.7, 122.0, 121.9, 119.1, 118.3, 45.6, 42.5, 32.5, 31.3, 27.2; IR (KBr)ν_{max}: 3367, 1687 cm^{-1}; HRMS (ESI) Calcd for $C_{27}H_{26}NO_2$ 396.1958 ($M + H^+$); Found 396.1958.

6-(5-Chloro-2-hydroxyphenyl)-8,9-dihydrobenzo[*c*]phenanthridin-10(7*H*)-one (10u)

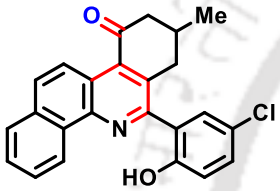

Yellow solid (257 mg, 69%); mp 258 °C; ^{1}H NMR (400 MHz, $CDCl_3$) δ 11.82 (s, 1H), 9.02 (d, *J* = 9.3 Hz, 1H), 8.95 (d, *J* = 9.4 Hz, 1H), 7.95 (dd, *J* = 9.3, 5.2 Hz, 2H), 7.77 – 7.74 (m, 2H), 7.55 (d, *J* = 2.4 Hz, 1H), 7.37 – 7.34 (m, 1H), 7.16 (d, *J* = 8.8 Hz, 1H), 3.31 – 3.27 (m, 2H), 2.92 (d, *J* = 6.7 Hz, 2H), 2.14 – 2.10 (m, 2H). ^{13}C NMR (100 MHz, CDCl3) δ 200.5, 155.9, 154.6, 143.9, 136.9, 136.6, 133.4, 131.0, 130.9, 130.0, 129.1, 128.1, 128.0, 123.8, 123.8, 122.9, 122.8, 122.6, 119.6, 40.3, 29.5, 23.1. IR (KBr)ν_{max}: 3400 (bs), 1686 cm^{-1}; HRMS (ESI) Calcd for $C_{23}H_{17}ClNO_2$ 374.0943 ($M + H^+$); Found 374.0956.

6-(5-Chloro-2-hydroxyphenyl)-8-methyl-8,9-dihydrobenzo[*c*]phenanthridin-10(7*H*)-one (10v)

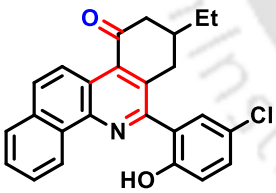

Yellow solid (271 mg, 70%); mp 268 °C; ^{1}H NMR (500 MHz, DMSO-d_6) δ 10.09 (s, 1H), 9.08 (d, *J* = 7.8 Hz, 1H), 9.04 (d, *J* = 9.4 Hz, 1H), 8.06 (d, *J* = 9.4 Hz, 1H), 8.02 (d, *J* = 7.6 Hz, 1H), 7.73 (q, *J* = 7.2 Hz, 2H), 7.39 (s, 2H), 7.02 (d, *J* = 9.4 Hz, 1H), 2.89 – 2.83 (m, 1H), 2.80 – 2.75 (m, 2H), 2.61 (dd, *J* = 16.1, 12.2 Hz, 1H), 2.34 – 2.28 (m, 1H), 1.04 (d, *J* = 6.5 Hz, 3H); ^{13}C NMR (125 MHz, DMSO) δ 201.2, 156.2, 153.7, 144.1, 137.2, 132.6, 132.3, 130.5, 129.9, 129.6, 129.5, 129.4, 128.3, 127.5, 127.2, 124.1, 122.6, 122.6, 121.4, 117.4, 48.0, 34.5, 29.3, 20.9; IR (KBr)ν_{max}: 3400 (bs), 1687 cm^{-1}; HRMS (ESI) Calcd for $C_{24}H_{19}ClNO_2$ 388.1099 ($M + H^+$); Found 388.1125.

6-(5-Chloro-2-hydroxyphenyl)-8-ethyl-8,9-dihydrobenzo[*c*]phenanthridin-10(7*H*)-one (10w)

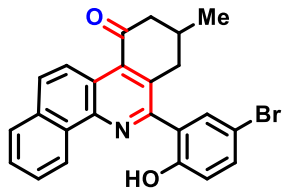

Yellow solid (285 mg, 71%); mp 268 °C; ^{1}H NMR (500 MHz, $CDCl_3$) δ 11.69 (s, 1H), 9.00 – 8.98 (m, 1H), 8.95 (d, *J* = 9.4 Hz, 1H), 7.94 (d, *J*= 9.3 Hz, 2H), 7.76 – 7.72 (m, 2H), 7.52 (d, *J* = 2.5 Hz, 1H), 7.35 (dd, *J* = 8.7, 2.5 Hz, 1H), 7.15 (d, *J* = 8.7 Hz, 1H), 3.30 (d, *J* = 16.1 Hz, 1H), 3.04 – 2.99 (m, 1H), 2.96 (dd, *J* = 15.0, 5.4 Hz, 1H), 2.55 – 2.49 (m, 1H), 2.01 (dt, *J* = 11.3, 5.8 Hz, 1H), 1.53 – 1.48 (m, 2H), 0.96 (t, *J* = 7.4 Hz, 3H); ^{13}C NMR (125 MHz, $CDCl_3$) δ 200.9, 155.8, 154.7, 143.8, 136.7, 135.7, 133.4, 131.0, 130.9, 129.9, 129.0, 128.1, 128.0, 123.9, 123.8, 123.1, 122.8, 122.5, 119.6, 46.2, 37.1, 35.5, 28.5, 11.2; IR (KBr)ν_{max}: 3400 (bs), 1686 cm^{-1}; HRMS (ESI) Calcd for $C_{25}H_{21}ClNO_2$ 402.1255 (M + H$^+$); Found 402.1256.

6-(5-Bromo-2-hydroxyphenyl)-8-methyl-8,9-dihydrobenzo[*c*]phenanthridin-10(7*H*)-one (10x)

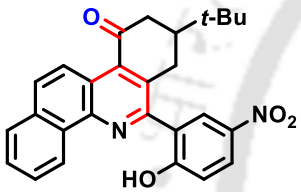

Yellow solid (297 mg, 69%); mp 266 °C; ^{1}H NMR (500 MHz, $CDCl_3$) δ 11.69 (s, 1H), 9.00 (t, *J* = 9.8 Hz, 2H), 7.95 (t, *J* = 8.5 Hz, 2H), 7.76 – 7.74 (m, 2H), 7.67 (d, *J* = 2.1 Hz, 1H), 7.50 (dd, *J* = 8.7, 2.1 Hz, 1H), 7.11 (d, *J* = 8.7 Hz, 1H), 3.29 (d, *J* = 16.2 Hz, 1H), 3.01 – 2.96 (m, 2H), 2.56 (dd, *J* = 17.7, 12.3 Hz, 1H), 2.27 – 2.21 (m, 1H), 1.20 (d, *J* = 6.5 Hz, 3H); ^{13}C NMR (125 MHz, $CDCl_3$) δ 200.8, 156.3, 154.6, 143.9, 136.6, 135.7, 133.9, 133.4, 132.8, 131.0, 130.0, 129.1, 128.1, 128.0, 123.8, 123.7, 122.8, 122.5, 120.0, 110.9, 48.4, 37.5, 30.7, 21.2; IR (KBr)ν_{max}: 3385 (bs), 1687 cm^{-1}; HRMS (ESI) Calcd for $C_{24}H_{19}BrNO_2$ 432.0594 (M + H$^+$); Found 432.0591 and 434.0580.

8-(*tert*-Butyl)-6-(2-hydroxy-5-nitrophenyl)-8,9-dihydrobenzo[*c*]phenanthridin-10(7*H*)-one (10y)

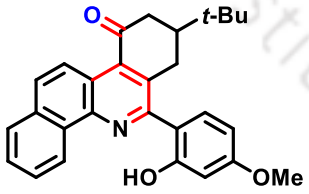

Yellow solid (299 mg, 68%); mp 284 °C; ^{1}H NMR (400 MHz, $CDCl_3$) δ 13.67 (s, 1H), 8.91 (t, *J* = 8.5 Hz, 2H), 8.64 (d, *J* = 2.6 Hz, 1H), 8.28 (dd, *J* = 9.1, 2.6 Hz, 1H), 7.96 – 7.93 (m, 2H), 7.82 – 7.75 (m, 2H), 7.24 (t, *J* = 9.1 Hz, 1H), 3.26 (dt, *J* = 15.9, 2.6 Hz, 1H), 3.00 – 2.90 (m, 2H), 2.53 – 2.45 (m, 1H), 1.81 – 1.74 (m, 1H), 0.95 (s, 9H); ^{13}C NMR (100 MHz, $CDCl_3$) δ 201.0, 163.9, 153.6, 143.1, 139.6, 136.5, 136.3, 133.4, 131.4, 129.4, 129.3, 128.3, 128.3, 126.8, 126.6, 123.5, 122.8, 122.7, 120.4, 118.8, 45.5, 42.3, 32.6, 31.3, 27.1; IR (KBr)ν_{max}: 3400 (bs), 1686 cm^{-1}; HRMS (ESI) Calcd for $C_{27}H_{25}N_2O_4$ 441.1809 (M + H$^+$); Found 441.1813.

8-(*tert*-Butyl)-6-(2-hydroxy-4-methoxyphenyl)-8,9-dihydrobenzo[*c*]phenanthridin-10(7*H*)-one (10z)

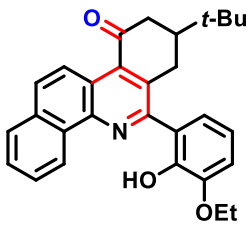

Yellow solid (259 mg, 61%); mp 256 °C; ^{1}H NMR (400 MHz, $CDCl_3$) δ 12.71 (s, 1H), 8.94 (dd, *J* = 6.4, 2.7 Hz, 1H), 8.89 (d, *J* = 9.3 Hz, 1H), 7.92 – 7.89 (m, 1H), 7.86 (d, *J* = 9.4 Hz, 1H), 7.73 – 7.70 (m, 2H), 7.46 (d, *J* = 8.8 Hz, 1H), 6.72 (d, *J* = 2.5 Hz, 1H), 6.58 (dd, *J* = 8.7, 2.5 Hz, 1H), 3.90 (s, 3H), 3.33 – 3.28 (m, 1H), 2.93 – 2.82 (m, 2H), 2.50 (dd, *J* = 17.5, 13.9 Hz, 1H), 1.80 – 1.72 (m, 1H), 0.96 (s, 9H); ^{13}C NMR (100 MHz, $CDCl_3$) δ 201.7, 162.0, 159.6, 156.3, 143.1, 136.3, 136.1, 133.4, 131.4, 129.9, 129.8, 128.7, 128.0, 127.7, 123.7, 122.8, 121.5, 114.6, 106.1, 102.5, 55.5, 45.6, 42.4, 32.5, 31.4, 27.2; IR (KBr)ν_{max}: 3350 (bs), 1687 cm^{-1}; HRMS (ESI) Calcd for $C_{28}H_{28}NO_3$ 426.2064 (M + H$^+$); Found 426.2063.

8-(*tert*-Butyl)-6-(3-ethoxy-2-hydroxyphenyl)-8,9-dihydrobenzo[*c*]phenanthridin-10(7*H*)-one (10aa)

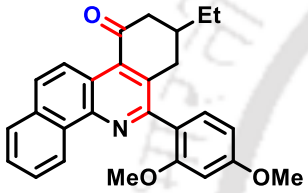

Yellow solid (272 mg, 62%); mp 228 °C; ^{1}H NMR (500 MHz, $CDCl_3$) δ 9.66 (s, 1H), 9.18 (d, *J* = 5.5 Hz, 1H), 9.02 (d, *J* = 9.3 Hz, 1H), 7.92 (t, *J* = 8.7 Hz, 2H), 7.69 (d,*J* = 4.5, 2H), 7.15 (d, *J* = 7.4 Hz, 1H), 7.03 – 6.97 (m, 2H), 4.24 (quin, *J* = 7.0 Hz, 2H), 3.24 (d, *J* = 16.1 Hz, 1H), 2.97 – 2.86 (m, 2H), 2.60 (t, *J* = 15.4 Hz, 1H), 1.89 (t, *J* = 12.7 Hz, 1H), 1.56 – 1.53 (m, 3H), 0.95 (s, 9H); ^{13}C NMR (100 MHz, $CDCl_3$) δ 202.2, 156.3, 147.6, 145.8, 144.3, 137.1, 135.1, 133.2, 130.6, 130.3, 128.5, 127.7, 127.4, 124.5, 124.2, 122.8, 122.6, 122.0, 119.1, 113.3, 64.8, 45.4, 42.7, 32.6, 30.4, 27.1, 15.1; IR (KBr)ν_{max}: 3350 (bs), 1682 cm^{-1}; HRMS (ESI) Calcd for $C_{29}H_{30}NO_3$ 440.2220 (M + H$^+$); Found 440.2222.

6-Phenyl-8,9-dihydrophenanthridin-10(7*H*)-one (11a)

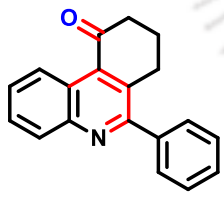

Green solid (150 mg, 55%); mp 155 °C; ^{1}H NMR (600 MHz, $CDCl_3$) δ 9.20 (d, *J* = 8.0 Hz, 1H), 8.15 (d, *J* = 8.3 Hz, 1H), 7.72 (t, *J* = 6.9 Hz, 1H), 7.67 (t, *J* = 7.7 Hz, 1H), 7.59 (d, *J* = 6.9 Hz, 1H), 7.52 (t, *J* = 7.3 Hz, 2H), 7.48 (t, *J* = 7.3 Hz, 1H), 6.82 (d, *J* = 7.8 Hz, 1H), 3.01 (t, *J* = 6.0 Hz, 2H), 2.85 (t, *J* = 6 Hz, 2H), 2.13 (quin, *J* = 6.4 Hz, 2H); ^{13}C NMR (150 MHz, $CDCl_3$) δ 201.0, 160.5, 147.4, 140.1, 136.7, 133.8, 130.0, 129.2, 129.0, 129.0, 128.8, 128.6, 126.1, 115.4, 40.6, 31.1, 23.0; IR (KBr)ν_{max}: 1686 cm^{-1}; HRMS (ESI) Calcd for $C_{19}H_{16}NO$ 274.1226 (M + H$^+$); Found 274.1232.

8-(*tert*-Butyl)-6-(4-methoxyphenyl)-8,9-dihydrophenanthridin-10(7*H*)-one (11b)

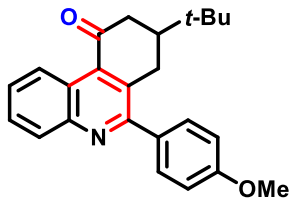

Green solid (215 mg, 60%); mp 160 °C; ^{1}H NMR (500 MHz, $CDCl_3$) δ 9.18 (d, *J* = 8.5 Hz, 1H), 8.13 (d, *J* = 8.3 Hz, 1H), 7.69 (t, *J* = 7.4 Hz, 1H), 7.63 (t, *J* = 7.1 Hz, 1H), 7.55 (d, *J* = 8.5 Hz, 2H), 7.05 (d, *J* = 8.6 Hz, 2H), 3.90 (s, 3H), 3.09 (dt, *J* = 16.8, 2.7 Hz, 1H), 2.91 (dt, *J* = 16.2, 2.8 Hz, 1H), 2.78 – 2.72 (m, 1H), 2.54 (dd, *J* = 16.1, 14.2 Hz, 1H), 1.95 – 1.88 (m, 1H), 0.93 (s, 9H).^{13}C NMR (100 MHz, $CDCl_3$) δ 202.1, 160.4, 160.1, 147.4, 136.7, 133.5, 132.7, 130.4, 129.9, 129.1, 128.7, 125.9, 123.2, 114.0, 55.5, 45.5, 42.7, 32.6, 30.9, 27.1; IR (KBr)ν_{max}: 1686 cm^{-1}; HRMS (ESI) Calcd for $C_{24}H_{26}NO_2$ 360.1958 (M + H$^+$); Found. 360.1958.

6-(2-Bromophenyl)-2-methoxy-8,9-dihydrophenanthridin-10(7*H*)-one (11c)

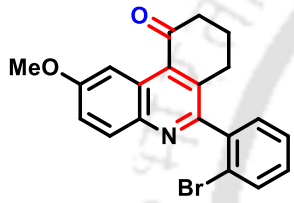

Brown gummy compound (229 mg, 60%); ^{1}H NMR (500 MHz, $CDCl_3$) δ 8.79 (s, 1H), 8.04 – 8.01 (m, 1H), 7.70 (d, J = 7.8 Hz, 1H), 7.48 – 7.45 (m, 1H), 7.40 – 7.37 (m, 2H), 7.34 – 7.32 (m, 1H), 4.00 (s, 3H), 2.95 – 2.90 (m, 1H), 2.84 – 2.81 (m, 2H), 2.70 – 2.67 (m, 1H), 2.18 – 2.13 (m, 2H).^{13}C NMR (125 MHz, $CDCl_3$) δ 201.2, 160.6, 157.0, 143.7, 141.3, 137.4, 132.9, 131.8, 131.4, 130.4, 130.1, 128.0, 125.5, 122.9, 121.9, 104.2, 55.8, 40.9, 27.8, 22.8. IR (KBr)ν_{max}: 1686 cm^{-1}; HRMS (ESI) Calcd for $C_{20}H_{17}BrNO_2$ 382.0437 (M + H$^+$); Found. 382.0415 and 384.0397.

6-(2-Bromophenyl)-8-(*tert*-butyl)-2-methoxy-8,9-dihydrophenanthridin-10(7H)-one (11d)

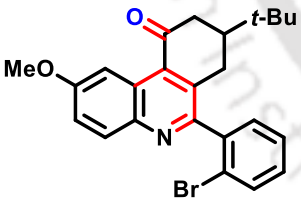

Brown semisolid (235 mg, 54%); ^{1}H NMR (600 MHz, $CDCl_3$) δ 8.77 (t, *J* = 2.8 Hz, 1H), 8.03 (dd, *J* = 9.1, 2.0 Hz, 1H), 7.71 (d, *J* = 8.1 Hz, 1H), 7.50 – 7.46 (m, 1H), 7.42 – 7.36 (m, 2H), 7.36 – 7.32 (m, 1H), 4.01 (s, 3H), 2.93 – 2.87 (m, 1H), 2.84 – 2.72 (m, 1H), 2.58 – 2.47 (m, 1H), 2.36 (dd, *J* = 16.5, 12.1 Hz, 1H), 2.08 (ddd, *J* = 18.8, 7.0, 3.5 Hz, 1H), 0.91 (s, 9H).^{13}C NMR (150 MHz, $CDCl_3$) δ 202.4, 160.6, 157.1, 143.7, 141.1, 137.6, 133.0, 132.7, 131.4, 130.6, 130.1, 128.1, 125.3, 122.7, 121.9, 104.0, 55.8, 45.5, 44.9, 42.9, 32.6, 27.0.IR (KBr)ν_{max}: 1686 cm^{-1}; HRMS (ESI) Calcd for$C_{24}H_{24}BrNO_2$ 438.1064 (M + H$^+$); Found. 438.1068 and 440.1051.

8-Ethyl-6-phenylbenzo[*c*]phenanthridin-10-ol (12i)

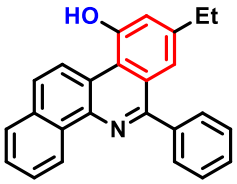

White solid (56 mg, 64%); mp 180 °C; ^{1}H NMR (500 MHz, $CDCl_3$) δ 9.54 (d, *J* = 9.3 Hz, 1H), 9.48 (d, *J* = 7.7 Hz, 1H), 7.99 (d, *J* = 9.3 Hz, 1H), 7.96 (d, *J* = 7.3 Hz, 1H), 7.88 (d, *J* = 7.8 Hz, 2H), 7.70 – 7.69 (m, 2H), 7.66 (dd, *J*= 7.1, 5.7 Hz, 1H), 7.59 (t, *J* = 6.4 Hz, 2H), 7.55 (td, *J* = 5.2, 4.5, 2.4 Hz, 1H), 7.07 (s, 1H), 5.97 (s, 1H), 2.76 (d, *J* = 7.6 Hz, 2H), 1.26 (s, 3H).^{13}C NMR (125 MHz, $CDCl_3$) δ 159.1, 154.0, 143.4, 141.2, 140.8, 132.9, 132.1, 130.5, 128.6, 128.3, 128.1, 127.2, 127.1, 127.0, 126.3, 125.4, 125.3, 121.9, 120.8, 120.1, 116.6, 28.9, 15.5. IR (KBr)ν_{max}: 3400 cm^{-1}; HRMS (ESI) Calcd for $C_{25}H_{20}NO$ 350.1539 (M + H$^+$); Found 350.1541.

8-Ethyl-6-(4-methoxyphenyl)benzo[*c*]phenanthridin-10-ol (12j)

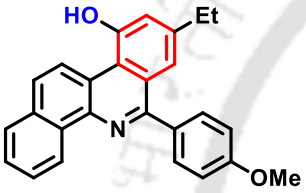

White solid (62 mg, 65%); mp 195 °C; ^{1}H NMR (500 MHz, DMSO-d_6) δ 11.03 (s, 1H), 9.69 (d, *J* = 9.2 Hz, 1H), 9.28 (d, *J* = 7.5 Hz, 1H), 8.05 (d, *J* = 7.4 Hz, 2H), 7.78 – 7.76 (m, 2H), 7.70 – 7.69 (m, 2H), 7.55 (s, 1H), 7.31 (s, 1H), 7.17 (t, *J* = 6.7 Hz, 2H), 3.90 (s, 3H), 2.74 – 2.71 (m, 2H), 1.24 – 1.20 (m, 3H);^{13}C NMR (125 MHz, DMSO-d_6) δ 159.6, 158.5, 156.1, 143.6, 139.3, 132.8, 132.1, 131.3, 131.1, 127.2, 127.0, 126.3, 125.2, 124.4, 120.9, 120.5, 117.4, 116.2, 113.7, 55.3, 28.3, 15.2.IR (KBr)ν_{max}: 3400 cm^{-1}; HRMS (ESI) Calcd for $C_{26}H_{22}NO_2$ 380.1645 (M + H$^+$); Found 380.1635.

6-(2-Hydroxyphenyl)benzo[*c*]phenanthridin-10-ol (12q)

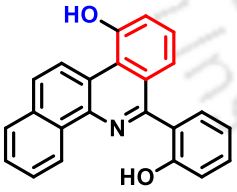

White solid (57 mg, 68%); mp 205 °C; ^{1}H NMR (500 MHz, DMSO-d_6) δ 11.02 (s, 1H), 9.74 (d, *J* = 9.3 Hz, 1H), 9.56 (s, 1H), 9.24 – 9.21 (m, 1H), 8.10 (d, *J* = 10.0 Hz, 1H), 8.08 – 8.06 (m, 1H), 7.72 – 7.68 (m, 2H), 7.53 (d, *J* = 7.9 Hz, 1H), 7.40 (d, *J* = 3.3 Hz, 2H), 7.36 (d, *J* = 8.2 Hz, 1H), 7.05 (d, *J* = 3.8 Hz, 1H), 7.02 (d, *J* = 7.6 Hz, 1H), 6.63 (s, 1H).^{13}C NMR (150 MHz, DMSO-d_6) δ 158.6, 155.8, 155.1, 139.8, 132.2, 131.1, 130.9, 129.7, 128.0, 127.8, 127.7, 127.2, 127.1, 126.4, 126.3, 125.3, 124.5, 121.9, 121.0, 119.6, 119.1, 115.9, 115.7; IR (KBr)ν_{max}: 3400 cm^{-1}; HRMS (ESI) Calcd for $C_{23}H_{16}NO_2$ 338.1176 (M + H$^+$); Found 338.1177.

8-(*tert*-Butyl)-6-(2-hydroxyphenyl)benzo[*c*]phenanthridin-10-ol (12t)

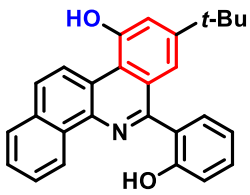

White solid (67 mg, 68%); mp 235 °C; ^{1}H NMR (500 MHz, $CDCl_3$) δ 9.52 (d, *J* = 9.1 Hz, 1H), 9.15 (d, *J* = 7.1 Hz, 5H), 8.18 (s, 1H), 7.96 – 7.94 (m, 2H), 7.79 (d, *J* = 7.3 Hz, 1H), 7.69 (dt, *J* = 23.9, 6.4 Hz, 2H), 7.45 (t, *J* = 7.2 Hz, 1H), 7.31 (s, 2H), 7.06 (t, *J* = 7.1 Hz, 1H), 1.36 (s, 9H); ^{13}C NMR (125 MHz, $CDCl_3$) δ 157.6, 157.5, 154.0, 150.7, 138.4, 133.0, 132.0, 131.0, 130.5, 127.7, 127.5, 127.4, 127.1, 125.3, 124.0, 122.6, 122.4, 121.1, 118.9, 118.1, 117.7, 115.4, 35.09, 31.2; IR (KBr)ν_{max}: 3400 cm^{-1}; HRMS (ESI) Calcd for $C_{27}H_{24}NO_2$ 394.1802 (M + H$^+$); Found 394.1797.

6-(5-Chloro-2-hydroxyphenyl)-8-methylbenzo[*c*]phenanthridin -10-ol (12u)

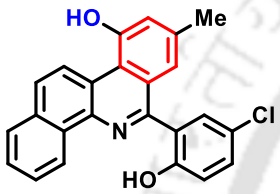

White solid (63 mg, 65%); mp 220 °C; ^{1}H NMR (500 MHz, DMSO-d_6) δ 10.96 (s, 1H), 9.82 (s, 1H), 9.69 (d, *J* = 9.3 Hz, 1H), 9.19 (dd, *J* = 6.1, 3.4 Hz, 1H), 8.08 (d, *J* = 9.4 Hz, 1H), 8.05 (dd, *J* = 6.1, 3.1 Hz, 1H), 7.69 (dd, *J* = 6.2, 3.2 Hz, 2H), 7.43 (dd, *J* = 8.6, 2.6 Hz, 1H), 7.41 (d, *J* = 2.6 Hz, 1H), 7.24 (s, 1H), 7.12 (s, 1H), 7.06 (d, *J* = 8.6 Hz, 1H), 2.40 (s, 3H); ^{13}C NMR (125 MHz, DMSO-d_6) δ 156.6, 155.7, 154.1, 139.3, 137.4, 132.0, 131.0, 130.1, 129.8, 129.3, 127.9, 127.2, 126.9, 126.6, 126.3, 125.1, 124.4, 122.5, 121.2, 120.1, 118.6, 117.4, 21.3; IR (KBr)ν_{max}: 3400 cm^{-1}; HRMS (ESI) Calcd for $C_{24}H_{17}ClNO_2$ 386.0942 (M + H$^+$); Found 386.0940.

6-(5-Chloro-2-hydroxyphenyl)-8-ethylbenzo[*c*]phenanthridin-10-ol (12v)

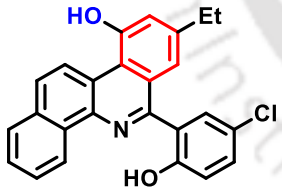

White solid (67 mg, 67%); mp 260 °C; ^{1}H NMR (500 MHz, DMSO-d_6) δ 10.04 (s, 1H), 9.66 (d, *J* = 9.3 Hz, 1H), 9.15 (d, *J* = 8.2 Hz, 1H), 8.07 – 8.02 (m, 2H), 7.68 – 7.67 (m, 2H), 7.41 (dd, *J* = 8.6, 2.4 Hz, 1H), 7.38 (d, *J* = 2.3 Hz, 1H), 7.26 (s, 1H), 7.12 (s, 1H), 7.04 (d, *J* = 8.7 Hz, 1H), 2.65 (q, *J* = 7.5 Hz, 2H), 1.16 (t, *J* = 7.5 Hz, 3H); ^{13}C NMR (125 MHz, DMSO-d_6) δ 157.2, 156.2, 154.5, 144.2, 139.8, 132.5, 131.4, 130.6, 130.2, 129.9, 128.3, 127.8, 127.6, 127.2, 127.0, 125.5, 124.7, 123.2, 121.6, 120.8, 118.0, 117.9, 116.8, 28.7, 15.7; IR (KBr)ν_{max}: 3400 cm^{-1}; HRMS (ESI) Calcd for $C_{25}H_{19}ClNO_2$ 400.1099 (M + H$^+$); Found 400.1108.

8-(*tert*-Butyl)-6-(4-methoxyphenyl)phenanthridin-10-ol (13b)

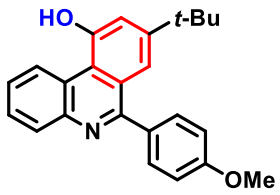

White solid (67 mg, 75%); mp 165 °C; ^{1}H NMR (500 MHz, DMSO-d_6) δ 10.94 (s, 1H), 9.55 (d, J = 8.3 Hz, 1H), 8.02 (d, J = 8.0 Hz, 1H), 7.70 (d, J = 7.0 Hz, 1H), 7.63 (s, 2H), 7.61 (d, J = 6.6 Hz, 2H), 7.49 (s, 1H), 7.12 (d, J = 8.6 Hz, 2H), 3.86 (s, 3H), 1.28 (s, 9H); ^{13}C NMR (125 MHz, DMSO-d_6) δ 160.3, 159.6, 155.9, 150.4, 143.4, 132.4, 131.1, 129.2, 127.6, 127.4, 126.7, 126.5, 123.3, 119.6, 115.4, 114.6, 113.6, 55.3, 34.6, 31.0; IR (KBr)ν_{max}: 3400 cm^{-1}; HRMS (ESI) Calcd for $C_{24}H_{24}NO_2$ 358.1802 (M + H$^+$); Found 358.1820.

6-(2-Bromophenyl)-8-(*tert*-butyl)-2-methoxyphenanthridin-10-ol (13d)

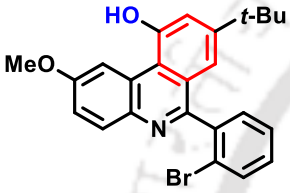

White solid (76 mg, 70%); mp 176 °C; ^{1}H NMR (500 MHz, DMSO-d_6) δ 10.93 (s, 1H), 9.11 (d, J = 2.8 Hz, 1H), 7.97 (d, J = 8.9 Hz, 1H), 7.82 (d, J = 7.9 Hz, 1H), 7.50 – 7.57 (m, 1H), 7.53 – 7.51 (m, 1H), 7.48 (d, J = 7.6 Hz, 1H), 7.43 (d, J = 1.5 Hz, 1H), 7.39 – 7.37 (m, 1H), 7.00 (d, J = 1.5 Hz, 1H), 3.95 (s, 3H), 1.21 (s, 9H); ^{13}C NMR (126 MHz, DMSO-d_6) δ 157.7, 157.6, 155.8, 150.6, 140.7, 138.2, 132.3, 131.2, 130.5, 130.2, 127.7, 126.7, 124.8, 122.3, 118.7, 116.5, 114.5, 114.0, 109.1, 55.3, 34.3, 30.7; IR (KBr)ν_{max}: 3400 cm^{-1} (bs); HRMS (ESI) Calcd for $C_{24}H_{23}BrNO_2$ 436.0907 (M + H$^+$); Found. 436.0911 and 438.0895.

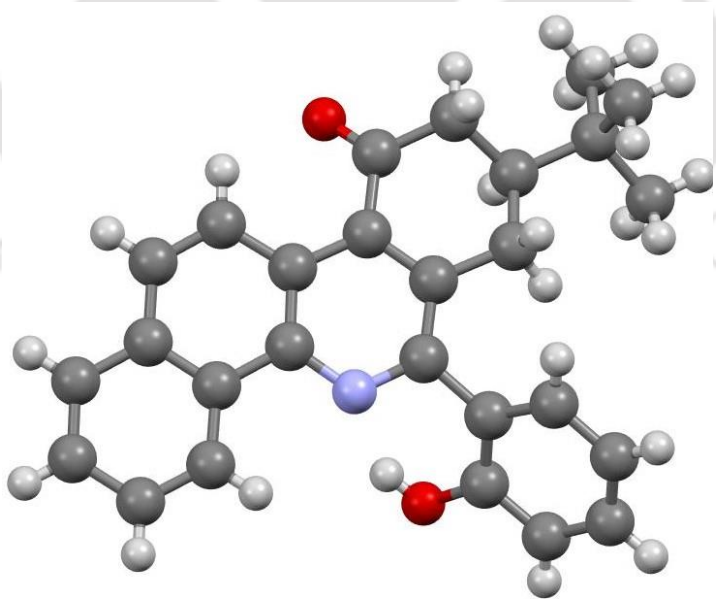

Figure 4.10. ORTEP Diagrams of compound 8-(*tert*-Butyl)-6-(2-hydroxyphenyl)-8,9-dihydrobenzo[*c*]phenanthridin-10(7*H*)-one **(10t)**.

Table 4.6. Crystal data and structure refinement for compound 8-(*tert*-Butyl)-6-(2-hydroxyphenyl)-8,9-dihydrobenzo[*c*]phenanthridin-10(7*H*)-one **(10t)**.

Entry	Identification Code	Compound 10t
01	Empirical formula	$C_{27}H_{25}NO_2$
02	Formula weight	395.48
03	Temperature	296 K
04	Wavelength	0.71073
05	Radiation type	Mo K\a
06	Radiation system	Fine-focus sealed tube
07	Crystal system	Monoclinic
08	Space group	P 21/c
09	Cell length	a 16.672(6) b 11.449(4) c 11.109(4)
10	Cell angle	α 90 β94.864(10) γ 90
11	Cell volume	2112.7(12)
12	Density	1.243
13	Completeness to theta	99.7
14	Absorption correction	multi-scan
15	Refinement method	Full-matrix least-squares on F2
16	Index ranges	-19<=h<=19, -13<=k<=13, -13<=l<=13
17	Reflection number	3640
18	Theta range	24.829
19	Cell formula units Z	4
20	CCDC no	2060048

4.3d Representative Characterization Spectra

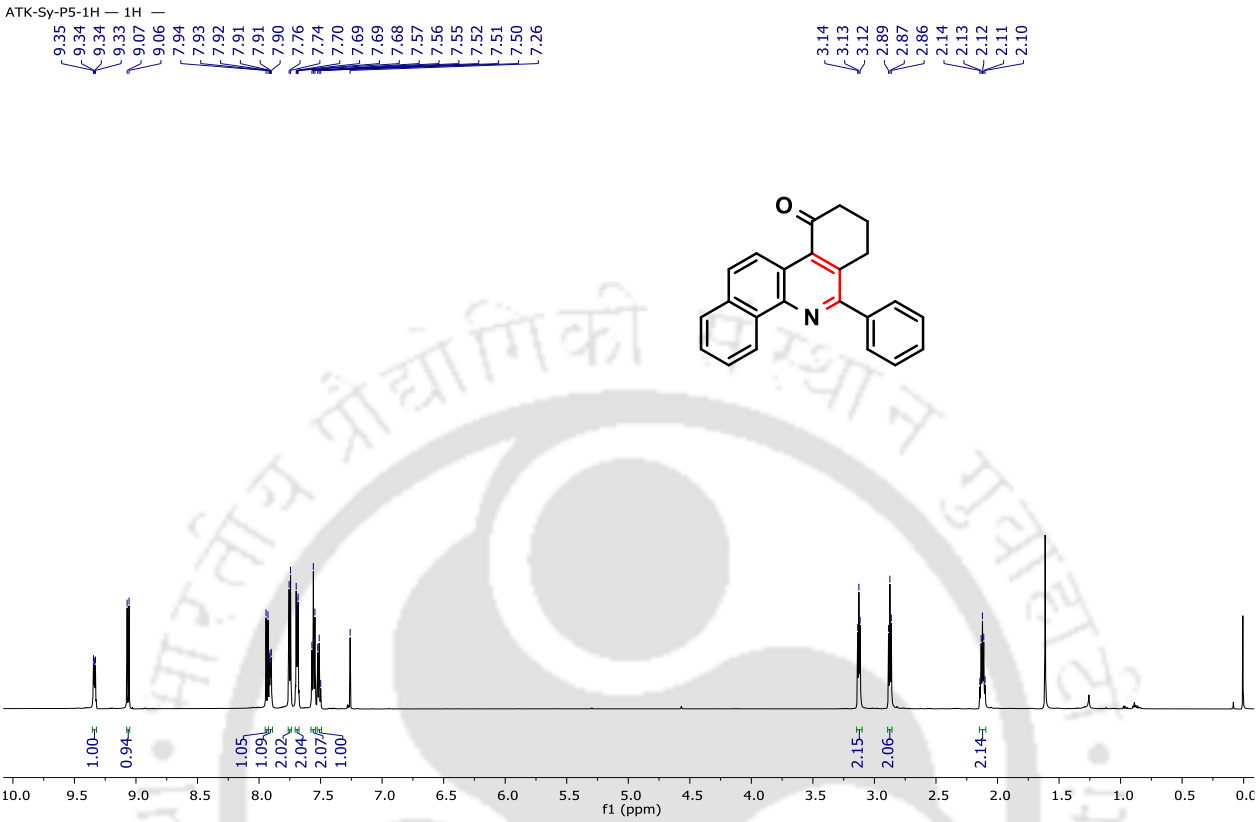

Figure 4.11. ^{1}H NMR Spectrum of 6-Phenyl-8,9-dihydrobenzo[*c*]phenanthridin-10(7*H*)-one (**10a**).

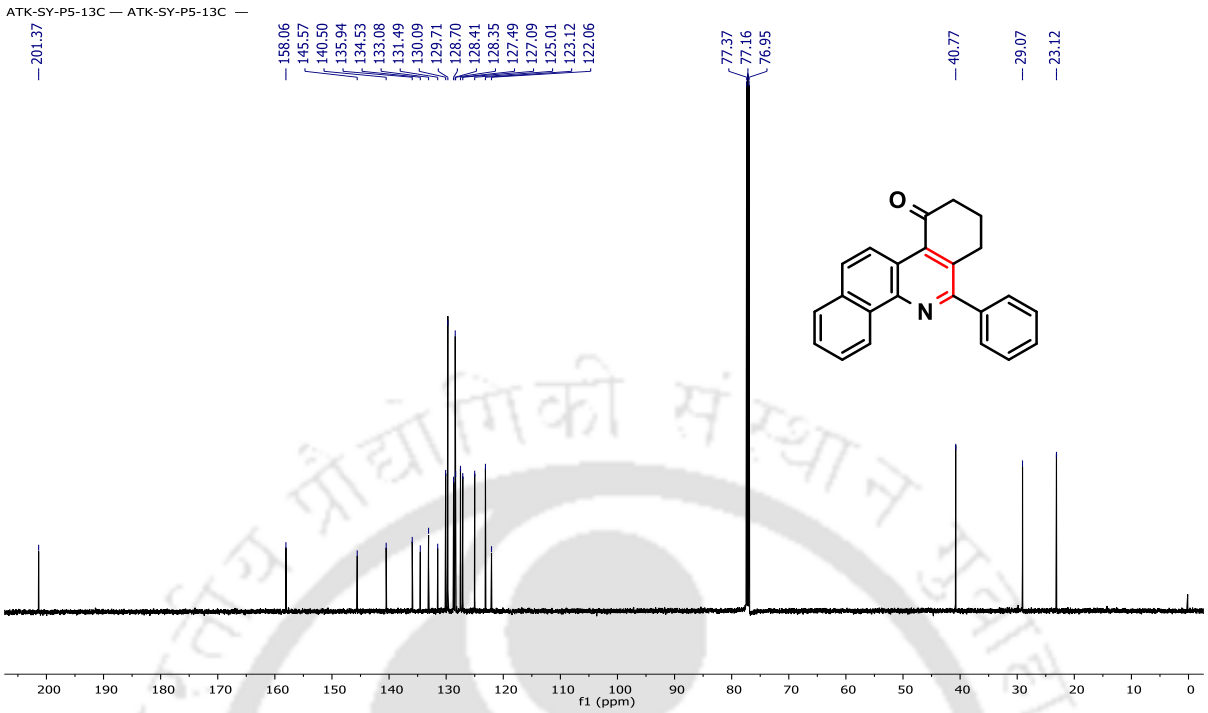

Figure 4.12. ^{13}C NMR Spectrum of 6-Phenyl-8,9-dihydrobenzo[*c*]phenanthridin-10(7*H*)-one (**10a**).

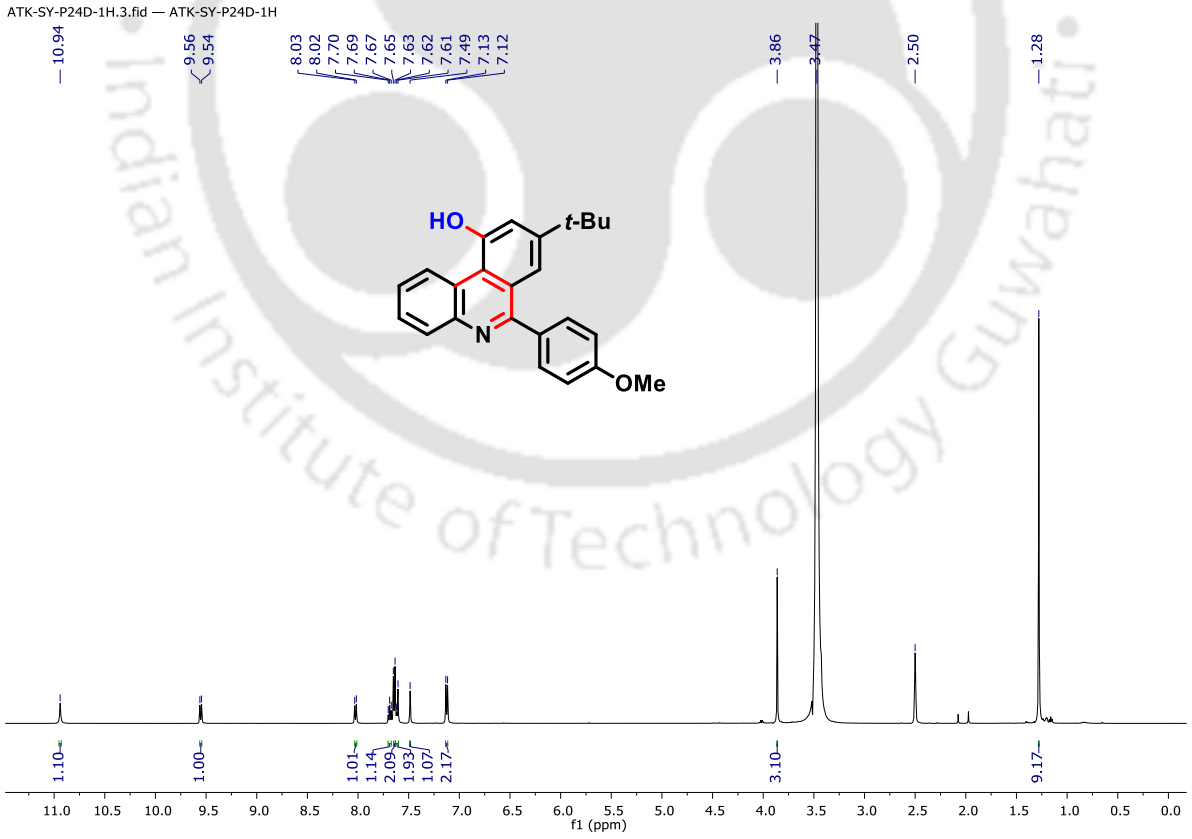

Figure 4.13. ^{1}H NMR Spectrum of of 8-(*tert*-butyl)-6-(4-methoxyphenyl)phenanthridin-10-ol (**13b**).

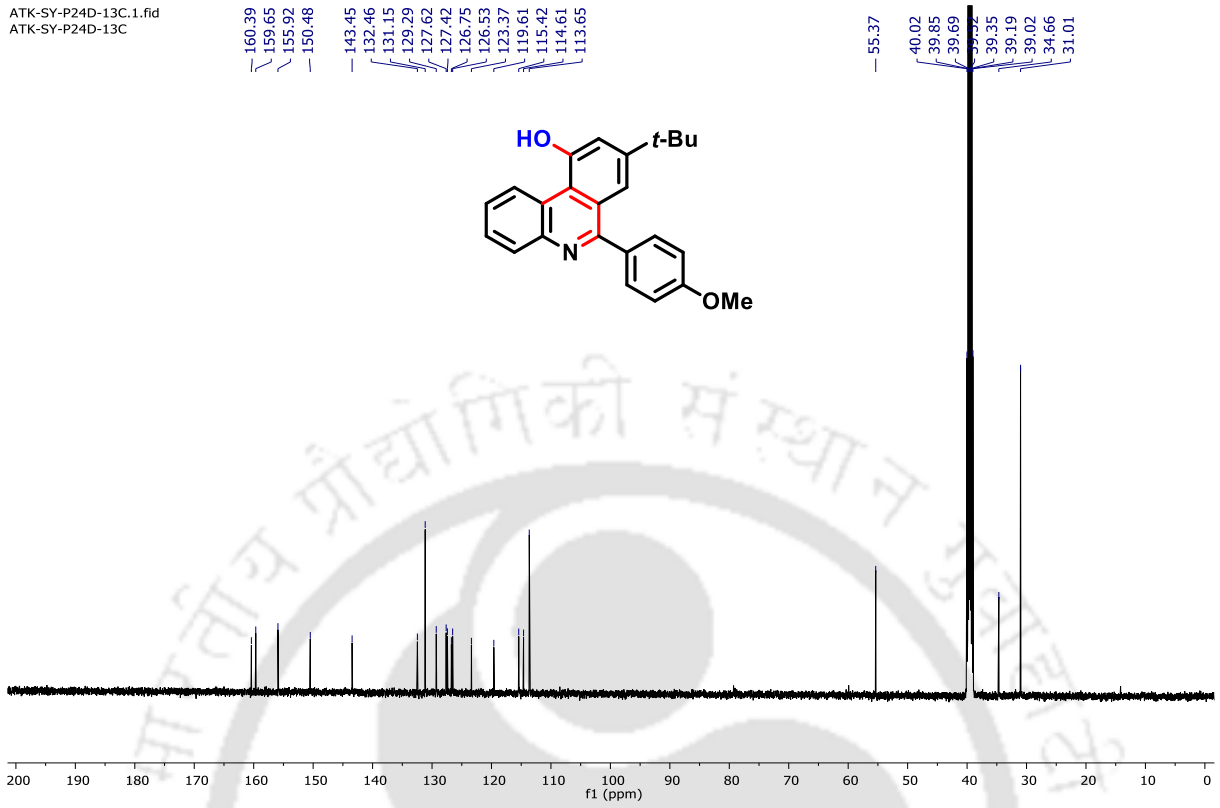

Figure 4.14. ^{13}C NMR Spectrum of 8-(*tert*-butyl)-6-(4-methoxyphenyl)phenanthridin-10-ol (**13b**).

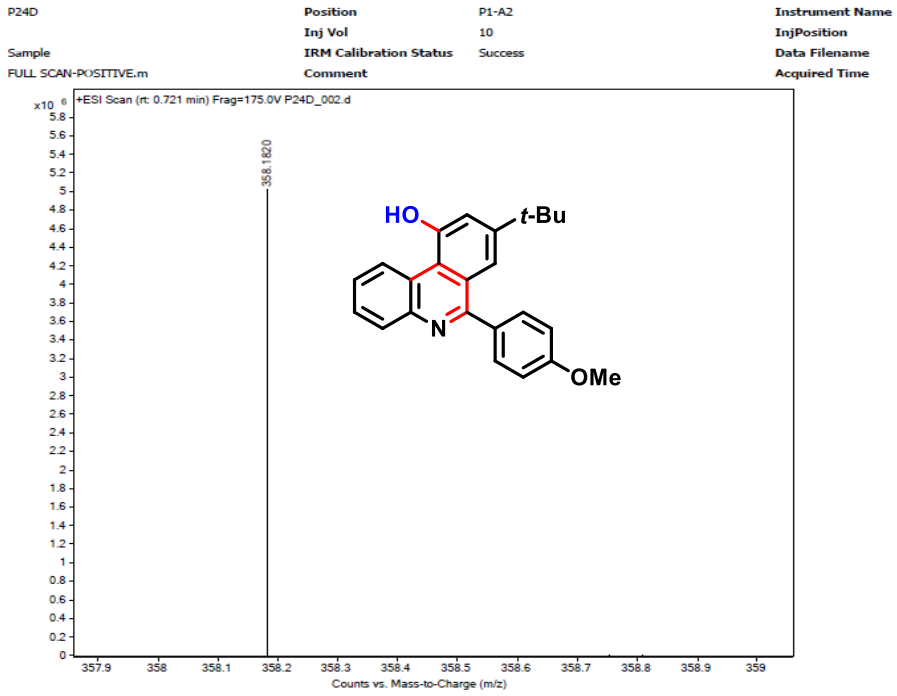

Figure 4.15. HRMS NMR Spectrum of 8-(*tert*-butyl)-6-(4-methoxyphenyl)phenanthridin-10-ol (**13b**).

4.4 References

1. A. Saytzeff, *Ann. Chem. Pharm.*, 1867, **144**, 148–156.

2. (a) I. Soroko, Y. Bhole and A. G. Livingston, *Green Chem.*, 2011, **13**, 162–168; (b) H. Tavallali, G. D. Rad, A. Parhami and E. Abbasiyan, *Spectrochim. Acta Part A*, 2012, **97**, 60–65.

3. **Review articles**: (a) Z. Tashrifi, M. M. Khanaposhtani, B. Larijani and M. Mahdavi, *Adv Synth Catal*, 2020, **362**, 65–86. (b) X. Li, X. Wang, Y. Li, J. Xiao and Y. Du, *Org. Biomol. Chem.*, 2022, **20**, 4471–4495; (c) X. Wu and K. Natte, *Adv Synth Catal*, 2016, **358**, 336–352; (d) E. Jones-Mensah, M. Karki and J. Magolan, *Synthesis*, 2016, **48**, 1421–1436.

4. (a) B. Yao, R. J. Song, Y. Liu, Y. X. Xie, J. H. Li, M. K. Wang, R. Y. Tang, X. G. Zhang and C. L. Deng, *Adv. Synth. Catal.*, 2012, **354**, 1890–1896; (b) O. P. Patel, D. Anand, R. K. Maurya and P. P. Yadav, *J. Org. Chem.*, 2016, **81**, 7626–7634; (c) Y.-F. Liu, P.-Y. Ji, J.-W. Xu, Y.-Q. Hu, Q. Liu, W.-P. Luo and C.-C. Guo, *J. Org. Chem.* 2017, **82**, 7159–7164; (d) J. Yuan, J. Li, B. Wang, S. Sun and J. Cheng, *Tetrahedron Lett.*, 2017, **58**, 4783–4785.

5 (a) M. Lu, H. Qin, Z. Lin, M. Huang, W. Weng and S. Cai, *Org. Lett.*, 2018, **20**, 7611–7615; (b) T. Shen, X. Huang, Y.-F. Liang and N. Jiao, *Org. Lett.*, 2015, **17**, 6186–6189; (c) F. Luo, C. Pan, L. Li, F. Chen and J. Cheng, *Chem. Commun*., 2011, **47**, 5304–5306; (d) G. Yuan, J. Zheng, X. Gao, X. Li, L. Huang, H. Chen and H. Jiang, *Chem. Commun*., 2012, **48**, 7513–7515; (e) P. Zhao, X. Wu, X. Geng, C. Wang, Y. Zhou, Y.-D. Wu and A.-X. Wu, *J. Org. Chem*., 2019, **85**, 8322–8329.

6. (a) Y.-F. Liang, K. Wu, S. Song, X. Li, X. Huang and N. Jiao, *Org. Lett.*, 2015, **17**, 876–879; (b) Z. Cao, H. Lv, Y. Liu, Z. Nie, H. Liu, T. Yang, W. Luo, Q. Liu and C. Guo, *Adv. Synth. Catal*., 2019, **361**, 1632–1640; (c) X. Zhang, S.-S. Li, L. Wang, L. Xu, J. Xiao and Z.-J. Liu, *Tetrahedron*, 2016, **72**, 8073–8077.

7. (a) K. Omura and D. Swern, *Tetrahedron*, 1978, **34**, 1651–1660; (b) N. Kornblum, W. J. Jones and G. J. Anderson, *J. Am. Chem. Soc.*, 1959, **81**, 4113–4114; (c) Y. Ashikari, T. Nokami and J.-I. Yoshida, J. *Am. Chem. Soc.*, 2011, **133**, 11840–11843.

8. R. Chebolu, A. Bahuguna, R. Sharma, V. K. Mishra and P. C. Ravikumar, *Chem. Commun.*, 2015, **51**, 15438–15441.

9. **Review article:** P. N. Reddy, B. V. S. Reddy and P. Padmaja, *Curr. Org. Synth.*, 2018, **15**, 815–838.

10. (a) M. S. Yusubov, V. D. Filimonov, V. P. Vasilyeva and K. Chi, *Synthesis*, 1995, **10**, 1234–1236; (b) M. V. Kadu, *Orient. J. Chem*., 2010, **26**, 1109–1112.

11. (a) P.D. Lokhande, K. Hasanzadeh, H. Khaledi and H. M. Ali, *J. Heterocyclic Chem*., 2012, **49**, 1398–1406; (b) V. Humne, Y. Dangat, K. Vanka and P. Lokhande, *Org. Biomol. Chem*., 2014, **12**, 4832–4836.

13. (a) M. Wenzel, J. R. Hiscock and P. A. Gale, *Chem. Soc. Rev*., 2012, **41**, 480–520; (b) R. Martinez-Manez and F. Sancenon, *Chem. Rev*., 2003, **103**, 4419–4476.

14. C.R. Wade, A.E.J. Broomsgrove, S. Aldridge and F. P. Gabbai, *Chem. Rev*., 2010, **110**, 3958–3984.

15. R. Waddington and M. Langley, *Tissue Res*., 2003, **44**, 88–95.

16. Y. Yu, W. Yang, Z. Dong, C. Wan, J. Zhang, J. Liu, K. Xiao, Y. Huang and B. Lu, *Fluoride*, 2008, **41**, 134–138.

17. S. Saha, A. Ghosh, P. Mahato, S. Mishra, S. K. Mishra, E. Suresh, S. Das and A. Das, *Org. Lett*., 2010, **12**, 3406–3409.

18. (a) Y.-P. Hang and J.-M. Liu, *J. Anal. Chem*., 2007, **62**, 583–587; (b) A.M. Bond and T.A. O'Donnell, *Anal. Chem*., 1968, **40**, 560–563; (c) R. Das, S. Bej, N.C. Murmu and P. Banerjee, *Anal. Chim. Acta*, 2022, **1202**, 339597.

19. S. Mondal, K. Mahato, N. Arora, D. Kankane, U. P. Singh, S. Ali, A. H. Khan, S. S. Ghosh and A. T. Khan, *Org. Biomol. Chem.*, 2020, **18**, 4104–4113.

20. (a) S. Yashmin, R. Ali, S. Mondal and A. T. Khan, *Chem. Commun.*, 2022, **58**, 5853–5856; (b) S. Yashmin, A. T. Khan, S. J. Akula, R. P and K. Bhattacharyya, *J. Org. Chem.*, 2023, **88**, 13622–13633; (c) R. Gattu, P. R. Bagdi, R. S. Basha and A. T. Khan, *J. Org. Chem.*, 2017, **82**, 12416–12429.

21. (a) R. Bharti and T. Parvin, *J. Heterocycl. Chem*., 2015, **52**, 1806–1811; (b) D. Kumbhara, R. Patila, D. Patil, A. Patravale, D. Chandam, S. Jadhava and M. Deshmukh, *Synth. Commun*., 2016, **46**, 85–92.

22. L.-W. Xu, C.-G. Xia and L. Li, *J. Org. Chem*., 2004, **69**, 8482–8484.

23. Y. Liang, X. Li, X. Wang, M. Zou, C. Tang, Y. Liang, S. Song and N. Jiao, *J. Am. Chem. Soc*., 2016, **138**, 12271–12277.

24. A. Sarkar, S. Bhattacharyya and A. Mukherjee, *Dalton Trans.*, 2016, **45**, 1166–1175.

25. Y. Wu, X. Peng, J. Fan, S. Gao, M. Tian, J. Zhao and S. Sun, *J. Org. Chem*., 2007, **72**, 62–70.

26. T. D. Thangadurai, C. J. Lee, S. H. Jeong, S. Yoon, Y. G. Seo and Y.-I. Lee, *Microchem. J*., 2013, **106**, 27–33.

CHAPTER V

Utilization of DMSO as a solvent-cum-reactant: Synthesis of fused 2-aryl-4-methylquinolines

- Introduction
- Results and Discussion
- Experimental Section

5.1. Introduction

5.1a. Importance of Quinoline Derivatives

Quinoline is a pivotal structural component within naturally occurring and synthetic compounds. These compounds exhibit a diverse array of biological applications, significantly impacting the realm of organic synthesis. A brief overview of their extensive importance and synthetic methods is provided in **Chapter I, Section 1.5**. Inspired by the literature review, our research is driven by exploring a novel pathway for synthesizing fused quinoline derivatives. The insights gained from the literature survey discussed below have played a crucial role in shaping the content of **Chapter V** of this thesis.

5.1b. DMSO as a Carbon Source

DMSO serves primarily as a highly efficient reaction medium. In addition to this role, it has been extensively employed both as a solvent and a reactant, providing a source of carbon (C), sulfur (S), and oxygen (O) for synthesizing crucial heterocyclic compounds. The utilization of DMSO as a reactant is briefly discussed in **Chapter IV**. Moreover, **Chapter IV** also consists of the investigation of DMSO as an oxygen source in the synthesis of derivatives of 6-arylbenzo[*c*]phenanthridine-10-ol, as shown in **Scheme 5.1**.[1]

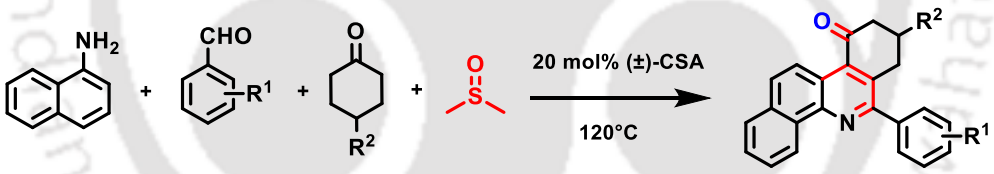

Scheme 5.1. The previously reported method utilizing DMSO as an oxygen source.

This section will focus on the utilization of DMSO as a carbon source, addressing its comprehensive role. Functioning as a carbon source, DMSO facilitates the transfer of various carbon moieties, including terminal methyl (-CH_3), bridged methylene (-CH_2-), terminal methylene (=CH_2), and methine (C=CH, N=CH, O=CH), in the synthesis of organic molecules. These aspects are thoroughly documented in numerous review articles.[2a-c]

Several studies indicate that DMSO functions as a singular methine (-CH) synthon in the synthesis of heterocycles which also includes substituted quinoline derivatives such as 3-ketoquinoline,[3a,b] 3,4-disubstituted quinoline,[3c] 4-arylquinoline,[3d,e] 2-arylquinoline.[3f] The synthesis of 3,4-disubstituted quinoline[3c] and 2-arylquinoline[3f] are depicted in **Scheme 5.2a** and **Scheme 5.2b** respectively.

Scheme 5.2a

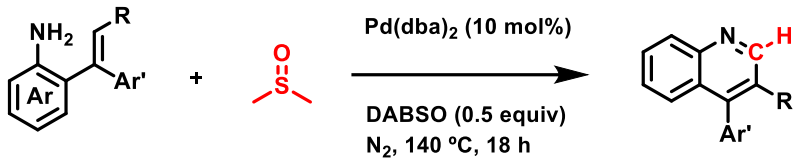

Scheme 5.2b

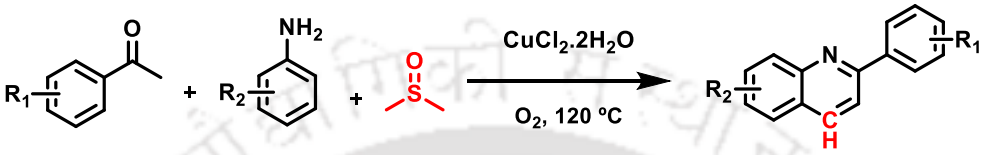

Scheme 5.2 DMSO as a single carbon synthon in the synthesis of quinolines.

Nevertheless, in the last five years, few reports are developed using DMSO as a dual carbon synthon in the field of organic synthesis, such as the construction of 5-methyl pyrimidine derivatives (=CH-, -CH_3),[4a] six-membered carbocycle (two -CH_2-),[4b] 1,3,5-oxadiazines (two -CH_2-),[4c] β-acyl allyl sulfones/β-acyl allyl benzotriazoles (=CH_2, -CH_2-),[4d] *N*-alkylated quinazolinones (=CH_2, -CH_2-).[4f]

Scheme 5.3a

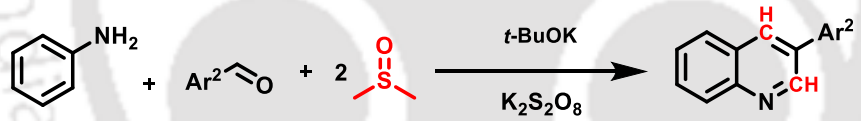

Scheme 5.3b

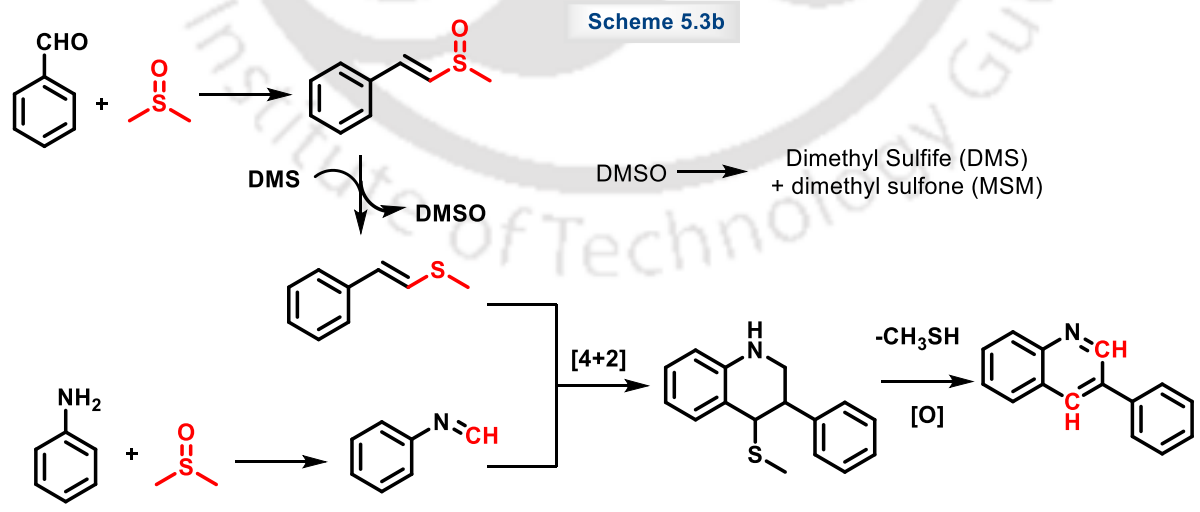

Scheme 5.3. Synthesis of 3-aryl quinoline using DMSO as a dual synthon.

Last year, Liu and Guo *et al*. also reported the synthesis of 3-aryl quinoline from aniline and aryl aldehyde using DMSO as a source of two methine groups in the presence of $K_2S_2O_8$ and base (**Scheme 5.3**).[4e] In all these cases, the transfer of carbon atoms is executed by the capture of sulfenium ion, which is generated *in situ* from the activation of DMSO in the presence of oxidants such as $K_2S_2O_8$ and selectfluor. The reaction mechanism for the formation of the product is given in **Scheme 5.3b**.

5.1c. Previously Reported Work from our Lab Group

In 2023, we disclosed the synthesis of 4-aryl quinoline from the reaction of arylamine and aryl acetylene using DMSO as a single methine synthon as well as a solvent in the presence of Bronsted acid *p*-toluenesulfonic acid monohydrate (*p*-TSA.H_2O). In **Scheme 5.4**, the sulfenium ion is generated *in-situ* induced by the *p*-TSA.H_2O and actively engages with the reactants to facilitate the transfer of a carbon atom during the reaction.[5]

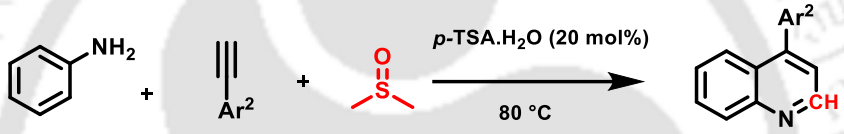

Scheme 5.4. DMSO is a single carbon synthon reported by our lab group.

This prompted us to dive deeper into exploring DMSO as a carbon synthon.

5.1d. Scope from the Literature Review

- Numerous studies have explored the use of DMSO as a sole carbon synthon, with only a few instances of its application as a dual carbon synthon reported. Notably, no documented case of DMSO being utilized as a triple carbon synthon to the best of our knowledge. This is a promising opportunity to leverage DMSO's potential as a triple carbon synthon.

- **Chapter I** highlights the prevalence of the quinoline skeleton in numerous polycyclic heteroaromatics. While the synthesis of substituted quinoline derivatives has been extensively investigated, there is comparatively less exploration in the realm of fused quinoline systems, such as substituted benzo[*h*]quinoline, benzo[*f*]quinoline, and naphtho[2,3-*f*]quinoline.

5.1e. Present Work

In this chapter, we report a pseudo-five component reaction for the synthesis of 4-methyl-2-arylbenzo[*h*]quinoline (**14a-j**) and 1-methyl-3-phenylbenzo[*f*]quinoline (**14k-r**), and 1-methyl-3-arylnaphtho[2,3-*f*]quinoline (**14s-x**) derivatives from the reaction of aryl aldehyde with 1-naphthylamine (**1a**), 2-naphthylamine (**1e**) and 2-aminoanthracene (**1f**) respectively in the presence of 30 mol% (±)-10-camphor sulfonic acid ((±)-CSA) as shown in **Scheme 5.5**. In addition, three 2-aryl-5,7-dimethoxy-4-methylquinoline derivatives (**15a-c**) are also synthesized from 3,5-dimethoxyaniline (**1g**) and aryl aldehyde. Interestingly, DMSO provides three carbon atoms, a -CH=C-CH_3 synthon, for constructing quinoline moiety.

The unique features of the reaction are: i) mild reaction condition, ii) oxidant-free activation of DMSO, and iii) as far as our knowledge goes, this is the first ever example where DMSO acts as a source of -CH=C-CH_3 atoms for the synthesis of organic compounds, iv) No activating agent is used to activate the DMSO.

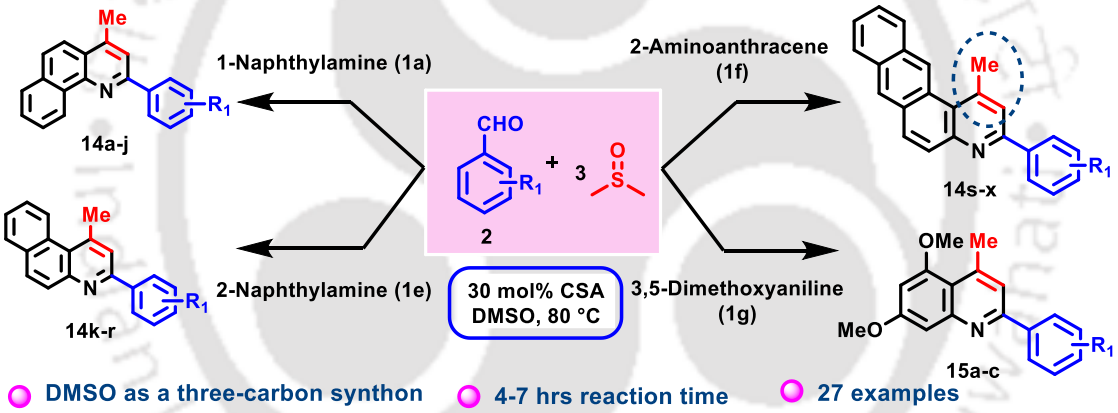

Scheme 5.5. Present work for the synthesis of 2,4-disubsituted fused quinolines using DMSO as a triple carbon synthon.

5.2. Results and Discussion

5.2a. Optimization of the Methodology

Intrigued by our previous works (**Scheme 5.1 & 5.4**) and literature, a reaction was tried with 1-naphthylamine (**1a**, 0.10 mmol) and benzaldehyde (**2b**, 0.10 mmol) in the presence of 10 mol% CSA at 80 ºC taking DMSO as a solvent. After 12 h, a different product was isolated and characterized from ^{1}H, ^{13}C, and HRMS spectra. Initially, the structure of the compound (**P$_x$**) was expected as imine product *N*-(naphthalene-2-yl)-1-phenylmethanimine (**P$_1$**, **Scheme 5.6**), which must have peaks of 12 aromatic protons in the ^{1}H NMR spectrum. It also includes one characteristic singlet for the methine proton of the imine group at 8.65 ppm. Whereas the isolated product **P$_x$** shows peaks for 11 protons in the aromatic region; in this case, a singlet peak at 8.65 ppm does not appear. This discarded the probability of being the compound **P$_x$** as imine (**P$_1$**). Another probability was the formation of 3-phenylbenzo[*h*]quinoline (**P$_2$**) if we conclude the incorporation of two carbons by the participation of two DMSO molecules according to the earlier reported literature (**Scheme 5.6**).[4e]

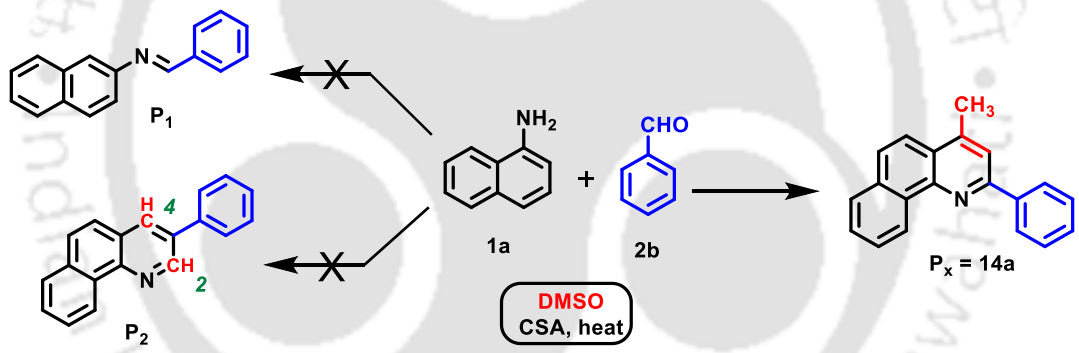

Scheme 5.6. Probabilities of the expected products from 1-naphthyl amine and benzaldehyde reaction.

Compound **P$_2$** has 13 aromatic protons with the two characteristic peaks at C2 and C4 positions, which appear at 9.28 (d, *J* = 2.3 Hz, 1H) and 8.34 (d, *J* = 2.3 Hz, 1H). Even so, the ^{1}H NMR pattern of the isolated product also does not match the compound **P$_2$**. Interestingly, apart from the 11 aromatic protons, the product **P$_x$** contains two characteristic singlets, such as one singlet at δ 7.86 ppm (1H) and another at δ 2.82 ppm (3H) from a CH_3 group in ^{1}H NMR spectra. In ^{13}C NMR spectra, it has one peak at 19.5 ppm, which might come from the aromatic CH_3 group. The meticulous literature shows that the NMR of the isolated compounds matches with 4-methyl-2-phenylbenzo[*h*]quinoline (**3a**).[6] The obtained HRMS of the predicted compound also matches with the calculated one. The obtained m/z value (ESI) is 270.1278, calculated for $C_{20}H_{16}N$ ($M + H^+$). Later on, the structure of the compound is also confirmed by XRD of another derivative (**14g**) mentioned below in the Results and Discussion section.

Table 5.1. Optimization of the Reaction Conditions[a,b]

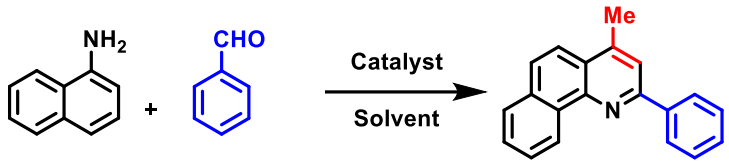

1a 2b 14a

Entry	Catalyst	Mol%	Solvent	Temp.	Time (h)	%Yield[b] (14a)
1	(±)-CSA	10	DMSO	rt	24	ND
2	(±)-CSA	10	DMSO	60 °C	12	20
3	(±)-CSA	10	DMSO	80 °C	12	40
4	(±)-CSA	10	DMSO	90 °C	12	42
5	(±)-CSA	20	DMSO	80 °C	8	55
6	**(±)-CSA**	**30**	**DMSO**	80 °C	**6**	**70**
7	(±)-CSA	40	DMSO	80 °C	6	72
8	No catalyst	-	DMSO	80 °C	24	-
9	*p*-TSA	30	DMSO	80 °C	12	60
10	TFA	30	DMSO	80 °C	12	20
11	Acetic acid	30	DMSO	80 °C	12	ND
12	(±)-CSA	30	DMF	80 °C	8	ND

[a]All reactions were carried out with 1-naphthylamine **1a** (14 mg, 0.10 mmol), benzaldehyde **2b** (11 mg, 0.10 mmol) in 1 mL of solvent at different temperatures mentioned above. [b]Yield of the isolated product. ND- No desired product.

However, the isolation of compound **14a** seems unusual as it contains an additional three carbons for constructing the quinoline skeleton. We suspect these three carbons are conferred by three molecules of DMSO, considering it a pseudo-five-component reaction.

After confirmation of the structure and assuming DMSO as a participant in the reaction, we tried to optimize the reaction conditions by taking 1-naphthylamine (**1a**, 0.10 mmol) and benzaldehyde (**2b**, 0.10 mmol) as a model substrate. The results are summarized in **Table 5.1**. Initially, a mixture of 1-naphthylamine and benzaldehyde was stirred at room temperature for 24 h in the presence of 10 mol% (±)-CSA in DMSO solvent, but no desired product was found (**Entry 1**). Then, a similar reaction was performed for 12 h at 60 °C; and compound **14a** was isolated in 20% yield (**Entry 2**). Then, the temperature was increased to 80 °C, and the yield of the desired product was also increased to 40% (**Entry 3**). Further, an

increase in temperature up to 90 °C of the reaction resulted in no effective change in the yield of product **14a** (**Entry 4**). Then, we tried to optimize the catalyst concentration. First, the amount of catalyst loading increased by 20%. After 8 h, the expected product, **14a** was achieved with a 55% yield (**Entry 5**). The amount of (±)-CSA was further increased up to 30 mol%, which furnished the product within 70% yield and only after 6 h (**Entry 6**). However, when 40 mol% (±)-CSA was taken for a similar reaction, the yield of the desired product was not improved satisfactorily (**Entry 7**). Another reaction was examined without a catalyst at 80 °C, but the reaction was futile (**Entry 8**). To check the efficacy of different catalysts, a few reactions were performed in other Bronsted acid catalysts such as *p*-toluenesulfonic acid (*p*-TSA), trifluoracetic acid (TFA) and acetic acid in 30 mol% amount. However, expected product **14a** was isolated in 60% and 20% yield in the presence of *p*-TSA and TFA, respectively (**Entries 9 & 10**). The desired product was not obtained with acetic acid (**Entry 11**). At last, a reaction was also performed in DMF, but the expected outcome was not achieved (**Entry 12**). Finally, it was concluded that the suitable reaction conditions for getting the quinoline derivative in maximum yield are 30 mol% (±)-CSA at 80 °C temperature in DMSO solvent (**Entry 6**).

5.2b. Exploration of the Substrate Scope

We then explored the substrate scope for 4-methyl-2-arylbenzo[*h*]quinoline derivatives with 1 naphthylamine and various aryl aldehydes with optimized reaction conditions. The results are summarized in **Table 5.2**. Initially, 1-naphthylamine was reacted to aryl aldehydes containing electron-withdrawing groups such as 2-fluoro and 2-chloro, 3-fluoro benzaldehyde to obtain the desired products **14b-d** in 54-60% yield. The 1-naphthyl amine and aryl aldehyde reaction with +R and -I effect, such as 4-methoxy and 3,4,5-methoxy benzaldehyde, provided the desired products **14e-f** in 60 and 50% yield respectively. 2-(4-Methylbenzo[*h*]quinolin-2-yl)phenol (**14g**) was obtained from the reaction of salicylaldehyde and 1-naphthylamine. The structure of compound **14g** has been ascertained with Single Crystal X-ray Data (**Figure 5.1** and **Table 5.6**). The **14h-i** products also included 5-chloro, 5-bromo, and 5-nitrosalicylaldehydes.

Then, the present methodology was extended further with 2-naphthylamine (**1e**) and various aryl aldehydes to produce different 1-methyl-3-arylbenzo[*f*]quinoline derivatives, as shown in **Table 5.3**. As 2-naphthylamine is very costly, it was prepared in the laboratory following the earlier reported method, illustrated in **Scheme 5.8** in the **Experimental Section**.[7] At first, the reaction of 2-naphthylamine and benzaldehyde produced 1-methyl-3-benzo[*f*]quinoline **14k** in 71% yield. Aryl aldehyde with electron-withdrawing groups such as 4-fluoro and 4-bromo benzaldehyde provided **14l** and **14m** in 60-61% yield. Again, 4-methyl and 4-methoxybenzaldehyde furnished the desired product 1-methyl-3-

arylbenzo[*f*]quinoline **14n** and **14o** in **65** % and **61**% yield. Compounds **14p**, **14q**, and **14r** were also obtained from the reaction of 2-naphthylamine with salicylaldehyde, 5-fluoro, and 5-chlorosalicylaldehyde.

Table 5.2. Scope of 4-Methyl-2-arylbenzo[*h*]quinoline Derivatives[a]

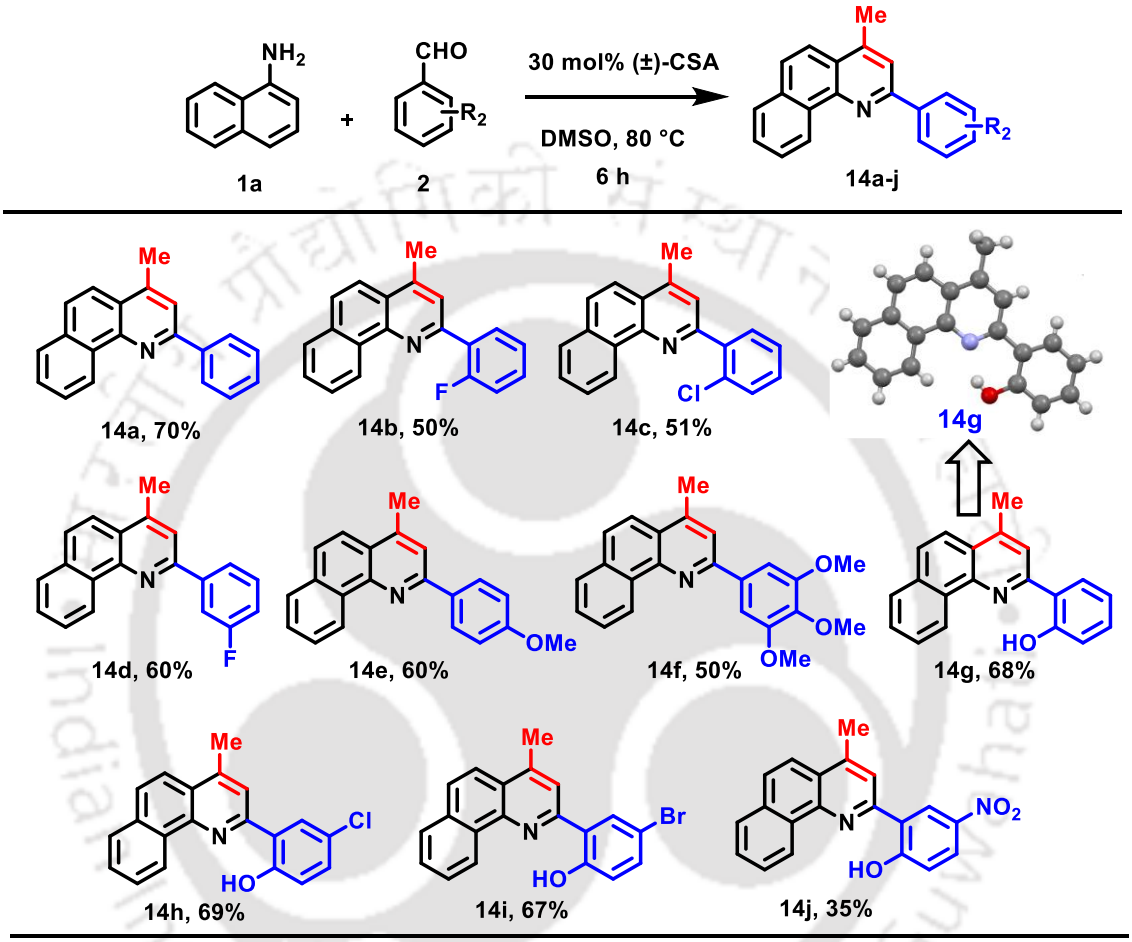

[a]All reactions were carried out using 1-naphthylamine (**1a**, 1 mmol), arylaldehyde (**2**, 0.10 mmol), and derivatives in 2 mL DMSO solvent at 80 °C.

Table 5.3. Scope of 1-Methyl-3-arylbenzo[*f*]quinoline Derivatives[a]

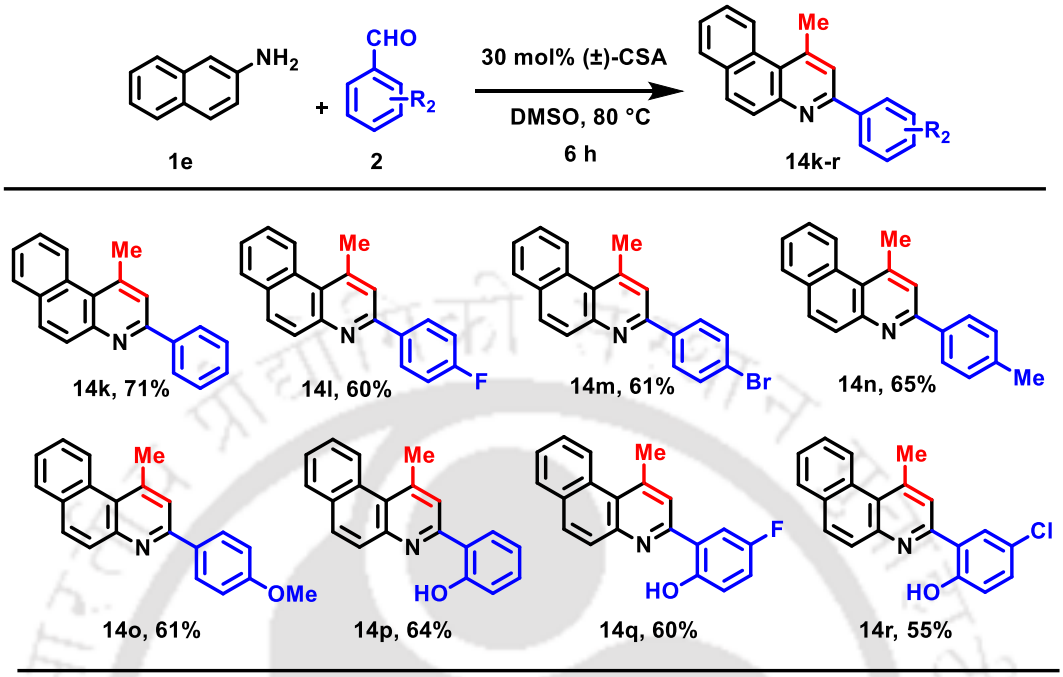

[a]All reactions were carried out with 2-naphthylamine (**1e**, 0.10 mmol), arylaldehyde (**2**, 0.10 mmol), and derivatives in 2 mL DMSO solvent at 80 °C.

Next, this protocol was further extended with 2-aminoanthracene (**1f**) to get 1-methyl-3-arylnaphtho[2,3-*f*]quinoline derivatives (**14s-x**), as shown in **Table 5.4**. The reaction of 2-aminoanthracene and benzaldehyde provided compound **14s** in 62% yield after 7 h. 2-Aminoanthracene was subjected to 3-fluoro, 3-bromo, and 4-chlorobenzaldehyde to deliver the desired products **14t-v** in 58-60% yield. However, 3-methoxybenzaldehyde and salicylaldehyde gave the expected product **14w** and **14x** in 58% and 48% respectively.

Next, the same protocol was examined with aniline, 4-chlorobenzaldehyde, *m*-anisidine, *p*-anisidine, 2,4-dimethoxy aniline, 3,4-dimethoxy aniline, 3,5-dimethoxy aniline, 3,4,5-trimethoxy aniline, 2,4-dimethylaniline, 3,5-dimethylaniline, and benzaldehyde. Unfortunately, the reaction was unsuccessful for all the anilines except 3,5-dimethoxyaniline. It furnished the desired product 2-phenyl-5,7-dimethoxy-4-methylquinoline (**15a**) in 57% yield. 3,5-Dimethoxyaniline was further reacted with 4-fluoro and 3-bromo benzaldehyde. Both the reactions produced expected 2-aryl-5,7-dimethoxy-4-methylquinoline **15b** and **15c** (**Table 5.5**).

Table 5.4. Scope of 1-Methyl-3-arylnaphtho[2,3-*f*]quinoline Derivatives[a]

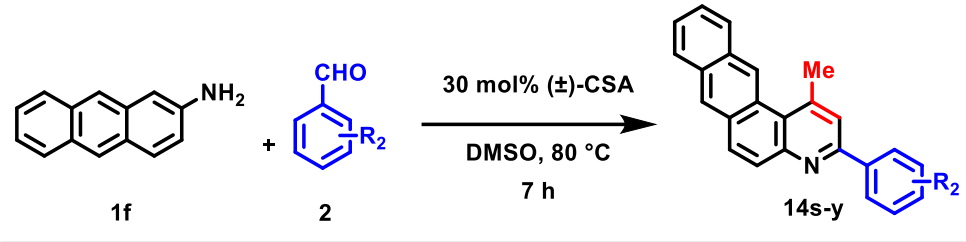

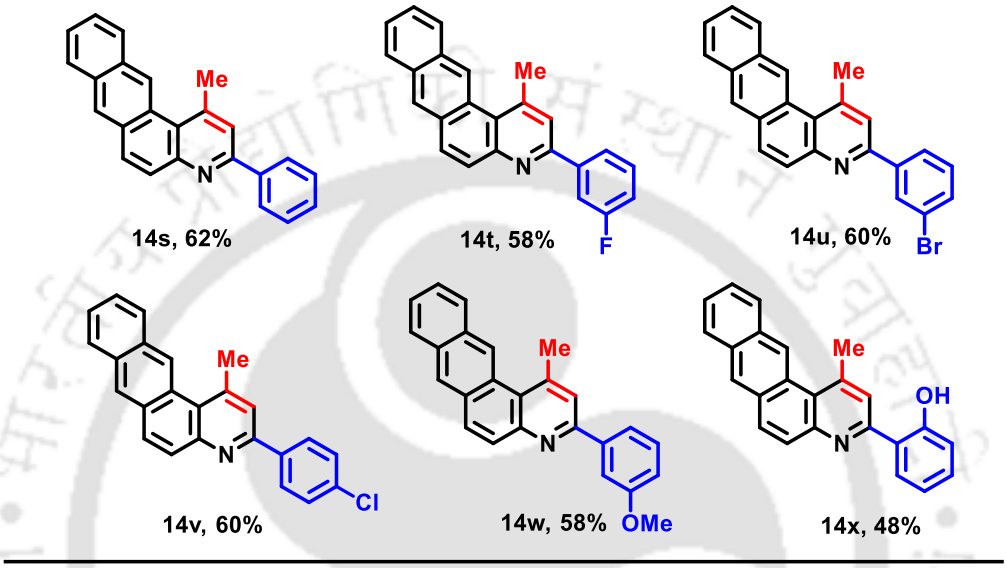

[a]All reactions were carried out with 1-aminoanthracene (**1f**, 0.10 mmol), arylaldehyde (**2**, 0.10 mmol), and derivatives in 2 mL DMSO solvent at 80 °C.

Table 5.5 Scope of 1-Methyl-3-arylnaphtho[2,3-*f*]quinoline Derivatives[a]

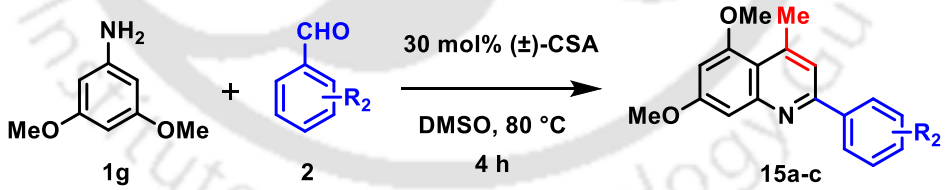

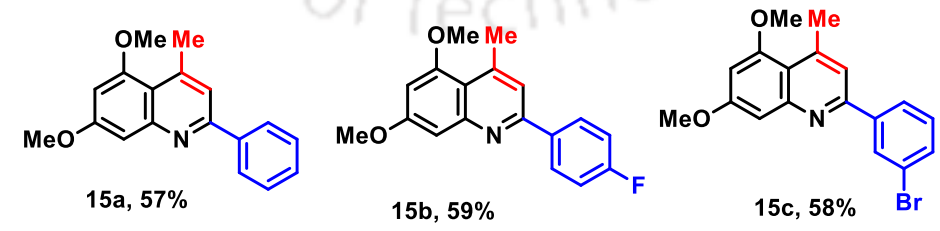

[a]All reactions were carried out with 3,5-dimethoxyquinoline (**1g**, 0.10 mmol), arylaldehyde (**2**, 0.10 mmol), and derivatives in 2 mL DMSO solvent at 80 °C.

5.2c. Establishment of the Reaction Mechanism

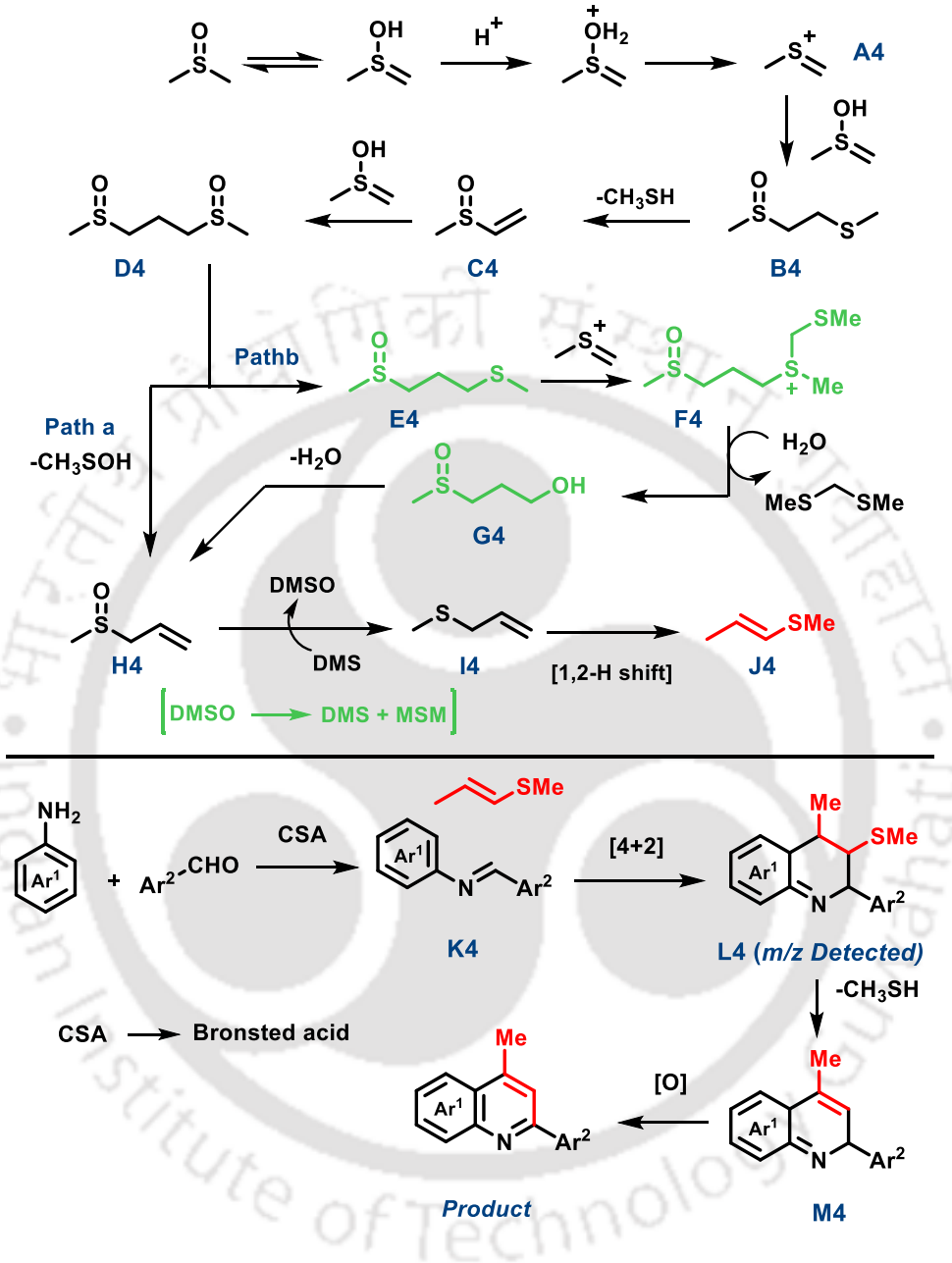

Scheme 5.7. Probable reaction mechanism for the formation of the product 1**3** & 1**4**.

The proposed reaction mechanism for product (**13** and **14**) formation is illustrated in **Scheme 5.7**. In this particular procedure, (±)-10-camphorsulfonic acid, (±)-CSA, serves as a Bronsted acid. Initially, DMSO gives rise to the sulfenium ion (**A4**).[8a] DMSO can also act as a nucleophile for carbon adduct.[8b] Subsequently, the interaction between the electrophilic sulfenium ion and nucleophilic DMSO generates the sulfinyl sulfane intermediate **B4**, which eliminates methane thiol to yield the methyl vinyl sulfone

intermediate **C4**. The nucleophilic addition of DMSO to sulfone **C4**, followed by the elimination of methanesulfenic acid (CH_3SOH), produces the allyl methyl sulfone intermediate **H4**.[8c] DMSO upon heating forms dimethylsulfide (DMS) and dimethyl sulfone (MSM). Then, DMS itself oxidized to DMSO, helping in the transformation of **H4** into allyl methyl sulfide intermediate **I4**,[4e] which undergoes a 1,2-H shift to form the methyl-1-propenyl sulfide intermediate **J4**. Intermediates **C4**, **H4**, **I4**, and **J4** are documented in the literature,[9] and listed in NIH, National Library of Medicine databook.

However, the formation of intermediate **H4** can also be explained via **Path b**. Intermediate **D4** can be reduced to intermediate **E4** which can attack another sulfenyl ion providing intermediate **F4**. Then, it forms intermediate **G4** upon hydroxylation and elimination of one molecule of bis(methylthio)methane. After that, intermediate **H4** can be generated by water elimination from intermediate **G4**.

Concurrently, the imine intermediate **K4** is formed through the reaction of aryl amine and aryl aldehyde in the presence of CSA. The imine (**K4**) and propenyl sulfide (**J4**) undergo a regioselective 4+2 cycloaddition, resulting in the cyclized intermediate **L4**. Upon elimination of one molecule of methyl thiol from **L4**, followed by aerobic oxidation of intermediate **M4**, the desired product is attained. Intermediates **B4**, **D4**, **H4** and **L4** are confirmed by HRMS analysis and given in the experimental section.

- ***All the synthesized compounds are characterized through ^{1}H, ^{13}C NMR, and HRMS spectra, and characterization data of all the compounds are given in the experimental section. A few representative spectra have also been attached in the experimental section.***

5.2d. Conclusion

In summary, we have developed a simple method for the synthesis of 4-methyl-2-arylbenzo[*h*]quinoline (**14a-j**), 1-methyl-3-arlbenzo[*f*]quinoline (**14k-r**) and 1-methyl-3-arylnaphtho[2,3-*f*]quinoline (**14s-x**) from the reaction of aryl aldehyde (**2**) with 1-naphthyl amine (**1a**), 2-naphthylamine (**1e**), and 2-aminoanthracene (**1f**) respectively at 80 °C in the presence of 30 mol% (±)-CSA using DMSO as a solvent-cum-reactant through a pseudo five component reaction. In addition, three 2-aryl-5,7-dimethoxy-4-methylquinoline derivatives (**15a-c**) have also been synthesized from 3,5-dimethoxyaniline (**1g**) and aryl aldehyde.

In this distinctive reaction, DMSO is utilized as a CH_3-C=CH_2- synthon for the incorporation of three carbon atoms in the target molecule. For this outcome in-situ generated methyl-1-propenyl sulfide intermediate participate in the reaction with imine regioselectively. To the best of our understanding, this represents the first documentation of such a scenario in the realm of organic synthesis. The other features of this methodology are: i) mild reaction condition, ii) oxidant-free activation of DMSO, iii) no other activating agent is used to activate the DMSO.

5.3. Experimental Section

5.3a. Synthesis of 2-Naphthylamine

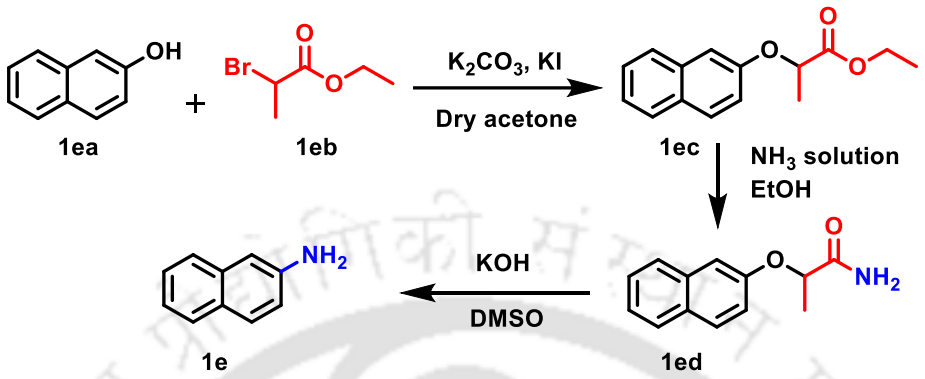

Scheme 5.8. General scheme for the synthesis of 2-naphthylamine (**1b**).

General Procedure for the Synthesis of Ethyl 2-(naphthalene-2-yloxy) Propanoate (1bc)

Into a 50 mL dry single-necked round-bottomed flask, 2-naphthol **1ba** (1.44.17 g, 10 mmol) was taken in 15 mL of dry acetone and K_2CO_3 (2.764 g, 20 mmol), KI (0.166 g 1.0 mmol) was added. Ethyl-2-bromopropionate **1bb** (1.687 mL, 13 mmol) was added successively, and the reaction was kept for reflux in a pre-heated oil bath with constant stirring. The reaction was monitored by TLC 10% (EtOH, hexane). After 8 h, when the reaction was completed, the reaction mixture was kept at room temperature. Then, excess acetone was removed in a rotary evaporator and extracted with ethyl-acetate (3x5 mL). The organic layer was washed with water and dried over anhydrous sodium sulphate. The organic layer was concentrated in a rotary evaporator under reduced pressure. The resultant maroon colour liquid (**1bc**, 2.325 g) with a fruity odour was obtained with an excellent yield of 95%.

General Procedure for the Synthesis` of 2-(Naphthalene-2-yloxy) Propenamide (1bd)

In a 50 mL single neck round-bottomed flask, compound **1bc** (2.281 g, 10 mmol) was dissolved in 15 mL of ethanol, and then 15 mL 25% ammonia solution was added. The reaction mixture was stirred for 24 h at room temperature (rt). The reaction was monitored by TLC 40% (EtOH, Hexane). After the completion of the reaction, the excess ammonia and ethanol were removed under reduced pressure in a rotary evaporator and filtered to obtain the white solid. Recrystallization of the crude product in ethanol gave the compound **1bd** (2.140 g) in nearly 93% yield.

General Procedure for the Synthesis of 2-Naphthylamine (1b)

Compound **1bd** (1.076 g, 5 mmol) was taken in a single-necked round-bottomed flask in DMSO. The solution was treated with KOH (2 equiv.) and refluxed at 140 °C for 6 hours. The completion of the reaction was monitored by TLC 10% (EtOH, hexane). After the completion of the reaction, the reaction mixture was cooled and extracted with DCM, dried over sodium sulphate, and concentrated under reduced pressure in a rotary evaporator. The residue was purified through column chromatography to obtain a yellowish solid. Recrystallization of the crude product in ethanol to obtain compound **3** (0.826 g) with 75-79% yield.

5.3b. General Procedure for the Synthesis of the Fused Quinoline (14 & 15)

General Procedure for the Synthesis of 4-Methyl-2-arylbenzo[h]quinoline (14a-j)

1-Naphthylamine (**1a**, 0.10 mmol) and aryl aldehyde (**2**, 0.10 mmol) are mixed in the round-bottomed flask. Then, 30 mol% (±)-CSA (7 mg) was added to the reaction mixture as a catalyst. The reaction mixture was then dissolved in 1 mL DMSO and kept in a pre-heated oil bath at 80 °C with constant stirring under an air atmosphere. The progress of the reaction was monitored by checking thin-layer chromatography (TLC) from time to time. After the completion of the reaction, the reaction mixture was brought to room temperature. Then, 5 mL of dichloromethane (DCM) was added to it. Then, it was transferred into a 25 mL separatory funnel, followed by the addition of 7 mL of water. The organic layer was collected into a 25 mL conical flask and dried with anhydrous sodium sulfate. The solvent was then removed from the rotary evaporator. Finally, the crude residue was purified by column chromatography (silica gel 60-120 mesh) using (9.8: 0.2, v/v) *n*-hexane and ethyl acetated mixture to obtain the final product 4-methyl-2-arylbenzo[*h*]quinoline derivatives (**14a-j**).

General Procedure for the Synthesis of 1-Methyl-3-arylbenzo[f]quinoline (14k-r)

Standard procedure was used to obtain 1-methyl-3-arylbenzo[*f*]quinoline **(14k-r)** using 2-naphthylamine (**1b**, 0.10 mmol), and aryl aldehyde (**2**, 0.10 mmol).

General Procedure for the Synthesis of 1-Methyl-3-arylnaphtho[2,3-f]quinoline (14s-x)

Standard procedure was used to obtain 1-methyl-3-arylnaphtho[2,3-*f*]quinoline **(14s-x)** using 2-aminoanthracene (**1c**, 0.10 mmol), and aryl aldehyde (**2**, 0.10 mmol).

General Procedure for the Synthesis of 1-Methyl-3-arylnaphtho[2,3-f]quinoline (15a-c)

Standard procedure was used to obtain 1-methyl-3-arylnaphtho[2,3-*f*]quinoline **(15a-c)** using 3,5-dimethoxyaniline (**1d**, 0.10 mmol), and aryl aldehyde (**2**, 0.10 mmol).

5.3c. Characterization Data

Ethyl 2-(naphthalene-2-yloxy)propanoate (1ec)

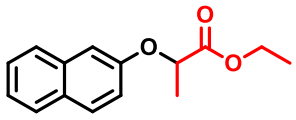

Yield 95% (2.325 g). Maroon liquid, ^{1}H NMR (400 MHz, $CDCl_3$) δ 7.71 (d, *J* = 9.0 Hz, 2H), 7.66 (d, *J* = 8.2 Hz, 1H), 7.39 (t, *J* = 7.3 Hz, 1H), 7.30 (t, *J* = 7.4 Hz, 1H), 7.18 (dd, *J* = 9.0, 2.3 Hz, 1H), 7.04 (d, *J* = 2.0 Hz, 1H), 4.86 (q, *J* = 6.8 Hz, 1H), 4.19 (dd, *J* = 7.1, 4.8 Hz, 2H), 1.65 (d, *J* = 6.8 Hz, 3H), 1.20 (t, *J* = 7.2 Hz, 3H). ^{13}C NMR (100 MHz, $CDCl_3$) δ 172.1, 155.5, 134.3, 129.6, 129.3, 127.6, 126.8, 126.4, 123.9, 118.9, 107.8, 72.7, 61.2, 18.5, 14.1; IR (KBr)ν_{max}: 1752, 1732 cm^{-1}; HRMS (ESI) Calcd for $C_{15}H_{17}O_3$ 245.1173 (M + H$^+$); Found 245.1173.

2-(Naphthalene-2-yloxy)propenamide (1ed)

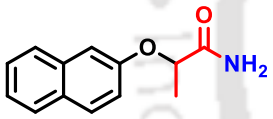

Yield 93% (2.14 g). White solid, mp 120 ºC, ^{1}H NMR (400 MHz, $CDCl_3$) δ 7.79 (d, *J* = 2.7 Hz, 1H), 7.77 (s, 1H), 7.73 (d, *J* = 8.2 Hz, 1H), 7.46 (t, *J* = 7.4 Hz, 1H), 7.37 (t, *J* = 7.4 Hz, 1H), 7.17 (m, 2H), 6.43 (s, 1H), 5.62 (s, 1H), 4.83 (q, *J* = 6.8 Hz, 2H), 1.67 (d, *J* = 6.8 Hz, 3H). ^{13}C NMR (100 MHz, $CDCl_3$) δ 175.1, 154.8, 134.4, 130.0, 129.6, 127.7, 127.1, 126.8, 118.6, 108.7, 75.0, 18.8. IR (KBr)ν_{max}: 3390, 3196, 1658 cm^{-1}; HRMS (ESI) Calcd for $C_{13}H_{14}NO_2$ 216.1020 (M + H$^+$); Found 216.1021.

2-Naphthylamine (1e)

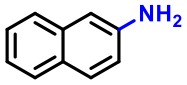

Yield 75-79% (0.826 g). Reddish-brown solid, mp 162-164 ºC; ^{1}H NMR (400 MHz, $CDCl_3$) δ 7.69 (d, *J* = 8.2 Hz, 1H), 7.66 (d, *J* = 8.7 Hz, 1H), 7.60 (d, *J* = 8.3 Hz, 1H), 7.37 (t, *J* = 7.5 Hz, 1H), 7.23 (t, *J* = 7.5 Hz, 1H), 6.99 (d, *J* = 2.1 Hz, 1H), 6.95 (dd, *J* = 8.6, 2.3 Hz, 1H), 3.84 (s, 2H). ^{13}C NMR (100 MHz, $CDCl_3$) δ 144.2, 135.0, 129.3, 128.1, 127.8, 126.4, 125.9, 122.6, 118.3, 108.7. IR (KBr)ν_{max}: 3411, 3328 cm^{-1}; HRMS (ESI) Calcd for $C_{10}H_{10}N$ 144.0808 (M + H$^+$); Found 144.0808.

4-Methyl-2-phenylbenzo[*h*]quinoline (14a)

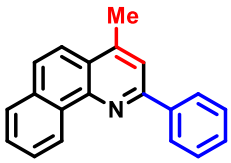

Yield 70% (19 mg), white solid, mp 128 °C; ^{1}H NMR (500 MHz, $CDCl_3$) δ 9.53 (d, *J* = 8.1 Hz, 1H), 8.34 (d, *J* = 7.8 Hz, 2H), 7.93 – 7.91 (m, 2H), 7.86 (s, 1H), 7.82 (d, J = 9.0 Hz, 1H), 7.74 (t, *J* = 7.5 Hz, 1H), 7.69 (t, *J* = 7.3 Hz, 1H), 7.56 (t, *J* = 7.5 Hz, 2H), 7.47 (t, *J* = 7.1 Hz, 1H), 2.82 (s, 3H). ^{13}C NMR (125 MHz, $CDCl_3$) δ 155.1, 146.1, 144.7, 140.0, 133.7, 132.3, 129.2, 128.9, 128.1, 127.7, 127.5, 127.2, 126.9, 125.3, 124.9, 121.3, 120.1, 19.5. IR (KBr)ν_{max}: 3062, 2956, 2924, 2849, 1623, 1591 cm^{-1}; HRMS (ESI) Calcd for $C_{20}H_{16}N$ 270.1278 (M + H$^+$); Found 270.1278.

2-(2-Fluorophenyl)-4-methylbenzo[*h*]quinoline (14b)

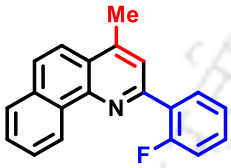

Yield 50% (14 mg), off-white solid, mp 147 °C; ^{1}H NMR (500 MHz, $CDCl_3$) δ 9.46 (d, *J* = 8.0 Hz, 1H), 8.38 (t, *J* = 7.7 Hz, 1H), 7.9 (t, *J* = 7.1 Hz, 3H), 7.85 (d, *J* = 9.1 Hz, 1H), 7.73 (t, *J* = 7.4 Hz, 1H), 7.71 – 7.68 (m, 1H), 7.46 – 7.42 (m, 1H), 7.36 (t, *J* = 7.3 Hz, 1H), 7.24 – 7.20 (m, 1H), 2.82 (s, 3H). ^{13}C NMR (125 MHz, $CDCl_3$) δ 162.1, 160.1, 151.7, 146.2, 144.3, 133.6, 132.2, 131.9 (d, *J* = 3.05 Hz), 130.6 (d, *J* = 8.5 Hz), 128.9 (d, *J* = 42 Hz), 127.5, 127.0, 125.1, 125.0, 124.7 (d, *J* = 3.4 Hz), 124.0, 123.9, 121.3, 116.4 (d, *J* = 23.1 Hz), 19.4. IR (KBr)ν_{max}: 3060, 2926, 2856, 1621, 1588 cm^{-1}; HRMS (ESI) Calcd for $C_{20}H_{15}FN$ 288.1184 (M + H$^+$); Found 288.1180.

2-(2-Chlorophenyl)-4-methylbenzo[*h*]quinoline (14c)

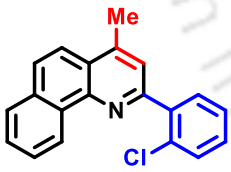

Yield 51% (15 mg), white solid, mp 136-138 °C; ^{1}H NMR (400 MHz, $CDCl_3$) δ 9.41 (d, *J* = 8 Hz, 1H), 7.95 (d, *J* = 8 Hz, 1H), 7.88 – 7.85 (m, 2H), 7.77 (s, 1H), 7.71 – 7.68 (m, 2H), 7.54 (d, *J* = 8.8 Hz, 1H), 7.45 (t, *J* = 7.3 Hz, 2H), 7.40 (dd, *J* = 7.7, 2.0 Hz, 1H), 2.82 (s, 3H). ^{13}C NMR (100 MHz, $CDCl_3$) δ 155.2, 146.1, 143.7, 140.0, 133.6, 132.7, 132.4, 132.2, 130.4, 129.7, 128.1, 127.7, 127.6, 127.1, 127.0, 125.3, 124.8, 124.2, 121.3, 19.4. IR (KBr)ν_{max}: 3051, 2956, 2924, 2848, 1622, 1591 cm^{-1}; HRMS (ESI) Calcd for $C_{20}H_{15}ClN$ 304.0888 (M + H$^+$); Found 304.0886.

2-(3-Fluorophenyl)-4-methylbenzo[*h*]quinoline (14d)

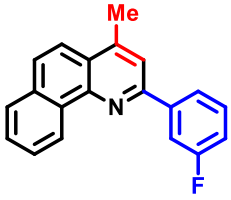

Yield 60% (17 mg), off-white solid, mp 112-114 °C; ^{1}H NMR (500 MHz, $CDCl_3$) δ 9.34 (d, *J* = 8.1 Hz, 1H), 7.95 (dt, *J* = 10.4, 2.0 Hz, 1H), 7.92 (d, *J* = 7.8 Hz, 1H), 7.76 (d, *J* = 8.9 Hz, 2H), 7.68 (d, *J* = 7.0 Hz, 2H), 7.61 – 7.58 (m, 1H), 7.55 (t, *J* = 6.7 Hz, 1H), 7.37 – 7.33 (m, 1H), 7.02 – 6.98 (m, 1H), 2.67 (s, 3H); ^{13}C NMR (125 MHz,

$CDCl_3$) δ 164.5, 162.6, 153.7, 153.6, 146.1, 145.0, 142.4 (d, *J* = 7.4 Hz), 133.7 (d, *J* = 8.0 Hz), 130.3 (d, *J* = 8.0 Hz), 128.2, 127.8, 127.5, 127.1, 125.2, 125.2, 123.0 (d, *J* = 2.6 Hz), 121.3, 120.0, 116.0 (d, *J* = 21.3 Hz), 114.4 (d, *J* = 22.7 Hz), 19.5. ^{19}F NMR (471 MHz, $CDCl_3$) δ -113.02; IR (KBr)ν_{max}: 3050, 2963, 2926, 2853, 1614, 1591 cm^{-1}; HRMS (ESI) Calcd for $C_{20}H_{15}FN$ 288.1184 ($M + H^+$); Found 288.1184.

2-(4-Methoxyphenyl)-4-methylbenzo[*h*]quinoline (14e)

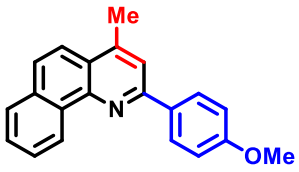

Yield 60% (18 mg), brown solid, mp 109-111 °C; ^{1}H NMR (500 MHz, $CDCl_3$) δ 9.51 (d, *J* = 8.1 Hz, 1H), 8.31 (d, *J* = 8.6 Hz, 2H), 7.90 (d, *J* = 8.8 Hz, 2H), 7.79 (d, *J* = 9.4 Hz, 2H), 7.73 (t, *J* = 7.5 Hz, 1H), 7.68 (t, *J* = 7.3 Hz, 1H), 7.08 (d, *J* = 8.6 Hz, 2H), 3.91 (s, 3H), 2.80 (s, 3H). ^{13}C NMR (125 MHz, $CDCl_3$) δ 160.8, 154.8, 146.1, 144.5, 133.7, 132.7, 132.3, 128.8, 128.0, 127.7, 126.8, 126.7, 125.2, 124.5, 121.4, 119.5, 114.3, 55.5, 19.5. IR (KBr)ν_{max}: 3048, 2956, 2928, 2835, 1608, 1591 cm^{-1}; HRMS (ESI) Calcd for $C_{21}H_{18}NO$ 300.1383 ($M + H^+$); Found 300.1382.

4-Methyl-2-(3,4,5-trimethoxyphenyl)benzo[*h*]quinoline (14f)

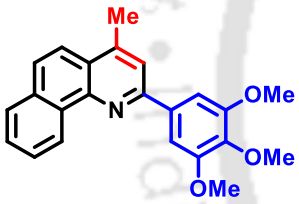

Yield 50% (18 mg), brown solid, mp 153 °C; ^{1}H NMR (500 MHz, $CDCl_3$) δ 9.46 (d, *J* = 7.7 Hz, 1H), 7.92 (d, *J* = 7.6 Hz, 2H), 7.82 (d, *J* = 9.2 Hz, 1H), 7.79 (s, 1H), 7.76 – 7.73 (m, 1H), 7.71 – 7.68 (m, 1H), 7.57 (s, 2H), 4.06 (s, 6H), 3.95 (s, 3H), 2.83 (s, 3H); ^{13}C NMR (125 MHz, $CDCl_3$) δ 154.8, 153.7, 146.0, 144.8, 139.5, 135.7, 133.8, 132.1, 128.1, 127.8, 127.2, 126.9, 125.1, 124.8, 121.3, 120.0, 104.9, 61.1, 56.5, 19.5; IR (KBr)ν_{max}: 3048, 2958, 2936, 2838, 1623, 1591 cm^{-1}; HRMS (ESI) Calcd for $C_{23}H_{22}NO_3$ 360.1595 ($M + H^+$); Found 360.1593.

2-(4-Methylbenzo[*h*]quinolin-2-yl)phenol (14g)

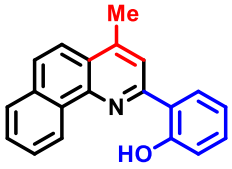

Yield 68% (19 mg), yellow solid, mp 144 °C; ^{1}H NMR (400 MHz, $CDCl_3$) δ 15.73 (s, 1H), 8.92 (d, *J* = 8.1 Hz, 1H), 7.97 (dd, *J* = 8.0, 1.3 Hz, 1H), 7.94 (s, 1H), 7.92 (d, *J* = 8.8 Hz, 1H), 7.88 – 7.79 (m, 2H), 7.78 – 7.73 (m, 1H), 7.73 – 7.69 (m, 1H), 7.41 – 7.36 (m, 1H), 7.14 (dd, *J* = 8.2, 1.0 Hz, 1H), 7.00 – 6.95 (m, 1H), 2.80 (s, 3H). ^{13}C NMR (150 MHz, $CDCl_3$) δ 160.8, 156.0, 146.2, 142.9, 133.9, 131.8, 129.9, 128.5, 128.3, 127.7, 127.6, 126.8, 124.6, 124.2, 121.0, 119.2, 118.9, 118.6, 118.5, 19.9. IR (KBr)ν_{max}: 3058, 2953, 2921, 2853,1626, 1591 cm^{-1}; HRMS (ESI) Calcd for $C_{20}H_{16}NO$ 286.1227 ($M + H^+$); Found 286.1226.

4-Chloro-2-(4-methylbenzo[*h*]quinolin-2-yl)phenol (14h)

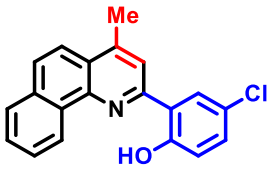

Yield 69% (22 mg), yellow solid, mp 218-219 °C; ^{1}H NMR (600 MHz, $CDCl_3$) δ 15.75 (s, 1H), 8.88 (d, *J* = 8.1 Hz, 1H), 7.94 (d, *J* = 7.8 Hz, 1H), 7.91 – 7.89 (m, 2H), 7.88 – 7.84 (m, 2H), 7.77 (t, *J* = 7.5 Hz, 1H), 7.73 (t, *J* = 7.3 Hz, 1H), 7.31 (dd, *J* = 8.7, 2.5 Hz, 1H), 7.06 (d, *J* = 8.7 Hz, 1H), 2.83 (s, 3H). ^{13}C NMR (150 MHz, CDCl3) δ 159.4, 154.6, 146.7, 142.9, 134.0, 131.5, 129.8, 128.7, 128.4, 128.1, 127.9, 126.4, 124.9, 124.1, 123.5, 121.0, 120.1, 119.9, 118.5, 19.9. IR (KBr)ν_{max}: 3048, 2955, 2923, 2853, 1626, 1596 cm^{-1}; HRMS (ESI) Calcd for $C_{20}H_{15}ClNO$ 320.0837 (M + H$^+$); Found 320.0837.

4-Bromo-2-(4-methylbenzo[*h*]quinolin-2-yl)phenol (14i)

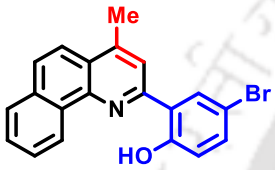

Yield 67% (24 mg), yellow solid, mp 212-214 °C; ^{1}H NMR (600 MHz, $CDCl_3$) δ 15.76 (s, 1H), 8.82 (d, *J* = 8.0 Hz, 1H), 7.98 (d, *J* = 2.2 Hz, 1H), 7.91 (d, *J* = 7.5 Hz, 1H), 7.83 – 7.79 (m, 3H), 7.75 (t, *J* = 8.0 Hz, 1H), 7.71 (t, *J* = 6.8 Hz, 1H), 7.42 (dd, *J* = 8.7, 2.3 Hz, 1H), 6.99 (d, *J* = 8.7 Hz, 1H), 2.78 (s, 3H). ^{13}C NMR (150 MHz, $CDCl_3$) δ 159.8, 154.4, 146.6, 142.7, 134.3, 133.9, 129.7, 129.2, 128.7, 128.4, 128.0, 127.8, 124.9, 124.0, 120.9, 120.7, 120.3, 118.4, 110.6, 19.9. IR (KBr)ν_{max}: 3045, 2958, 2923, 1625, 1594 cm^{-1}; HRMS (ESI) Calcd for $C_{20}H_{15}BrNO$ 364.0332 (M + H$^+$); Found 364.0336.

2-(4-Methylbenzo[*h*]quinolin-2-yl)-4-nitrophenol (14j)

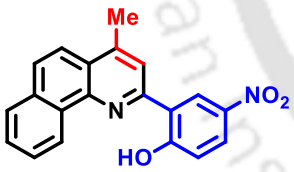

Yield 35% (11 mg), brown solid, mp 315-317 °C; ^{1}H NMR (400 MHz, $CDCl_3$) δ 17.28 (s, 1H), 8.99 (d, *J* = 2.6 Hz, 1H), 8.91 (d, *J* = 8.1 Hz, 1H), 8.31 – 8.26 (m, 1H), 8.12 (s, 1H), 8.00 (d, *J* = 9.3 Hz, 1H), 7.95 (d, *J* = 4.3 Hz, 2H), 7.82 (dt, *J* = 14.3, 7.0 Hz, 2H), 7.19 (d, *J* = 9.1 Hz, 1H), 2.93 (s, 3H); ^{13}C NMR (126 MHz, $CDCl_3$) δ 147.7, 134.2, 129.4, 129.1, 128.8, 128.6, 128.4, 128.2, 127.3, 124.0, 124.0, 123.4, 121.4, 121.0, 119.3, 118.5, 20.0. IR (KBr)νmax: 3048, 2958, 2916, 2851, 1628, 1596 cm^{-1}; HRMS (ESI) Calcd for $C_{20}H_{15}N_2O_3$ 331.1078 (M + H$^+$); Found 331.1072.

1-Methyl-3-phenylbenzo[*f*]quinoline (14k)

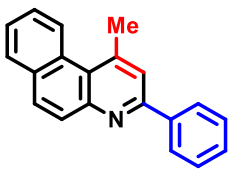

Yield 71% (19 mg), white solid, mp 157-159 °C; ^{1}H NMR (400 MHz, $CDCl_3$) δ 8.81 (d, *J* = 8.1 Hz, 1H), 8.23 (d, *J* = 7.2 Hz, 2H), 8.10 (d, *J* = 9.0 Hz, 1H), 7.97 (d, *J* = 9.5 Hz, 2H), 7.81 (s, 1H), 7.69 – 7.62 (m, 2H), 7.55 (t, *J* = 7.5 Hz, 2H), 7.48 (t, *J* = 7.3 Hz, 1H), 3.17 (s, 3H). ^{13}C NMR (100 MHz, $CDCl_3$) δ 155.5, 149.8, 145.5, 139.3, 133.0, 131.1, 130.9, 129.7, 129.2, 129.1, 128.9, 127.5, 127.4, 126.4, 126.3, 124.8, 122.7, 27.0. IR (KBr)ν_{max}:

3055, 2970, 2926, 2871, 1606, 1582 cm^{-1}; HRMS (ESI) Calcd for $C_{20}H_{16}N$ 270.1278 (M + H^+); Found 270.1278.

3-(4-Fluorophenyl)-1-methylbenzo[*f*]quinoline (14l)

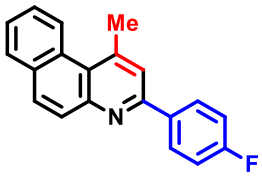

Yield 60% (18 mg), off-white solid, mp 127-129 °C; ^{1}H NMR (500 MHz, $CDCl_3$) δ 8.83 (d, *J* = 8.3 Hz, 1H), 8.22 – 8.1 (m, 2H), 8.06 (d, *J* = 9.0 Hz, 1H), 7.97 (d, *J* = 9.1 Hz, 2H), 7.78 (s, 1H), 7.70 – 7.63 (m, 2H), 7.22 (t, *J* = 8.7 Hz, 2H), 3.20 (s, 3H).^{13}C NMR (125 MHz, $CDCl_3$) δ 164.8, 162.8, 154.5, 149.8, 145.7, 135.5, 133.0, 131.3, 130.9, 129.6, 129.3 (d, *J* = 8.8 Hz), 129.2, 127.6, 126.5 (d, *J* = 4.28 Hz), 124.7, 122.4, 115.8 (d, *J* = 21.4 Hz), 27.1.^{19}F NMR (471 MHz, $CDCl_3$) δ -112.80; IR (KBr)ν_{max}: 3060, 2978, 2926, 2856, 1621, 1596 cm^{-1}; HRMS (ESI) Calcd for $C_{20}H_{15}FNO$ 288.1184 (M + H^+); Found 288.1184.

3-(4-Bromophenyl)-1-methylbenzo[*f*]quinoline (14m)

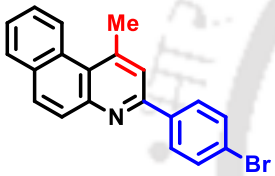

Yield 61% (19 mg), off-white solid, mp 177 °C; ^{1}H NMR (400 MHz, $CDCl_3$) δ 8.82 (d, *J* = 8.1 Hz, 1H), 8.10 (d, *J* = 8.5 Hz, 2H), 8.05 (d, *J* = 9.0 Hz, 1H), 7.97 (d, *J* = 8.9 Hz, 2H), 7.78 (s, 1H), 7.70 – 7.63 (m, 4H), 3.19 (s, 3H); ^{13}C NMR (125 MHz, $CDCl_3$) δ 154.2, 149.8, 145.8, 138.1, 133.1, 132.0, 131.4, 130.9, 129.6, 129.2, 129.0, 127.6, 126.5, 125.0, 123.8, 122.3, 27.1; IR (KBr)ν_{max}: 3053, 2958, 2925, 2850, 1626, 1581 cm^{-1}; $C_{20}H_{15}BrN$ 348.0383 (M + H^+); Found 348.0378 & 350.0358.

1-Methyl-3-(*p*-tolyl)benzo[*f*]quinoline (14n)

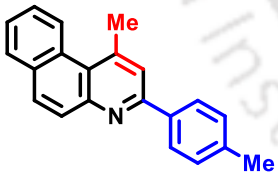

Yield 65% (18 mg), off-white solid, mp 152-154 °C; ^{1}H NMR (400 MHz, $CDCl_3$) δ 8.83 (d, *J* = 8.3 Hz, 1H), 8.12 (d, *J* = 8.1 Hz, 2H), 8.08 (d, *J* = 9.0 Hz, 1H), 7.97 (d, *J* = 9.0 Hz, 2H), 7.81 (s, 1H), 7.70 – 7.62 (m, 2H), 7.35 (d, *J* = 8.0 Hz, 2H), 3.20 (s, 3H), 2.45 (s, 3H). ^{13}C NMR (100 MHz, $CDCl_3$) δ 155.6, 149.8, 145.4, 139.3, 136.5, 133.0, 131.0, 129.8, 129.6, 129.1, 127.5, 127.3, 126.4, 126.3, 124.6, 122.5, 27.1, 21.5. IR (KBr)ν_{max}: 3058, 2957, 1604, 1581 cm^{-1}; HRMS (ESI) Calcd for $C_{21}H_{18}N$ 284.1434 (M + H^+); Found. 284.1441.

3-(4-Methoxyphenyl)-1-methylbenzo[*f*]quinoline (14o)

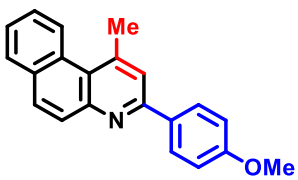

Yield 61% (17.6 mg), yellow solid, mp 124-126 °C; ^{1}H NMR (500 MHz, $CDCl_3$) δ 8.82 (d, *J* = 8.4 Hz, 1H), 8.19 (d, *J* = 8.7 Hz, 2H), 8.06 (d, *J* = 9.0 Hz, 1H), 7.96 (d, *J* = 8.5 Hz, 2H), 7.78 (s, 1H), 7.67 (t, *J* = 7.0 Hz, 1H), 7.63 (t, *J* = 7.2 Hz, 1H), 7.06 (d, *J* = 8.7 Hz, 2H), 3.90 (s, 3H), 3.19 (s, 3H). ^{13}C NMR (125

MHz, $CDCl_3$) δ 160.7, 155.1, 149.7, 145.3, 132.8, 131.8, 130.9, 129.6, 129.0, 128.6, 127.4, 126.2, 126.1, 124.3, 122.1, 114.2, 55.4, 26.9. IR (KBr)ν_{max}: 3051, 2958, 2921, 2833, 1604, 1581 cm^{-1}; HRMS (ESI) Calcd for $C_{21}H_{18}NO$ 300.1383 ($M + H^+$); Found 300.1378.

2-(1-Methylbenzo[*f*]quinolin-3-yl)phenol (14p)

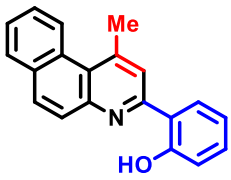

Yield 64% (17 mg), yellow solid, mp 139 °C; ^1H NMR (400 MHz, $CDCl_3$) δ 15.10 (s, 1H), 8.81 (d, *J* = 8.3 Hz, 1H), 7.99 – 7.90 (m, 5H), 7.62 – 7.63 (m, 2H), 7.35 (t, *J* = 7.7 Hz, 1H), 7.09 (d, *J* = 8.2 Hz, 1H), 6.96 (t, *J* = 7.5 Hz, 1H), 3.21 (s, 3H). ^{13}C NMR (125 MHz, $CDCl_3$) δ 161.0, 156.0, 146.7, 146.4, 132.9, 132.2, 131.8, 130.6, 129.4, 127.5, 127.4, 126.9, 126.8, 126.7, 124.3, 120.9, 118.9, 118.8, 118.7, 27.3. IR (KBr)ν_{max}: 3055, 2956, 2921, 2851, 1605, 1584 cm^{-1}; HRMS (ESI) Calcd for $C_{20}H_{16}NO$ 286.1227 ($M + H^+$); Found 286.1231.

4-Fluoro-2-(1-methylbenzo[*f*]quinolin-3-yl)phenol (14q)

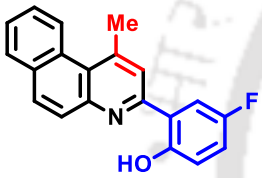

Yield 60% (18 mg), yellow solid, mp 202 °C; ^1H NMR (500 MHz, $CDCl_3$) δ 14.84 (s, 1H), 8.79 (d, *J* = 8.3 Hz, 1H), 7.97 (t, *J* = 7.2 Hz, 2H), 7.88 (d, *J* = 8.9 Hz, 1H), 7.81 (s, 1H), 7.62 – 7.65 (m, 2H), 7.60 (dd, *J* = 9.9, 2.8 Hz, 1H), 7.08 – 7.04 (m, 1H), 7.01 (dd, *J* = 8.9, 5.0 Hz, 1H), 3.20 (s, 3H). ^{13}C NMR (125 MHz, $CDCl_3$) δ 157.0, 156.7, 154.9, 154.8 (d, *J* = 2.7 Hz), 147.0, 146.3, 133.0, 132.4, 130.5, 129.4, 127.4 (d, *J* = 13 Hz), 127.0 (d, *J* = 19.8 Hz), 124.6, 120.8, 119.5 (d, *J* = 7.68 Hz), 118.8, 118.7, 118.5, 112.4 (d, *J* = 24.0 Hz), 27.3.; ^{19}F NMR (471 MHz, $CDCl_3$) δ -125.64; IR (KBr)ν_{max}: 3050, 2961, 2924, 2853, 1604, 1581 cm^{-1}; HRMS (ESI) Calcd for $C_{20}H_{15}FNO$ 304.1133 ($M + H^+$); Found 304.1133.

4-Chloro-2-(1-methylbenzo[*f*]quinolin-3-yl)phenol (14r)

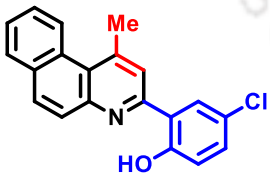

Yield 55% (17 mg), yellow solid, mp 245-246 °C; ^1H NMR (500 MHz, $CDCl_3$) δ 8.84 (d, *J* = 8.4 Hz, 1H), 8.03 – 7.99 (m, 2H), 7.95 – 7.92 (m, 3H), 7.73 (t, *J* = 8 Hz, 1H), 7.69 (t, *J* = 6 Hz, 1H), 7.29 (dd, *J* = 8.8, 2.4 Hz, 1H), 7.03 (d, *J* = 8.7 Hz, 1H), 3.25 (s, 3H). ^{13}C NMR (125 MHz, $CDCl_3$) δ 159.6, 154.7, 147.2, 146.3, 133.0, 132.5, 131.5, 130.5, 129.5, 127.8, 127.5, 127.3, 127.1, 127.0, 126.3, 124.7, 123.6, 120.8, 120.1, 27.4; IR (KBr)ν_{max}: 3054, 2924, 2854, 1606, 1578 cm^{-1}; HRMS (ESI) Calcd for $C_{20}H_{15}ClNO$ 320.0837 ($M + H^+$); Found 320.0834.

1-Methyl-3-phenylnaphtho[2,3-*f*]quinoline (14s)

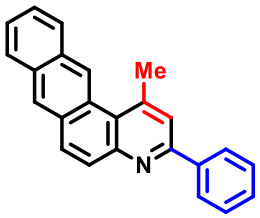

Yield 62% (19 mg), white solid, mp 198-200 °C; ^{1}H NMR (400 MHz, DMSO-d_6) δ 9.49 (s, 1H), 9.43 – 9.41 (m, 1H), 8.63 (s, 1H), 8.32 (d, *J* = 7.6 Hz, 2H), 8.17 (m, 2H), 7.87 (t, *J* = 9.9, Hz, 1H), 7.67 – 7.64 (m, 2H), 7.58 (d, *J* = 7.6 Hz, 2H), 7.53 – 7.50 (m, 1H), 3.31 (s, 3H). ^{13}C NMR (125 MHz, DMSO-d_6) δ 132.6, 131.9, 129.7, 129.6, 129.2, 129.1, 129.0, 128.5, 128.3, 128.0, 127.2, 127.1, 127.1, 126.6, 126.6, 126.4, 122.6, 122.4, 119.0, 26.4; IR (KBr)ν_{max}: 3053, 2923, 2858, 1568 cm^{-1}; HRMS (ESI) Calcd for $C_{24}H_{18}N$ 320.1434 (M + H$^+$); Found. 320.1434.

3-(3-Fluorophenyl)-1-methylnaphtho[2,3-*f*]quinoline (14t)

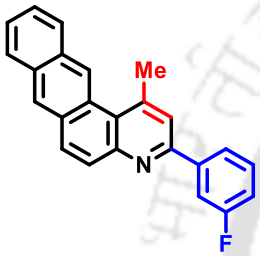

Yield 58% (19 mg), off-white solid, mp 112-113 °C; ^{1}H NMR (500 MHz, $CDCl_3$) δ 9.26 (s, 1H), 8.41 (s, 1H), 8.13 – 8.05 (m, 2H), 8.02 (d, *J* = 9.1 Hz, 1H), 7.97 (d, *J* = 7.5 Hz, 2H), 7.92 (d, *J* = 9.1 Hz, 1H), 7.80 (s, 1H), 7.62 – 7.58 (m, 2H), 7.49 (q, *J* = 8.0 Hz, 1H), 7.15 (t, *J* = 8.4 Hz, 1H), 3.29 (s, 3H). ^{13}C NMR (125 MHz, $CDCl_3$) δ 164.5, 162.5, 153.8, 150.5, 145.7, 141.6 (d, *J* = 7.5 Hz), 131.9, 131.7, 131.4 (d, *J* = 11.1 Hz), 130.4 (d, *J* = 8.1 Hz), 129.6, 129.0, 128.9, 127.6 (d, *J* = 5.5 Hz), 127.3, 126.6, 126.2, 125.4, 122.9, 122.9, 122.6, 116.0 (d, *J* = 21.1 Hz), 114.3 (d, *J* = 22.6 Hz), 27.0; ^{19}F NMR (471 MHz, $CDCl_3$) δ -112.87; IR (KBr)ν_{max}: 3053, 2963, 2921, 2853, 1623, 1573 cm^{-1}; HRMS (ESI) Calcd for $C_{24}H_{17}FN$ 338.1340 (M + H$^+$); Found 338.1340.

3-(3-Bromophenyl)-1-methylnaphtho[2,3-*f*]quinoline (14u)

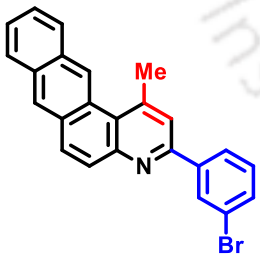

Yield 60% (24 mg), yellow solid, mp 194-196 °C; ^{1}H NMR (400 MHz, $CDCl_3$) δ 9.26 (s, 1H), 8.41 – 8.39 (m, 2H), 8.12 (t, *J* = 6.7 Hz, 2H), 8.08 – 8.05 (m, 1H), 8.02 (d, *J* = 9.2 Hz, 1H), 7.92 (d, *J* = 9.2 Hz, 1H), 7.79 (s, 1H), 7.62 – 7.57 (m, 3H), 7.40 (t, *J* = 7.9 Hz, 1H), 3.29 (s, 3H); ^{13}C NMR (125 MHz, $CDCl_3$) δ 153.6, 150.6, 145.8, 141.3, 132.1, 131.9, 131.7, 131.5, 131.4, 130.5, 130.4, 129.6, 129.0, 128.9, 127.7, 127.6, 127.3, 126.6, 126.2, 125.9, 125.4, 123.2, 122.6, 27.0; IR (KBr)ν_{max}: 3050, 2921, 2853, 1623, 1573 cm^{-1}; HRMS (ESI) Calcd for $C_{24}H_{17}BrN$ 398.0539 (M + H$^+$); Found 398.0539 and 400.0520.

3-(4-Chlorophenyl)-1-methylnaphtho[2,3-*f*]quinoline (14v)

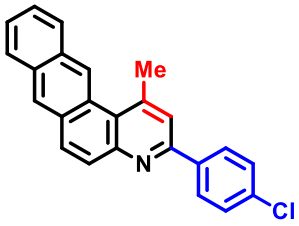

Yield 60% (20 mg), yellow solid, mp 224-226 °C; ^{1}H NMR (500 MHz, $CDCl_3$) δ 9.27 (s, 1H), 8.41 (s, 1H), 8.17 (d, *J* = 8.3 Hz, 2H), 8.13 – 8.05 (m, 2H), 8.02 (d, *J* = 9.2 Hz, 1H), 7.91 (d, *J* = 9.1 Hz, 1H), 7.80 (s, 1H), 7.62 – 7.58 (m, 2H), 7.50 (d, *J* = 8.3 Hz, 2H), 3.29 (s, 3H). ^{13}C NMR (125 MHz, $CDCl_3$) δ 154.0, 150.6, 145.7, 137.7, 135.4, 131.9, 131.7, 131.5, 131.4, 129.6, 129.1, 129.1, 128.9, 128.7, 127.6, 127.3, 126.6, 126.2, 125.2, 122.4, 27.09; IR (KBr)ν_{max}: 3050, 2923, 2853, 1601, 1572 cm^{-1}; HRMS (ESI) Calcd for $C_{24}H_{17}ClN$ 354.1045 ($M + H^+$); Found 354.1045.

3-(3-Methoxyphenyl)-1-methylnaphtho[2,3-*f*]quinoline (14w)

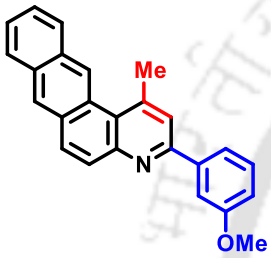

Yield 58% (21 mg), off-white solid, mp 132-134 °C; ^{1}H NMR (500 MHz, $CDCl_3$) δ 9.29 (s, 1H), 8.43 (s, 1H), 8.14 – 8.07 (m, 2H), 8.03 (d, *J* = 9.1 Hz, 1H), 7.96 (d, *J* = 9.1 Hz, 1H), 7.83 (d, *J* = 8.2 Hz, 2H), 7.76 (d, *J* = 7.6 Hz, 1H), 7.62 – 7.58 (m, 2H), 7.45 (t, *J* = 7.9 Hz, 1H), 7.02 (d, *J* = 8.1 Hz, 1H), 3.96 (s, 3H), 3.31 (s, 3H); ^{13}C NMR (125 MHz, $CDCl_3$) δ 160.3, 155.2, 150.5, 145.6, 140.8, 131.7, 131.7, 131.4, 131.4, 129.9, 129.8, 129.2, 128.9, 127.6, 127.6, 127.3, 126.5, 126.1, 125.2, 122.9, 119.9, 115.3, 112.6, 55.6, 27.0; IR (KBr)ν_{max}: 3050, 2956, 2923, 2851, 1626, 1580 cm^{-1}; HRMS (ESI) Calcd for $C_{25}H_{20}NO$ 350.1540 ($M + H^+$); Found 350.1545.

2-(1-Methylnaphtho[2,3-*f*]quinolin-3-yl)phenol (14x)

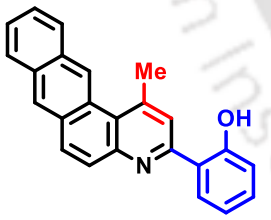

Yield 48% (16 mg), brown solid, mp 132-135 °C; ^{1}H NMR (400 MHz, DMSO-d_6) δ 9.49 (s, 1H), 8.72 (s, 1H), 8.40 (s, 1H), 8.38 – 8.36 (m, 1H), 8.32 (d, *J* = 9.2 Hz, 1H), 8.21 – 8.19 (m, 1H), 8.15 (d, *J* = 8.8 Hz, 1H), 7.88 (d, *J* = 9.1 Hz, 1H), 7.71 (dd, *J* = 6.6, 2.9 Hz, 2H), 7.42 (t, *J* = 7.7 Hz, 1H), 7.05 – 7.02 (m, 2H), 3.39 (s, 3H); ^{13}C NMR (125 MHz, DMSO-d_6) δ 134.0, 132.2, 131.7, 131.1, 130.3, 129.2, 129.1, 128.3, 127.9, 127.7, 127.5, 127.4, 127.2, 126.7, 125.2, 124.3, 122.7, 119.2, 118.4, 117.7, 26.6; IR (KBr)ν_{max}: 3053, 2921, 2856, 1581 cm^{-1}; HRMS (ESI) Calcd for $C_{24}H_{18}NO$ 336.1383 ($M + H^+$); Found 336.1383.

5,7-Dimethoxy-4-methyl-2-phenylquinoline (15a)

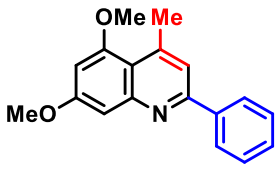

Yield 57% (16 mg), off-white solid, mp 116-117 °C; ^{1}H NMR (500 MHz, $CDCl_3$) δ 8.10 (d, *J* = 8.1 Hz, 2H), 7.50 (t, *J* = 7.4 Hz, 2H), 7.44 (d, *J* = 10.9 Hz, 2H), 7.13 (s, 1H), 6.49 (s, 1H), 3.96 (s, 3H), 3.92 (s, 3H), 2.89 (s, 3H); ^{13}C NMR (125

MHz, $CDCl_3$) δ 160.6, 158.6, 157.3, 129.2, 128.8, 127.5, 119.3, 115.7, 101.1, 98.5, 55.7, 55.6, 24.7; IR (KBr)ν_{max}: 3046, 2956, 2924, 2853, 1619, 1588 cm^{-1}; HRMS (ESI) Calcd for $C_{18}H_{18}NO_2$ 280.1333 (M + H^+); Found 280.1348.

2-(4-Fluorophenyl)-5,7-dimethoxy-4-methylquinoline (15b)

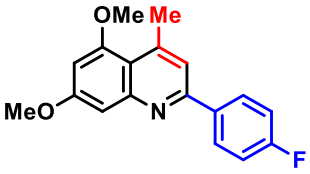

Yield 59% (17 mg), brown solid, mp 177-179 °C; ^1H NMR (500 MHz, $CDCl_3$) δ 8.11 – 8.08 (m, 2H), 7.37 (s, 1H), 7.17 (t, *J* = 8.6 Hz, 2H), 7.08 (d, *J* = 2.0 Hz, 1H), 6.48 (d, *J* = 1.9 Hz, 1H), 3.95 (s, 3H), 3.91 (s, 3H), 2.87 (s, 3H); $^{13}C\{^1H\}$ NMR (125 MHz, $CDCl_3$) δ 163.7 (d, *J* = 246.8 Hz), 160.7, 158.6, 156.2, 151.8, 146.5, 135.9, 129.3 (d, *J* = 8.3 Hz), 118.9, 115.7 (d, *J* = 21.3 Hz), 115.6, 101.0, 98.5, 55.6, 55.6, 24.7; ^{19}F NMR (471 MHz, $CDCl_3$) δ -113.01; IR (KBr)ν_{max}: 3049, 2968, 2928, 2871, 1614, 1580 cm^{-1}; HRMS (ESI) Calcd for $C_{18}H_{17}FNO_2$ 298.1238 (M + H^+); Found 298.1238.

2-(3-Bromophenyl)-5,7-dimethoxy-4-methylquinoline (15c)

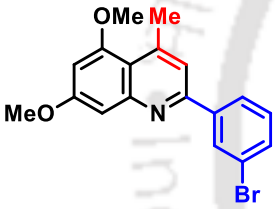

Yield 58% (21 mg), off-white solid, mp 118-120 °C; ^1H NMR (500 MHz, $CDCl_3$) δ 8.29 (s, 1H), 8.02 (d, *J* = 7.7 Hz, 1H), 7.56 (d, *J* = 7.8 Hz, 1H), 7.38 – 7.34 (m, 2H), 7.10 (s, 1H), 6.50 (s, 1H), 3.96 (s, 3H), 3.93 (s, 3H), 2.89 (s, 3H); ^{13}C NMR (125 MHz, $CDCl_3$) δ 160.8, 158.6, 155.6, 151.9, 146.7, 141.9, 132.1, 130.6, 130.3, 126.0, 123.1, 118.9, 116.0, 101.1, 98.8, 55.7, 55.6, 24.6; IR (KBr)ν_{max}: 2962, 2931, 1616, 1586 cm^{-1}; HRMS (ESI) Calcd for $C_{18}H_{17}BrNO_2$ 358.0438 (M + H^+); Found 358.0438 & 360.0417.

Methyl(2-(methylsulfinyl)ethyl)sulfane (Intermediate B4)

HRMS (ESI) Calcd for $C_4H_{11}OS_2$ 139.0246 (M + H^+); Found 139.0004.

1,3-*bis*(Methylsulfinyl)propane (Intermediate D4)

HRMS (ESI) Calcd for $C_5H_{13}O_2S_2$ 169.0352 (M + H^+); Found 168.9920.

3-(Methylsulfinyl)prop-1-ene (Intermediate H4)

HRMS (ESI) Calcd for C_4H_9OS 105.0369 (M + H^+); Found 105.9347.

1-Methyl-2-(methylthio)-3-phenyl-1,2,3,10b-tetrahydrobenzo [*f*]quinoline (Intermediate L4 of compound 3K)

HRMS (ESI) Calcd for $C_{21}H_{22}NS$ 320.1468 (M + H^+); Found 320.1436.

Table 5.6. Crystal data and structure refinement for 2-(4-methylbenzo[*h*]quinolin-2-yl)phenol (14g).

Entry	Identification code	Compound 14g
1	Empirical formula	$C_{20}H_{15}NO$
2	Formula weight	285.3
3	Temperature	297 K
4	Wavelength	0.71073
5	Radiation type	MoK\a
6	Radiation system	Fine-focus sealed tube
7	Crystal system	Monoclinic
8	Space group	P 21/n
9	Cell length	a=16.9016 (15) b=8.6430 (8) c=21.0199 (8)
10	Cell angle	α=90 β=108.891 (3) γ=90
11	Cell volume	2905.2 (5)
12	Density	1.305
13	Completeness to theta	99.4
14	Absorption correction	multi-scan
15	Refinement method	Full-matrix least-squares on F2
16	Index ranges	-10<=h<=10, -24<=k<=24, -13<=l<=13
17	Reflection number	3415
18	Theta (max)	25.02
19	Theta (min)	2.57
20	Cell formula units Z	4
21	CCDC no	2291148

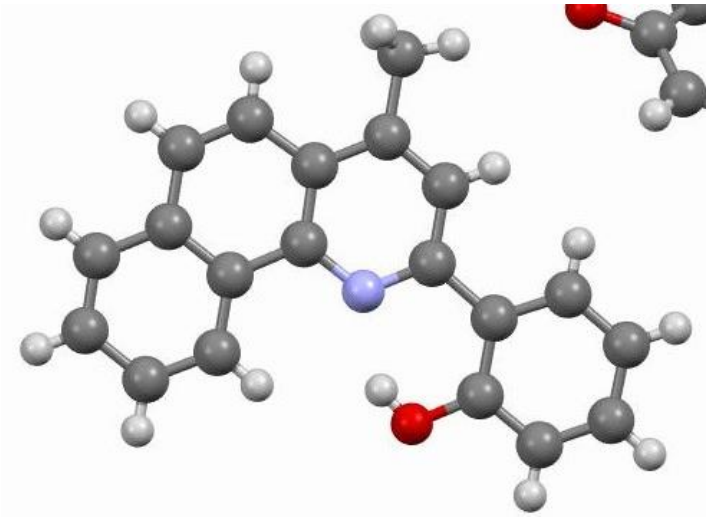

Figure 5.1. ORTEP diagrams of compound **14g**.

5.3d. Representative Characterization Spectra

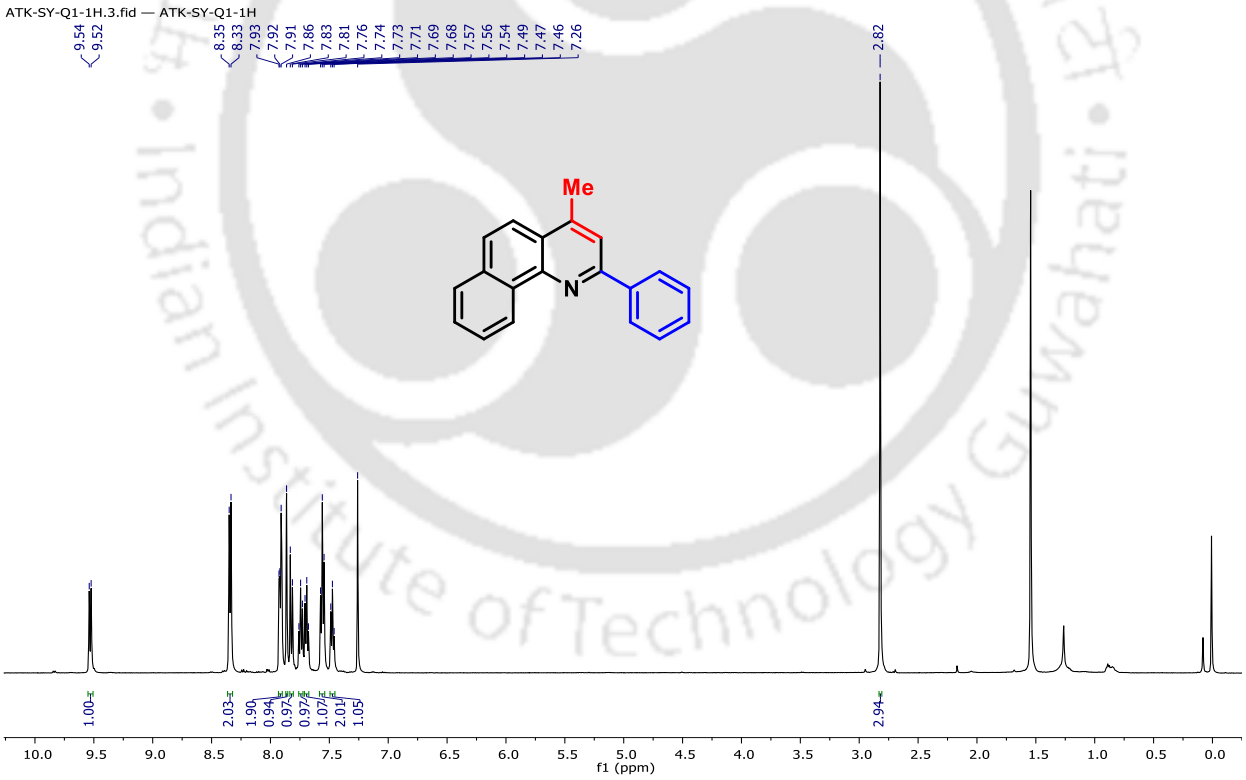

Figure 5.2. ^{1}H NMR Spectra of 4-methyl-2-phenylbenzo[*h*]quinoline (**14a**).

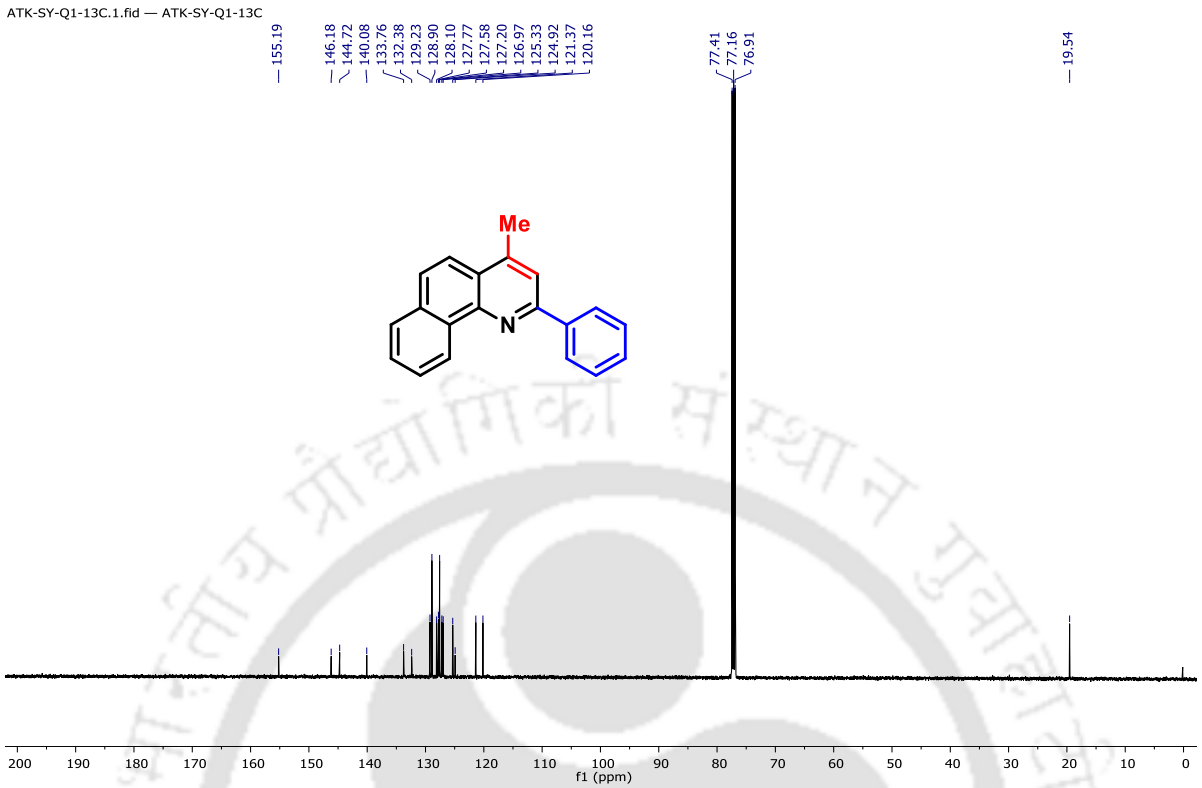

Figure 5.3. ^{13}C NMR Spectra of 4-methyl-2-phenylbenzo[*h*]quinoline (**14a**).

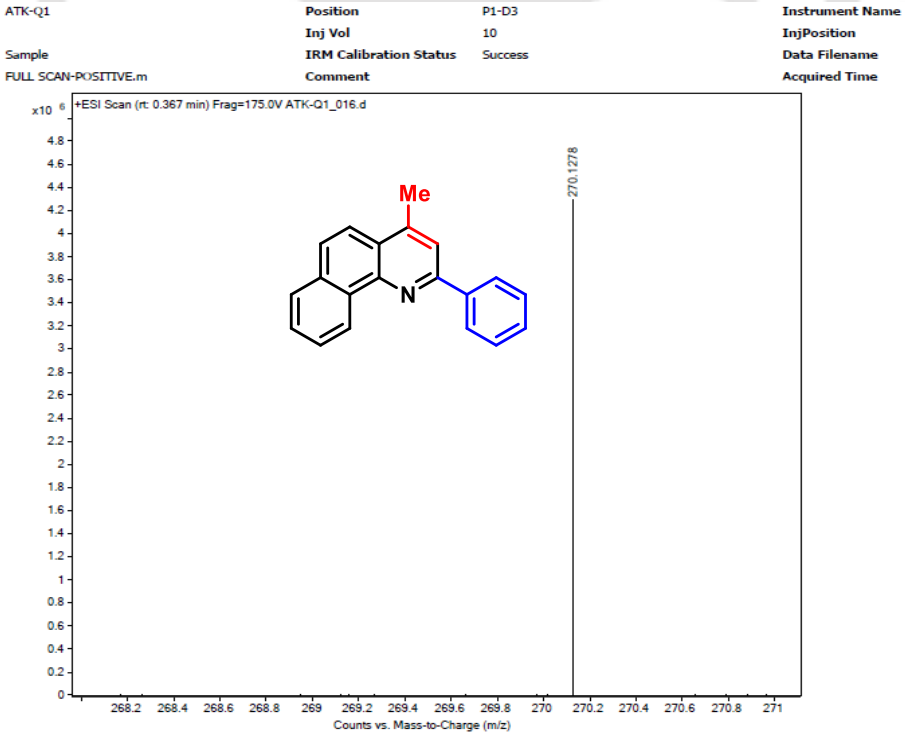

Figure 5.4. HRMS Spectra of 4-methyl-2-phenylbenzo[*h*]quinoline (**14a**).

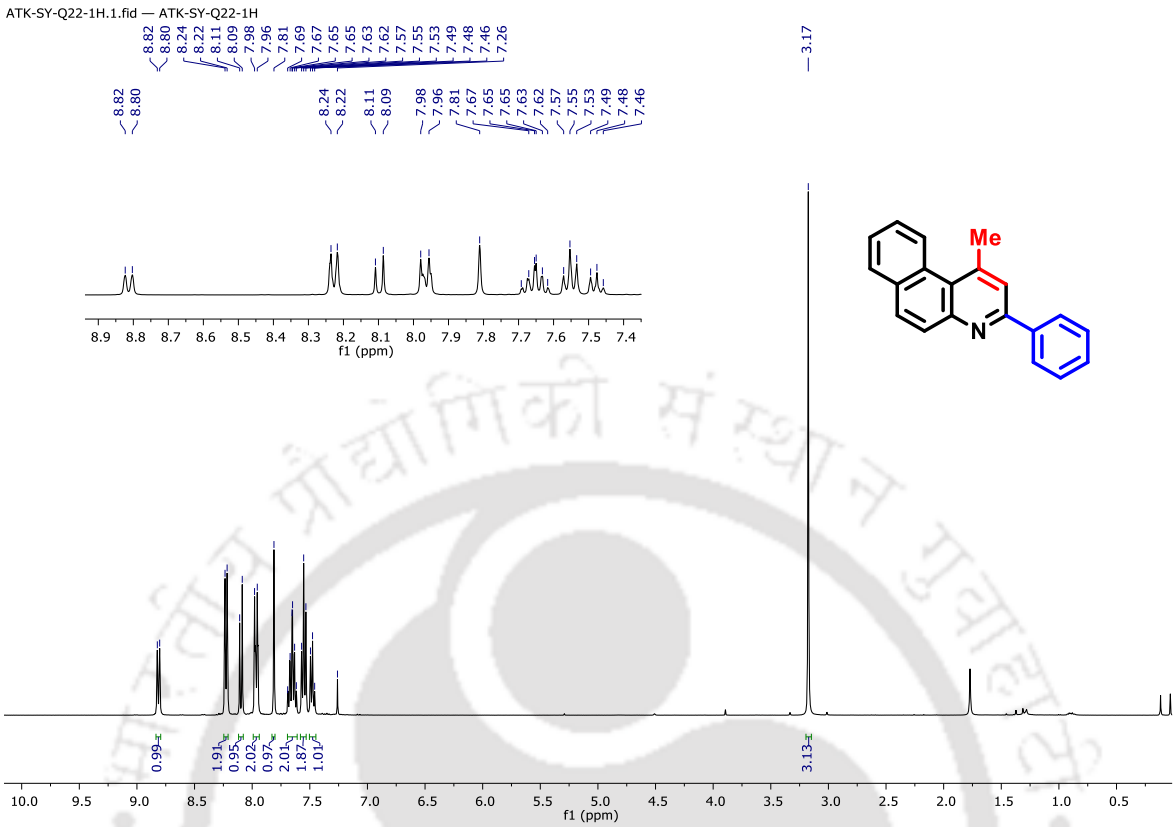

Figure 5.5. ^{1}H NMR Spectra of compound 1-methyl-3-phenylbenzo[*f*]quinoline **(14k)**.

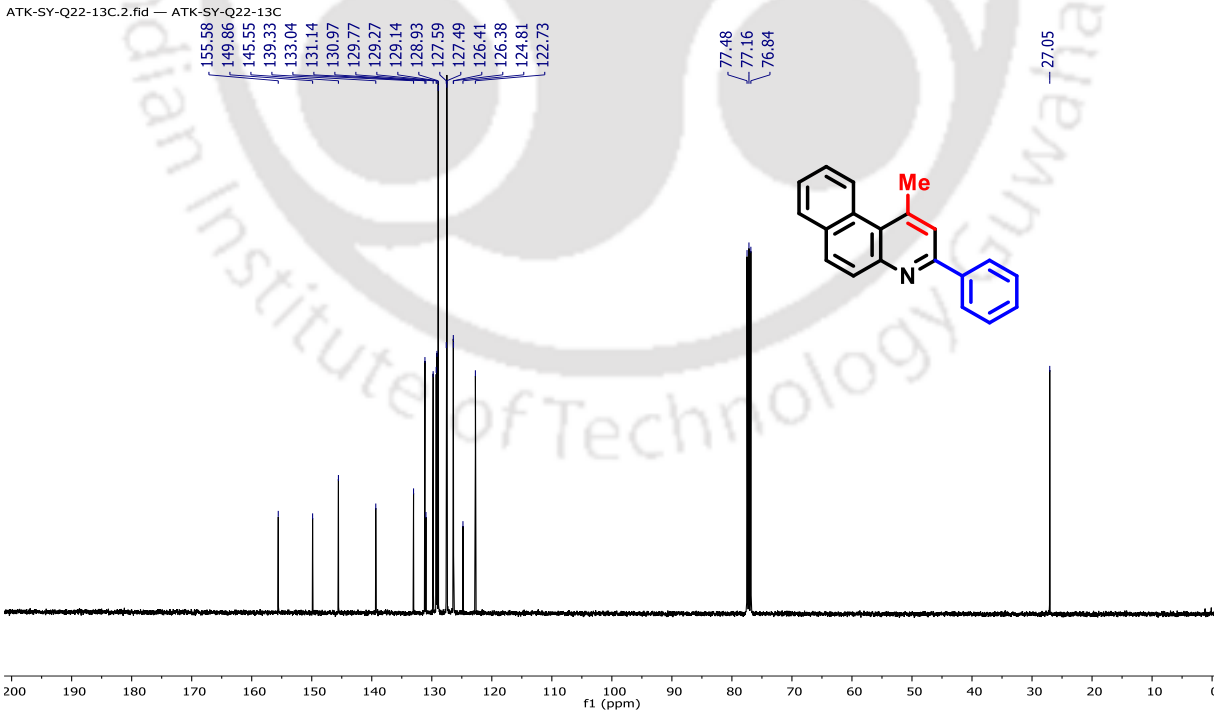

Figure 5.6. ^{13}C NMR Spectra of 1-methyl-3-phenylbenzo[*f*]quinoline **(14k)**.

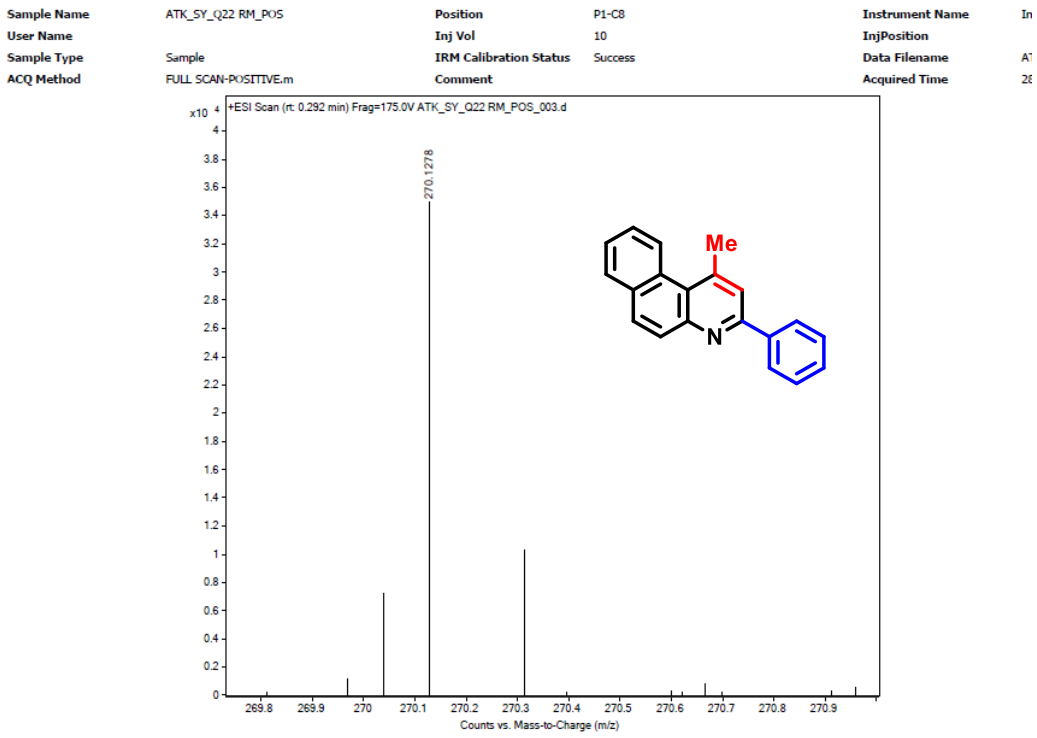

Figure 5.7. HRMS Spectra of 1-methyl-3-phenylbenzo[*f*]quinoline **(14k)**.

5.4. References

1. S. Yashmin, S. Mondal, R. Das, P. Banerjee and A. T. Khan, *Org. Biomol. Chem.*, 2022, **20**, 7302–7315.

2. **Review articles**: (a) Z. Tashrifi, M. M. Khanaposhtani, B. Larijani and M. Mahdavia, *Adv. Synth. Catal.*, 2020, **362**, 65–86; (b) S.-Q. Cai, K.-F. Zhang and X.-H. Cai, *Curr. Org. Chem.*, 2022, **26**, 91-121; (c) X.-F. Wua and K. Natte, *Adv. Synth. Catal.*, 2016, **358**, 336–352.

3. (a) S. B. Wakade, D. K. Tiwari, P. S. K. P. Ganesh, M. Phanindrudu, P. R. Likhar and D. K. Tiwari, *Org. Lett.*, 2017, **19**, 4948−4951; (b) S. B. Wakade, D. K. Tiwari, M. Phanindrudu, Pushpendra and D. K. Tiwari, *Tetrahedron*, 2019, **75**, 4024–4030; (c) J. Yuan, J. T. Yu, Y. Jiang and J. Cheng, *Org. Biomol. Chem.*, 2017, **15**, 1334−1337; (d) T.-S. Jiang, X. Wang and X. Zhang, *Tetrahedron Lett.*, 2018, **59**, 2979–2982; (e) S. D. Jadhav and A. Singh, *Org. Lett*., 2017, **19**, 5673−5676; (f) Y. Liu, Y. Hu, Z. Cao, X. Zhan, W. Luo, Q. Liu and C. Guo, *Adv. Synth. Catal*., 2018, **360**, 2691–2695.

4. (a) C. Xu, S.-F. Jiang, X.-H. Wen, Q. Zhang, Z.-W. Zhou, Y.-D. Wu, F.-C. Jia and A.-X. Wua, *Adv. Synth. Catal.*, 2018, **360**, 2267–2271; (b) H. Li, M. Su, Z. Nie, T. Yang, W. Luo, Q. Liu and C. Guoa, *Adv. Synth. Catal*., 2021, **363**, 3127–3137; (c) Y. Zhang, J. Kuang, X. Xiao, L. Wang and Y. Ma, *Org. Lett.*, 2021, **23**, 3960−3964; (d) S. Kalari, U. B. Karale and H. B. Rode, *J. Org. Chem.*, 2022, **87**, 2435−2445; (e) T. Yang, H. Li, Z. Nie, M.-d. Su, W.-p. Luo, Q. Liu and C.-C. Guo, *J. Org. Chem.*, 2022, **87**, 2797−2808; (f) P. Yadav, S. Yadav, A. Awasthi, M. Phanindrudu, S. Bhowmicka and D. K. Tiwari, *New J. Chem.*, 2022, **46**, 16289–16296.

5. S. Faraz and A. T. Khan, *Org. Biomol. Chem*., 2023, **21**, 7553–7560.

6. C. Zhu, R. Guo, Z. Sheng, Y. Li and C. Chu, *Chin. J. Chem.*, 2017, **35**, 1595–1600.

7. J. Yu, P. Zhang, J. Wua and Z. Shang, *Tetrahedron Lett.*, 2013, **54**, 3167–3170.

8. (a) A. Wang, X. Liu, Y. Kong, J. Wang and T.-S. Jiang, *Org. Chem. Front.*, 2021, **8**, 947–952; (b) D. Fu, J. Dong, H. Du, and J. Xu, *J. Org. Chem.*, 2020, **85**, 4, 2752–2758; (c) P. Yang, W. Xu, R. Wang, M. Zhang, C. Xie, X. Zeng and M. Wang, *Org. Lett*., 2019, **21**, 3658−3662.

9. L. Huang, Z. Liu, J. Wang, J. Fu, Y. Jia, L. Ji and T. Wang, *Food Sci. Nutr.*, 2023, **11**, 2450–2470.

APPENDIX

- **Thesis Conclusion**
- **Future Perspectives**
- **List of Publications**

Thesis Conclusion

Before presenting a comprehensive conclusion for this thesis, it is essential to provide the contextual background of ***Domino and Multicomponent reactions***. **Chapter I** delves into the significance of PHAs and briefly describes various well-known methodologies for synthesizing a broad spectrum of PHAs. The ***Domino/Tandem/Cascade reactions*** are a particularly convenient method due to their remarkable efficiency and selectivity, involving at least two consecutive reactions within a single step. This approach eliminates the need for isolating intermediates, introducing new reagents and generating fewer by-products, which makes this one-pot reaction superior to other multi-step syntheses of PHAs. While cascade reactions typically involve intramolecular transformations, they can also occur as intermolecular reactions, alternatively called ***Multicomponent reactions***. In this document, the research conducted throughout the PhD program is outlined and presented as a thesis overview in **Scheme A1**.

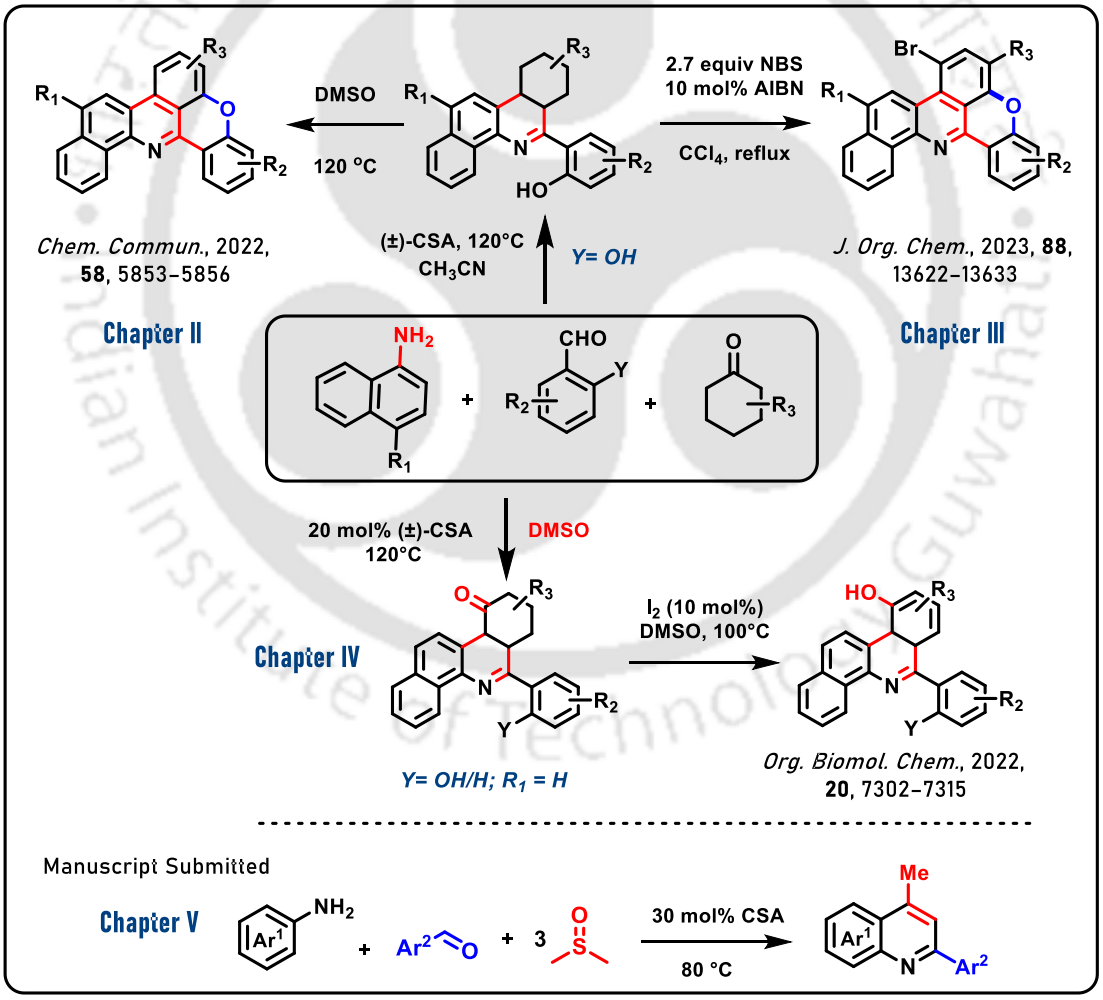

Scheme A1. Thesis Overview

Conclusion

In summary, this thesis documents the synthesis of tricyclic, tetracyclic and hexacyclic heteroaromatics through the strategic application of the ***Domino*** and ***Multicomponent reactions*** as presented in **Scheme A1**.

1. **Chapter II** describes the preparation of 2-(7,8,9,10-tetrahydrobenzo[*c*]phenanthridin-6-yl)phenol derivatives as a precursor from the multicomponent reaction of 1-naphthylamine, salicylaldehyde and cyclohexanones. Then, the synthesis of benzo[*c*]chromeno[4,3,2-*gh*]phenanthridine derivatives is accomplished using the precursor in a one-step cascade reaction. This includes a consecutive series of reactions such as the formation of *o*-quinone methide intermediate, 6pe ring closure reaction, hydroxylation, and H_2O elimination reactions for the aromatization.

2. **Chapter III** illustrates the synthesis of 7-bromobenzo[*c*]chromeno[4,3,2-*gh*]phenanthridine from the tandem reaction of the same phenolic precursors with a regioselective instalment of the bromo group. This methodology showcases the involvement of radical catalyzed di-bromination, pyran ring formation by intramolecular substitution, and aromatization reactions in a step employing NBS/AIBN.

3. **Chapter IV** delves into the synthesis of 6-aryl-8,9-dihydrobenzo[*c*]phenanthridine-10(7*H*)-ones by using solvent-dependent multicomponent reaction of 1-naphthylamine, salicylaldehyde and cyclohexanones. This methodology flaunts imine formation, adding imine and cyclohexanone, cyclization followed by regioselective benzylic oxygenation using DMSO as a solvent-cum-reactant. Finally, 6-arylbenzo[*c*]phenanthridin-10-ol derivatives are obtained from the ketone precursor.

4. **Chapter V** consists of the pseudo-multicomponent reaction of aryl amine (mainly 1-naphthylamine, 2-naphthylamine, 2-aminoanthracene), aryl aldehyde and solvent-cum-reactant dimethyl sulfoxide (DMSO). Herein, DMSO is used as a three-carbon synthon.

5. The thesis also demonstrates the brief AIE study of a 7-bromo-benzo[*c*]chromeno[4,3,2-*gh*]phenanthridine compound and fluoride sensing study of few 6-(2-hydroxyaryl)-8,9-dihydro-benzo[*c*]phenanthridine-10(7*H*)-one derivative.

Future Perspectives

1. *Exploration of 2-(7,8,9,10-Tetrahydrobenzo[c]phenanthridin-6-yl)phenol Derivatives*

2-(7,8,9,10-Tetrahydrobenzo[*c*]phenanthridin-6-yl)phenol derivatives obtained from the multicomponent reaction of 1-naphthylamine, salicylaldehyde and cyclohexanone derivatives can be utilized as a precursor further (**Scheme A2**). These compounds can be applied in established organic reactions as well as the development of new methodologies for synthesizing a diverse range of polycyclic heteroaromatic compounds (PHAs).

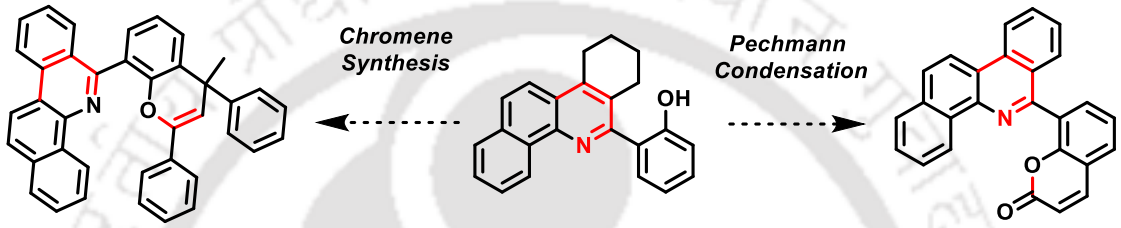

Scheme A2

2. *Exploration of 2-Naphthylamine*

The thesis predominantly focuses on the examination of 1-naphthylamine through multicomponent or pseudo-multicomponent reactions, significantly contributing to multiple polycyclic heteroaromatic (PHAs) syntheses. However, 2-naphthylamine is specifically highlighted in **Chapter V**, alongside 1-naphthylamine and 2-aminoanthracene. Herein, it is proposed that 2-naphthylamine can be exclusively explored to achieve novel PHAs, as illustrated in **Scheme A3**.

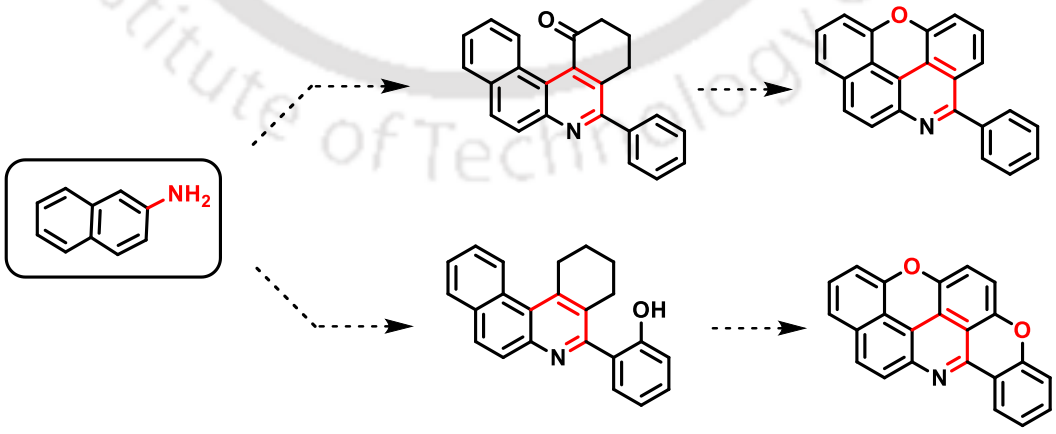

Scheme A3

3. Biological Applications

In **Chapter I**, **Section 1.4**, the significance of the benzophenanthridine skeleton is emphasised, as it plays a crucial role in numerous naturally occurring benzophenanthridine alkaloids. These alkaloids are predominantly bioactive and possess various anti-disease properties. In **Chapter IV**, we successfully synthesized derivatives of 6-arylbenzo[*c*]phenanthridin-10-ol. These compounds offer potential for studying various biological properties, including but not limited to anti-cancer, anti-bacterial, and anti-fungal activities.

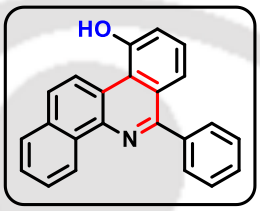

4. Applications in Organic-semiconducting-diodes and Photophysical Studies

Chapter I, **Section 1.1** highlights the noteworthy contribution of polycyclic heteroaromatic compounds to organic semiconducting diodes (OSCs), including OLEDs, OFETs, and solar cells. **Chapter I**, **Section 1.3** mentions the intriguing photoluminescence properties of polyheteroaromatics containing chromeno[4,3,2-*gh*]phenanthridine. Therefore, future research may focus exclusively on studying the applications of the synthesized compounds, specifically benzo[*c*]chromeno[4,3,2-*gh*]phenanthridine and 7-benzo[*c*]chromeno[4,3,2-*gh*]phenanthridine derivatives in OSCs.

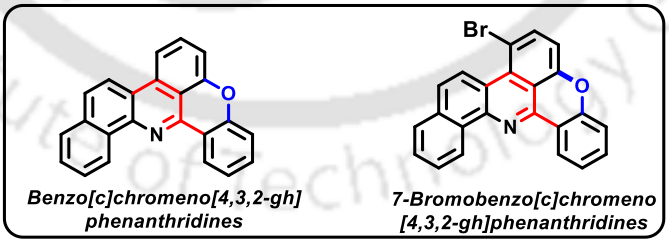

In **Chapter III**, we conducted a partial investigation into the Aggregation-Induced Emission (AIE) study and the Fluoride Sensing study has also been illustrated in **Chapter IV**. Since all the compounds synthesized in this thesis exhibit fluorescence properties, future research can be expanded absolutely to their remaining photophysical studies.

List of Publications

Research Publications, Accomplished from the Thesis work

1. **S. Yashmin**, R. Ali, S. Mondal and A. T. Khan. DMSO-assisted environmentally benign synthesis of benzo[*c*]chromeno[4,3,2-*gh*]phenanthridines by remote oxidative hetero cross-coupling cyclization and aromatization reaction. *Chem. Commun.*, 2022, **58**, 5853–5856.

2. **S. Yashmin**, S. Mondal, R. Das, P. Banerjee, and A. T. Khan, Regioselective synthetic approach for key precursors of 6-arylbenzo[*c*]phenanthridin-10-ol derivatives: A useful compound for selective chromogenic recognition of fluoride. *Org. Biomol. Chem.*, 2022, **20**, 7302–7315.

3. **S. Yashmin**, A. T. Khan, S. J. Akula, R. P, K. Bhattacharyya, One-Step Synthesis of 7-Bromobenzo[*c*]chromeno[4,3,2-*gh*]phenanthridines through a Sequential Bromination/ Cyclization/Aromatization Reaction Using *N*-Bromosuccinimide (NBS). *J. Org. Chem.*, 2023, **88**, 13622–13633.

4. **S. Yashmin**, K. AM, A. T. Khan, 'Utilization of DMSO as a solvent-cum-reactant: Synthesis of fused 2-aryl-4-methylquinolines' *Org. Biomol. Chem.*, 2024, **22**, 0000–0000

Publications which are not included in the Thesis

5. S. Mondal, **S. Yashmin**, R. Ali, R. Soundaram, S. S. Ghosh and A. T. Khan, Synthesis of biologically active fused 1,4-oxathiin derivatives from 4-hydroxydithiocoumarins, arylacetylenes and dimethyl sulfoxide by Cu(I) catalyzed C-H functionalization and cross-dehydrogentive C-S coupling reactions. *Org. Biomol. Chem.*, 2021, **19**, 5818–5826.

6. S. Mondal, **S. Yashmin** and A. T. Khan. Synthesis of vinyl sulfides and thioethers via hydrothiolation reaction of 4-hydroxydithiocoumarin and arylacetylenes/styrenes. *Org. Biomol. Chem.*, 2021, **19**, 9223–9230.

7. M. Belal, S. Mondal, **S. Yashmin** and A. T. Khan. Reactivity switch-over of 4-hydroxydithiocoumarin under various conditions and their application in organic synthesis. *Org. Biomol. Chem.*, 2022, **20**, 715–726.

8. S. Faraz, **S. Yashmin**, M. D. Marathe, A. T. Khan, Environmentally benign synthesis of 2,4-diarylquinolines under metal- & solvent-free conditions. *Tetrahedron Lett.*, 2023, **120**, 154433.